THE DYNAMIC RESPONSE OF FINITE CYLINDRICAL SHELLS ACCORDING TO TWO SHELL THEORIES

by

SELIG FISHER

A dissertation submitted to the Graduate Faculty in Engineering in partial fulfillment of the requirements for the degree of Doctor of Philosophy, The City University of New York

1970

This manuscript has been read and accepted for the Graduate Faculty in Engineering in satisfaction of the dissertation requirement for the degree of Doctor of Philosophy.

5/13/70
date

Chairman of Examining Committee

13 May 1970
date

Executive Officer

David Cheng, Civil Engineering

Gerald G. Lowen, Mechanical Engineering

Richard Stoneham, Mathematics

(Chairman) Sherwood B. Menkes, Mechanical Engineering
Supervisory Committee

The City University of New York

Abstract

THE DYNAMIC RESPONSE OF FINITE CYLINDRICAL SHELLS ACCORDING TO TWO SHELL THEORIES

Adviser: Professor Sherwood B. Menkes

The forced response of finite, linearly elastic cylindrical shells with prescribed edge conditions has not been sufficiently studied. Various shell theories have been proposed to examine this problem. The simpler bending theories (called herein classical theories), more amenable to engineering approximation, having been examined by other criteria, may not actually be appropriate to all dynamic problems. Only limited use has been made of these classical theories for dynamic problems, and then only with very specialized edge conditions. More inclusive theories, which include transverse shear deformation and rotary inertia (usually termed refined or SR theories), though developed, have not been used to analyze dynamic problems of this nature. This thesis compares the results obtained with two shell theories, one classical and one SR theory, when they are used to analyze the forced dynamic deformation of a cylindrical shell with free or clamped edges. An essential feature of the analysis is a reliance on Hamilton's Variational Principle as the underlying, dominant governing physical law. Beginning with Hamilton's Principle, I have formulated two mutually consistent sets of descriptive equations and bound-

ary conditions, as well as the required conditions of orthogonality. The equilibrium portions of these equations are shown to be identical with particular shell theories, previously developed by Yu, in part by different means. The two dimensional shell equations are formed after making a power series approximation for the particle displacement, applying the variation to the mid-surface motion coordinates, and integrating over the cylinder thickness. The mid-surface motion is composed of a dimensionally separable series of orthogonal functions containing exponential axial terms. A computer program has been developed which identifies the natural frequencies and boundary dependent normal deformation modes associated with force-free vibration. The separable Lagrange equations developed within Hamilton's Integral are numerically solved for three time-impulsive type forcing functions. The cumulative deformation pattern of all modulated normal modes excited by these forcing functions create a particle stress intensity at a critical point on the cylinder's surface. The stress intensity history of the SR and Classical models are examined. Differences are noted and analyzed. The effects of the spatial character of the forcing functions, alternate model rigidity and different natural boundary conditions for each model are considered.

SUMMARY AND CONCLUSIONS

An investigation has been made of the dynamic response of two short, thick cylindrical shells, with clamped and free edges, to three different impulsive loadings. The comparison is taken between two models of elastic restraint to deformation: a classical type model (CL) and an SR model, in which transverse deformation is permitted and rotary inertia effects are included.

The investigation was performed by means of a computer program, briefly described in Chapter IX. The actual program is written in FORTRAN IV and is suitable for use with the IBM 360 or CDC 6600. Readers who are interested in these details, or in securing the program listing, are urged to communicate with the author.

The reasons for the choice of loading and configurations are set forth in Chapter XI.

The major comparison parameter was the stress intensity history at a critical point on the cylinder surface. This stress intensity was developed from a truncated series of the infinite normal deformation modes, oscillating at their appropriate natural frequencies, which were excited by the three forcing functions. The loads were all time-impulsive, and described spatially as cosine frontal, tri-

angular and exponential.

The stress intensity histories are shown in Figures 7,9 and 11 for the fixed cylindrical shell, for low, intermediate and high truncations of the frequencies examined.

The major sources of difference between the response of each model were attributed to two factors: the admission of transverse shear deformation in the SR model (the pliancy effect) and to the different natural boundary conditions of each model, formulated within Hamilton's Integral. These are described in 11.2 and 11.3 respectively.

The clamped cylinder had normal deformation modes whose natural frequencies, according to the alternate models, followed a consistent pattern. As the normal mode structural waves became progressively shorter, the CL frequency became increasingly larger than the SR frequency of oscillation for a given mode. Frequency values are shown in Tables I and II, as well as Figure 5.

The stress intensities for the clamped cylindrical shell, as more short structural waves were incorporated in the truncated series, differed significantly for the two models. These results have been analyzed (11.5) and attributed to the pliancy effect.

It may be concluded that: sufficient differences

exist between the models to recommend that the SR model should be chosen for a fixed cylindrical shell undergoing transient dynamic loading.

With respect to possible future work, the following comments are offered:

1. This conclusion is reached for a short, thick cylinder. Other geometries, e.g., short, thin; long, thick and long, thin might be considered to determine the effect of length and thickness parameters. A preliminary judgment would be that for these other cases, the CL model will probably be adequate.

2. Some consideration should be given to loads that are not purely impulsive, but are instead distributed in time. A preliminary judgment is that for these cases, the CL model may be adequate.

For the free cylindrical shell, the stress intensity histories are shown in Figures 8, 10 and 12. The free cylinder showed the effect of different natural boundary conditions for the two models. The SR frequency was initially greater than that for the CL model, with the longer structural waves. These normal modes had deformation patterns which are influenced

throughout the length of the cylinder by conditions at the boundary. Refer to Figures 30 and 31. When the axial waves are shorter, the boundary effects are isolated, and the general pliancy effect dominated. The CL frequency was then found to be larger than for the SR model with such waves. Frequencies are tabulated in Tables III and IV, and differences between frequencies in Table V. Note also Figure 29.

Differences in the stress intensity histories between the models were as great when only long waves were included in the (very limited) truncated series as was the case when many more terms, incorporating the shorter structural waves, excited by the transient dynamic loading, were included in the series.

It may be concluded that: <u>for the impulsive loadings, and the free cylinder the use of the SR theory is not required</u>.

With respect to possible future work on the free cylinder, the following comments are offered:

1. Examination of other geometries will probably not be fruitful and is not recommended.

In either case (fixed or free), it is evident that it will be necessary to establish an entirely different approach for an examination of the post-yield behavior of such structures. It seems to me that this will be the most interesting area for further research.

The material in this thesis has been partially presented in a CUNY report, TR 68-15, prepared for the U. S. Army Research Office, entitled, "The Dynamic Response of Finite Elastic Cylinders according to various Shell Theories," Volume I. This report has been cited in the NASA/SCAN Notifications of September 1969, and the NASA/STAR Notifications, January 1970. The work in this thesis not covered in Volume I, will be included in a subsequent Volume to be prepared later this year.

TABLE OF CONTENTS

LIST OF TABLES

LIST OF ILLUSTRATIONS

NOMENCLATURE
(PARTIAL)

The following list is an inventory of most of the symbols and letters used in this report. I have not made a serious attempt to restrict this nomenclature to unique or individual interpretation. Certain algebraic letters have historically been used so often to represent particular concepts that it would seriously detract from the presentation were other letters or symbols to be used. In addition, I have attempted to preserve much of the notation used in certain references, so as to make it easier to compare this material with that in the reference.

As a consequence, more than one meaning is often shown for a letter or symbol. The one which should be used will be clear in the context of the application. Not all symbols are listed; where the use of the character is restricted to only a few pages, and in a very narrow sense, it has not been included in this glossary of terms.

A_1	The determinant a_{rs} (see equation 76)
A_2	Frequency determinant (see equation 78)
C_{mN}	A constant, expressing amplitude of a solution u_k^n
C	Midsurface line (see Figure 4)
D	Linear operator on x
E	Modulus of elasticity
$\bar{F}$	Force
$F_k^n(x,\phi)$	Those terms in free vibration equations that are multiplied by ω_{mN}. (See 103). Traceable to K.E. variation.
G	Lame's constant
G'	KG

H_k^n	Free vibration, deformation equilibrium equations
I	Hamilton's Integral
I_2'	Second invariant of deviatoric stress tensor
K_{mN-ps}	Stiffness coefficient (See equation E-24)
L	Length of cylinder
L	Lagrangian = T + U-W
M	Mass of entire cylinder
$M_{x,\phi}$	Moment resultants (equation 43)
M_{mN}	Generalized mass associated with mN^{th} mode (Eq.129)
$N_{x,\phi}$	Stress resultants (equation 43)
N	Index of infinite number of eigenvalues of ω_m
$\bar{P}$	Pressure on surface of cylinder
P_o	Maximum value of $\bar{P}$, as scalar
Q^E	Generalized external force in the "direction" of $q(t)_{mN}$
Q_x, Q_ϕ	Shear stress resultant
$\bar{\sigma}_r$	Dimensionless parameter = $\dfrac{\sigma_r}{(P_o\tau/2)(1+h/a)(a/h)\omega_o}$
dS_k	Incremental distance along vector $\bar{e}_k$
S_{ik}^n	Components of boundary value determinant, free ends (see Eq. 94)
T	System kinetic energy
U	System strain energy
dV	Unit volume
V	Volume
W	System external work
Y_B	Location of center of gravity
a	mean radius of cylinder
a_{rs}	Free vibration coefficient matrix (see equation 75)
a_r	Coefficients of Fourier series (equation 168)
b_k^n	$(1+\frac{h}{a})h^n$
b_p	Coefficients of Fourier series (equation 166)

c_k^n	$-2\,\gamma\, h^* \left(\frac{h}{\sqrt{3}a}\right)^{2n}$
$\bar{e}_k$	Body fixed triad
$f_k^n(x)$	Axial function in assumed solution
g	Coefficients in equation 79
h	Half-thickness of cylinder
h_k	Proportionality constant (see equation 13)
h ( )	Unit step function
k	$1/3\ (h/a)^2$
m	Number of circumferential waves
$\bar{n}$	Vector normal to a surface $d\Sigma$ (Figure 2)
q	Generalized coordinate (t)
$\bar{r}$	Inertial vector location of typical particle
t	Time
t_1	Time terms involving rotary inertia
$\bar{u}$	Deformation vector
u_k^n	Midsurface deformation or rotation
x	Axial coordinate
z	Radial coordinate
Γ_{mi}	A constant amplitude factor (see equation 77)
K	$\kappa(1-\nu)/2$
	Terms in free vibration equilibrium equations due to strain energy variation (See 103)
$\bar{\bar{=}}_k^n$	Deformation equilibrium equations
$d\Sigma$	Surface element (see equation 11)
ϕ_k^n	Used in boundary condition equation (see equation 49)
X	Space dependent terms in Free Vibration equation (102)
ψ_k^n	Stress-motion equilibrium equations (see equation 44)
Ω_k^n	Used in boundary condition equations (see equation 50)
Ω_{mN}	Non-dimensional parameter (equation 177)
ϵ	Parameter varied as coefficient of perturbation function.

α	Parameter varied as coefficient of perturbation function
γ	Mass density
γ	Shear strain
δ	variational sign
δ_{ik}	Kronecker delta
ϵ	Strain
ϵ_{ik}	Strain tensor
ζ_p	Perturbation Function
ζ^n_{kmi}	Relative amplitudes of axial modes
η_k	Perturbation function
θ	Perturbation function (t) in generalized coordinate
κ	Mindlin's constant
λ_k	Body referenced coordinates (see equation 12)
λ_{ni}	A root of determinant A_2
ν	Poisson's ratio
ξ_p	Inertial axes
$\bar{\rho}$	Location vector to particle from center of gravity
σ	Stress (general notation)
σ_{ik}	Stress tensor
σ^n_{ik}	Stress or Moment Resultant (see equation 42)
σ_o	Yield stress in simple tension
σ_r	Stress intensity (see equation 182)
τ	Time of action of a pressure pulse
ϕ	Circumferential coordinate
ω_{mN}	Natural frequency
ω_o	Lowest extensional frequency $= \sqrt{\frac{E}{\gamma a^2 (1-\nu^2)}}$
∇	Del operator
$\cup$	Mathematical notation: "or"

$\bullet$	Notation for scalar multiplication
*	Arithmetic multiplier
$\{\}$	A column vector
λ	Lame's constant

Dimensionless quantity	To convert to dimensional form multiply by	Physical Interpretation
$\bar{\sigma}_{11}'$	$\left(\frac{E2}{1-\nu^2}\right) a$	stress resultant (moment)
$\bar{\sigma}_{11}^{\circ}, \bar{\sigma}_{12}^{\circ}$	$\frac{E2}{(1-\nu^2)}$	Stress resultant (force)
$\bar{U}$	$\left(\frac{E}{1-\nu^2}\right)\left(\frac{1}{a}\right)$	Strain energy
Ω_{mn}	$\omega_0=\left[\frac{E}{\gamma a^2(1-\nu^2)}\right]^{1/2}$	natural frequency
t'	ω_0^{-1}	time
$\bar{\sigma}_r$	$\left(\frac{P_0 r}{2}\right)\left(1+\frac{h}{a}\right)\left(\frac{a}{h}\right)\omega_0$	stress intensity
$\bar{\bar{\sigma}}_r$	$\bar{\sigma}_{r_{max}(CL)}$	$\bar{\sigma}_r$

SECTION I INTRODUCTION

1.1 Statement of the Problem

Many shell theories have been developed to predict the deformation response of thin cylinders to external stimuli. Shell theory is based upon the premise that deformation throughout the thickness of the shell is a function of the mid-surface motion (linear displacement, rotation, variation of rotation per inch, etc.), and the original distance of an element from the mid-surface. These mathematical models, when possible, have been compared with the assumed exact model, the three-dimensional theory of elasticity. Such comparisons have been limited due to the unavailability of exact (elasticity) solutions for other than extremely specialized loadings, constraints and response patterns, as for example, the axial shear vibrations of an infinite cylinder.

The classical shell theories are developed for a cylinder whose transverse shear deformation is considered negligible and whose rotary inertia is disregarded. Rotation of the mid-surface is seen then to be a dependent function of its linear displacement. The mathematical model to predict deformation response is therefore constructed from 3 independent variables, i.e., the orthogonal mid-surface displacements.

A more complete (non-classical) shell theory (SR) would account for transverse shear deformation and rotary inertia. Mid-surface variables are the linear displacements and rotation in the transverse planes. These develop a transverse shear strain approximately constant throughout the thickness. The five

variables are independent.

In only one instance (wave propagation during free vibration of an infinite cylinder) has a dynamic characteristic of the models for both of these shell theories been compared with the exact three dimensional elastic solution (36). In that one case, the 5 variable shell theory can duplicate the elasticity solution while the classical (3 variable) shell theory is in substantial error in predicting the cycle time of the higher frequency oscillations associated with short structural wavelengths.

My intention was to discover how this divergence of dynamic response characteristics between the two shell theories manifests itself in more typical engineering structures (finite cylinders, clamped and free-ended) subjected to familiar impulsive loadings. The comparison parameter was the time history of the Hencky stress intensities developed on the cylinder's surface. A measurable difference in results for a particular shell geometry or impulse pattern could indicate hesitation in the unlimited usage of the popular classical shell theories as models for many dynamic problems.

No forced dynamic response problem for a finite cylinder with edge conditions other than simply supported has been attempted using a non-classical theory. Nor has a free vibration problem, with the free and clamped boundary conditions, been attempted with a non-classical theory. Even with the classical theories, analytical dynamic response investigations are very limited. The deformation history for the finite - clamped or free cylinder under dynamic loading has not been investigated previously with either theory.

Shell equilibrium equations and required boundary conditions will be developed from Hamilton's Principle both for a classical theory and a shear deformation theory. The alterations necessary in both the equilibrium equations and the boundary requirements to transform one theory into its conjugate will be accomplished within Hamilton's integral and will therefore be consistent with the minimization principle.

The solution of the force-free equations is an infinite series of separable space (normal mode) and time (natural frequency) functions. Proof of the orthogonality of the normal mode functions will also be accomplished within the Hamilton Integral by a procedure shown to be applicable for any model, when the strain energy density of the shell is a quadratic function of the strains. This orthogonality is necessary to reduce Hamilton's Integral to a set of uncoupled Lagrange equations. The Lagrange equations determine the time functions necessary to construct the deformation response pattern during a forced vibration.

The truncation of the stress intensity series for both theories rests upon upper limits of natural frequency magnitudes, which are selected on the basis of the precision desired in making the comparison.

1.2 History of Dynamic Analysis of Elastic Cylinders

Several authors have considered the free vibration characteristics of thin shells with various end conditions. In 1894, Rayleigh (1)* found the natural frequencies of a

---

* Numbers in brackets ( ) refer to References

cylindrical shell with free edges, based upon an inextension of the mid-surface. Frequencies for an infinite cylinder were also computed for a pure inextensional and a pure extensional mode. Baron & Bleich (2), adding bending to Rayleigh's extensional energy, applied Rayleigh's Principle to the combined energy to construct a table of natural frequencies for an infinite cylinder. Arnold & Warburton (3) investigated the free vibrations of the simply supported cylinder. Later, (4) using the Rayleigh-Ritz procedure of assuming an axial mode shape, they developed the Lagrange equilibrium equations from a minimization of Hamilton's Integral and computed an approximation to the natural mode frequencies of the clamped cylinder. In both cases, Arnold and Warburton used the classical strain expressions of Love. In 1955, Yu (5) also studied finite cylinders with clamped and simply supported edges, with Donnell's simplified equation. Yu employed an approximation which effectively restricted the minimum permissible wave length.

Recently Forsberg, (7), (8), presented a computational procedure to determine the exact mode shapes and frequencies for any edge conditions, using the classical theory of Flugge. The method was suggested by Flugge in 1934 but awaited the advent of the high speed computer. Warburton (9), used a variation of this procedure, with Flugge's equations, to present the edge condition neglected by Forsberg, but in my opinion used inappropriate stresses at the boundary. Edge conditions do affect natural frequency, as shown by Weingarten (10).

Yu, (6), in 1958 included shear deformation and rotatory inertia (SR) in analyzing the five natural fre-

quency branches for a simply-supported and an infinite cylinder. Other attempts to compute natural frequencies using a non-classical shell theory were made by Herrmann and Mirsky, (12), (13), for an infinite cylinder. The first was for an SR theory of five independent deformation coordinates and the latter for a six variable shell theory, including transverse normal stress (an SRN theory).

Weingarten (11), used a very much simplified classical theory (the Donnell equations with no longitudinal or circumferential inertia) and found that many classical theories (as well as many assumed mode shapes) lead to approximately the same values of natural frequencies.

The literature on the forced vibration problem of shell structures under transient loading is rather meager. Dynamic response of cylinders to an impulsive load has been investigated in a few cases of simplified geometry, using either a membrane theory or a classical bending theory. Payton (14) determined the dynamic membrane stress in an infinite cylinder for a number of radial pressure distributions. Humphreys and Winter (15), using Flugge's bending theory, solved the same problem and compared numerical results with Payton.

Sheng (16), Bushnell (17) and Yao (18) using, respectively, the classical theories of Donnell, Flugge, and again Donnell as equilibrium equations, have solved the response of a simply supported cylinder to a radial impulse. This was accomplished in a closed form solution, using the normal mode method. The complexity of the problem was greatly reduced, as the normal modes are well known as trigonometric functions for a simply-supported structure (19), (3). This condition

applies to infinite cylinders as well. Very recent work done by Reismann and his associates, (62)-(65), has concentrated on the response of simply supported and infinite cylinders under the influence of impulsive radial loads. SR as well as Classical theories were used in the first three of these analyses.

Wah (2) considered the dynamic response of clamped-ended structures, but used Yu's approximation (see 5) after choosing the form of the axial normal mode. Therefore, he accepted, for the forcing function problem, an unproved (and incorrect) normal mode orthogonality.

A numerical solution by finite difference methods for an elastic (small deflection) cylinder by Johnson and Greif (21), was constructed from a classical shell theory (22), assuming first a normal mode solution. Results were indicated for various modal shapes for a clamped-free cylinder with a blast loading. Another numerical program (23) was developed for axisymmetric dynamic loading of an elastic cylinder, from a momentum distribution caused by traveling elastic waves.

Finite difference codes for large deformation, elastic-plastic response have been developed at MIT. An extensive account of the two-dimensional problem (axisymmetric loading) is presented by Witmer, et al, in reference (24). Pian extended the theoretical basis of the method to include the general three-dimensional shell (25). Recently Leech (26) offered the first 3 dimensional shell code, capable of handling large deflections and rotations.

A serious limitation to the numerical approach is in computer storage capability. This necessitates the use of a very coarse space mesh, which in turn restricts the precision of the result.

1.3 Various Shell Theories

Many shell theories have been proposed. The particular ones reviewed here have had considerable engineering application. The methods of developing these theories have been different, but they all rest on the premise that the mid-surface motion of the shell controls the behavior of the structure, and a particular motion is prescribed, either explicitly or implicitly.

Classical Theories

Usually, the dynamic equilibrium for a finite element as thick as the shell is considered. The forces and moments acting upon this element are expressed first in terms of strain and change in curvature of the mid-surface and finally as functions of the mid-surface displacement. For a classical bending theory, where the normals to the median surface of the undeformed shell remain straight and normal to the median surface after deformation, the change in curvatures (rotations) of the mid-surface are directly dependent on the space-derivatives of the translation of the mid-surface. For a membrane theory, where deviations throughout the cross-section are disregarded, the effect of median-surface rotation, with respect to its contribution to this change of deformation throughout the cross-section, at least, is neglected.

Cylinder bending theories, developed following this finite element procedure, that have enjoyed wide usage, are those of Love (27), Timoshenko (28), Flugge (29) and Donnell (30). Love and Flugge make allowances for the trapezoidal shape of two faces of the element in computing the stress resultant. Timoshenko does not. Donnell's

equations are derivable from those of Timoshenko or Flugge, by neglecting the first power of the thickness-mean radius ratio when compared with unity. The Donnell equations are applied most frequently as they can be easily manipulated to give an uncoupled equation in the transverse deformation coordinate and because they are amenable to approximate analytical solutions.

Other bending theories, perhaps more rigorously developed, have been compared by Budiansky and Sanders (31), and were justified for a variety of theoretical considerations. Two of the engineering theories above, Love's first approximation and Timoshenko's, yield unsymmetrical equilibrium equations and are therefore in contradiction to the principle of conservation of energy (32). Their strain energy would not be invariant with a coordinate transformation (33). This implies that the structure was not linearly elastic as assumed, Betti's law being violated (34). The major practical consequence of unsymmetric equilibrium equations is that a series solution of assumed normal mode functions would not be orthogonal and therefore not truly separable for analytical and computational purposes.

Non-Classical Shell Theories

Higher order (non-classical) shell theories have been developed which attempt to include the transverse shear strains and transverse normal stress. Such theories differ from the classical shell theories in that the material normal to the median surface of the undeformed shell no longer remains normal to the median surface after deformation. Shear deformation theories, including the effects of rotary inertia, are called SR theories, while the further inclusion of the

normal stress creates what is termed as SRN theory .

A different approach was necessary to create these theories as the geometry of the deformation is not as evident as in the classical bending theory. In a manner originally proposed by Cauchy and Poisson, and revived by Mindlin (35), the deformation of each particle throughout the thickness was described by a truncated power series for the transverse position coordinate of the shell;

$$u_k(x,\phi,z,t) = \sum_{n=0}^{N} z^n u_k^n(x,\phi,t)$$

where the superscript terms described the motions of the mid-surface. For an SR theory the circumferential and axial coordinates, u_1 and u_2, are linear functions of z. The radial deformation, u_3, is independent of z. This is necessary to define $u_1^{(1)}$ and $u_2^{(1)}$, the rotations of the original normal to the median surface, as functions of the transverse strain.*

Consistent with the displacement of a particle, the three-dimensional stress-motion equilibrium of a particle is studied. The elastic constitutive equations at a point (with appropriate modifications for a transverse shear factor), coupled with exact strain-displacement relationships for curvilinear coordinates, transform the particle equilibrium equations into functions of the mid-surface motion coordinates, $u_k^{(n)}$. An integration of these equilibrium equations over the thickness produces the shell equilibrium equations as a function of these coordinates. Herrmann and Mirsky (36)

---

* As stated before, the classical bending theories use this method implicitly. When the transverse strain is set equal to zero, the dependency of the rotation $u_k^{(1)}$ on the translation of the mid-surface $u_k^{(o)}$ is found.

and Yu (6) developed their shell equilibrium equations in this manner. Herrmann and Mirsky determined their shear factor by studying the free, axi-symmetric motion of an infinite cylinder (36) by the three-dimensional theory of elasticity and comparing their shell theory to this.

Utilizing the true dynamic equilibrium equations at a point is the sufficient condition to satisfy the Virtual Work integral when there is a variation of the equilibrating displacements. Recognizing this, further work in developing shell equations was done, utilizing Hamilton's principle of minimizing the time integral of generalized Lagrange energy. The results should be exactly equivalent, as was checked by Yu (37) and Herrmann and Mirsky (12), as they redeveloped their shell theory equations, using the Hamilton method.* A great advantage of this procedure is that it readily and consistently permits the establishment of the appropriate boundary conditions. A further advantage, is that being developed from an energy basis, for a linear elastic system, the differential equations of motion (the equilibrium equations) possess the symmetry necessary for a series of orthogonal solutions.

Klosner and Levine (38) developed two shear deformation theories starting with Donnell's and Flugge's bending theory by assuming changes in these bending strains consistent with transverse shear deformation and constant radial displacement. The strain energy was constructed and Hamilton's principle applied to develop the shell equilibrium equations.

---

* This is a form of a Rayleigh-Ritz procedure. The actual deformations are approximated by Mindlin's series within the Hamilton integral and the mid-surface coordinates are minimized.

The more complex SRN theories have also been developed using Hamilton's principle and the Mindlin power series deformation. Herrmann and Mirsky (13) proposed a linear power series for all three displacements. Naghdi, (43), applying the variational principle of Reissner (39), used a radial deformation that was a function of mid-surface coordinate terms up until the second power of z. The normal stress was not disregarded and the shear constants were obtained as a natural consequence of the displacement assumptions.

I have used Hamilton's principle to formulate my own shell equations of both the SR type and the classical bending type. These will prove to be the same as equations developed previously by Yu, by different means. This has incorporated a selection of the appropriate Mindlin deformation series (linear in the line-of-curvature coordinates and with only one transverse coordinate). The equilibrium equations in each case will be symmetric. This is a necessary requirement for solving a dynamic problem by the normal mode method. The boundary conditions, taken from within the Hamilton integral, will be consistent for each type of theory.

1.4 Comparison of Shell Theory Solutions - Dynamic & Static Response

The free vibration characteristics of infinite cylinders, analyzed by both the three dimensional theory of elasticity and various shell theories (classical and non-classical) have been investigated and compared. Mindlin (45) investigated flexural wave propagation in an infinite plate and compared the known elasticity solution for the slowest

moving wave for each structural wave length (first branch of the phase velocity spectrum) to solutions found from the membrane theory, a classical bending theory and a non-classical SR theory which used a shear factor, K . All theories gave the same results as the membrane theory for long wave lengths but only the theory accounting for shear deformation could duplicate the elasticity solution (with an adjustment of K as a function of Poisson's ratio) for short wave lengths. If the first mode of thickness-shear vibration is compared, K must have another value. The classical bending theory erroneously predicts wave propagation velocities for short structural wave lengths (high frequency terms).

Mindlin (46) did a similar analysis for axially symmetric flexural vibrations of a circular disk with free boundaries, comparing an SR with a classical theory where the rotary inertia is included. Natural frequencies for all mode shapes were compared. There was a significant difference in the high frequency range, (short structural wave length). The classical bending theory computes higher magnitudes for these frequencies due to the constraint imposed in suppressing shear deformation.

Herrmann and Mirsky (36) developed classical and SR shell equations (beginning with stress-equilibrium at a point and assuming a linear deformation pattern) and extended Mindlin's procedure of comparing first branch flexural wave propagation velocities, in an infinite cylinder with axisymmetric loading. Those computed from these shell theories were compared with the elastic solution. Mindlin's plate conclusions were verified for the cylinder. Interestingly, the effects of shell curvature were negligible for short

structural wavelengths, and Mindlin's plate shear factor, K could be used in the SR theory to produce the elasticity results. The bending theory prediction of wave velocities for these wave lengths were in error, while for long wavelengths the membrane theory was adequate.

Greenspon (40) compared the natural frequencies (associated with wave propagation) of an infinite shell computed from the membrane theory, various classical theories and non-classical SR theories. This was done for a range of structural wave lengths with more than one branch of the frequency spectrum studied. The upper branches contain higher frequencies associated with the same wave length (mode shape). The shear deformation theories were most successful in predicting the elasticity solution for the higher frequencies. Greenspon also found that, for this free vibration case, the deformations for thin shells according to the linear SR theory approached the theory of elasticity solution more successfully than did the classical bending theory. Even the SR deformations became less valid as the shell thickness increased.

Herrmann and Mirsky (12) duplicated the elasticity solution for the first mode frequency of an infinite cylinder, during thickness-shear vibration, with an SR theory, using Mindlin's plate shear factor. In their work (13) with an SRN shell theory the same results were obtained. (The shear factor, though, was slightly different from Mindlin's). In (13), where general vibration frequencies for six branches were obtained for each structural wavelength, and in another work (41), with their SRN theory, but with axi-symmetric vibrations, limitations of the shell theory were uncovered. The higher branches of the short structural wavelength fre-

quencies (extremely high) were not predicted accurately for thick shells. This is partially accounted for by the non-universality of the shear factor, the thickness-shear factor having been developed for a lower first mode frequency.

The forced dynamic response of infinite cylinders has been analyzed (at separate times) using the membrane theory, a classical bending theory, and the SR theory of Herrmann and Mirsky. Spillers (42) used the SR theory to describe the response of a semi-infinite cylinder to an axi-symmetric longitudinal impact at one end. He finds that at times shortly after the impact the deformation and stress could have been adequately described by the membrane theory. This must be due to high wave velocity of long structural wave lengths that are primarily associated with shell compression. At a later time, when the effects of bending and shear deformation (associated with the slower moving waves of short structural wavelengths) are felt, the membrane theory is invalid. Spillers did not differentiate between the effects of bending and shear deformation. Recently, Reismann (65) analyzed an infinite cylinder in plane-strain under the influence of a radially directed concentrated impulse. A membrane, bending, and SR solution were compared. Results similar to Spillers' were obtained for the membrane and SR solution. At times shortly after the impact, though, Flugge's Classical theory predicts a different response than the other two. At a later time, when flexural waves are more significant, the Classical theory response is closer to the SR response. Humphrey and Winter (15) compared their work to Payton (14) to differentiate between the membrane and bending effects on an infinite cylinder in plane strain with radial impulsive loading. They found (29) their stresses, from Flugge's bending theory,

diverged from the membrane solution only after some time.

The membrane-bending, membrane-shear deformation, and bending-SR comparisons in an infinite cylinder during forced impulsive loading, therefore, do exhibit the characteristics found for free vibration wave propagation. As already noted, the free vibration analysis of an infinite cylinder also indicates in exactness (towards the elasticity solution) of the SR theory over the classical bending theory.

This difference in results between these theories has recently been verified for the forced response of a simply supported finite cylinder. Reisman and Padlog (64) used the classical theory of Timoshenko-Love and the SR theory of Herrmann-Mirsky to compute the response of a simply supported cylinder to axisymmetric line loads and moving pressure loads. With the moving pressure load a percentage difference of 34% was noted between the axial moment developed by each theory. This was almost four times the difference noted with the line load and accentuates the effect of short force waves in exciting each model. In a slighty later work in 1968, Medige, Lin, and Reisman (64) extended the comparison with a non-axisymmetric cosine frontal impulse. Flugge's equations were used for the classical model. Moment Resultants and Stresses on the cylinder surface, in both the axial and circumferential direction, differed appreciably in each model for a thicker cylinder. The effect of end conditions in no other finite cylinder in influencing any difference in response had been investigated.*

---

* Bushnell (17) discovered marked differences in radial displacement and frequencies associated with this displacement when comparing a simply-supported and infinite shell response to radial impulse, using a classical theory.

My investigations involve a fixed edge cylinder and a free edge cylinder, and continue this line of research. Differences that have been uncovered are assumed to reinforce the superiority of the SR theory.

This supposition of the superiority of the SR theory is by no means valid a priori if the criterion of comparison is the static response. Klosner and Levine (38) employing 5 shell theories (two classical, two SR, and the SRN theory of Naghdi) have investigated the displacement and stresses produced in an infinite cylinder, according to these theories, by axi-symmetric, periodically spaced radial loads. These results have been compared with the solution of the theory of elasticity. All shell theories predict stress and displacement erroneously in the vicinity of the applied loads. In predicting longitudinal stress and displacement the classical theory gave the best results. In predicting the circumferential stress, the classical theory gave better results than the shear deformation theory and was only inferior in predicting radial displacement. The authors attribute these seemingly surprising results to the particular static load used, which produces large circumferential stresses and constant longitudinal displacement throughout the shell thickness. The shell theories, though, assume a longitudinal displacement varying linearly throughout the thickness. The cross-section rotation coordinate, which accounts for this linear effect, is computed as overly large with the SR theory not suppressing the shear deformation. Iyengar and Yoganda (44) also found the classical shell theories acceptable in predicting deformations and stresses in a semi-infinite shell with a concentrated axi-symmetric line load at one end, especially for thin shells. The deformations and stresses in the vicinity of the concentrated load were in error. They did not investigate a shear-defor-

mation theory in their paper.

1.5 Summary of Analysis

Forced Response of the Finite Elastic, Cylinder

The structural dynamic response of the free cylinder subjected to time dependent mechanical loading will be described by the resulting rigid body motion and the elastic deformation of the structure. The elastic deformation will be expressed in terms of modes of free vibration of the mathematical model chosen to represent the structure. The model will rest upon the choice of elastic parameters, permissible stresses and strains, and most importantly, the choice of displacement coordinates to define the shape of a deformed element within the structure.

Hamilton's Variation Principle

Hamilton's Integral, for an elastic cylinder in motion, is rearranged internally by choosing a set of displacement coordinates (Mindlin's power series, truncated,) [30] * leading to a particular shell theory. Utilizing Hamilton's principle to develop the ordinary differential equations associated with the rigid body motions, the partial differential equations associated with a finite element of the structure, and the natural form of required boundary conditions, mode shapes and oscillation frequencies can be computed to construct a deformation pattern minimizing the Hamilton integral in the absence of external loadings (free vibration.)

---

* bracketed terms refer to subsequent equations

A variation of the propagation times for developing these mode shapes, is the method used to minimize the Integral formed when external loadings are applied. A set of generalized Lagrange equations are developed, as a consequence of this, which will define these required time functions. When the deformation pattern for this forced response is constructed, the stress pattern is, of course, determined.

Variation Technique - The Shell Equation

I have used the conventional variation to develop the three-dimensional, particle equilibrium equations within the time dependent Hamilton integral. In this method, all terms of the Lagrangian energy density are expressed as functions of the particle displacements. These displacements are ultimately varied during the variation of the entire integral. The applicability of this method for a continuous elastic structure was suggested by Love (27), Goldstein (47) and Wang (48). The actual variation technique (perturbation from a solution value) is described by Goldstein and also by Courant and Hilbert (49). Other variation forms have been suggested. Reisner (39) (50) varies displacement and stress independently. Yu has done considerable work (37) (51) (52), extending Washizu's method (53) of varying strain, displacement, and stresses independently, from the static to the dynamic case.

The SR shell equations are formed after making the power series approximation for the particle displacement, applying the variation to the mid-surface motion coordinates, and integrating over the cylinder thickness. The five shell equilibrium equations [53] - [57] as well as the five natural boundary conditions [59] - [60], are developed within Hamilton's integral, as functions of the five mid-surface coordinates, as

a natural consequence of the variation principle. These are identical to Yu's (37) developed by his variational technique and those found when he used the three-dimensional stress-motion equations (6). The consistency of these two models within the same variational integral had not been examined.

The transformation of Hamilton's integral when the rotary inertia is disregarded and the shear factor, K (inversely proportional to shear strain) approaches infinity, i.e.,

$$\text{Lim}_{K\to\infty} \left(\delta \int_{t_o}^{t_1} L\,dt \Big|_{K\to\infty} = 0 \right)$$

results in a classical bending theory. The three equilibrium equations [69] - [71] and the four natural boundary conditions [68] are taken from within Hamilton's integral (see Appendix D).

Free Vibration Solution - Normal Modes, Natural Frequencies

As stated earlier, the only method of obtaining the exact mode shapes and natural frequencies, of a finite cylinder, with end conditions other than simply supported, was presented by Forsberg (7) in 1964. Many procedures are available to obtain approximations to the natural frequencies for a given modal pattern. These are either through approximations to the equilibrium equations (11) (5) or, Warburton's (3) (4) (9), assumed approximation to the mode shapes (the Rayleigh-Ritz procedure) which gives better results. Forsberg's work is invaluable in solving the free vibration problem.

An assumed solution for the mid-surface deformation coordinates, in modal vibration, is made (54):

$$u_k^n = \left(\sum_{i=1}^{8,10} \mathcal{L}_{ki}^n \Gamma_i e^{\lambda_i x}\right)(\cos m\phi \text{ U } \sin m\phi) e^{i\omega t}$$

$K = 1,2,3$
$n = 0,1$

where the series of eight axial functions applies to the classical theory and the series of ten to the SR theory.

Substitution of these expressions into the homogeneous differential equations of equilibrium, after a Donnell-type manipulation, leads to a tenth (or eighth) order algebraic equation for λ_i as function of ω and equations involving the proportionality of $\mathcal{L}_{ki}^{(n)}$. With the boundary conditions specified, the problem is entirely determined. The detailed statement of these conditions leads directly to ten (eight) simultaneous algebraic equations for the ten (eight) unknown constants. These equations involve the roots of $\lambda_i(\omega)$. Since the boundary conditions will be homogeneous, the determinant [84] or [94] of these equations must be zero for a non-trival solution. A computer procedure solves the equilibrium equation and the boundary value determinant simultaneously, for a chosen circumferential wave pattern, m. A trial value of ω is chosen to determine λ_i, and $\mathcal{L}_{ki}^{(n)}$ for the determinant, which must go to zero, if the chosen ω was a true eigenvalue (natural frequency. If not, we iterate by trial increments to find the values of ω which will converge the determinant through zero. Initially, the successive eigenvalues found will be from the lower branch spectrum for axial structural waves of increasing node number (long waves). They should be nearly the same for either shell theory, as the effects of shear deformation are only evident at higher frequencies, i.e., at

shorter structural wavelengths.

Forced Vibrations - Lagrange Equation - Orthogonality of Normal Modes: Comparison of Shell Theories

Once the mode shapes and natural frequencies are determined, the forced vibration problem is solved, within Hamilton's Integral, by a variation of the time function [116], [121], [122]. This is the procedural form of the normal mode method, when Hamilton's principle is applied. The Lagrange equations can be taken from the Hamilton integral in uncoupled form, if the orthogonality of normal modes can be verified.

Kraus and Kalnins (55) demonstrated the appropriateness of a normal mode dynamic solution for a bending theory shell with homogeneous boundary conditions. They need symmetric equilibrium equations to prove orthogonality by a particular Green identity. Tso (56) verified the orthogonality result, using the equilibrium equations and boundary conditions generated from Hamilton's principle, for a classical theory. His proof rests upon homogeneous boundary conditions (leading to a separable (space-time) solution series) and a linear elastic structure, where the strain energy is a symmetric quadratic function of the displacement variables and their space derivatives. Love (27), proves orthogonality for the normal modes of vibration for a structure whose strain energy is a quadratic function of the strain. For his proof, he utilizes the symmetry of the energy expression for this linear elastic system that makes Betti's law valid. I have extended and applied a similar orthogonality proof to both the 3 variable and 5 variable (SR) case. The need for this orthogonality (to uncouple the Lagrange equations) will

manifest itself within Hamilton's integral. The orthogonality, therefore, is also proved within Hamilton's integral.

When the orthogonality proof is completed, the uncoupled Lagrange equations to determine the time coordinate as a function of an arbitrary force input are developed, [128] . The deformation patterns for an impulsive force input are examined, [175] and the resulting stress intensity on the cylinder's surface is computed, [186] [194] . The stress intensity history is recorded for different truncations of the natural frequency bandwidth.

The results of utilizing the bending theory or the shear deformation theory have been compared for various edge conditions, shell geometry, and truncations of the deformation series. Previous dynamic solutions for a finite cylinder have only been attempted for simply-supported edges, where the normal mode functions are known. At the time the proposal for this thesis was presented, this work on simply supported cylinders had only been done with a classical bending theory. Reismann's recent work has considered the response of simply supported cylinders with an SR theory also. No attempt has been made previously to solve any forcing function problem for a free or fixed edge finite cylinder by either a non-classical (SR) or a classical theory. The comparison of the SR solution to a classical bending theory solution, therefore, has not been previously attempted.

SECTION II CO-ORDINATE SYSTEMS

The cylinder has length L, inside radius (a-h) and thickness 2h. It is subjected to an arbitrary pressure $\bar{P}$ on its surfaces. The usual practical case encountered would be that the pressure was exerted only on the outer cylindrical surface, but our analysis is not so restricted. We do require, however, that the body undergo only translation with respect to the inertial axes $\bar{\varepsilon}_1$, $\bar{\varepsilon}_2$, and $\bar{\varepsilon}_3$. (See Figure 1). With this limitation, only certain patterns of surface pressures are permitted.*

A point m in the material is located by means of the vector $\bar{\rho}$ from the center of gravity B. The body fixed triad $\bar{e}_1$, $\bar{e}_2$, $\bar{e}_3$ serves as a reference coordinate system both for the surface pressure $\bar{P}$ and for the subsequent deformation vector $\bar{u}$, locating the displaced particle at m'.

The symbol $\bar{e}_k$ is used to represent any one of the vectors $\bar{e}_1$, $\bar{e}_2$, $\bar{e}_3$, which are seen to retain their orientation with respect to the inertial set $\bar{\varepsilon}$ p.

---

*Note: This particular limitation is not really essential to the analysis, but is chosen for the convenience it affords in presenting the problem clearly. The general desire is to prevent rigid body rotation, so the requirement is that there be no resultant external moment. If, for example, the loads are radially directed, rotation is automatically prevented about the $\bar{\varepsilon}_3$ axis. To avoid rotation about the $\bar{\varepsilon}_2$ axis they must be symmetric with respect to $\phi = 0$, and to prevent rotation about the $\bar{\varepsilon}_1$ axis, symmetric about $x = L/2$.

If there were a rigid body rotation, in the subsequent

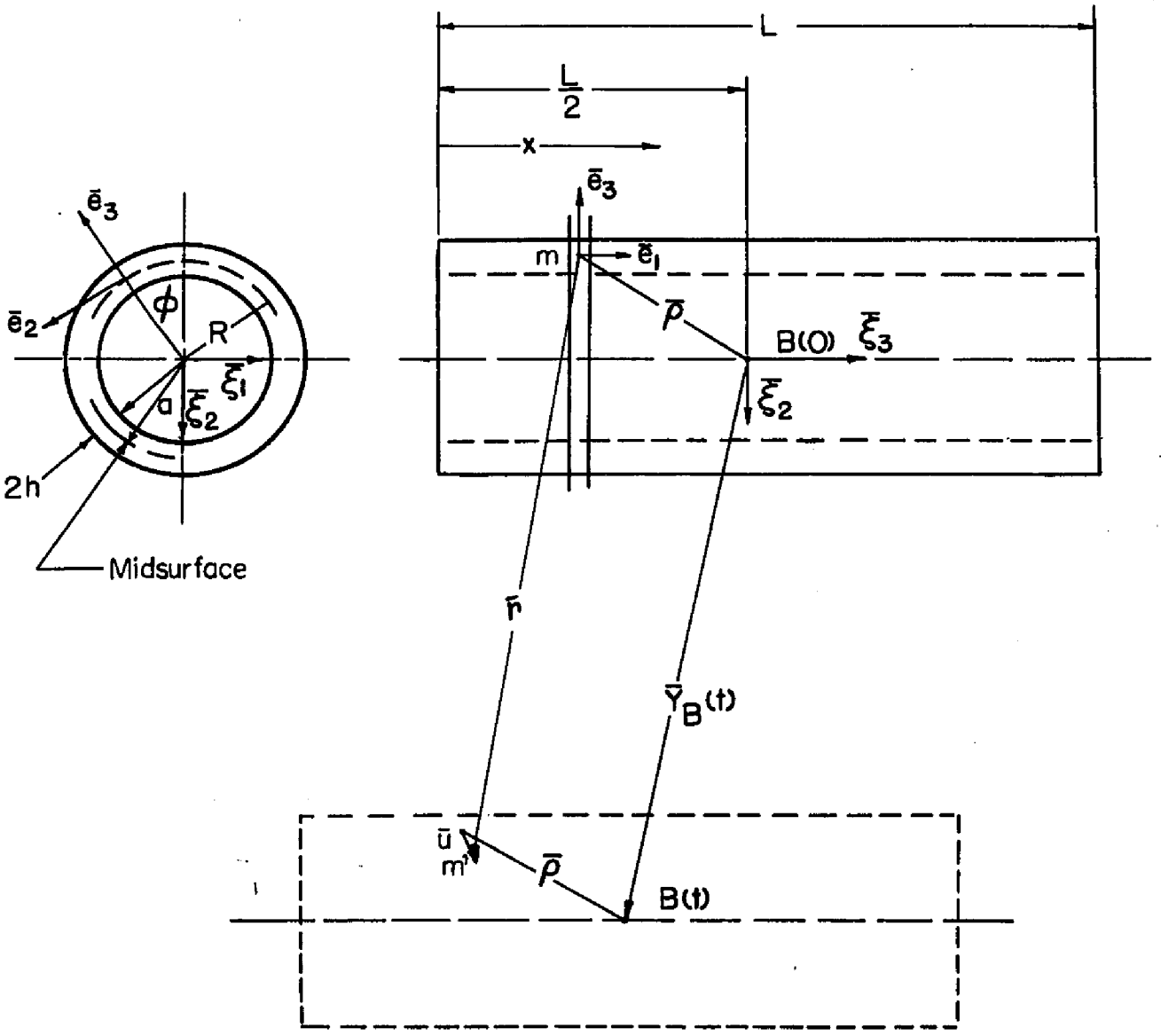

FIGURE 1: CO-ORDINATE SYSTEM

The point m may be visualized also as being located by the coordinates x, ϕ and z. x is taken as the distance from the left end, ϕ as positive counterclockwise from the vertical zero position, and z as the distance from the mid-surface, measured positive radially outward.

When the body has translated, the location of the center of gravity at time t_i is given by $\bar{Y}_B(t)$. The location vector $\bar{\rho}$ is considered not to vary in time. The new position of m is given in inertial space by the vector $\bar{r}$. We may thus write:

$$(1) \qquad \bar{r}(x,\phi,z,t) = \bar{Y}_B(t) + \bar{u}(x,\phi,z,t)$$

We now define the components of $\bar{Y}_B$ along the space-fixed axes as:

$$(2) \qquad Y_B(t)_p = \bar{Y}_B(t) \cdot \bar{e}_p$$

and along the body fixed axes as:

$$(3) \qquad Y_B(t)_k = \bar{Y}_B(t) \cdot \bar{e}_k$$

The components of the deformation coordinate, $\bar{u}$, along the body-fixed axes are:

$$(4) \qquad \bar{u}(x,\phi,z,t) = u_k(x,\phi,z,t)\, \bar{e}_k(\phi)$$

(Continuation of Note on preceding page)

application of Hamilton's principle, terms deriving from the variation of strain energy would not be affected. The variation in Kinetic energy and work would produce additional terms, identifiable as being associated with the rigid body rotation, but otherwise not particularly useful.

Equation (1) now may be written:

$$\bar{r} = \gamma_B(t)_K \bar{e}_K + u_K \bar{e}_K \tag{5}$$

with the right hand terms understood to be in indicial notation.

Differentiating with respect to t,

$$\dot{\bar{r}} = \frac{d}{dt}(\gamma_B)_K \bar{e}_K + \frac{\partial u_K}{\partial t} \bar{e}_K \tag{6}$$

Repeating the $\partial/\partial t$ operation, and employing the conventional dot notation:

$$\ddot{\bar{r}} = (\ddot{\gamma}_B)_K \bar{e}_K + \ddot{u}_K \bar{e}_K \tag{7}$$

Expression (6) will be useful in formulating the system kinetic energy, and equation (7) in understanding the part played by the rigid body motion.

SECTION III DETERMINATION OF STRESS EQUATIONS OF MOTION AND STRESS BOUNDARY CONDITIONS

Hamilton's principle states that the motion of the system from time t_o to the time t_f is such that the line integral I is an extremum for the path of motion:

$$I = \int_{t_o}^{t_f} (T - U + W)\, dt \tag{8}$$

The integral I is defined by equation (8), in which the kinetic energy T is:

$$T = \int_V \frac{1}{2} \gamma \dot{\bar{r}} \cdot \dot{\bar{r}}\, dV \tag{9}$$

The system potential (strain) energy is:

$$U = \int_V \frac{1}{2} \sigma_{ik} \epsilon_{ik}\, dV \tag{10}$$

and the term W is taken as:

(11) $$W = \int_{\Sigma} \bar{P} \cdot \bar{r} \, d\Sigma$$

In equations (9) - (11), we use

γ = density per unit volume

σ_{ik} = stress tensor component

ϵ_{ik} = strain tensor component

dV = unit volume

$d\Sigma$ = unit surface area

and $\bar{P}$, $\bar{r}$ are used as before. Some explanation of these terms is helpful.

The unit volume is defined as:

(12) $$dV = dS_1 dS_2 dS_3$$

where dS_k is the incremental distance along the body-fixed vector $\bar{e}_k$. The origin of the orthogonal body-fixed vector triad $\bar{e}_1$, $\bar{e}_2$, and $\bar{e}_3$ is formally located by the body referenced coordinates λ_1, λ_2, and λ_3. In the particular cylindrical coordinate system of Figure 1;

λ_1	=	x	dS_1	=	1 dx
λ_2	=	ϕ	dS_2	=	R dϕ
λ_3	=	R = a+z	dS_3	=	1 dz

We will find it more convenient; however, to retain a more general symbolism:

(13) $$dS_k = (h \, d\lambda)_k$$

In the form of (13), we can use Hamilton's principle for any orthogonal curvilinear co-ordinate system.

The term $d\Sigma$ requires additional explanation. In equation (11) it is understood that the integration is taken over the entire surface of the body under study. In the actual case, which involves a cylinder, the surface occurs at either end of the cylinder, and on the inner and outer curved surfaces. At these boundaries, $d\Sigma$ has different forms:

Boundary		$d\Sigma$	
$\lambda_1 = x = 0$		$Rd\phi dz$	$= dS_2 dS_3$
$\lambda_1 = x = L$		$Rd\phi dz$	$= dS_2 dS_3$
$\lambda_3 = R = a+h$	$(a+h)$	$d\phi dx$	$= dS_2)^+ dS_1$
$\lambda_3 = R = a-h$	$(a-h)$	$d\phi dx$	$= dS_2)^- dS_1$

The boundary is encountered in the first two cases, by traversing the body in the direction $\bar{e}_1$. In the latter two cases, the boundary is encountered by traversing in the direction $\bar{e}_3$. No boundary exists for a traversal in the direction $\bar{e}_2$.

In each of these cases, the surface $d\Sigma$ could be called $d\Sigma_1$ and $d\Sigma_3$ to reference the direction of traversal. Also, and fortuitously, the elemental surfaces at the actual boundary are normal to the direction of traversal.

In order to preserve the generality of the indicial notation, we do not assume that the surface $d\Sigma$ must lie in a plane normal to a body-fixed coordinate vector. Instead, we take the surface $d\Sigma$ as in figure 2, so oriented that $\bar{n}$ is normal to $d\Sigma$. The projection of $d\Sigma$ on any coordinate plane is found from:

$$(14) \qquad (d\Sigma)\,\bar{n}\cdot\bar{e}_k = dS_i\, dS_j \quad (i \neq j = k)$$

Furthermore, we assign a subscript to $d\Sigma$, e.g., $d\Sigma_k$, to reference the direction traversed in the body to encounter the surface. Thus (in this case) equation (11) should be understood to imply:

$$W = \int_\Sigma \bar{P}\cdot\bar{r}\, d\Sigma_1 + \int_\Sigma \bar{P}\cdot\bar{r}\, d\Sigma_3$$

The stress and strain tensor components σ_{ik} and ϵ_{ik} follow the conventional notation that the first subscript

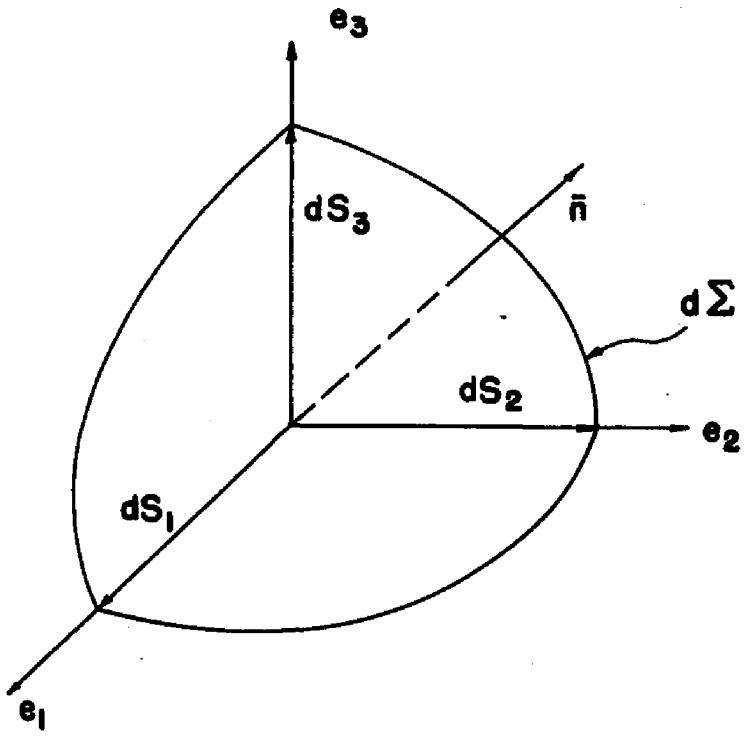

FIGURE 2: BOUNDARY SURFACE AREA $d\Sigma$

indicates the plane on which the stress acts (normal to $\bar{e}_i$) and the second subscript the direction in which it acts.

Now, the extremum requirement on equation (8) is equivalent to :

$$\delta I = 0 \tag{15}$$

Setting L = T - U + W, equation (15) becomes:

$$\delta \int_{t_o}^{t_f} L\,dt = 0 \tag{16}$$

L is known to be a function of the displacement coordinates $Y_B(t)_p$ and u_k (x,ϕ,z,t) as well as of their appropriate space and time derivatives. (See Appendix A for details). Conventionally, u_k and Y_{Bp} are assumed in the form of a minimizing function plus a perturbation function:

$$U_k(X,\Phi,Z,t,\alpha) = (U_k)_{MIN} + \alpha \eta_k(x,\phi,z,t) * \tag{17}$$

$$Y_{Bp}(t,\beta) = (Y_{Bp})_{MIN} + \beta \mathcal{L}_p(t) * \tag{18}$$

The terms η_k and $\mathcal{L}_p$ are the perturbation functions and α and β are the parameters to be varied. The minimum forms $(u_k)_{MIN}$ and $(Y_B)_{MIN}$ are the forms of u_k and Y_{Bp} when α and β are set equal to zero. The perturbation functions η_k and $\mathcal{L}_p$ are required to be zero at t_o and t_f. The variation δI thus requires that:

$$\delta I(\alpha,\beta) = \frac{\partial I}{\partial \alpha}\bigg|_{\alpha=0} d\alpha + \frac{\partial I}{\partial \beta}\bigg|_{\beta=0} d\beta \quad ** \tag{19}$$

---

*See Reference 47

**Bibliography. Reference 48

The application of equation (19) involves differentiation under the integral sign in (8) of the form:

$$(20) \qquad \left(\frac{\partial T}{\partial \dot{u}_k}\right)\left(\frac{\partial \dot{u}_k}{\partial \alpha}\right)\Big|_{\alpha=0} d\alpha \quad \text{or} \quad \left(\frac{\partial U}{\partial \sigma_{ik}}\right)\left(\frac{\partial \sigma_{ik}}{\partial \epsilon_{ik}}\right)\left(\frac{\partial \epsilon_{ik}}{\partial\left(\frac{\partial u_k}{\partial s_i}\right)}\right)\left(\frac{\partial\left(\frac{\partial u_k}{\partial s_i}\right)}{\partial \alpha}\right)\Big|_{\alpha=0} d\alpha$$

so that we must also use the notation:

$$(21) \qquad \delta u_k = \frac{\partial u_k}{\partial \alpha}\Big|_{\alpha=0} d\alpha = \eta_k d\alpha$$

$$(22) \qquad \delta \dot{u}_k = \frac{\partial \dot{u}_k}{\partial \alpha}\Big|_{\alpha=0} d\alpha = \dot{\eta}_k d\alpha = \frac{\partial}{\partial t}(\delta u_k)$$

$$(23) \qquad \delta\left(\frac{\partial u_k}{\partial s_i}\right) = \frac{\partial\left(\frac{\partial u_k}{\partial s_i}\right)}{\partial \alpha}\Big|_{\alpha=0} d\alpha = \frac{\partial\left(\frac{\partial u_k}{\partial \alpha}\right)}{\partial s_i}\Big|_{\alpha=0} = \frac{\partial \eta_k}{\partial s_i} d\alpha = \frac{\partial(\delta u_k)}{\partial s_i}$$

Expression (11) is an artificial form, chosen so that δW will be equal to the virtual work done by the surface tractions $\bar{P}$ during a virtual displacement. Equation (16) becomes:

$$(24) \qquad \delta I = \delta \int_t T dt - \delta \int_t U dt + \delta \int W dt = 0$$

Substituting (9), (10) and (11) in (24):

$$(25) \qquad \int_t \int_V \left[\delta\left(\tfrac{1}{2}\gamma \dot{\bar{r}} \cdot \dot{\bar{r}}\right) - \delta\left(\tfrac{1}{2}\sigma_{ik}\epsilon_{ik}\right)\right] dV dt + \int_t \int_\Sigma \bar{P} \cdot \delta \bar{r}\, d\Sigma dt = 0$$

The actual variation of equation (25) is performed in Appendix A. The result is:

$$(26) \qquad \delta \int_t L dt = \int_t \int_V \left[\frac{\partial \sigma_{ik}}{\partial s_i} + \sigma_{ik}\left(\bar{e}_t \cdot \frac{\partial \bar{e}_i}{\partial s_t}\right) + \sigma_{ti}\left(\bar{e}_k \cdot \frac{\partial \bar{e}_i}{\partial t}\right) - \gamma\left(\ddot{Y}_\beta(t)_k + \ddot{U}_{kl}\right)\delta u_k\right] dV dt$$

$$+ \int_t \int_{\Sigma_i} \left[P_k \delta u_k - \bar{n} \cdot \bar{e}_i \left\{\left(\sigma_{ik}\delta U_k\right)^{\lambda \mu \nu \rho} + \left(\sigma_{ik}\delta U_k\right)^{\lambda \mu \nu \rho}\right\}\right] d\Sigma_i dt$$

$$+ \int_t \left[F(t)_\rho - M\ddot{Y}_\beta(t)_\rho\right] \delta Y_\beta(t)_\rho dt = 0$$

---

* The equations are written to be most accessible for a free-

In equation (26), the first integral provides the stress-motion equilibrium equations for a volumetric element. The second integral prescribes the boundary conditions and the third integral demonstrates the equilibrium equations for rigid body motion.

In the second integral, we interpret the subscript i as being associated with the traversal of the direction $\bar{e}_i$ to encounter a boundary surface element $d\Sigma_i$. The equation requires an evaluation of (σ_{ik} δu_k) at the extreme values of the body referenced coordinate λ_i.

The stress-motion equilibrium equations (without the boundary conditions and rigid-body equations) may be separately obtained by setting the time integral of the virtual work equal to zero:

(27) $$\int W_{VIRT} = \int_t \int_V \bar{F}_{DYN} \cdot \delta \bar{r} \, dV dt = 0$$

(Continuation of Note on preceding page)
body in space. For a constrained cylinder, the deformation (and strain energy) would referred to an inertial reference. As rigid body motion does not contribute to the strain energy of deformation, the Hamilton integral, as developed in Appendix A, would be acceptable for a constrained cylinder. The form of (26) would change:

In the first and second integral on the right hand side:

- δu_k would become δr_k
- $u_k + Y_B(t)_k$ would be r_k, as the c.g. acceleration is absorbed in the deformation coordinate

The third integral would be absorbed. It depends on the unspecified, (for the constrained case), motion of the c.g. of the body.

The stress, σ_{ik}, would be developed as functions of the displacement coordinate, r_k, and its space derivatives.

In the conventional form, using $\tilde{\tau}$ as the stress tensor at a point, and ∇ as the del operator:

(28)

$$\int_t W_{VIRT} = \int_t \int_V (\nabla \cdot \tilde{\tau} - \gamma \ddot{\vec{r}}) \cdot \delta \vec{r} \, dV dt = 0 \qquad *$$

---

* Note: This is shown as follows: $\nabla \cdot \tilde{\tau} = \bar{\delta}_K \frac{\partial ()}{\partial S_K} \cdot \sigma_{ij} \bar{e}_i \bar{e}_j$

in which $\sigma_{ij} \bar{e}_i \bar{e}_j$ is the stress dyad. Carrying out the differentiation:

$$\nabla \cdot \tilde{\tau} = \bar{e}_K \cdot \left[\frac{\partial \sigma_{ij}}{\partial S_K} \bar{e}_i \bar{e}_j + \sigma_{ij} \frac{\partial \bar{e}_i}{\partial S_K} \bar{e}_j + \sigma_{ij} \bar{e}_i \frac{\partial \bar{e}_j}{\partial S_K} \right]$$

continuing

$$\nabla \cdot \tilde{\tau} = \bar{e}_K \cdot \bar{e}_i \frac{\partial \sigma_{ij}}{\partial S_K} \bar{e}_j + (\bar{e}_K \cdot \frac{\partial \bar{e}_i}{\partial S_K}) \sigma_{ij} \bar{e}_j + (\bar{e}_K \cdot \bar{e}_i) \sigma_{ij} \frac{\partial \bar{e}_j}{\partial S_K}$$

Using the Kronecker delta:

$$\nabla \cdot \tilde{\tau} = \delta_{Ki} \frac{\partial \sigma_{ij}}{\partial S_K} \bar{e}_j + (\bar{e}_K \cdot \frac{\partial \bar{e}_i}{\partial S_K}) \sigma_{ij} \bar{e}_j + (\delta_{Ki}) \sigma_{ij} \frac{\partial \bar{e}_j}{\partial S_K}$$

or, contracting the first and third terms:

$$\nabla \cdot \tilde{\tau} = \frac{\partial \sigma_{Kj}}{\partial S_K} \bar{e}_j + (\bar{e}_K \cdot \frac{\partial \bar{e}_i}{\partial S_K}) \sigma_{ij} \bar{e}_j + \sigma_{Kj} \frac{\partial \bar{e}_j}{\partial S_K}$$

We now make use of the idemfactor $I = \delta_{tn} \bar{e}_t \bar{e}_n$ which has the property $I \cdot \bar{e}_1 = \bar{e}_1$

$$\sigma_{Kj} \delta_{tM} \bar{e}_t \bar{e}_M \cdot \frac{\partial \bar{e}_j}{\partial S_K} = \sigma_{Kj} \delta_{tM} \bar{e}_t (\bar{e}_m \cdot \frac{\partial \bar{e}_j}{\partial S_K})$$

$$= \sigma_{Kj} \bar{e}_M (e_m \cdot \frac{\partial \bar{e}_j}{\partial S_K})$$

Replace m by t and interchange j and t to find

$$= \sigma_{Kt} \bar{e}_j (\bar{e}_j \cdot \frac{\partial \bar{e}_t}{\partial S_K}) = \sigma_{Kt} \bar{e}_j \cdot \frac{\partial \bar{e}_t}{\partial S_K} \bar{e}_j$$

Return to the expression for $\nabla \cdot \tilde{\tau}$ to find:

$$\nabla \cdot \tilde{\tau} = \frac{\partial \sigma_{Kj}}{\partial S_K} \bar{e}_j + (\bar{e}_K \cdot \frac{\partial \bar{e}_i}{\partial S_K}) \sigma_{ij} \bar{e}_j + \sigma_{Kt} \bar{e}_j \cdot \frac{\partial \bar{e}_t}{\partial S_K} \bar{e}_j$$

Replacing the index j by k, k by t and t by i:

$$\nabla \cdot \tilde{\tau} = \left[\frac{\partial \sigma_{tk}}{\partial S_t} + \bar{e}_t \cdot \frac{\partial \bar{e}_i}{\partial S_t} \sigma_{ik} + \sigma_{ti} \bar{e}_k \cdot \frac{\partial \bar{e}_i}{\partial S_t} \right] \bar{e}_k$$

In the first expression replace t by i, and note that $\sigma_{ti} = \sigma_{it}$ to obtain

$$\nabla\cdot\tilde{\tau} = \left[\frac{\partial\sigma_{ik}}{\partial s_i} + \tilde{e}_t\cdot\frac{\partial e_i}{\partial s_t}\,\sigma_{ik} + \sigma_{ti}\,\tilde{e}_k\cdot\frac{\partial e_i}{\partial s_t}\right]\tilde{e}_k = (\nabla\cdot\tilde{\tau})_k\,\tilde{e}_k$$

The balance of the proof follows readily from the definition of $\bar{r}$.

SECTION IV THE TWO-DIMENSIONAL THEORY - THE "SR" THEORY

The next step is to isolate the z dependence of the deformation coordinate u_k (x,ϕ,z,t), and to integrate equation (26) with respect to z over the thickness of the cylinder.

This will result in stress-motion equilibrium equations in terms of shell variables, i.e., as functions of x and ϕ, where the point x,ϕ is a location on the cylinder mid-surface. This is then a two-dimensional theory.

The first step is to assume that the deformation coordinate u_k can be expanded in the form:

(29)
$$U_k(X,\Phi,Z,t) = \sum_{n=0}^{\infty} U_k^{(n)}(x,\phi,t)\,Z^n \qquad *$$

where the superscript (n) indicates a mid-surface property. Several prior investigators have found it appropriate to truncate this series as follows:

(30)
$$\begin{aligned} U_1(X,\Phi,Z,t) &= U_1^{\circ}(x,\phi,t) + Z\,U_1^{1}(x,\phi,t) \\ U_2(X,\Phi,Z,t) &= U_2^{\circ}(x,\phi,t) + Z\,U_2^{1}(X,\phi,t) \\ U_3(X,\Phi,Z,t) &= U_3^{\circ}(x,\phi,t) \end{aligned} \qquad **$$

---

* See Reference 35

** For a constrained cylinder, with inertially referenced deformation, the following condition holds:

$$u_k + Y_{B',k} = r_k$$
$$u_k^{\,o} + z u_k^{\,1} + Y_{B',k} = r_k^{\,o} + z r_k^{\,1}$$
$$(u_k^{\,o} + Y_{B',k}) + z\,(u_k^{\,1}) = r_k^{\,o} + z\,(r_k^{\,1})$$

In equations (30), the superscript 0 refers to a mid-surface deformation and the superscript 1 to a mid-surface rotation.

Since we require arbitrary variations in δu_k, it is necessary to develop equivalent expressions involving $\delta u_k{}^0$ and $\delta u_k{}^1$. This is done as follows:

We have taken (see equation 17, repeated below for convenience):

$$(17) \qquad u_k(x,\phi,z,t,\alpha) = u_k(x,\phi,z,t,0)_{MIN} + \alpha \eta_k(x,\phi,z,t)$$

With the assumed z dependence:

$$(31) \qquad u_k(x,\phi,z,t,\alpha) = u_k^{\circ}(x,\phi,t,\alpha) + z u_k'(x,\phi,t,\alpha_k)$$

Now, if the variations of $u_k{}^0$ and $u_k{}^1$ are similarly defined:

$$(32) \qquad u_k^{\circ}(x,\phi,t,\alpha) = u_k^{\circ}(x,\phi,t,0)_{MIN} + \alpha \eta_k^{\circ}(x,\phi,t)$$

$$(33) \qquad u_k'(x,\phi,t,\alpha) = u_k'(x,\phi,t,0)_{MIN} + \alpha \eta_k'(x,\phi,t)$$

We note that η_k^n (x,ϕ,t) are zero at t_o and t_f, but are arbitrary at other times.

(Continuation of Note on preceding page)

The deformation for constrained cylinder is a function of the inertially referenced, mid-surface motion, r_k^n.

Since any variation is still defined as:

(34) $$\left.\frac{\partial(\ )}{\partial\alpha}\right|_{\alpha=0} d\alpha + \left.\frac{\partial(\ )}{\partial\dot{\phi}}\right|_{\dot{\phi}=0} d\dot{\phi}$$

We operate on (32) and (33) to yield:

(35) $$\delta U_k^\circ = \eta_k^\circ(X,\Phi,t)\,d\alpha$$
$$\delta U_k^1 = \eta_k^1(X,\Phi,t)\,d\alpha$$

Since:

(36) $$U_k(X,\Phi,Z,t,\alpha) = \left[U_k^\circ(X,\Phi,t,0) + Z U_k^1(X,\Phi,t,0)\right] + \alpha\left[\eta_k^\circ(X,\Phi,t) + Z\eta_k^1(X,\Phi,t)\right]$$

it becomes apparent that

(37) $$\delta U_k = \delta U_k^\circ + Z\,\delta U_k^1$$

We also require the volume element, which for cylindrical coordinates becomes:

(38) $$dV = (a+Z)\,d\Phi\,dX\,dZ = \left(1+\frac{Z}{a}\right) a\,d\Phi\,dX\,dZ$$

As has been explained, the boundary conditions may be related to several surfaces. We employ the table developed in section II to denote the proper forms of $d\Sigma_i$.

Using (37), (38) and $d\Sigma_i$ as needed, equation (26) becomes:

(39)
$$0 = \int_t\int_x\int_\phi \Big[\int_{-h}^{+h} \Big\{\frac{\partial \sigma_{ik}}{\partial s_k} + \sigma_{ik}\Big(\bar{e}_t \cdot \frac{\partial \bar{e}_i}{\partial s_t}\Big) + \sigma_{ti}\Big(\bar{e}_k \cdot \frac{\partial \bar{e}_i}{\partial s_t}\Big) - \gamma\big(\ddot{Y}_{Bk} + \ddot{u}_k^\circ + z\,\ddot{u}_k'\big)\Big\}\big\{\delta u_k^\circ + z\,\delta u_k'\big\}\Big(1+\frac{z}{a}\Big)dz\Big] a\,d\phi\,dx\,dt$$

$$+\int_t\int_x\int_\phi \big(P_k - \sigma_{ik}\,\bar{e}_3\cdot\bar{e}_i\big)_{z=h}\big(\delta u_k^\circ + h\,u_k'\big)(a+h)\,d\phi\,dx\,dt$$

$$+\int_t\int_x\int_\phi \big(P_k + \sigma_{ik}\,\bar{e}_3\cdot\bar{e}_i\big)_{z=-h}\big(\delta u_k^\circ - h\,u_k'\big)(a-h)\,d\phi\,dx\,dt$$

$$+\int_t\int_\phi \Big[\int_{-h}^{+h}\big\{P_k + \sigma_{ik}\,\bar{e}_1\cdot\bar{e}_i\big\}_{x=0}\big\{\delta u_k^\circ + z\,\delta u_k'\big\}_{x=0}\Big(1+\frac{z}{a}\Big)dz\Big] a\,d\phi\,dt$$

$$+\int_t\int_\phi \Big[\int_{-h}^{h}\big\{P_k - \sigma_{ik}\,\bar{e}_1\cdot\bar{e}_i\big\}_{x=L}\big\{\delta u_k^\circ + z\,\delta u_k'\big\}_{x=L}\Big(1+\frac{z}{a}\Big)dz\Big] a\,d\phi\,dt$$

$$+\int_t\big\{F_p(t) - M\ddot{Y}(t)_p\big\}\,\delta Y_B(t)_p\,dt$$

The detailed treatment of equation (39) is given in Appendix B. It is necessary, on a term by term basis, to assign the values 1, 2 and 3 to the index k, as well as to completely evaluate such terms as $\bar{e}_k \cdot \frac{\partial \bar{e}_i}{\partial s_t}$ For a better understanding of the form of the results, we consider equations (39) on a term by term basis.

The first part requires that:

(40)
$$0 = \int_t\int_x\int_\phi \Big[\int_{-h}^{+h} \Big\{\frac{\partial \sigma_{ik}}{\partial s_i} + \sigma_{ik}\Big(\bar{e}_t \cdot \frac{\partial \bar{e}_i}{\partial s_t}\Big) + \sigma_{ti}\Big(\bar{e}_k \cdot \frac{\partial \bar{e}_i}{\partial s_t}\Big) - \gamma\big(\ddot{Y}_{Bk} + \ddot{u}_k^\circ + z\,\ddot{u}_k'\big)\Big\}\big(\delta u_k^\circ + z\,\delta u_k'\big)\Big(1+\frac{z}{a}\Big)dz\Big] a\,d\phi\,dx\,dt$$

Manipulation of equation (40) results in the following equation assembled from terms developed in Appendix B:

(41)

$$\int_t\int_x\int_\phi \Big[\Big\{\int_{-h}^{h}\Big[\frac{\partial\sigma_{11}}{\partial s_1}+\frac{\partial\sigma_{21}}{\partial s_2}+\frac{\partial\sigma_{31}}{\partial s_3}+\frac{1}{a+z}\sigma_{31}-\gamma(\ddot{Y}_{B_1}+\ddot{u}_1^\circ+z\ddot{u}_1')\Big](\frac{a+z}{a})\,dz\Big\}\delta u_1^\circ$$

$$+\Big\{\int_{-h}^{h}\Big[\frac{\partial\sigma_{11}}{\partial s_1}+\frac{\partial\sigma_{21}}{\partial s_2}+\frac{\partial\sigma_{31}}{\partial s_3}+\frac{1}{a+z}\sigma_{31}-\gamma(\ddot{Y}_{B_1}+\ddot{u}_1^\circ+z\ddot{u}_1')\Big]z(1+\frac{z}{a})\,dz\Big\}\delta u_1'$$

$$+\Big\{\int_{-h}^{h}\Big[\frac{\partial\sigma_{12}}{\partial s_1}+\frac{\partial\sigma_{22}}{\partial s_2}+\frac{\partial\sigma_{32}}{\partial s_3}+\frac{\sigma_{32}}{a+z}+\frac{\sigma_{23}}{a+z}-\gamma(\ddot{Y}_{B_2}+\ddot{u}_2^\circ+z\ddot{u}_2')\Big](1+\frac{z}{a})\,dz\Big\}\delta u_2^\circ$$

$$+\Big\{\int_{-h}^{h}\Big[\frac{\partial\sigma_{12}}{\partial s_1}+\frac{\partial\sigma_{22}}{\partial s_2}+\frac{\partial\sigma_{32}}{\partial s_3}+\frac{\sigma_{32}}{a+z}+\frac{\sigma_{23}}{a+z}-\gamma(\ddot{Y}_{B_2}+\ddot{u}_2^\circ+z\ddot{u}_2')\Big]z(1+\frac{z}{a})\,dz\Big\}\delta u_2'$$

$$+\Big\{\int_{-h}^{h}\Big[\frac{\partial\sigma_{13}}{\partial s_1}+\frac{\partial\sigma_{23}}{\partial s_2}+\frac{\partial\sigma_{33}}{\partial s_3}+\frac{\sigma_{33}-\sigma_{22}}{a+z}-\gamma(\ddot{Y}_{B_3}+\ddot{u}_3^\circ)\Big](1+\frac{z}{a})\,dz\Big\}\delta u_3^\circ\Big]a\,d\phi\,dx\,dt\equiv 0$$

Equation (41) is thus seen to contain in itself a series of five terms, which add up to zero because this is implicit in the independence of the terms in (39)'. In addition, each term in equation (41) is multiplied by an arbitrary integrating term, of the form δu_k^n. Therefore, each one of the $\{\ \}$ terms, after integrating must equal zero. This result is obtained in Appendix B and summarized below.

(42)

$$\int_t\int_x\int_\phi \Big[\Big\{\frac{\partial\sigma_{11}^\circ}{\partial x}+\frac{1}{a}\frac{\partial\sigma_{21}^\circ}{\partial\phi}+P_1^+(1+\frac{h}{a})-2\gamma h\ddot{Y}_B(t)\cdot\bar{e}_1-2\gamma h\ddot{u}_1^\circ-\frac{2\gamma h^3}{3a}\ddot{u}_1'\Big\}\delta u_1^\circ$$

$$+\Big\{\frac{\partial\sigma_{11}'}{\partial x}+\frac{1}{a}\frac{\partial\sigma_{21}'}{\partial\phi}+P_1^+(h)(1+\frac{h}{a})-\sigma_{13}^\circ-\frac{2\gamma h^3}{3a}\ddot{Y}_B(t)\cdot\bar{e}_1-\frac{2\gamma h^3}{3a}\ddot{u}_1^\circ-\frac{2\gamma h^3}{3}\ddot{u}_1'\Big\}\delta u_1'$$

$$+\Big\{\frac{\partial\sigma_{12}^\circ}{\partial x}+\frac{1}{a}\frac{\partial\sigma_{22}^\circ}{\partial\phi}+\frac{\sigma_{23}^\circ}{a}+P_2^+(1+\frac{h}{a})-2\gamma h\ddot{Y}_B(t)\cdot\bar{e}_2-2\gamma h\ddot{u}_2^\circ-\frac{2\gamma h^3}{3a}\ddot{u}_2'\Big\}\delta u_2^\circ$$

$$+\Big\{\frac{\partial\sigma_{12}'}{\partial x}+\frac{1}{a}\frac{\partial\sigma_{22}'}{\partial\phi}+P_2^+(1+\frac{h}{a})h-\sigma_{23}^\circ-\frac{2\gamma h^3}{3a}\ddot{Y}(t)\cdot\bar{e}_2-\frac{2\gamma h^3}{3a}\ddot{u}_2^\circ-\frac{2\gamma h^3}{3}\ddot{u}_2'\Big\}\delta u_2'$$

$$+\Big\{\frac{\partial\sigma_{13}^\circ}{\partial x}+\frac{1}{a}\frac{\partial\sigma_{23}^\circ}{\partial\phi}-\frac{\sigma_{33}^\circ}{a}+P_3^+(1+\frac{h}{a})-2\gamma h\ddot{Y}_B(t)\cdot\bar{e}_3-2\gamma h\ddot{u}_3^\circ\Big\}\delta u_3^\circ\Big]a\,d\phi\,dx\,dt$$

$$\equiv 0$$

In equation (42), it is to be understood that there is no surface traction on the inside of the cylinder. The terms

P_1^+, P_2^+ and P_3^+ represent the surface tractions on the outside of the cylinder. The meaning of such terms as σ_{11}^0, σ_{11}^1, etc. is shown on Figure 3. Generally speaking, the superscript 0 refers to a force resultant, and the superscript 1 to a moment resultant. The first index designates the plane on which the resultant acts, and the second index the direction in which it acts. Stress resultants are to be taken as "per unit length" of surface on which they act.

These equations may be more familiar if the notations for stress resultants N and Q, and moment resultants M, as discussed in Appendix B, are employed:

(43)

$$\int_t \int_x \int_\phi \Big[\Big\{ \frac{\partial N_x}{\partial x} + \frac{1}{a}\frac{\partial N_{\phi x}}{\partial \phi} + P_1^+\Big(1+\frac{h}{a}\Big) - 2\gamma h\Big(\ddot{Y}_s(t)\cdot\bar{e}_1 + \ddot{u}_1^0 + \frac{h^2}{2a}\ddot{u}_1^1\Big)\Big\}\delta u_1^0$$

$$+ \Big\{ \frac{\partial M_x}{\partial x} + \frac{1}{a}\frac{\partial M_{\phi x}}{\partial \phi} - Q_x + P_1^+\Big(1+\frac{h}{a}\Big)h - \frac{2\gamma h^3}{3}\Big(\frac{\ddot{Y}_s(t)\cdot\bar{e}_1 + \ddot{u}_1^0}{a} + \ddot{u}_1^1\Big)\Big\}\delta u_1^1$$

$$+ \Big\{ \frac{\partial N_{x\phi}}{\partial x} + \frac{1}{a}\frac{\partial N_\phi}{\partial \phi} + Q_\phi + P_2^+\Big(1+\frac{h}{a}\Big) - 2\gamma h\Big(\ddot{Y}_s(t)\cdot\bar{e}_2 + \ddot{u}_2^0 + \frac{h^2}{3a}\ddot{u}_2^1\Big)\Big\}\delta u_2^0$$

$$+ \Big\{ \frac{\partial M_{x\phi}}{\partial x} + \frac{1}{a}\frac{\partial M_\phi}{\partial \phi} - Q_\phi + P_2^+\Big(1+\frac{h}{a}\Big)h - \frac{2\gamma h^3}{3}\Big(\frac{\ddot{Y}_s(t)\cdot\bar{e}_2 + \ddot{u}_2^0}{a} + \ddot{u}_2^1\Big)\Big\}\delta u_2^1$$

$$+ \Big\{ \frac{\partial Q_x}{\partial x} + \frac{1}{a}\frac{\partial Q_\phi}{\partial \phi} - \frac{N_\phi}{a} + P_3^+\Big(1+\frac{h}{a}\Big) - 2\gamma h\Big(\ddot{Y}_s(t)\cdot\bar{e}_3 + \ddot{u}_3^0\Big)\Big\}\delta u_3^0 \Big] a\,d\phi\,dx\,dt$$

$$\equiv 0$$

In equations 42, 43, u_k^0 represent the second derivative (with respect to time) of the mid-surface deformation and u_k^1 represent the second derivative (with respect to time) of the mid-surface rotations.

We note that equation 42 (or, alternately, 43) in general forms a series

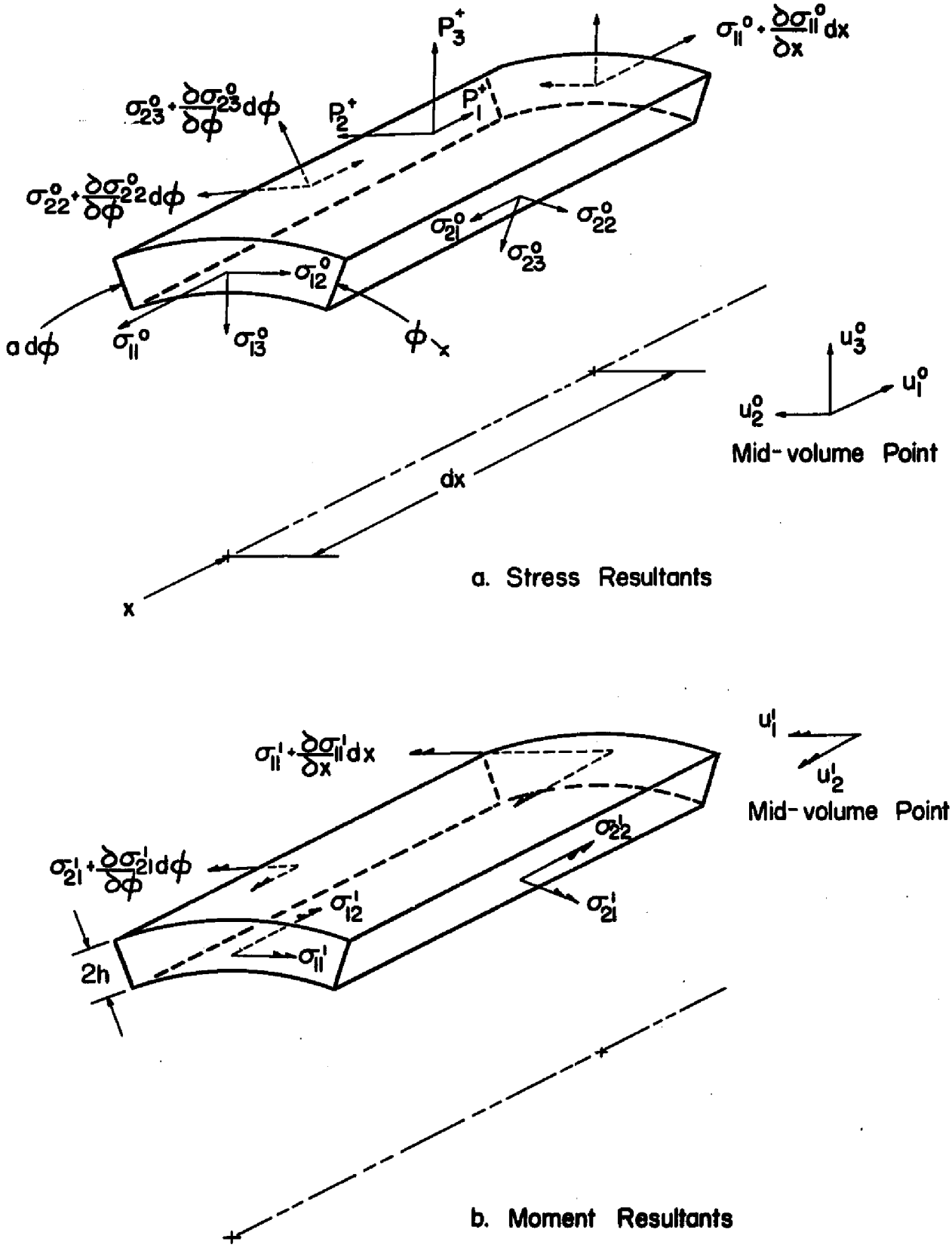

FIGURE 3: STRESS AND MOMENT RESULTANTS ON CYLINDRICAL ELEMENT

(44)

$$\iiint_{t\,x\,\phi} \Psi_k^n \delta U_k^n \, a\, d\Phi\, dx\, dt \equiv 0$$

in which k = 1,2,3 and n = 0,1. (There is no term corresponding to δu_3^1.) Since, in general $\delta u_k^n \neq 0$, this requires that the individual terms $\Psi_k^n \equiv 0$ identically. The set of five equations that results is known as the group of "forced dynamic equilibrium equations".

Returning to equation (39), the second, third, fourth and fifth integrals refer to the boundary conditions at the following boundaries:

At	z = h	Outer Cylindrical Surface
At	z = -h	Inner Cylindrical Surface
At	x = 0	Left end
At	x = L	Right end

The results are found in Appendix B, and the end products summarized below:

<u>At z = h</u>

(45)

$$\iiint_{t\,x\,\phi} \Big[(P_1^+ - \sigma_{31})_{z=h} (\delta U_1^o) + (P_1^+ - \sigma_{31})_{z=h} (\delta U_1' * h) + (P_2^+ - \sigma_{32})_{z=h} (\delta U_2^o) + (P_1^+ - \sigma_{32})_{z=h} (\delta U_2' * h) + (P_3^+ - \sigma_{33})_{z=h} (\delta U_3^o) \Big] (a+h)\, d\phi\, dx\, dt$$

At z = -h

(46)

$$\int_t\int_x\int_\phi \Big[-(P_1^- - \sigma_{31})_{z=-h}(\delta u_1^\circ) + (P_1^- + \sigma_{31})_{z=-h}(\delta u_1' * h) + (P_2^- + \sigma_{32})_{z=-h}(\delta u_2^\circ) + (P_2^- + \sigma_{32})_{z=-h}(\delta u_2' * h) + (P_3^- + \sigma_{33})_{z=-h}(\delta u_3^\circ)\Big](a-h)\, d\phi\, dx\, dt$$

At x = 0

(47)

$$\int_t\int_\phi \Big[\{\sigma_{11}^\circ + \int_{-h}^{h} P_1(1+\tfrac{z}{a})dz\}_{x=0}(\delta u_1^\circ)_{x=0} + \{\sigma_{11}' + \int_{-h}^{h} P_1(1+\tfrac{z}{a})z\,dz\}_{x=0}(\delta u_1')_{x=0} + \{\sigma_{12}^\circ + \int_{-h}^{h} P_2(1+\tfrac{z}{a})dz\}_{x=0}(\delta u_2^\circ)_{x=0} + \{\sigma_{12}' + \int_{-h}^{h} P_2(1+\tfrac{z}{a})z\,dz\}_{x=0}(\delta u_2')_{x=0} + \{\sigma_{13}' + \int_{-h}^{h} P_3(1+\tfrac{z}{a})dz\}_{x=0}(\delta u_3^\circ)_{x=0}\Big] a\, d\phi\, dt = 0$$

At x = L

(48)

$$\int_t\int_\phi \Big[\{\sigma_{11}^{\circ} - \int_{-h}^{h} P_1\left(1+\frac{z}{a}\right) dz\}_{x=L} (\delta u_1^{\circ})_{x=L}$$

$$+ \{\sigma_{11}^{1} - \int_{-h}^{h} P_1\left(1+\frac{z}{a}\right) z\, dz\}_{x=L} (\delta u_1^{1})_{x=L}$$

$$+ \{\sigma_{12}^{\circ} - \int_{-h}^{h} P_2\left(1+\frac{z}{a}\right) dz\}_{x=L} (\delta u_2^{\circ})_{x=L}$$

$$+ \{\sigma_{12}^{1} - \int_{-h}^{h} P_2\left(1+\frac{z}{a}\right) z\, dz\}_{x=L} (\delta u_2^{1})_{x=L}$$

$$+ \{\sigma_{13}^{\circ} - \int_{-h}^{h} P_3\left(1+\frac{z}{a}\right) dz\}_{x=L} (\delta u_3^{\circ})_{x=L}\Big] a\, d\phi\, dt = 0$$

In the boundary condition equations (45 - 48) the quantities P_k refer to the external surface tractions at the boundary and the σ_{ik}^{n} to the stress resultants at the boundary. Equations (45) and (46) are of the form:

(49)

$$\int_t\int_x\int_\phi \bar{\Phi}_k^n \delta u_k^n (a+h)\, d\phi\, dx\, dt \equiv 0$$

while equations (47) and (48) are of the form:

(50)

$$\int_t\int_\phi \Omega_k^n \delta u_k^n a\, d\phi\, dt \equiv 0$$

There are only two ways of satisfying equations (49) and (50). Either the $\delta u_k^n \neq 0$, in which case $\bar{\Phi}_k^n = 0$ and $\Omega_k^n = 0$, or alternately, the $\delta u_k^n = 0$. This prescription will later be considered in more detail.

Finally, the last term in equation (39), in this form, clearly demonstrates that Newton's second law must also hold for the entire body. The requirement is stated:

(51) $$F_p(t) - M\ddot{Y}_B(t)_p \equiv 0$$

This fact, too, will be useful in our later development.

SECTION V
EQUATIONS IN TERMS OF DEFORMATION COORDINATES

The next step is the transformation of the stress-motion equations into a similar set involving deformation displacement coordinates. This work is done in Appendix C.

For the equilibrium equation 42, the result becomes:

(52) $$\int_t \int_x \int_\phi \equiv^n_\kappa \delta u^n_\kappa \, a \, d\phi \, dx \, dt \equiv 0$$

where the individual values $(\equiv)^n_k$ are, $(\delta u^n_k \neq 0)$:

(53)
$$\equiv^\circ_i = \frac{2Eh}{1-\nu^2}\left\{\frac{\partial^2 u_i^\circ}{\partial x^2} + \frac{1-\nu}{2a^2}\frac{\partial^2 u_i^\circ}{\partial \phi^2} + \frac{1+\nu}{2a}\frac{\partial^2 u_2^\circ}{\partial x \partial \phi} + \frac{\nu}{a}\frac{\partial u_3^\circ}{\partial x}\right.$$
$$\left. + k a\left[\frac{\partial^2 u_i'}{\partial x^2} - \frac{(1-\nu)}{2a^2}\frac{\partial^2 u_i'}{\partial \phi^2}\right]\right\} + P_i^+\left(1+\frac{h}{a}\right)$$
$$- 2\gamma h \ddot{Y}_B(t)\cdot \bar{e}_i - 2\gamma h \frac{\partial^2 u_i^\circ}{\partial t^2} - \frac{2\gamma h^3}{3a}\frac{\partial^2 u_i'}{\partial t^2} = 0$$

Note: In equations 53-60, replace u^n_k by r^n_k if dealing with an unconstrained cylinder.

(54)

$$\equiv_1' = \frac{2Eh^3}{3a(1-\nu^2)}\left\{\frac{\partial^2 u_1^\circ}{\partial x^2} - \frac{(1-\nu)}{2a^2}\frac{\partial^2 u_1^\circ}{\partial \phi^2} + a\frac{\partial^2 u_3'}{\partial x^2} + \frac{1-\nu}{2a}\frac{\partial^2 u_3'}{\partial \phi^2}\right.$$

$$\left. + \frac{1+\nu}{2}\frac{\partial^2 u_2'}{\partial x \partial \phi} - \frac{K}{ka}\left(u_1' + \frac{\partial u_3^\circ}{\partial x}\right)\right\} + P_1^+ h\left(1+\frac{h}{a}\right)$$

$$- \frac{2\gamma h^3}{3a}\ddot{Y}_B(t)\cdot\bar{e}_1 - \frac{2\gamma h^3}{3}\left(\frac{\partial^2 u_1^\circ}{a\,\partial t_1^2} + \frac{\partial^2 u_1'}{\partial t_1^2}\right) = 0$$

(55)

$$\equiv_2^\circ = \frac{2Eh}{1-\nu^2}\left\{\frac{(1+\nu)}{2a}\frac{\partial^2 u_2^\circ}{\partial x \partial \phi} + \frac{(1-\nu)}{2}\frac{\partial^2 u_2^\circ}{\partial x^2} + \frac{1}{a^2}\frac{\partial^2 u_2^\circ}{\partial \phi^2} + \frac{1}{a^2}\frac{\partial u_3^\circ}{\partial \phi}\right.$$

$$\left. + ka\left[\frac{(1-\nu)}{2}\frac{\partial^2 u_2'}{\partial x^2} - \frac{1}{a^2}\frac{\partial^2 u_2'}{\partial \phi^2}\right] - K\left[\frac{u_2^\circ}{a^2} - \frac{1}{a^2}\frac{\partial u_3^\circ}{\partial \phi} - \frac{u_2'}{a}\right]\right\}$$

$$+ P_2^+\left(1+\frac{h}{a}\right) - 2\gamma h\ddot{Y}_B(t)\cdot\bar{e}_2 - \frac{2\gamma h^3}{3a}\frac{\partial^2 u_2'}{\partial t_1^2} - 2\gamma h\frac{\partial^2 u_2^\circ}{\partial t_2^2} = 0$$

(56)

$$\equiv_2' = \frac{2Eh^3}{3a(1-\nu^2)}\left\{\frac{(1-\nu)}{2}\frac{\partial^2 u_2^\circ}{\partial x^2} - \frac{\partial^2 u_2^\circ}{a^2\partial\phi^2} - \frac{1}{a^2}\frac{\partial u_3^\circ}{\partial \phi} + \frac{(1+\nu)}{2}\frac{\partial^2 u_1'}{\partial x \partial \phi}\right.$$

$$\left. + \left(\frac{(1-\nu)}{2}\right)a\frac{\partial^2 u_2'}{\partial x^2} + \frac{1}{a}\frac{\partial^2 u_2'}{\partial \phi^2} + \frac{K}{k}\left(\frac{u_2^\circ}{a^2} - \frac{1}{a^2}\frac{\partial u_3^\circ}{\partial \phi} - \frac{u_2'}{a}\right)\right\}$$

$$+ P_2^+\left(1+\frac{h}{a}\right)h - \frac{2\gamma h^3}{3a}\ddot{Y}(t)\cdot\bar{e}_2 - \frac{2\gamma h^3}{3}\left(\frac{\partial^2 u_2^\circ}{a\,\partial t_1^2} + \frac{\partial^2 u_2'}{\partial t_1^2}\right) = 0$$

(57)

$$\equiv_3^\circ = \frac{-2hE}{1-\nu^2}\left\{\frac{\nu}{a}\frac{\partial u_1^\circ}{\partial x} + \frac{1}{a^2}\frac{\partial u_2^\circ}{\partial \phi} + \frac{u_3^\circ}{a^2} - \frac{k}{a}\frac{\partial u_2'}{\partial \phi}\right.$$

$$\left. + K\left(\frac{1}{a^2}\frac{\partial u_2^\circ}{\partial \phi} - \nabla^2 u_3^\circ - \frac{\partial u_1'}{\partial x} - \frac{1}{a}\frac{\partial u_2'}{\partial \phi}\right)\right\}$$

$$+ P_3^+\left(1+\frac{h}{a}\right) - 2h\gamma\frac{\partial^2 u_3^\circ}{\partial t_2^2} - 2h\gamma\ddot{Y}_B(t)\cdot\bar{e}_3 = 0$$

Equations (53-57) were obtained by Yu * in 1958, except for the terms involving the external forces and the rigid body motion.

In equations (53-57)

(58)

$$k = \frac{1}{3}\left(\frac{h}{a}\right)^2$$

$$K = \frac{\kappa(1-\nu)}{2}$$

The significance of K is explained in part in Appendix C and also in Appendix D. The notation t_1 is used to indicate those terms which are related to the inclusion of rotary inertia. This is further discussed in Section VI.

Boundary conditions (45) and (46) are in an appropriate form for use when the outer and inner cylindrical surfaces are free to move, and are not transformed.

Boundary conditions (47) and (48) transform as follows:

At x (59)
$$\int_t\int_\phi \Big[\Big\{\frac{2Eh}{1-\nu^2}\Big(\frac{\partial u_1^\circ}{\partial x}+\frac{h^2}{3a}\frac{\partial u_1'}{\partial x}+\frac{\nu}{a}\frac{\partial u_2^\circ}{\partial\phi}+\frac{\nu}{a}u_3^\circ\Big)+\int_{-h}^{h}P_1\Big(1+\frac{z}{a}\Big)dz\Big\}_{x=0}(\delta u_1^\circ)_{x=0}$$

(59)
$$+\Big\{\frac{E}{1-\nu^2}\cdot\frac{2h^3}{3}\Big(\frac{1}{a}\frac{\partial u_2^\circ}{\partial x}+\frac{\partial u_1'}{\partial x}+\frac{\nu}{a}\frac{\partial u_2'}{\partial\phi}\Big)+\int_{-h}^{h}P_1(z)\Big(1+\frac{z}{a}\Big)dz\Big\}_{x=0}(\delta u_1')_{x=0}$$

$$+\Big\{\frac{E}{1-\nu^2}\cdot\frac{1-\nu}{2}\cdot 2h\Big(\frac{\partial u_2^\circ}{\partial x}+\frac{1}{a}\frac{\partial u_1^\circ}{\partial\phi}+\frac{h^2}{3a}\frac{\partial u_2'}{\partial x}\Big)+\int_{-h}^{h}P_2\Big(1+\frac{z}{a}\Big)dz\Big\}_{x=0}(\delta u_2^\circ)_{x=0}$$

$$+\Big\{\frac{2Eh^3}{3(1-\nu^2)}\cdot\frac{1-\nu}{2}\Big(\frac{1}{a}\frac{\partial u_2^\circ}{\partial x}+\frac{\partial u_2'}{\partial x}+\frac{1}{a}\frac{\partial u_1'}{\partial\phi}+\int_{-h}^{h}P_2 z\Big(1+\frac{z}{a}\Big)dz\Big\}_{x=0}(\delta u_2')_{x=0}$$

$$+\Big\{\frac{2Eh^3}{3(1-\nu^2)}\cdot\frac{1-\nu}{2}\Big(\frac{1}{a}\frac{\partial u_2^\circ}{\partial x}+\frac{\partial u_2'}{\partial x}+\frac{1}{a}\frac{\partial u_1'}{\partial\phi}+\int_{-h}^{h}P_2 z\Big(1+\frac{z}{a}\Big)dz\Big\}_{x=0}(\delta u_2')_{x=0}$$

$$+\Big\{\frac{\kappa E}{1-\nu^2}\cdot\frac{1-\nu}{2}\cdot 2h\Big(u_1'+\frac{\partial u_3^\circ}{\partial x}\Big)+\int_{-h}^{h}P_3\Big(1+\frac{z}{a}\Big)dz\Big\}_{x=0}(\delta u_3^\circ)_{x=0}\Big]a\,d\phi\,dt=0$$

---

* Reference 6

At x = L

$$(60)\quad \int_t\int_\phi \Big[\Big\{\frac{2Eh}{1-\nu^2}\Big(\frac{\partial u_1^\circ}{\partial x}+\frac{h^2}{3a}\frac{\partial u_1'}{\partial x}+\frac{\nu}{a}\frac{\partial u_2^\circ}{\partial\phi}+\frac{\nu}{a}u_3^\circ\Big)-\int_{-h}^{h}P_1\Big(1+\frac{z}{a}\Big)dz\Big\}_{x=L}(\delta u_1^\circ)_{x=L}$$

$$+\Big\{\frac{E}{1-\nu^2}\cdot\frac{2h^3}{3}\Big(\frac{1}{a}\frac{\partial u_1^\circ}{\partial x}+\frac{\partial u_1'}{\partial x}+\frac{\nu}{a}\frac{\partial u_2'}{\partial\phi}\Big)-\int_{-h}^{h}P_1\Big(1+\frac{z}{a}\Big)z\,dz\Big\}_{x=L}(\delta u_1')_{x=L}$$

$$+\Big\{\frac{E}{1-\nu^2}\cdot\frac{1-\nu}{2}\cdot 2h\Big(\frac{\partial u_2^\circ}{\partial x}+\frac{1}{a}\frac{\partial u_1^\circ}{\partial\phi}+\frac{h^2}{3a}\frac{\partial u_2'}{\partial x}\Big)-\int_{-h}^{h}P_2\Big(1+\frac{z}{a}\Big)dz\Big\}_{x=L}(\delta u_2^\circ)_{x=L}$$

$$+\Big\{\frac{2Eh^3}{3(1-\nu^2)}\cdot\frac{1-\nu}{2}\Big(\frac{1}{a}\frac{\partial u_2^\circ}{\partial x}+\frac{\partial u_2'}{\partial x}+\frac{1}{a}\frac{\partial u_1'}{\partial\phi}\Big)-\int_{-h}^{h}P_2\,z\Big(1+\frac{z}{a}\Big)dz\Big\}_{x=L}(\delta u_2')_{x=L}$$

$$+\Big\{\frac{KE}{1-\nu^2}\cdot\frac{1-\nu}{2}\cdot 2h\Big(u_1'+\frac{\partial u_3^\circ}{\partial x}\Big)-\int_{-h}^{h}P_3\Big(1+\frac{z}{a}\Big)dz\Big\}_{x=L}(\delta u_3^\circ)_{x=L}\Big]a\,d\phi\,dt=0$$

We retain this material for later use while we briefly consider its relationship to conventional treatments. This is discussed in Section VI.

SECTION VI
NEGLECT OF ROTARY INERTIA AND TRANSVERSE SHEAR DEFORMATION - THE "CLASSICAL" THEORY

Most frequently in classical engineering shell theory, the various descriptive equations are developed under the assumptions that there is no transverse shear deformation and that terms involving rotary inertia may be neglected. When this is done, the five differential equations reduce to a set of three, and the boundary conditions are also simplified. (Not all investigators have obtained the same set of three. This depends on the precise point at which these assumptions are made, as well as on the nature of other simplifying assumptions).

The usual next step is the transformation of the stress-motion equations into a similar set involving displacement (deformation) coordinates. From this point, some solutions have been found for the lower modes.* Prior studies have been directed generally at the free vibration problem. It has been found that slight differences in the original differential equations do not cause very much change in the natural frequencies found. It has also been demonstrated that for each set of mode parameters, three natural frequencies result from the set of three equilibrium equations. Similarly, one might expect five natural frequencies from the five equation set.

We are, however, interested in the response of the shell to impulsive loading, rather than in the uni-modal

---

*NOTE: A mode is characterized by the size of an axial and a circumferential wave length Ordinarily, only the lowest natural frequency for the mode is found.

free vibration problem. The response is formed from an infinite series of expressions for shell deformations, each term of which is at one of the shell natural frequencies.

Lacking information to the contrary, it is premature to assert that these assumptions may be made, and the problem simplified, without loss of accuracy. The actual response will depend on the nature of the load. Different forcing functions will certainly excite different combinations of the normal modes.

In order to assure complete consistency with the equilibrium equations and boundary conditions already obtained for five variables we essentially return to equation (39) et seq., obtained directly from Hamilton's principle. (The details are included in Appendix D.)

Neglect of rotary inertia affects only equation 42, in a relatively minor way. Terms in h^3 are dropped from each one. The result is the equation (D-7).

Neglect of transverse shear deformation is considerably more subtle. Essentially we require:

(61) $$\epsilon_{13} = 0 = \epsilon_{23}$$

This is the same as requiring that:

(62) $$U_1' + \frac{\partial U_3^\circ}{\partial x} = 0 = U_2' + \frac{1}{a}\frac{\partial U_3^\circ}{\partial \phi} - \frac{1}{a}U_2^\circ$$

This can be accomplished by letting Mindlin's Constant $\kappa \to \infty$ so long as σ_{13}° and σ_{23}° remain finite although undefined.

The Hamilton Integral as $\kappa \to \infty$, leads to the

following stress-motion equilibrium equations which are (D-22, D-23) and (D-24), shown below as (63-65), ($\delta u_k^{\circ} \neq 0$);

(63)

$$\left\{ \frac{\partial \sigma_{11}^{\circ}}{\partial x} + \frac{1}{a} \frac{\partial \sigma_{21}^{\circ}}{\partial \phi} + P_1^{+}\left(1+\frac{h}{a}\right) - 2\gamma h \ddot{Y}_s(t)\cdot \bar{e}_1 - 2\gamma h \ddot{u}_1^{\circ} \right\} \delta u_1^{\circ} = 0$$

(64)

$$\left\{ \frac{\partial \sigma_{12}^{\circ}}{\partial x} + \frac{1}{a} \frac{\partial \sigma_{22}^{\circ}}{\partial \phi} + P_2^{+}\left(1+\frac{h}{a}\right) - 2\gamma h \ddot{Y}_s(t)\cdot \bar{e}_2 - 2\gamma h \ddot{u}_2^{\circ} \right.$$
$$\left. + \frac{1}{a} \frac{\partial \sigma_{12}^{1}}{\partial x} + \frac{1}{a^2} \frac{\partial \sigma_{22}^{1}}{\partial \phi} + P_2^{+} \cdot \frac{h}{a} \cdot \left(1+\frac{h}{a}\right) \right\} \delta u_2^{\circ} = 0$$

(65)

$$\left\{ P_3^{+}\left(1+\frac{h}{a}\right) - \frac{\sigma_{22}^{\circ}}{a} - 2\gamma h \ddot{Y}_s(t)\cdot \bar{e}_3 - 2\gamma h \ddot{u}_3^{\circ} + \frac{\partial^2 \sigma_{11}^{1}}{\partial x^2} + \frac{1}{a} \frac{\partial^2 \sigma_{21}^{1}}{\partial x \partial \phi} \right.$$
$$\left. + \frac{\partial P_1^{+}}{\partial x}\left(1+\frac{h}{a}\right) h + \frac{1}{a} \frac{\partial^2 \sigma_{12}^{1}}{\partial x \partial \phi} + \frac{1}{a} \frac{\partial^2 \sigma_{22}^{1}}{\partial \phi^2} + \frac{\partial P_2^{+}}{\partial \phi} \cdot \frac{h}{a} \cdot \left(1+\frac{h}{a}\right) \right\} \delta u_3^{\circ} = 0$$

Boundary condition equations (45) and (46) are unaffected by this assumption.

The complete set of boundary conditions (as $K \longrightarrow \infty$) at x = 0 is given below for reference purposes:

<u>At x = 0</u>

(66)

$$\int_t \int_{\phi} \Big[\left\{ \sigma_{11}^{\circ} + \int_{-h}^{h} P_1 \left(1+\frac{z}{a}\right) dz \right\}_{x=0} (\delta u_1^{\circ})_{x=0}$$
$$- \left\{ \sigma_{11}^{1} + \int_{-h}^{h} P_1 z \left(1+\frac{z}{a}\right) dz \right\}_{x=0} \left(\delta \frac{\partial u_1^{\circ}}{\partial x}\right)_{x=0}$$
$$+ \left\{ \sigma_{12}^{\circ} + \int_{-h}^{h} P_2 \left(1+\frac{z}{a}\right) dz + \frac{\sigma_{12}^{1}}{a} + \frac{1}{a} \int_{-h}^{h} P_2 z \left(1+\frac{z}{a}\right) dz \right\}_{x=0} (\delta u_2^{\circ})_{x=0}$$
$$+ \left\{ P_1^{+}\left(1+\frac{h}{a}\right) h + \frac{\partial \sigma_{11}^{1}}{\partial x} + \frac{\partial \sigma_{21}^{1}}{\partial x} + \frac{1}{a} \frac{\partial \sigma_{12}^{1}}{\partial \phi} + \int_{-h}^{h} P_3 \left(1+\frac{z}{a}\right) dz \right.$$
$$\left. + \frac{1}{a} \frac{\partial}{\partial \phi} \int_{-h}^{h} P_2 \left(1+\frac{z}{a}\right) z \, dz \right\}_{x=0} (\delta u_3^{\circ})_{x=0} \Big] a \, d\phi \, dt = 0$$

For a clamped (fixed-ended) cylinder, at both x = 0, and x = L, the end conditions are prescribed and reduce to:

(67)

$$r_1^\circ = 0 = r_2^\circ$$

$$r_3^\circ = 0 = \frac{\partial r_3^\circ}{\partial x}$$

For a free ended cylinder, $P_1 = P_2 = P_3 = 0$ and for arbitrary $\delta u_k{}^\circ \neq 0$, the boundary conditions at x = 0 and x = L become:

(68)

$$\sigma_{11}^\circ = N_x = 0$$

$$\sigma_{11}' = M_x = 0$$

$$\sigma_{12}^\circ + \frac{1}{a}\sigma_{12}' = N_{x\phi} + \frac{1}{a}M_{x\phi} = 0$$

$$0 = P_1^+(1+\frac{h}{a})h + \frac{\partial \sigma_{11}'}{\partial x} + \frac{\partial \sigma_{21}'}{a\partial \phi} + \frac{1}{a}\frac{\partial \sigma_{12}'}{\partial \phi} = P_1^+(1+\frac{h}{a})h + \frac{\partial M_x}{\partial x} + \frac{\partial M_{\phi x}}{a\partial \phi} + \frac{1}{a}\frac{\partial M_{x\phi}}{\partial \phi}$$

where the first 3 terms of the last equation define $Q_x\,|_{x=0,L}$ with no rotary inertia considered.

In addition, we can obtain the appropriately consistent set of three equations in deformation displacement coordinates. A new set of stress resultant equations as $K \to \infty$ (see equations (D-30 a-j)) is formed by using equation (62). The set is then substituted in equations

(63-65) to form:* (assuming $\delta u_1^\circ \neq \delta u_2^\circ \neq \delta u_3^\circ \neq 0$).

(69)
$$+\frac{2Eh}{1-\nu^2}\left\{\frac{\partial^2 u_1^\circ}{\partial x^2}+\frac{(1-\nu)}{2a^2}\frac{\partial^2 u_1^\circ}{\partial \phi^2}+\frac{(1+\nu)}{2a}\frac{\partial^2 u_2^\circ}{\partial x\partial\phi}+\frac{\nu}{a}\frac{\partial u_3^\circ}{\partial x}+k\left(\frac{1-\nu}{2a}\frac{\partial^3 u_2^\circ}{\partial x\partial\phi^2}-a\frac{\partial^3 u_3^\circ}{\partial x^3}\right)\right\}$$

$$-\left\{2\gamma h\ddot{Y}_B(t)\cdot\bar{e}_1+2\gamma h\ddot{u}_1-P_1^+\left(1+\frac{h}{a}\right)\right\}=0$$

(70)

$$+\frac{2Eh}{1-\nu^2}\left\{\frac{1+\nu}{2a}\cdot\frac{\partial^2 u_1^\circ}{\partial x\partial\phi}+\frac{1-\nu}{2}\cdot\frac{\partial^2 u_2^\circ}{\partial x^2}+\frac{1}{a^2}\cdot\frac{\partial^2 u_2^\circ}{\partial\phi^2}+\frac{1}{a^2}\frac{\partial u_3^\circ}{\partial\phi}\right.$$

$$\left.+k\left[\frac{3}{2}(1-\nu)\frac{\partial^2 u_2^\circ}{\partial x^2}-\frac{1}{a^2}\frac{\partial^2 u_2^\circ}{\partial\phi^2}-\frac{1}{a^2}\frac{\partial u_3^\circ}{\partial\phi}-\frac{(3-\nu)}{2}\cdot\frac{\partial^3 u_2^\circ}{\partial\phi\partial x^2}\right]\right\}$$

$$-\left\{2\gamma h\ddot{Y}_B(t)\cdot\bar{e}_2+2\gamma h\ddot{u}_2^\circ-P_2^+\left(1+\frac{h}{a}\right)-P_2^+\cdot\left(\frac{h}{a}\right)\cdot\left(1+\frac{h}{a}\right)\right\}=0$$

(71)

$$-\frac{2Eh}{1-\nu^2}\left\{\frac{1}{a^2}\frac{\partial u_2^\circ}{\partial\phi}+\frac{u_3^\circ}{a^2}+\frac{\nu}{a}\cdot\frac{\partial u_1^\circ}{\partial x}-ka^2\left[\frac{1}{a}\frac{\partial^2 u_1^\circ}{\partial x^2}-\frac{(1-\nu)}{2a^2}\frac{\partial^3 u_1^\circ}{\partial x\partial\phi^2}+\frac{(3-\nu)}{2a^2}\frac{\partial^3 u_2^\circ}{\partial\phi\partial x^2}+\frac{1}{a^3}\frac{\partial u_2^\circ}{\partial\phi}\right.\right.$$

$$\left.\left.-\frac{2}{a^3}\frac{\partial^2 u_3^\circ}{\partial\phi^2}-\nabla^4 u_3^\circ\right]\right\}-\left\{2\gamma h\ddot{Y}_B(t)\cdot\bar{e}_3+2\gamma h\ddot{u}_3^\circ-P_3^+\left(1+\frac{h}{a}\right)-\frac{\partial P_1^+}{\partial x}\cdot h\cdot\left(1+\frac{h}{a}\right)\right.$$

$$\left.-\frac{\partial P_2^+}{\partial\phi}\cdot\frac{h}{a}\left(1+\frac{h}{a}\right)\right\}=0$$

---

* The four stress boundary conditions can also be related to the deformation coordinates at the edges through D-30.

SECTION VII
THE FREE VIBRATION PROBLEM

7.1 The SR Model

We have obtained the shell equilibrium equations, expressed in terms of the mid-surface variables. (Equations (53-57)). The set may be written as:

(72)

$$\overline{\overline{=}}_K^n\left(U_K^n, \frac{\partial U_K^n}{\partial S_i}, \frac{\partial U_K^n}{\partial S_\nu}, \frac{\partial^2 U_K^n}{\partial S_i\,\partial S_j}, \frac{\partial^2 U_K^n}{\partial t^2}, \nu, a, \frac{h}{a}, E, P_K, \ddot{\bar{Y}}_B(t)\right)=0$$

where it is understood that

$$k = 1,\ 2,\ 3$$

$$n = 0,\ 1$$

$$S_1 = x$$

$$S_2 = a\phi$$

$$S_3 = R$$

The solution to this general problem (which includes the surface tractions and the acceleration of the mass-center) is discussed in Section VIII.

In the free vibration problem, the surface tractions P_k^+ and the acceleration $\ddot{\bar{Y}}_B(t)$ are eliminated from the set $\overline{\overline{=}}$. For clarity of notation, we write the set now as:

(73)

$$H_K^n\left(U_K^n, \frac{\partial U_K^n}{\partial S_\nu}, \frac{\partial^2 U_K^n}{\partial S_i}, \frac{\partial^2 U_K^n}{\partial S_i\,\partial S_j}, \frac{\partial^2 U_K^n}{\partial t^2}, \nu, a, \frac{h}{a}, E\right)=0$$

It should be emphasized that H_k^n will refer only to the free vibration problem, and that the only difference between $\overline{\overline{=}}_k^n$ and H_k^n is in the elimination of the P_k^+ and $\ddot{\bar{Y}}_B(t)$ terms.

We assume that the solutions u_k^n may be expressed as an infinite series of terms, separable in the functions x, ϕ, t:

(74)

a. $$U_1^\circ = \sum_{m=0}^{\infty} f_1^\circ(x)_m \cos m\phi \, C_m e^{i\omega_m t}$$

b. $$U_1' = \sum_{m=0}^{\infty} f_1'(x)_m \cos m\phi \, C_m e^{i\omega_m t}$$

c. $$U_2^\circ = \sum_{m=0}^{\infty} f_2^\circ(x)_m \sin m\phi \, C_m e^{i\omega_m t}$$

d. $$U_2' = \sum_{m=0}^{\infty} f_2'(x)_m \sin m\phi \, C_m e^{i\omega_m t}$$

e. $$U_3^\circ = \sum_{m=0}^{\infty} f_3^\circ(x)_m \cos m\phi \, C_m e^{i\omega_m t}$$

where $f_k^n(x,m)$ $\cos m\phi$ U $\sin m\phi$ is a normal mode deformation during free vibration at frequency ω_m. When these solutions are substituted in the set $\{H_k^n\}$ the result becomes:

(75)

a. $$H_1^\circ = \sum_{m=0}^{\infty} \cos m\phi \, C_m e^{i\omega_m t}\left[a_{11}f_1^\circ + a_{12}f_1' + a_{13}f_2^\circ + a_{14}f_2' + a_{15}f_3^\circ\right] = 0$$

b. $$H_1' = \sum_{m=0}^{\infty} \cos m\phi \, C_m e^{i\omega_m t}\left[a_{21}f_1^\circ + a_{22}f_1' + a_{23}f_2^\circ + a_{24}f_2' + a_{25}f_3^\circ\right] = 0$$

c. $$H_2^\circ = \sum_{m=0}^{\infty} \sin m\phi \, C_m e^{i\omega_m t}\left[a_{31}f_1^\circ + a_{32}f_1' + a_{33}f_2^\circ + a_{34}f_2' + a_{35}f_3^\circ\right] = 0$$

d. $$H_2' = \sum_{m=0}^{\infty} \sin m\phi \, C_m e^{i\omega_m t}\left[a_{41}f_1^\circ + a_{42}f_1' + a_{43}f_2^\circ + a_{44}f_2' + a_{45}f_3^\circ\right] = 0$$

e. $$H_3^\circ = \sum_{m=0}^{\infty} \cos m\phi \, C_m e^{i\omega_m t}\left[a_{51}f_1^\circ + a_{52}f_1' + a_{53}f_2^\circ + a_{54}f_2' + a_{55}f_3^\circ\right] = 0$$

The trigonometric terms satisfy the necessary angular periodicity and the imaginary exponential time terms satisfy

the periodicity requirements of free vibration.

The coefficients a_{rs} are functions of K, a, m, ω_m, ν, $\frac{h}{a}$, D and D^2, where D signifies differentiation with respect to x. Since these equations are valid for any value of ϕ or t, the bracketed terms must be equal to zero for any value of m. *

Thus, equations (75) reduce to a matrix equation:

(76)

$$\begin{bmatrix} H_1^0 \\ H_1' \\ H_2^0 \\ H_2' \\ H_3^0 \end{bmatrix}_m \equiv \begin{bmatrix} & & \\ & A_1 & \\ & & \end{bmatrix}_m \begin{bmatrix} f_1^0 \\ f_1' \\ f_2^0 \\ f_2' \\ f_3^0 \end{bmatrix}_m \equiv \begin{bmatrix} 0 \\ 0 \\ 0 \\ 0 \\ 0 \end{bmatrix}_m$$

in which A_1 is a 5 x 5 determinant, as a function of γ, K, a, m, ω_n, ν, $\frac{h}{a}$, D and D^2. This can be solved if the typical solution is taken as:

(77)
$$f_k^n(x,m)_{mi} = \sum_i \mathcal{L}_{kmi}^n \Gamma_{mi} e^{\lambda_{mi}\frac{x}{L}}$$

The subscripts i indicate that more than one such solution will be possible. The term Γ_{mi} refers to a factor of the solution common to all f_k^n for a particular m, i set of five. The terms $\mathcal{L}_{kmi}^n$ then express the relative amplitudes for each f_k^n for a particular m, i set.

---

* Note: A special case develops for m = 0, which has axisymmetric deformation (i.e., $U_2^0 = U_2^0(x,t)$ sin 0, $U_2^1 = U_2^1(x,t)$ sin 0, and $\frac{\partial(\ )}{\partial\phi} = 0$. The third and fourth equations of the set (75) are zero irrespective of the value of the bracketed terms, as sin 0 = 0. Matrix A, reduces to order 3 x 3, leading to an axial function containing six terms, in a form analogous to equation (80).

Using this postulated solution form, the determinantal equation becomes:

(78)

$$\sum_i \left[A_2 (\omega_m, m, \frac{h}{a}, \frac{a}{L}, \lambda_{mi}) \right]_{mi} \left[\begin{matrix} \chi_{i-1}^{0} \\ \chi_{i-2}^{0} \\ \chi_{i-3}^{0} \\ \chi_{i}^{0} \end{matrix} \right]_{mi} \Gamma_{mi} e^{\lambda_{mi} \frac{x}{L}} \equiv 0$$

The matrix A_2 is of course also a function of γ, ν and K, but the form chosen highlights the variable factors in it.

To satisfy equation (78), the determinant of the matrix A_2 must equal zero for each value of i and m. Expansion of the determinant would result in an equation of the form:

(79) $$\Delta \cdot A_2 = \lambda_i^{10} + g_{8i} \lambda_i^{8} + g_{6i} \lambda_i^{6} + g_{4i} \lambda_i^{4} + g_{2i} \lambda_i^{2} + g_{0i} \equiv 0$$

In equation (79), the coefficients g_{pi} are functions of h/a, a/L, ω_m and m. For specified values of h/a, ω_m and m, there are five values of λ_i^2, or ten values of λ_i, that will satisfy equation (79). There must be at least one real root λ_i^2, and this will be associated either with four other real roots, or with either one or two pairs of complex conjugate roots.

Assuming for the moment that the 10 values of λ_i are known, the index i in equation (77) is seen to take the values 1 - 10. Equation (77) thus yields:

(80) $$f_k^n(x,m)_m = \sum_{i=1}^{10} f_k^n(x,m)_{mi} = \sum_{i=1}^{10} \mathcal{L}_{kmi}^n \Gamma_{mi} e^{\lambda_{mi} \frac{x}{L}}$$

It is convenient to set $(\mathcal{Z}^{\circ}_{3})$ mi = 1, for normalizing purposes. Now, if λ_{mi} can be obtained as analytic functions of ω_m, it will be possible to obtain the relative amplitude factor:

$$(81) \quad \mathcal{Z}^{n}_{kmi}(\omega_m, \lambda_{mi}) = \frac{U^{n}_{kmi}}{U^{\circ}_{3mi}}$$

(This is done by substituting the λ_{mi} into four of the five equations (78).)

To reiterate, it is at this point possible to write equation (80) in the form:

(82)

a. $f^{\circ}_{1}(x,m)_m = \mathcal{Z}^{\circ}_{1m1}\Gamma_{m1}e^{\lambda m1 x/L} + \mathcal{Z}^{\circ}_{1m2}\Gamma_{m2}e^{\lambda m2 x/L} + \ldots + \mathcal{Z}^{\circ}_{1m10}\Gamma_{m10}e^{\lambda m10 x/L}$

b. $f^{1}_{1}(x,m)_m = \mathcal{Z}^{1}_{1m1}\Gamma_{m1}e^{\lambda m1 x/L} + \mathcal{Z}^{1}_{1m2}\Gamma_{m2}e^{\lambda m2 x/L} + \ldots + \mathcal{Z}^{1}_{1m10}\Gamma_{m10}e^{\lambda m10 x/L}$

c. $f^{\circ}_{2}(x,m)_m = \mathcal{Z}^{\circ}_{2m1}\Gamma_{m1}e^{\lambda m1 x/L} + \mathcal{Z}^{\circ}_{2m2}\Gamma_{m2}e^{\lambda m2 x/L} + \ldots + \mathcal{Z}^{\circ}_{2m10}\Gamma_{m10}e^{\lambda m10 x/L}$

d. $f^{1}_{2}(x,m)_m = \mathcal{Z}^{1}_{2m1}\Gamma_{m1}e^{\lambda m1 x/L} + \mathcal{Z}^{1}_{2m2}\Gamma_{m2}e^{\lambda m2 x/L} + \ldots + \mathcal{Z}^{1}_{2m10}\Gamma_{m10}e^{\lambda m10 x/L}$

e. $f^{\circ}_{3}(x,m)_m = 1\ \Gamma_{m1}e^{\lambda m1 x/L} + 1\ \Gamma_{m2}e^{\lambda m2 x/L} + \ldots + 1\ \Gamma_{m10}e^{\lambda m10 x/L}$

Until the value of ω_m is found, it should be noted that the values of $\mathcal{Z}^{\circ}_{1m1}$, $\mathcal{Z}^{\circ}_{1m2}$, etc. are undetermined.

In order to proceed further, it is necessary to appreciate that the five functions (74 a-e) must satisfy problem boundary conditions, as presented in equations (59) and (60).

BOUNDARY CONDITIONS FOR CLAMPED ENDS

For the purpose of continuing this discussion, we now note that for clamped ends equations (59) and (60) yield the following 10 homogeneous boundary conditions.

(83)

At X = 0	At X = L
$r_1^0 = 0$	$r_1^0 = 0$
$r_1^1 = 0$	$r_1^1 = 0$
$r_2^0 = 0$	$r_2^0 = 0$
$r_2^1 = 0$	$r_2^1 = 0$
$r_3^0 = 0$	$r_3^0 = 0$

When boundary conditions (83) are substituted in equations (74 a-e), each m dependent term will yield 10 equations. Since the boundary conditions do not depend on either ϕ or t, these essentially reduce to the 10 equations found by setting equations (82 a-e) equal to zero at x = 0 and x = L.

(84)

$$\begin{bmatrix} \mathcal{L}^0_{im1} & \mathcal{L}^0_{im2} & \mathcal{L}^0_{im3} & \cdots & \mathcal{L}^0_{im10} \\ \mathcal{L}^1_{im1} & \mathcal{L}^1_{im2} & \mathcal{L}^0_{im2} & \cdots & \mathcal{L}^0_{im10} \\ \mathcal{L}^0_{2m1} & \cdot & \cdot & \cdots & \cdot \\ \mathcal{L}^1_{2m1} & \cdot & \cdot & \cdots & \cdot \\ 1 & \cdot & \cdot & \cdots & 1 \\ \mathcal{L}^0_{im1} e^{\lambda m1} & \mathcal{L}^0_{im2} e^{\lambda m2} & \cdot & \cdots & \mathcal{L}^0_{im10} e^{\lambda m10} \\ \cdot & \cdot & \cdot & \cdots & \cdot \\ \cdot & \cdot & \cdot & \cdots & \cdot \\ \cdot & \cdot & \cdot & \cdots & \cdot \\ 1 e^{\lambda m1} & \cdot & \cdot & \cdots & 1 e^{\lambda m10} \end{bmatrix}_n \begin{bmatrix} [m1] \\ [m2] \\ [m3] \\ [m4] \\ [m5] \\ [m6] \\ [m7] \\ [m8] \\ [m9] \\ [m10] \end{bmatrix}_m = 0$$

Since the column $\Gamma_{m1} \ldots \Gamma_{m10}$ is arbitrary, the determinant of the coefficient matrix must = 0 for a non-trivial solution.

Recall that both equation (79) and the determinant of equation (84) are functions of ω for a particular value of $\underline{m}$. Equation (79) is imagined to provide λ_{mi} as functions of ω_m, so that all that remains is to find the value or values of ω_m that satisfy equation (84).

The determinant of equation (84) is a transcendental equation which yields an infinite number of solutions. We employ the index N to denote these values. Thus N = 1,2,3. The natural frequency ω should thus be subscripted as ω_{mN}, and is seen (in this case) to be one of the eigenvalues of ω in the determinant of (84). Thus, to recapitulate:

- Each value of ω_{mN} (N=1,2,3... ∞) determines λ_{mN1} and $\mathcal{L}_{kmNi}$
- Placing one value of ω_{mN} in 9 of 10 equations (84) produces Γ_{mNi}, the relative amplitudes of the axial functions, where Γ_{mN10} is taken as 1.
- Thus, equation (80) may be written:

$$(85) \quad f_k^n(x,m)_m = f_k^n(x,m,N)_{mN} = \sum_{i=1}^{10} \mathcal{L}_{kmNi} \Gamma_{mNi} e^{\lambda_{mNi} \frac{x}{L}}$$

There are an infinite number of solutions N = 1,2,3... ∞ for each $\underline{m}$ that will satisfy the boundary conditions (83) and the equilibrium equations (75). Each of these solutions may be conveniently expressed:

$$(86) \quad U_{kmN}^n = C_{mN} e^{i\omega_{mN}t} \cos m\phi \; U \sin m\phi \; f_k^n(x,m,N)_{mN}$$

The set of solutions corresponding to the eigenvalue ω_{mN} is represented by the solution vector:

$$(87)\quad \left\{U^n_{KmN}\right\} = C_{mN} e^{i\omega_{mN}t} \cos m\phi \cup \sin m\phi \left\{f^n_K(x,m,N)_{mN}\right\}$$

Each of these solution vectors exist independently for each ω_{mN}. Thus the complete solution is represented by a doubly infinite series formed as a linear combination of the solution vectors:

$$(88)\quad \left\{U^n_K\right\} = \sum_{m=0}^{\infty}\sum_{N=1}^{\infty} \left\{U^n_{KmN}\right\}$$

or,

$$(89)\quad \left\{U^n_K\right\} = \sum_{m=0}^{\infty}\sum_{N=1}^{\infty} C_{mN} e^{i\omega_{mN}t} \cos m\phi \cup \sin m\phi \left\{f^n_K(x,m,N)_{mN}\right\}$$

Before proceeding further, let us also develop the boundary conditions for free ends.

BOUNDARY CONDITIONS FOR FREE ENDS:

For the free ended cylinder, the boundary conditions can be obtained from equations (59) and (60), by noting that the variables u_1^0, u_1^1, etc. are not prescribed, so that the several terms $\delta u^n_k \neq 0$. If we take no surface tractions on the end faces, equations (59) and (60) reduce to a system of 10 equations:

(90)

At $x=0$	At $x=L$
$\sigma_{11}^{\circ} = 0$	$\sigma_{11}^{\circ} = 0$
$\sigma_{11}^{1} = 0$	$\sigma_{11}^{1} = 0$
$\sigma_{12}^{\circ} = 0$	$\sigma_{12}^{\circ} = 0$
$\sigma_{12}^{1} = 0$	$\sigma_{12}^{1} = 0$
$\sigma_{13}^{\circ} = 0$	$\sigma_{13}^{\circ} = 0$

These are, of course, expressible in terms of deformation coordinates as follows:

(91)

a. $$\frac{2Eh}{1-\nu^2}\left(\frac{\partial U_1^{\circ}}{\partial x}+\frac{h^2}{3a}\frac{\partial U_1^{1}}{\partial x}+\frac{\nu}{a}\frac{\partial U_2^{\circ}}{\partial \phi}+\frac{\nu}{a}U_3^{\circ}\right)\Big|_{x=0,L}=0$$

b. $$\frac{2Eh}{1-\nu^2}\cdot\frac{h^2}{3}\left(\frac{1}{a}\frac{\partial U_1^{\circ}}{\partial x}+\frac{\partial U_1^{1}}{\partial x}+\frac{\nu}{a}\frac{\partial U_2^{1}}{\partial \phi}\right)\Big|_{x=0,L}=0$$

c. $$\frac{2Eh}{1-\nu^2}\cdot\frac{(1-\nu)}{2}\left(\frac{\partial U_2^{\circ}}{\partial x}+\frac{1}{a}\frac{\partial U_1^{\circ}}{\partial \phi}+\frac{h^2}{3a}\frac{\partial U_2^{1}}{\partial x}\right)\Big|_{x=0,L}=0$$

d. $$\frac{2Eh}{1-\nu^2}\cdot\frac{h^2}{3}\left(\frac{1}{a}\frac{\partial U_2^{\circ}}{\partial x}+\frac{\partial U_2^{1}}{\partial x}+\frac{1}{a}\frac{\partial U_1^{1}}{\partial \phi}\right)\Big|_{x=0,L}=0$$

e. $$\frac{2Eh}{1-\nu^2}\cdot\frac{K(1-\nu)}{2}\left(U_1^{1}+\frac{\partial U_2^{\circ}}{\partial x}\right)\Big|_{x=0,L}=0$$

By way of example, consider (91a) in terms of equations (74) and (80). This becomes:

(92)
$$\frac{2Eh}{1-\nu^2}\sum_{m=0}^{\infty}\Bigg(\sum_{i=1}^{10}\mathcal{L}_{1mi}^{\circ}\lambda_{mi}e^{\lambda_{mi}\frac{x}{L}}\Gamma_{mi}\cos m\phi + \frac{h^2}{3a}\sum_{i=1}^{10}\mathcal{L}_{1mi}^{1}\lambda_{mi}e^{\lambda_{mi}\frac{x}{L}}\Gamma_{mi}\cos m\phi + \frac{\nu}{a}m\sum_{i=1}^{10}\mathcal{L}_{2mi}^{\circ}\Gamma_{mi}e^{\lambda_{mi}\frac{x}{L}}\cos m\phi + \frac{\nu}{a}\sum_{i=1}^{10}1\cdot\Gamma_{mi}e^{\lambda_{mi}\frac{x}{L}}\cos m\phi\Bigg)\Big|_{x=0,L}\cdot C_m e^{i\omega_m t}=0$$

Factoring and simplifying:

(93)
$$\frac{2Eh}{1-\nu^2}\sum_{m=0}^{\infty} C_m e^{i\omega_m t}\cos m\phi\left\langle\sum_{i=1}^{10}\Gamma_{mi}\left[e^{\lambda_{mi}\frac{x}{a}}\left(\mathcal{L}_{1mL}\lambda_{mi}+\frac{h^2}{3a}\mathcal{L}'_{1mi}\lambda_{mi}+\frac{\partial}{a}\mathcal{L}^{\circ}_{2mi}+\frac{\partial}{a}\cdot 1\right)\right]\right\rangle_{x=0,L}\equiv 0$$

We designate the term in $\langle\ \rangle$ brackets as $S^{n}_{1k}(x)_m$ and in $[\ ]$ brackets as $S^{n}_{1k}(x)_{mi}$ where the subscript k and superscript n serve to associate it with the corresponding stress resultant. The i subscript, of course, again serves to identify $S^{n}_{1k,mi}$ with one of the 10 roots λ_{mi}. Since a similar development can be made for each of the terms of equation (91) the result is again a 10 x 10 determinantal equation:

(94)
$$\begin{bmatrix} S^{\circ}_{11,m1} & S^{\circ}_{11,m2} & \cdots & S^{\circ}_{11,m10} \\ S'_{11,m1} & S'_{11,m2} & & \\ S^{\circ}_{12,m1} & & & \\ S'_{12,m1} & & & \\ S^{\circ}_{13,m1} & & & \\ S^{\circ}_{91,m1}e^{\lambda_{m1}} & & & \\ & & & \\ & & & \\ S^{\circ}_{13,m1}e^{\lambda_{m1}} & & & S^{\circ}_{13,m10}e^{\lambda_{m10}} \end{bmatrix}_m \begin{bmatrix} \Gamma_{m1} \\ \Gamma_{m2} \\ \cdot \\ \cdot \\ \cdot \\ \cdot \\ \cdot \\ \cdot \\ \Gamma_{m10} \end{bmatrix}_m \equiv 0$$

where all terms in the left matrix are analytic functions of ω_m, and the solution for ω_{mN} will proceed in an analgous manner as with clamped ends.

We now consider the forms of the equilibrium equations and the boundary conditions when the solution is taken in the form of equation (89), the doubly infinite series.

First, noting the form of equation (85), we write the solution set for a given m, N pair as:

(95)
$$(U_1^o)_{mN} = C_{mN} e^{i\omega_{mN}t} \cos m\phi \; f_1^o(x,m,N)_{mN}$$
$$(U_1^e)_{mN} = C_{mN} e^{i\omega_{mN}t} \cos m\phi \; f_1^e(x,m,N)_{mN}$$
$$(U_2^o)_{mN} = C_{mN} e^{i\omega_{mN}t} \sin m\phi \; f_2^o(x,m,N)_{mN}$$
$$(U_2^e)_{mN} = C_{mN} e^{i\omega_{mN}t} \sin m\phi \; f_2^e(x,m,N)_{mN}$$
$$(U_3^o)_{mN} = C_{mN} e^{i\omega_{mN}t} \cos m\phi \; f_3^o(x,m,N)_{mN}$$

Now, substitute the solution vector $\left\{u_k^n\right\}_{mN}$ into the set of equilibrium equations. In the process, we note from equations (75) that each one of the terms f_k^n is multiplied by a coefficient of the form a_{rs}. The coefficient is identified by row with a term H_k^n and by column with a term f_j^r. We therefore find it convenient to display the equilibrium equations in the form:

(96)
$$(H_1^o)_{mN} = C_{mN} e^{i\omega_{mN}t} \cos m\phi \left[a_{11}^{oo} f_1^o + a_{11}^{oe} f_1^e + a_{12}^{oo} f_2^o + a_{12}^{oe} f_2^e + a_{15}^{oo} f_3^o\right]_{mN}$$
$$(H_1^e)_{mN} = C_{mN} e^{i\omega_{mN}t} \cos m\phi \left[a_{11}^{eo} f_1^o + a_{11}^{ee} f_1^e + a_{12}^{eo} f_2^o + a_{12}^{ee} f_2^e + a_{15}^{eo} f_3^o\right]_{mN}$$
$$(H_2^o)_{mN} = C_{mN} e^{i\omega_{mN}t} \sin m\phi \left[a_{21}^{oo} f_1^o + a_{21}^{oe} f_1^e + a_{22}^{oo} f_2^o + a_{22}^{oe} f_2^e + a_{23}^{oo} f_3^o\right]_{mN}$$
$$(H_2^e)_{mN} = C_{mN} e^{i\omega_{mN}t} \sin m\phi \left[a_{21}^{eo} f_1^o + a_{21}^{ee} f_1^e + a_{22}^{eo} f_2^o + a_{22}^{ee} f_2^e + a_{23}^{eo} f_3^o\right]_{mN}$$
$$(H_3^o)_{mN} = C_{mN} e^{i\omega_{mN}t} \cos m\phi \left[a_{31}^{oo} f_1^o + a_{31}^{oe} f_1^e + a_{32}^{oo} f_2^o + a_{32}^{oe} f_2^e + a_{33}^{oo} f_3^o\right]_{mN}$$

Equation set (96 a-e) may be more compactly displayed as the column vector:

$$(97)\quad \left\{H_\kappa^n\right\}_{mN} = C_{mN}\, e^{i\omega_{mN}t} \sin m\phi \cup \cos m\phi \left\{a_{kr}^{nj} f_r^j(x)\right\}$$

It should be carefully noted that the coefficients a_{kr}^{nj} are functions of m, D and ω^2 , and that they are precisely the same as those displayed in equation (75). The only difference is that ω has been shown to be dependent not only on m but also on N.

Since these coefficients formed the matrix of equation (76), we may now write:

$$(98)\quad \left\{H_\kappa^n\right\}_{mN} = 0$$

The notation cos mø ∪ sin mø may be incorporated into each term f_k^n by defining:

$$(99)\quad f_\kappa^n(x,\phi)_{mN} = (\cos m\phi \cup \sin m\phi)\, f_\kappa^n(x,m,N)_{mN}$$

Thus we write:

$$(100)\quad \left\{U_\kappa^n\right\} = \sum_{m=0}^{\infty}\sum_{N=1}^{\infty} C_{mN}\, e^{i\omega_{mN}t}\left\{f_\kappa^n(x,\phi)_{mN}\right\}$$

By considering the development of equation (96), it is also evident that:

$$(101)\quad \left\{H_\kappa^n\right\} = 0 = \sum_{m=0}^{\infty}\sum_{N=1}^{\infty} C_{mN}\, e^{i\omega_{mN}t}\left\{a_{kr}^{nj} f_r^j(x,\phi)_{mN}\right\}$$

It is convenient to write

$$(102)\quad \left\{ a^{nj}_{kr} f^{j}_{r}(x,\phi)_{mN} \right\} = \left\{ \chi^{n}_{k}(x,\phi)_{mN} \right\}$$

and then to separate out the terms containing ω^2 in each function:

$$(103)\quad \left\{ \chi^{n}_{k}(x,\phi)_{mN} \right\} = \left\{ \Lambda^{n}_{k}\left(\left\{ f^{n}_{k}(x,\phi)_{mN} \right\}\right) + F^{n}_{k}(x,\phi)_{mN}\, \omega^{2}_{mN} \right\}$$

Equation (101) is now written:

$$(104)\quad \left\{ H^{n}_{k} \right\} = 0 = \sum_{m=0}^{\infty} \sum_{N=1}^{\infty} C_{mN} e^{i\omega_{mN} t} \left\{ \Lambda^{n}_{k}\left(\left\{ f^{n}_{k}(x,\phi)_{mN} \right\}\right) + F^{n}_{k}(x,\phi)_{mN}\, \omega^{2}_{mN} \right\}$$

In equations (103) and (104), the terms $\Lambda^{n}_{k,\,mN}$ are due to terms with just space derivatives, and stem from a variation of the strain energy. The terms $F^{n}_{k}(x,\phi)_{mN}\ \omega^{2}_{mN}$ come from terms with just time derivatives, and are due to the variation in kinetic energy.

(Each term $\Lambda^{n}_{k,\,mN}$ and $\omega^{2}_{mN} F_{k,mN}$ is formed by using one of the mN series of $\left\{ (u^{k}_{n})_{mN} \right\}$ in the equilibrium equations.)

Similarly, from equations (90-93), for any one of the series of $\left\{ (u^{k}_{n})_{mN} \right\}$ the boundary conditions for free ends are typically noted as:

(105)

$$a^{n}_{ik}(x,\phi,t)_{mN}\Big|_{x=0,L} = 0 = S^{n}_{ik}(x,\phi)_{mN}\Big|_{x=0,L} C_{mN} e^{i\omega_{mN} t}$$

where $S^{n}_{1k}(x)_{mN} \cos m\phi \ \cup \sin m\phi = S_{1k}(x,\phi)_{mN}$ (see, typically, equation (92).

It is thus also evident that we may define

$$(106)\quad \sigma^n_{ik}(x,\phi,t)\big|_{x=0,L} = 0 = \sum_{m=0}^{\infty}\sum_{N=1}^{\infty} S^n_{ik}(x,\phi)_{mN}\big|_{x=0,L} C_{mN} e^{i\omega_{mN} t}$$

Later, consideration is given as to whether or not the series of equations (100), (104) and (106) actually do effect the required minimization of Hamilton's Integral for Free Vibration.

Now, we pause to note another important point. Equation (79) was displayed as an equation of the 10th order in λ_i. It could also have been shown as of the 10th order in ω_m or more precisely, of the fifth order in ω_m^2 Thus, having located any one set of λ_i values which, together with <u>one</u> value of ω , satisfy both equation (79) and (84) or (94) there must be four other values of ω that are compatible with each of the λ_{mi} set.

The interpretation of this situation is that a nodal pattern is established, consisting of <u>m</u> circumferential waves and <u>r</u> axial half waves. For each such nodal pattern there are five natural frequencies. (The <u>r</u> axial half waves are interpreted as having r+1 axial nodes).

Thus, as equation (84) or (94) is solved for the successive values of ω , corresponding to N = 1, 2 ... ∞ , we may expect that we could, with some effort, identify the particular five values of N corresponding to the same number of axial nodes. (This requires plotting the axial function, equation (85) for each N). Thus, the following notations are equally appropriate:

(107) $\omega_{mN} \rightleftharpoons \omega_{mrj}$

$\mathcal{L}^{n}_{KmNi} \rightleftharpoons \mathcal{L}^{n}_{Kmrji}$ $\qquad j = 1,5$

$\lambda_{mNi} \rightleftharpoons \lambda_{mrji}$

$\Gamma_{mNi} \rightleftharpoons \Gamma_{mrji}$

$$f^{n}_{K}(x,m,N)_{mN} \rightleftharpoons f^{n}_{K}(x,m,r,j)_{mrj} \rightleftharpoons \sum_{i=1}^{10} \Gamma_{mrji}\, \mathcal{L}^{n}_{Kmrji}\, e^{\lambda_{mrji} x}$$

We should emphasize that for the response problem there is no need to identify the actual numbers of axial nodes, r + 1. We will be concerned rather with simply establishing a cutoff frequency as a truncation criterion for the deformation series, equation (100). This will be further considered in the next section.

We now proceed to consider the actual approach to be used in the numerical solution of the problem of free vibration.

NUMERICAL APPROACH

In reviewing the steps necessary to isolate the values of ω_m which satisfy the boundary value determinant, we note that it was necessary to develop the values of λ_{mi} as functions of ω , explicitly. Having these values, it was then necessary to use equations (78) to find $\mathcal{L}^{n}_{kmi}$ also as explicit functions of ω .

Since it did not appear feasible to obtain analytic expressions for λ_{mi}, an alternate approach was necessary. This was suggested by Forsberg (Reference 7). This method is outlined below:

- We assume a given shell ($\frac{L}{a}$, $\frac{h}{a}$, ν) at circumferential wave form, m=0.
- Use a trial value for ω close to zero.
- For the shell, determine λ_{mi} from equation (79). Also find ζ_{kmi}.
- Using the appropriate boundary condition determinant (84 or 93), test whether the determinant = 0.
- Iterate on ω until the result converges, repeating the above process.
- From this starting frequency, a detailed, small increment in ω upwards should yield, for a given m, the eigenvalues corresponding to N = 1,2,3... ∞

It will be noted that computations on χ^{n}_{kmi} are in themselves also laborious. This effort can be somewhat reduced by applying a Donnell type manipulation to the equilibrium equation set (73). The method is alluded to in Reference 6.

The result of the Donnell manipulation will be to provide an equivalent set of five equilibrium equations. One of the equations will be a function of u_3^o alone, and the four other equations are each functions of u_3^o and one other (unique) variable:

(108)

a. $\Theta_1(U_3^o) = 0$

b. $\Theta_2(U_3^o, U_1^o) = 0$

c. $\Theta_3(U_3^o, U_2^o) = 0$

d. $\Theta_4(U_3^o, U_1') = 0$

e. $\Theta_5(U_3^o, U_2') = 0$

Equation (108a) is essentially the same as equation (79). The other equations (108 a-e) provide algebraic expressions for $\mathcal{L}^{n}_{kmi}$. The complete operational requirements are not given here, because they are very lengthy, and because they are available in Reference 57. The latter equations are identical to those obtainable by handling the first four equations of (78) according to Cramer's Rule, when $\mathcal{L}^{o}_{s} = 1$.

7.2 The Classical Model

Beginning with three classical equilibrium equations (69-71) a wave form is developed:

$$(109)\quad U^{o}_{\kappa,mN} = \sum_{i=1}^{8} \mathcal{L}^{\bullet}_{kmNi}\, \Gamma_{mNi}\, e^{\lambda_{mNi}\frac{x}{L}} \cos m\phi \cup \sin m\phi \qquad m \neq 0^{*}$$

which will satisfy the eighth order (in $\lambda(w)$) eigenvalue determinant analagous to (79) as well as the other two equivalent equilibrium equations in terms of only two deformation coordinates ($u^{\bullet}_{1,mNi}$, $u^{o}_{3,mNi}$). These three are obtainable by a Donnell manipulation of (69-71).

Eight boundary conditions are satisfied with this

---

* Note: For the special case of m = 0, a sixth order eigenvalue determinant is formed from equations (69) and (71) when $u^{o}_{2} = u^{o}_{2}(x,t)$ sin 0, and $\frac{\partial}{\partial\phi}(u^{\bullet}_{\kappa,oN}) = 0$. The axial function contains six terms. Correspondingly, only six boundary conditions are not identically zero.

deformation function, (109), when the determinant of the 8 x 8 boundary coefficient matrix, analagous to (84) or (94) is equal to zero.

The fixed edge boundary matrix equation is formed from equation (67) in the following manner:

(110)

a. $$f_K^0(x)\big|_{x=0,L} = 0 = \sum_{i=1}^{8} \left[\mathcal{L}_{ki}^0\right]\left(e^{\lambda_i \frac{x}{L}}\right)\Big|_{x=0,L} * \Gamma_i \qquad K = 1,3$$

b. $$\frac{\partial f_s^0(x)}{\partial x}\Big|_{x=0,L} = 0 = \frac{1}{L} \sum_{i=1}^{8} \left[\lambda_i \mathcal{L}_{si}^0\right]\left(e^{\lambda_i \frac{x}{L}}\right)\Big|_{x=0,L} * \Gamma_i$$

For the free cylinder, the form of the eight necessary boundary conditions are:

(111)

a. $$S_{11}^0(x)\big|_{x=0,L} = 0 = \frac{2Eh}{(1-\vartheta^2)a} * \sum_{i=1}^{8} \left[\frac{\lambda_i a}{L}\mathcal{L}_{1i}^0 + \vartheta m \mathcal{L}_{2i}^0 - \frac{1}{3}\left(\frac{h}{a}\right)^2\left(\frac{\lambda_i a}{L}\right)^2 \mathcal{L}_{3i}^0 + \vartheta \mathcal{L}_{3i}^0\right]\left(e^{\lambda_i \frac{x}{L}}\right)\Big|_{x=0,L} * \Gamma_i$$

b. $$S_{11}'(x)\big|_{x=0,L} = 0 = \frac{2Eh^3}{3(1-\vartheta^2)a^2} * \sum_{i=1}^{8} \left[\frac{\lambda_i a}{L}\mathcal{L}_{1i}^0 + \vartheta m \mathcal{L}_{2i}^0 - \left(\vartheta m^2 + \left(\frac{\lambda_i a}{L}\right)^2\right)\mathcal{L}_{3i}^0\right]\left(e^{\lambda_i \frac{x}{L}}\right)\Big|_{x=0,L} * \Gamma_i$$

c. $$S_{12}^0(x) + \frac{1}{a}S_{12}'(x)\big|_{x=0,L} = 0 = \frac{2E\left(\frac{1-\vartheta}{2}\right)h}{(1-\vartheta^2)} * \sum_{i=1}^{8} \left[-m\mathcal{L}_{1i}^0 + \frac{\lambda_i a}{L}\left(1+\left(\frac{h}{a}\right)^2\right)\mathcal{L}_{2i}^0 + \left(\frac{h}{a}\right)^2 \frac{m\lambda_i a}{L}\mathcal{L}_{3i}^0\right] e^{\lambda_i \frac{x}{L}}\Big|_{x=0,L} * \Gamma_i$$

d. $$\frac{\partial S_{11}'}{\partial x} + \frac{1}{a}\frac{\partial S_{11}'(x)}{\partial \phi} + \frac{1}{a}\frac{\partial S_{12}'(x)}{\partial \phi}\Big|_{x=0,L} = 0 = \frac{2E}{1-\vartheta^2} * \frac{1}{3}\left(\frac{h}{a}\right)^3 * \sum_{i=1}^{8} \left[\left\langle\left(\frac{1-\vartheta^2}{2}\right)m^2 + \left(\frac{\lambda_i a}{L}\right)^2\right\rangle \mathcal{L}_{1i}^0 + \left(\frac{3-\vartheta}{2}\right)\left(\frac{\lambda_i a}{L}\right) m \mathcal{L}_{2i}^0 + \left\langle(2-\vartheta)m^2 * \frac{\lambda_i a}{L} - \left(\frac{\lambda_i a}{L}\right)^3\right\rangle \mathcal{L}_{3i}^0\right]\left(e^{\lambda_i \frac{x}{L}}\right)\Big|_{x=0,L} * \Gamma_i$$

These are derivable from equation (68) applied to the free vibration problem.

SECTION VIII
THE FORCED VIBRATION PROBLEM

8.1 Manipulation of The Hamilton Integral

To reiterate, the free vibration problem (in which both the surface tractions $\bar{P}$ and the acceleration $\ddot{\bar{Y}}_B$ of the center of gravity vanish) is solved by the equation set (100). This is repeated below for convenience, except that we now use the subscripts p, s instead of m, N. (The reason for this change is associated with a desire for clarity in the development of the orthogonality requirements later in the section):

$$(100)\quad \left\{U_k^n\right\} = \sum_{p=0}^{\infty}\sum_{s=1}^{\infty} C_{ps}\, e^{i\omega_{ps}t} \left\{f_k^n(x,\phi)_{ps}\right\}$$

The equilibrium equations became equation (104):

$$(104)\quad \left\{\equiv_k^n\right\} \Rightarrow \left\{H_k^n\right\} = \sum_{p=0}^{\infty}\sum_{s=1}^{\infty} C_{ps}\, e^{i\omega_{ps}t}\left\{\Lambda_k^n\left(\left\{f_k^n(x,\phi)_{ps}\right\}\right)_{ps} + \omega_{ps}^2 F_k^n(x,\phi)_{ps}\right\} = 0$$

and the boundary conditions for the free ended cylinder became equation (106):

$$(106)\quad \sigma_{ik}^n(x,\phi,t)\big|_{x=0,L} = 0 = \sum_{p=0}^{\infty}\sum_{s=1}^{\infty} S_{ik}^n(x,\phi)_{ps}\big|_{x=0,L}\, C_{ps}\, e^{i\omega_{ps}t}$$

Each p, s solution set independently and sequentially satisfy the equilibrium equations and the boundary conditions.

The original variation was presented in equation (39). Making use of the transformation to deformation coordinates (refer to equations (52-56), and of expressions (45-48), we recast the variation as follows:

$$(112)\quad 0 = \delta I = \int_t \int_x \int_\phi \underline{\underline{\Xi}}^n_k \, \delta U^n_k \, a \, d\phi \, dx \, dt + \int_t \int_{\Sigma_3} \Phi_k \, \delta U_k \, d\Sigma_3 \, dt + \int_t \int_C \left([P^n_k - \sigma^n_{ik} \bar{n} \cdot \bar{e}_i] \, \delta U^n_k \right)_c \, dC \, dt$$

In equation (112) $d\Sigma_3$ refers to the element of surface $(a \pm h)\, d\phi dx$, and C is the midsurface line. (See Figure 4). The term P^n_k is defined:

$$(113)\quad P^n_k|_c = \int_{-h}^{h} P_k|_c \left(1 + \frac{z}{a}\right) z^n \, dz \quad \text{or} \quad \int_{-h}^{h} P_k|_c \, z^n \, dz$$

Of the three terms in equation (112), the first includes the set of terms $\underline{\underline{\Xi}}^n_k$ (52-56). The second integral may be summarized:

$$(114)\quad \int_t \int_{\Sigma_3} \Phi \, \delta U_k \, d\Sigma_3 \, dt = \int_t \int_\phi \int_x \left(P_k(z) \mp \sigma_{3k}\right) \delta U_k (a+z)|_{h,-h} \, d\phi \, dx \, dt$$

Since in both free and forced vibration, δu_k on the cylindrical surface is <u>not</u> defined, equation (114) serves here

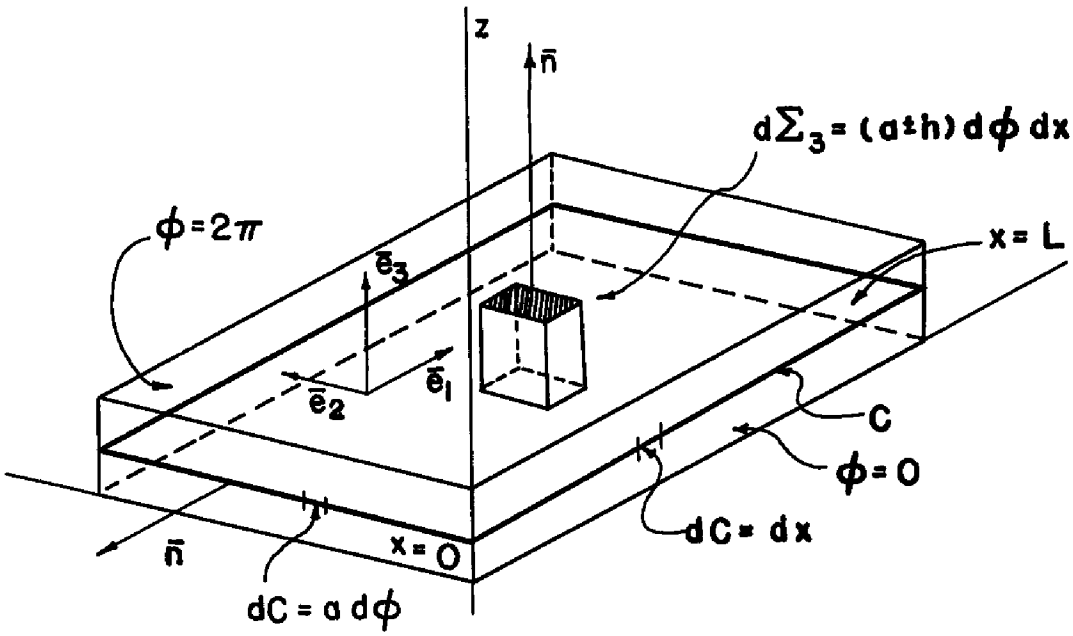

FIGURE 4: DEVELOPED CYLINDER SECTION

merely to emphasize that $P_k \mid h, -h = \pm\sigma_{3k}\mid h, -h$

Because of the equivalence of forces and deflections at $\phi = o$ and $\phi = 2\pi$, the third integral reduces to:

$$(115) \quad \int_t \int_\phi (P_k^n \mp \sigma_{ik}^n)(\delta U_k^n)\Big|_{x=0,L} \, a \, d\phi \, dt$$

in which

$$P_k^n\Big|_{x=0,L} = \int_{-h}^{h} P_k\Big|_{x=L,0} \left(1 + \frac{z}{a}\right) z^n \, dz$$

To solve the forced vibration Hamilton Integral, a proposed deformation function must:

a. Satisfy the third (boundary condition) integral

b. Satisfy the first (equilibrium) integral

c. Satisfy the limit of the integral as $\bar{P}$ and $\ddot{\bar{Y}}_B \to 0$ (i.e., the free vibration integral).

We propose a deformation function similar to equation (100), with the same function but a different time function:

$$(116) \quad \{U_k^n\} = \sum_{p=0}^{\infty} \sum_{s=1}^{\infty} q(t)_{ps} \{f_k^n(x,\phi)_{ps}\}$$

and will also require that:

(117) $$\underset{\ddot{\bar{P}},\ddot{Y}\to 0}{\text{Limit}}\; q(t)_{ps} = C_{ps}\, e^{i\omega_{ps}t}$$

The proposal follows the classical concept of the so-called "normal mode" method of solution.

The obvious reason for such a choice is that all the axial functions already found for the free vibration solution have satisfied the appropriate boundary conditions.

From an examination of equations (100) and (104), it is evident that were we to have used equation (116) for the free vibration problem, the set representing the five equations of equilibrium (104) would have become:

(118) $$\{H_k^n\} = \sum_{p=0}^{\infty}\sum_{s=1}^{\infty}\left[\Lambda_k^n\left(\{f_k^n(x,\phi)_{ps}\}\right) q(t)_{ps} - F_k^n(x,\phi)_{ps}\,\ddot{q}(t)_{ps}\right]$$

One of the equations would have read:

(119) $$H_k^n = \sum_{p=0}^{\infty}\sum_{s=1}^{\infty}\left[\Lambda_k^n\left(\{f_k^n(x,\phi)_{ps}\}\right) q(t)_{ps} - F_k^n(x,\phi)_{ps}\,\ddot{q}(t)_{ps}\right]$$

The difference between the term H_k^n and Ξ_k^n is in the existence of the terms dealing with P_k^+ and $\ddot{Y}_B(t)_k$. Thus, if equation (116) is now substituted into (112) we obtain:

$$(120)\quad 0 = \delta I = \int_t \iint_{k} \iint_{\phi} \Big[\Big(\sum_{p=0}^{\infty} \sum_{s=1}^{\infty} \Big[\Lambda_k^n \big(\{ f_k^n(x,\phi)_{ps} \} \big) q(t)_{ps} - F_k^n(x,\phi)_{ps} \ddot{q}(t)_{ps} \Big] \Big) + \Big\langle P_k^+ \Big(1+\frac{h}{a}\Big) h^n - \ddot{Y}_{B,k} 2\gamma h \cdot \frac{h^{2n}}{(3a)^n} \Big\rangle \Big] \big[\delta U_k^n \big] a \, d\phi \, dx \, dt$$

$$+ \int_t \iint_{\Sigma} \Phi_k \delta U_k \, d\Sigma_s \, dt$$

$$+ \int_t \iint_{\phi} P_k^n \delta U_k^n \big|_{x=L,0} - \delta U_k^n \Big(\sum_{p=0}^{\infty} \sum_{s=1}^{\infty} S_{ik,ps}^n \big(f_k^n(x,\phi)_{ps} \big) q(t)_{ps} \Big|_{x=0}^{x=L} a \, d\phi \, dt$$

We now recognize that the term δu_k^n also involves a doubly summed series. In order to distinguish the modal pairs in the δu_k^n term from those used elsewhere in (120), we call these by the indices m, N. The variation δu_k^n (with the space dependent function $f_k^n(x,\phi)_{mN}$ already defined) involves the variation of the time function $q(t)_{mN}$:

(121)

$$\delta U_k^n = \sum_{m=0}^{\infty} \sum_{N=1}^{\infty} f_k^n(x,\phi)_{mN} \, \delta q(t)_{mN} \qquad *$$

Now, we substitute equation (121) for δu_k^n into (120) to obtain:

---

* Note: We take $U_k^n(x,\phi,t,\alpha) = U_k^n(x,\phi,t,0) + \alpha \eta_k^n(x,\phi,t)$

$$= \sum_{m=0}^{\infty} \sum_{N=1}^{\infty} f_k^n(x,\phi)_{mN} \big[q(t,0)_{mN} + \alpha \Theta_{mN}(t) \big]$$

$$= \sum_{m=0}^{\infty} \sum_{N=1}^{\infty} f_k^n(x,\phi)_{mN} \, q(t,0)_{mN} + \alpha \sum_{m=0}^{\infty} \sum_{N=1}^{\infty} f_k^n(x,\phi)_{mN} \, \Theta(t)_{mN}$$

$$(122)\quad 0=\delta I=\int_{t}\sum_{m=0}^{\infty}\sum_{N=1}^{\infty}\delta q(t)_{mN}\Big[\iint_{x\,\phi}\Big[\Big(\sum_{p=0}^{\infty}\sum_{s=1}^{\infty}\Big[\Lambda_{k}^{n}\big(\{f_{k}^{n}(x,\phi)_{ps}\}\big)q(t)_{ps}-F_{k,ps}^{n}\ddot{q}(t)_{ps}\Big]\Big)$$
$$+\Big\langle P_{k}^{n}\Big(1+\frac{h}{a}\Big)h^{n}-\ddot{Y}_{B,k}\,2\gamma h\cdot\frac{h^{2n}}{(3a)^{n}}\Big\rangle\Big]f_{k}^{n}(x,\phi)_{mN}\,a\,d\phi\,dx\Big]dt$$
$$+\int_{t}\iint_{\Sigma_{3}}\bar{\Phi}_{k}\,\delta U_{k}\,d\Sigma_{3}\,dt$$
$$+\int_{t}\sum_{m=0}^{\infty}\sum_{N=1}^{\infty}\delta q(t)_{mN}\Big[\int_{0}^{2\pi}P_{k}^{n}f_{k}^{n}(x,\phi)_{mN}\big|_{x=L,0}\,a\,d\phi$$
$$-\sum_{p}^{\infty}\sum_{s}^{\infty}q(t)_{ps}\int_{0}^{2\pi}S_{1k,ps}^{n}\big(\{f_{k}^{n}(x,\phi)_{ps}\}\big)f_{k}^{n}(x,\phi)_{mN}\big|_{x=0}\,a\,d\phi\Big]dt$$

In equation (122), the second integral is equal to zero for arbitrary δu_{k}^{n}. The third integral is also equal to zero for arbitrary $\delta q(t)_{mN}$; as long as the deformation coordinates were chosen in the form of equation (116).

For free ended cylinders: (at x = 0 and x = L)

$$(123)\qquad P_{k}^{n}=0 \qquad \text{and} \qquad S_{1k,ps}^{n}\big(\{f_{k}^{n}(x,\phi)_{ps}\}\big)=0$$

For clamped end cylinders: (at x = 0 and x = L)

$$(124)\qquad r_{k,mN}^{n}=0 \qquad ; \qquad f_{k}^{n}(x,\phi)_{mN}=0$$

Note from preceding page:

therefore:

$$\delta U_{k}^{n}=\frac{\partial U_{k}^{n}}{\partial\alpha}\Big|_{\alpha=0}d\alpha=\sum_{m=0}^{\infty}\sum_{N=1}^{\infty}f_{k}^{n}(x,\phi)_{mN}\theta(t)_{mN}\,d\alpha=\sum_{m=0}^{\infty}\sum_{N=1}^{\infty}f_{k}^{n}(x,\phi)_{mN}\delta q(t)_{mN}$$

Because

$$\delta q(t)_{mN}=\frac{\partial q(t)_{mN}}{\partial\alpha}\Big|_{\alpha=0}d\alpha=\theta(t)_{mN}\,d\alpha$$

The entire third integral is thus demonstrated also to be zero, using the mode shapes which were developed individually in solving the free vibration problem.

Our assumed choice thus satisfied requirement a. Before examining the criteria involved in the satisfaction of requirement b (which will incorporate an orthogonality condition as a subsidiary requirement), we seek to demonstrate that requirement c is satisfied. This would necessitate using:

$$(117)\quad \lim_{\bar{P},\ddot{Y}_B \to 0} q(t)_{PS} = C_{PS} e^{i\omega_{PS} t}$$

to demonstrate that $\delta I|_{\bar{P},\ddot{Y}_B \to 0} = 0$

We write:

$$(125)\quad \delta I|_{\bar{P},\ddot{Y}_B \to 0} = 0 = \int_t \sum_m \sum_N \delta(C_{mN} e^{i\omega_{mN} t}) \Big[\sum_P \sum_S C_{PS} e^{i\omega_{PS} t} \iint_x \iint_\phi \Big\langle \Lambda^n_{K,PS}\left(f^n_{K,PS} + F^n_{K,PS}\, \omega^2_{PS} \right) \Big\rangle * f^n_K(x,\phi)_{mN}\, a\, d\phi\, dx \Big] dt$$

$$+ \int_t \int_{\Sigma_S} \Phi_K\, \delta U_K\, d\Sigma_S\, dt$$

$$+ \int \sum_m \sum_N \delta(C_{mN} e^{i\omega_{mN} t}) \Big[\int_0^{2\pi} P^n_K f^n_{K,mN}\Big|_{x=L,0} a\, d\phi$$

$$- \sum_P \sum_S C_{PS} e^{i\omega_{PS} t} \int_0^{2\pi} S^n_{IK,PS} f^n_{K,mN}\Big|_{x=0}^{x=L} a\, d\phi \Big] dt$$

Each component of this integral may readily be shown to be equal to zero for any arbitrary variation of $C_{mN} e^{i\omega_{mN} t}$. The terms within the brackets are the free vibration equilibrium equations (see (104)) and are equal to zero with each mode shape. Requirement c is therefore satisfied.

We now return to equation (122) for an examination of

the first integral when a forcing function is present For the Hamilton condition to be satisfied, it must be equal to zero for any arbitrary variation $q(t)_{mN}$. Therefore the term within the [ ] brackets must be brought to zero. This will require a minimization of each time coordinate, $\delta q(t)_{mN}$, (see equation (128)). Specifically, this requirement (the equilibrium equation) is written:

$$(125)\quad 0 = \int_x \int_\phi \sum_P^{\infty} \sum_S^{\infty} \Big[\Big(\Lambda^n_{k,PS} \big(\{ f^n_k(x,\phi)_{PS} \} \big) q(t)_{PS} - F^n_{K,PS} \ddot{q}(t)_{PS} \Big) + \Big(P^+_K \big(1 + \frac{h}{a}\big) h^n - \ddot{Y}_{B,K} 2\gamma h \cdot \frac{h^{2n}}{(3a)^n} \Big) \Big] * f^n_K(x,\phi)_{mN}\, a\, d\phi\, dx$$

To equation (125), add and subtract:

$$(126)\quad \int_x \int_\phi \sum_P \sum_S F^n_{K,PS}\, \omega^2_{PS}\, q(t)_{PS}\, f^n_K(x,\phi)_{mN}\, a\, d\phi\, dx$$

So that equation (125) becomes:

$$(125a)\quad \sum_P^{\infty} \sum_S^{\infty} q(t)_{PS} \int_x \int_\phi \Big(\Lambda^n_{k,PS} \big(\{ f^n_K(x,\phi)_{PS} \} \big) + F^n_{K,PS}\, \omega^2_{PS} \Big) * f^n_K(x,\phi)_{mN}\, a\, d\phi\, dx$$
$$- \sum_{P=0}^{m} \sum_{S=1}^{\infty} \Big[\ddot{q}(t)_{PS} + \omega^2_{PS}\, q(t)_{PS} \Big] \int_0^L \int_0^{2\pi} F^n_K(x,\phi)_{PS}\, f^n_K(x,\phi)_{mN}\, a\, d\phi\, dx$$
$$+ \int_0^L \int_0^{2\pi} \Big(P^+_K \big(1 + \frac{h}{a}\big) h^n - \ddot{Y}_{B,K} 2\gamma h * \frac{h^{2n}}{(3a)^n} \Big) * f^n_K(x,\phi)_{mN}\, a\, d\phi\, dx \equiv 0$$

In equation (125a) the first term does equal zero, because it contains the factor H^n_K, ps = 0.

Now if the following orthogonality requirement is satisfied:

(127) $$\iint_{x\,\phi} F^n_K(x,\phi)_{ps}\, f^n_K(x,\phi)_{mN}\, a\, d\phi\, dx \begin{cases} = 0 & m \neq p,\ s \neq N \\ \neq 0 & m = p,\ s = N \end{cases}$$

then the first integral of equation (125a) leads to the Lagrange equilibrium equations for principal (separable) time coordinates, as the coefficient of the arbitrary variation of these time coordinates:

(128) $$\delta I = 0 = \int_t \sum_{m}^{\infty} \sum_{N}^{\infty} \delta\, q(t)_{mN} \left[Q^E_{mN}(t) - M_{mN}\left(\ddot{q}(t)_{mN} + \omega^2_{mN}\, q(t)_{mN}\right)\right] dt$$

where the generalized mass associated with the mNth normal mode is:

(129)

$$M_{mN} = \int_x \int_\phi F^n_K(x,\phi)_{mN}\, f^n_K(x,\phi)_{mN}\, a\, d\phi\, dx \qquad *$$

---

* Note: For the classical model, the generalized mass is:

$$M_{mN} = 2\gamma h \iint_{x\,\phi} f^o_K(x,\phi)_{mN}\, f^o_K(x,\phi)_{mN}\, a\, d\phi\, dx$$

and the generalized force is:

$$Q^E(t)_{mN} = \iint_{x\,\beta} \left(P^+_K\left(1+\frac{h}{a}\right) + P_K - \ddot{Y}_{B,K}\, 2\gamma h\right) f^o_K(x,\phi)_{mN}\, a\, d\phi\, dx$$

where:

$$P_1 = 0$$

$$P_2 = P^+_2\left(1+\frac{h}{a}\right)\left(\frac{h}{a}\right)$$

$$P_3 = \frac{\partial P^+_1}{\partial x}(h)\left(1+\frac{h}{a}\right) + \frac{\partial P^+_2}{\partial \phi}\left(\frac{h}{a}\right)\left(1+\frac{h}{a}\right)$$

and the generalized external force in the "direction" of $q(t)_{mN}$ associated with that mode is:

$$(130)\quad Q^{*}(t)_{mN} = \int_{x}\int_{\phi} \left(P_{\kappa}^{*}\left(1+\frac{h}{a}\right)h^{n} - \ddot{Y}_{s,x}\,2\gamma h^{n}\frac{h^{2n}}{(3a)^{n}}\right) * f_{\kappa}^{n}(x,\phi)_{mN}\, a\, d\phi\, dx$$

The proof of required orthogonality is shown in Appendix E.

This proof is interesting because it proceeds from Hamilton's integral directly, and does not require examination of the actual mode shapes.

The following pre-conditions are necessary:

- The system must be linearly elastic, with no dissipation of energy internally possible.
- The mode shapes must satisfy the equilibrium equations for free vibration.
- The mode shapes must satisfy the boundary conditions.

It then rests on Betti's Law, which is an implicit generalization of Maxwell's Law of Reciprocal relations. Eventually, we demonstrate that since the natural frequencies for any two modal pairs are not equal, equation (127) must be satisfied.

8.2 Solution of the Forced Vibration Problem

With an assumed solution of the form:

$$(131)\quad \left\{U_{\kappa,mN}^{n}\right\} = \left\{ f_{\kappa}^{n}(x,\phi)_{mN}\right\} q(t)_{mN}$$

we have shown that the Lagrange equation (128) is to be satisfied. Equation (128) is repeated below for convenience:

$$(128)\quad \ddot{q}(t)_{mN} + \omega^2_{mN}\, q(t)_{mN} = \frac{Q(t)_{mN}}{M_{mN}}$$

The definitions for the generalized mass M_{mN} and the generalized force $Q(t)_{mN}$ are given in equations (129) and (130).

We now consider a forcing function which is arbitrary when taken as a function of x and ϕ, but restricted to a step time function from o to τ and zero thereafter. Thus, the forcing function is written:

$$(132)\quad \bar{P}^{+}(x,\phi,\tfrac{h}{2},t) = P^{+}_{k}\bar{e}_{k} = P_o\left[h(t) - h(t-\tau)\right]\bar{G}(x,\phi)$$

or, alternately:

$$(133)\quad P^{+}_{k}\,\bar{e}_{k} = P_o\left[h(t) - h(t-\tau)\right]G_{k}(x,\phi)\,\bar{e}_{k}$$

We note also that one of the terms required in equation (130) is $\ddot{Y}_B(t)_k$.

At this point, we should emphasize that although we have frequently referred to a "fixed-end" boundary, the constrained end structure equations are developed for the absolute (space-referenced) coordinate $\bar{r}$ and the c.g. motion is absorbed in this displacement coordinate. Therefore, any reference to the deformation coordinate u, and the rigid body displacement, $\bar{Y}$, refers to the free cylinder in space. The acceleration of $\bar{Y}_B(t)$ with respect to the space fixed origin, is then found by computing the resultant force acting on the whole body, and dividing by the entire mass:

$$(134)\quad \ddot{\bar{Y}}_B(t) = \frac{\int_x\int_\phi (\bar{P}\cdot\bar{\xi}_\rho)\,\bar{\xi}_\rho (a+h)\,d\phi\,dx}{\gamma\int_x\int_\phi\int_z (a+z)\,dz\,d\phi\,dx}$$

From (134) and, using (133), we may write the components of $\ddot{\bar{Y}}_B(t)$ along the body-fixed triad $\bar{e}_K$:

$$(135)\quad \ddot{Y}_B(t)_K = \ddot{\bar{Y}}_B(t)\cdot\bar{e}_K = \bar{\xi}_\rho\cdot e_K \left[\frac{P_o\left[h(t)-h(t-\tau)\right]\int_x\int_\phi \bar{G}(x,\phi)\cdot\bar{\xi}_\rho(1+\frac{h}{a})\,a\,d\phi}{4h\pi a L\gamma}\right]$$

We now apply the Laplace transform operation to equation (128) (assuming zero initial conditions).

$$(136)\quad q(s)_{mN} = \frac{Q(s)_{mN}}{(s^2+\omega^2_{mN})M_{mN}}$$

We find it convenient to use the following notation for generalized force:

$$(137)\quad Q(t)_{mN} = \int_x\int_\phi \left(b^n_K P^+_\kappa + C^n_\kappa \ddot{Y}_B(t)_K\right) * f^n_\kappa(x,\phi)_{mN}\,a\,d\phi\,dx$$

in which:

$$(138)\quad b^n_K = \left(1+\frac{h}{a}\right)h^n$$

$$(139)\quad C^n_K = -2\gamma h * \frac{h^{2n}}{(3a)^n}$$

In order to transform $Q(t)_{mN}$, we consider the transform first of the component (133) and then the transform of (134). We pause to note that the era of interest is $t > \tau$, and that we intend to consider the limit, of pure impulse ($P_o \tau$ constant as $\tau \to o$). The transform of (133) is:

$$(140)\quad P_k(s) = \mathcal{L}P_k(t) = \frac{P_o}{s} G_k(x,\phi)(1 - e^{-s\tau}) \qquad \text{For } t > \tau$$

Expanding the exponential term in (140):

$$(141)\quad P_k(s) = \frac{P_o G_k(x,\phi)}{s}\left[1 - \left(1 - s\tau + \frac{s^2\tau^2}{2} - \frac{s^3\tau^3}{3} + \dots\right)\right]$$

We now recognize that as $\tau \to 0$, the influence of the latter terms may be discounted. The expression becomes:

$$(142)\quad P_k(s)\Big|_{\tau \to o} = P_o \tau\, G_k(x,\phi)$$

In the same way we can write, for $t > \tau$, as $\tau \to o$ and $P_o \tau$ constant,

$$(143)\quad \ddot{Y}_\beta(s)_k = (\bar{\xi}_p \cdot \bar{e}_k)\frac{P_o \tau}{4\pi h a L \gamma} \int_x \int_\phi \left[\bar{G}(x,\phi) \cdot \bar{\xi}_p\right]\left(1 + \frac{h}{a}\right) a\, d\phi\, dx$$

We now transform equation (137), making use of (142) and (143):

(144)

$$Q(s)_{mN} = P_0 \tau \iint_x \iint_\phi \left\langle \left[b_K^n G_K(x,\phi) + \frac{C_K^n (\bar{\xi}_p \cdot \bar{e}_K)}{4\pi h a L \gamma} \int_x \int_\phi \bar{G}(x,\phi) \cdot \bar{\xi}_p \left(1 + \frac{h}{a}\right) a \, d\phi \, dx \right] * f_K^n(x,\phi)_{mN} \right\rangle a \, d\phi \, dx$$

We substitute (144) into (136), and at the same time, take the inverse Laplace transform:

$$(145)\quad q(t)_{mN} = \frac{P_0 \tau}{\omega_{mN} M_{mN}} \left[\iint_x \iint_\phi \left[b_K^n G_K(x,\phi) + \frac{C_K^n (\bar{\xi}_p \cdot \bar{e}_K)}{4\pi h a L \gamma} \int_x \int_\phi \bar{G}(x,\phi) \cdot \bar{\xi}_p \left(1 + \frac{h}{a}\right) a \, d\phi \, dx \right] f_{K,mN}^n \, a \, d\phi \, dx \right] \sin \omega_{mN} t$$

We substitute equation (145) in (131), and sum over all mN modes:

$$(146)\quad \left\{ U_K^n \right\}_{t>\tau} = \sum_{mN}^{\infty} \left\{ f_K^n(x,\phi)_{mN} \right\} \frac{P_0 \tau}{\omega_{mN} M_{mN}} \left[\int_x \int_\phi h^n G_K(x,\phi) f_K^n(x,\phi)_{mN} (a+h) \, d\phi \, dx - \left(\iint_x \iint_\phi \frac{G_L(x,\phi)(\bar{e}_L \cdot \bar{\xi}_p) a \, d\phi \, dx}{4\pi h a L \gamma} \right) \iint_x \iint_\phi (\bar{\xi}_p \cdot \bar{e}_K) \frac{h^{2n} (2\gamma h)}{(3a)^n} f_K^n(x,\phi)_{mN} (a+h) \, d\phi \, dx \right] \sin \omega_{mN} t$$

Equation (146), it should be recalled, is the solution to the problem for the <u>limiting case</u> of the <u>forcing function in equation (132)</u>.

We seek to compare this solution with the one to be derived for the "initial velocity" problem:

$$(147)\quad \left\{ U_K^n \right\}_{t=0} = 0 \qquad \left\{ \dot{U}_K^n \right\}_{t=0} \neq 0$$

For this we use the free vibration solution, equation (100),

repeated below for convenience:

$$(100)\quad \{U_k^n\} = \sum_m \sum_N \{f_k^n(x,\phi)_{mN}\} C_{mN} e^{i\omega_{mN}t}$$

We find it convenient to use the trigonometric equivalent (when adding the complex conjugate of the time term to (100):

$$(148)\quad \{U_k^n\} = \sum_m \sum_N \{f_k^n(x,\phi)_{mN}\}(A_{mN} \sin \omega_{mN}t + B_{mN} \cos \omega_{mN}t)$$

Since the initial displacement is taken equal to zero, the terms $B_{mN} \equiv 0$. Equation (148) reduces to:

$$(149)\quad \{U_k^n\} = \sum_m \sum_N \{f_k^n(x,\phi)_{mN}\} A_{mN} \sin \omega_{mN}t$$

Differentiate with respect to time, and substitute t = 0 to obtain:

$$(150)\quad \{\dot{U}_k^n\}_{t=0} = \sum_m \sum_N \{f_k^n(x,\phi)_{mN}\} \omega_{mN} A_{mN}$$

We select <u>one</u> coefficient A_{mN} for one frequency $\omega_{\underline{mN}}$ for examination. Multiply each one of the five equations represented in 150 by the appropriate $F_k^n(x,\phi)_{mN}$, and integrate over the limits of x and ø:

(151) $$\int_x \int_\phi (\dot{U}^n_k|_{t=0})(F^n_k(x,\phi)_{\underline{mN}}\, a\, d\phi\, dx = \int_x \int_\phi \sum_m \sum_N f^n_k(x,\phi)_{mN} F^n_k(x,\phi)_{\underline{mN}}\, \omega_{\underline{mN}}\, A_{\underline{mN}}\, a\, d\phi dx$$

Due to the orthogonality relationship (see Appendix E), only one term remains on the right hand side. Thus, for each nodal paid $\underline{mN}$:

(152) $$A_{\underline{mN}} = \frac{\int_x \int_\phi (\dot{U}^n_k|_{t=0})\, F^n_k(x,\phi)_{\underline{mN}}\, a\, d\phi\, dx}{\omega_{\underline{mN}} \int_x \int_\phi f^n_k(x,\phi)_{\underline{mN}}\, F^n_k(x,\phi)_{mN}\, a\, d\phi\, dx}$$

Thus, equation (149) becomes:

(153) $$\{U^n_k\} = \sum_m \sum_N \{f^n_k(x,\phi)_{mN}\} \left[\frac{\int_x \int_\phi (\dot{U}^n_k|_{t=0}) F^n_k(x,\phi)_{mN}\, a\, d\phi\, dx}{\omega_{mN} \int_x \int_\phi f^n_k(x,\phi)_{mN} F^n_k(x,\phi)_{mN}\, a\, d\phi\, dx} \right] \sin \omega_{mN} t$$

If we state $\dot{u}^n_k|_{t=0}$, equation (153) may be used to present the solution to the initial velocity problem.

In order to specify the initial velocity distribution, we examine the equilibrium equations for forced vibration, (53-57).

We make the important assumption that at very short times, no deformation or strain terms exist. These equations then reduce to:

(154)

a. $P_1^+(1+\frac{h}{a}) - 2\gamma h \ddot{Y}_B(t)\cdot\bar{e}_1 - 2\gamma h \frac{\partial^2 U_1^0}{\partial t^2} - \frac{2\gamma h^2}{3a}\frac{\partial^2 U_1^1}{\partial t^2} = 0$

b. $P_1^+ h(1+\frac{h}{a}) - \frac{2\gamma h^3}{3a}\ddot{Y}_B(t)\cdot\bar{e}_1 - \frac{2\gamma h^2}{3a}\frac{\partial^2 U_1^0}{\partial t^2} - \frac{2\gamma h^3}{3}\frac{\partial^2 U_1^1}{\partial t^2} = 0$

c. $P_2^+(1+\frac{h}{a}) - 2\gamma h \ddot{Y}_B(t)\cdot\bar{e}_2 - 2\gamma h \frac{\partial^2 U_2^0}{\partial t^2} - \frac{2\gamma h^2}{3a}\frac{\partial^2 U_2^1}{\partial t^2} = 0$

d. $P_2^+(h)(1+\frac{h}{a}) - \frac{2\gamma h^3}{3a}\ddot{Y}_B(t)\cdot\bar{e}_2 - \frac{2\gamma h^2}{3a}\frac{\partial^2 U_2^0}{\partial t^2} - \frac{2\gamma h^3}{3}\frac{\partial^2 U_2^1}{\partial t^2} = 0$

e. $P_3^+(1+\frac{h}{a}) - 2\gamma h \ddot{Y}_B(t)\cdot\bar{e}_3 - 2\gamma h \frac{\partial^2 U_3^1}{\partial t^2} = 0$

During the period $o < t < \tau$, P_k^+ is constant:

(155) $$P_k^+ = P_o G_k(x,\phi)$$

Since P_k^+ is constant, the acceleration $\ddot{Y}_{B,k}$ for $o < t < \tau$ is also constant, and by equation (135):

(156) $$\ddot{Y}_{B,k}(o<t<\tau) = (\bar{\xi}_p\cdot\bar{e}_k)\frac{P_o\int_x\int_\phi G_k(x,\phi)(\bar{e}_k\cdot\bar{\xi}_p)(1+\frac{h}{a})\,a\,d\phi\,dx}{4\pi h a L\gamma}$$

We now note that we can represent (154) in a shorthand (although not entirely satisfactory) manner:

$$(157)\quad P_k^+\left(1+\frac{h}{a}\right)h^n - 2\gamma h\frac{h^{2n}}{(3a)^n}\ddot{Y}_{B,K} - 2\gamma h * \frac{h^{2n}}{3^n}\ddot{U}_K^n - \frac{2\gamma h^3}{3a}\ddot{U}_K^{n\pm1} = 0$$

(In the last term, the plus and minus signs alternate in a, b, c and d).

Since $\ddot{u}_k^{\,n}$ and $\ddot{u}_k^{\,n+1}$ are constant during this interval, the velocity components are given by:

$$(158)\quad \dot{U}_K^n(\tau) = \int_0^\tau \ddot{U}_K^n(t)\,dt = \ddot{U}_K^n\tau$$

We solve (157) for $\ddot{u}_k^{\,n}$ and multiply by τ :

$$(159)\quad \dot{U}_K^n(\tau) = \ddot{U}_K^n\tau = (P_K^+\tau)\frac{3^n}{(2\gamma h)}\frac{(1+\frac{h}{a})h^n}{(h^{2n})} - \frac{3^n}{2\gamma h(h^{2n})}\cdot\frac{2\gamma h(h^{2n})}{(3a)^n}\ddot{Y}_{B,K}$$
$$-\frac{3^n}{2\gamma h}(h^{2n})\cdot\frac{2\gamma h^3}{3a}\cdot\ddot{U}_K^{n\pm1}\tau$$

Substituting for $P_k^{\,+}$ and $\ddot{Y}_{B,k}$:

$$(160)\quad \dot{U}_K^n(\tau) = \frac{1}{2\gamma h}\left[\frac{3}{h^2}\right]^2 P_0\tau G_K(x,\phi)\left(1+\frac{h}{a}\right)h^n$$
$$-\frac{1}{2\gamma h}\left[\frac{3}{h^2}\right]^n\frac{P_0\tau(\bar{\xi}_P\cdot\bar{e}_K)}{4\pi a L h\gamma}\int_x\int_\phi G_x(x,\phi)(\bar{e}_x\cdot\bar{\xi}_P)2\gamma h\left[\frac{h^2}{3a}\right]^n\left(1+\frac{h}{a}\right)a\,d\phi\,dx$$
$$-\frac{1}{2\gamma h}\left[\frac{3}{h^2}\right]^n\left[\frac{2\gamma h^3}{3a}\dot{U}_K^{n\pm1}(\tau)\right]$$

We now substitute equation (160) into equation (153) (noting that the demoninator of (153) can be expressed as M_{mN}). Note we are considering the initial velocity as

$\dot{u}_k^{\,n}(\tau)$ and that equation (153) will be valid for $t > \tau$

$$(161)\quad \left\{U_\kappa^n\right\}_{t>\tau} = \sum_m \sum_N \left\{f_\kappa^n(x,\phi)_{mN}\right\} \frac{\sin \omega_{mN} t}{\omega_{mN} M_{mN}} \left[P_0 \tau \iint_{x\,\phi} \frac{h^n}{2\gamma h}\left[\frac{3}{h^2}\right]^n G_\kappa(x,\phi) F_\kappa^n(x,\phi)_{mN}(a+h)\,d\phi\,dx \right.$$
$$- P_0\tau \iint_{x\,\phi} \frac{G_\rho(x,\phi)(\bar{e}_\rho \cdot \bar{e}_\rho)\,a\,d\phi\,dx}{4\pi a L h \gamma} \iint_{x\,\phi} 2\gamma h \left[\frac{h^2}{3a}\right]^n \frac{(\bar{\xi}_\rho \cdot \bar{e}_\kappa) F_\kappa^n(x,\phi)_{mN}(a+h)\,d\phi\,dx}{2\gamma h\left[\frac{h^2}{3}\right]^n}$$
$$\left. - \iint_{x\,\phi} 2\gamma h \left[\frac{h^2}{3a}\right]^n U_\kappa^{n\pm1}(\tau)\ \frac{F_\kappa^n(x,\phi)_{mN}}{2\gamma h\left[\frac{h^2}{3}\right]^n}\ a\,d\phi\,dx \right]$$

But we have used $F_k^{\,n}(x, \phi)_{mN}$ to refer to those portions of the solution multiplied by ω^2_{mN}. From equation (103) and (157):

$$(162)\quad F^n_{\kappa,mN} = 2\gamma h \left[\frac{h^2}{3}\right]^n f^n_{\kappa,mN} + \frac{2\gamma h^3}{3a} \rho^{n\pm1}_{\kappa,mN}$$

We substitute (162) into (161) to obtain:

$$(161a)\quad \left\{U_\kappa^n\right\}_{t>\tau} = \sum_m \sum_N \left\{f_\kappa^n(x,\phi)_{mN}\right\} \frac{\sin \omega_{mN} t}{\omega_{mN} M_{mN}} \left[P_0 \tau \iint_{x\,\phi} h^n G_\kappa(x,\phi) f_\kappa^n(x,\phi)_{mN}(a+h)\,d\phi\,dx \right.$$
$$- P_0\tau \iint_{x\,\phi} \frac{G_\rho(x,\phi)(\bar{e}_\rho \cdot \bar{e}_\rho)\,a\,d\phi\,dx}{4\pi a L \gamma} \iint_{x\,\phi} 2\gamma h \left[\frac{h^2}{3a}\right]^n (\bar{\xi}_\rho \cdot \bar{e}_\kappa) f_\kappa^n(x,\phi)_{mN}(a+h)\,d\phi\,dx$$
$$+ \frac{2\gamma h^3}{3a} + \left[\frac{3}{h^2}\right]^n \frac{1}{2\gamma h} \iint_{x\,\phi} \left\langle P_0 \tau\, G_\kappa(x,\phi) h^2 \left(1+\frac{h}{a}\right) - P_0 \tau \iint_{x\,\phi} \frac{G_\rho(x,\phi)(\bar{e}_\rho \cdot \bar{e}_\rho)\,a\,d\phi\,dx}{4\pi a L h \gamma} \right.$$
$$\left. * 2\gamma h \left[\frac{h^2}{3a}\right]^n (\bar{\xi}_\rho \cdot \bar{e}_\kappa)\left(1+\frac{h}{a}\right) - \frac{2\gamma h^3}{3a} U_\kappa^{n\pm1} \right\rangle f_\kappa^{n\pm1}(x,\phi)_{mN}\ a\,d\phi\,dx$$
$$\left. - \frac{2\gamma h^3}{3a} \iint_{x\,\phi} U_\kappa^{n\pm1}\, f_\kappa^n(x,\phi)_{mN}\ a\,d\phi\,dx \right]$$

The first two terms of (162) are identically equal to (146).

It remains to show that the latter four terms vanish.

Compare the section between $\langle\ \rangle$ brackets to equation (160), and it is then seen that the last four terms reduce to:

(163) $$+\frac{2\gamma h^3}{3a}\int_{x=0}^{L}\int_{\phi=0}^{2\pi}\left(\dot{U}_k^n(\tau)\, f_k^{n\pm1}(x,\phi)_{mN} - \dot{U}_k^{n\pm1}(\tau)\, f_k^n(x,\phi)_{mN}\right) a\, d\phi\, dx$$

In the integral the terms k, n, $n\pm1$ have the following values:

(164)

$k=1$	$n=0$	$n\pm1=1$
	$n=1$	$n\pm1=0$
$k=2$	$n=0$	$n\pm1=1$
	$n=1$	$n\pm1=0$
$k=3$	$n=0$	$n\pm1$ (not defined)

In the summation, the terms under the integral add to zero.

We conclude that equation (162) is identically equal to equation (146) in the limit, so that the forcing function problem and the initial velocity problem both yield the same answer.

We now briefly consider the characteristics of three typical radial forcing functions:

Cosine Frontal

The so-called "cosine frontal" loading is often used as a mathematical model for certain nuclear weapons effects on ICBM structures. In our nomenclature, the "cosine frontal" loading is specified:

(165)

a. $\text{For} \quad |\phi| < \frac{\pi}{2} \quad ; \quad \bar{P}^+ = -P_o \left[h(t) - h(t-\tau)\right] \cos\phi \; h(x) \bar{e}_3$

b. $\pi > |\phi| > \frac{\pi}{2} \quad ; \quad \bar{P}^+ = 0$

In expression (165a), h(t) and h(x) are unit step functions. τ represents the time duration of the pressure pulse. The load is thus seen to be directed radially inward, and symmetric in the xz plane with respect to ϕ=0, and uniform along the longitudinal axis.

The fact that the loading around the circumference exists only over the top half is mathematically cumbersome. We replace equations (165) by the equivalent expression involving a Fourier Series expansion in ϕ:

(166) $$P^+ = -\bar{e}_3 P_o \left[h(t) - h(t-\tau)\right] \sum_{p=0}^{\infty} b_p \cos p\phi$$

In equation (166), the Fourier coefficients are:

(167)

$$b_o = \frac{1}{\pi}$$

$$b_1 = 0.5$$

$$b_p = \frac{(-2)(-1)^{p/2}}{\pi(p^2-1)} \qquad p = 2, 4, 6, \cdots$$

$$b_p = 0 \qquad p = 1, 3, 5, \cdots$$

We see that this series, which includes all the even cosine waves, may not yield the most information, because the coefficients of the series diminish rapidly in magnitude.

A similar problem exists with respect to a Fourier series expansion in the x direction. The double series becomes:

$$(168) \qquad p^+ = -\varepsilon_3 P_o[h(t)-h(t-\tau)] \sum b_r \cos p\phi \sum_{r=1,3,5} a_r \sin \frac{\pi r x}{L}$$

The coefficients a_r are found by:

$$(169) \qquad a_r = \frac{4}{r\pi} \qquad r = 1,3,5.$$

and are also noted as diminishing rapidly in magnitude. In actual usage, it is much simpler to consider:

$$(170) \qquad G_3\left(\frac{x}{L}\right) = 1$$

In order to transmit force waves of shorter length in significant quantity, two other impulsive loads were considered.

Triangular Impulse

The space dependent function $G_3(x\ \phi)$ is symmetric about L/2 and ϕ =0 and is separable with respect to ϕ and x:

(171)

a. $G_3(\frac{X}{L}) = 2(\frac{X}{L})$ $\qquad 0 < X < \frac{L}{2}$

b. $G_3(\phi) = 1 - \phi\frac{2}{\pi}$ $\qquad 0 < \phi < \frac{\pi}{2}$

The Fourier expansion components in Ø are:

(172)

a. $b_0 = .25$

b. $b_p = \frac{4}{\pi^2 p^2}(1 - \cos p\frac{\pi}{2})$ $\qquad p = 1,2,3,4$

and would have a similar form in the x expansion.

Exponential Impulse

This is an approximation of a point impulse, symmetric about L/2 and Ø=0.

(173)

a. $G_3(\frac{X}{L}) = \frac{e^{20\frac{X}{L}R_1} - 1}{e^{10R_1} - 1}$; $R_1 = \frac{\ln 1000}{10}$ $\qquad 0 < X < \frac{L}{2}$

b. $G_3(\phi) = \frac{e^{(\frac{\pi}{2} - \phi)R_2} - 1}{e^{\frac{\pi}{2}R_2} - 1}$; $R_2 = \frac{\ln 1000}{\frac{\pi}{2}}$ $\qquad 0 < \phi < \frac{\pi}{2}$

The Fourier expansion components in Ø are:

(174)

a. $b_o = .0718$

b. $$b_p = \frac{.002}{\pi}\left[\left(\frac{4.396(1000-\cos\frac{p\pi}{2}) + p\sin\frac{p\pi}{2}}{4.396^2+p^2}\right) - \frac{\sin\frac{p\pi}{2}}{p}\right] \qquad p=1,2,3,4\ldots$$

and would have a similar form in the x expansion.

These latter (two) forcing functions are more revealing in comparing the response of the classical model to the SR model. Differences in response are more pronounced with normal modes of short structural wavelength.

Equation (146) can be put into a more concise form for these radial loads:

(175) $$\left\{U_k^n\right\} = \frac{P_o \tau (1+\frac{h}{a})}{2\gamma\omega_o \frac{h}{a} + a} \sum_{mN} \left\{f_k^n(x,\phi)_{mN}\right\} * A_{mN} \sin \Omega_{mN} t'$$

A normalizing factor was introduced for the natural frequency, ω_o, which is the lowest extensional frequency of a ring in plane strain:

(176) $$\omega_o = \left[\frac{E}{\gamma a^2(1-\nu^2)}\right]^{\frac{1}{2}}$$

Correspondingly, we write:

(177) $$\omega_{mN} = \Omega_{mN}\omega_o$$

in which Ω_{mN} is a non-dimensional parameter.

We will also define a normalized time, $t' = \omega_0 t$.

A_{mN} is the amplification factor of the mNth normal mode to a particular forcing function. It has the following form, if the cylinder is being analyzed according to the SR model:

(178)
$$A_{mN}(SR) = \left\langle b_m * \int_{t=0}^{t} f_3^0\left(\frac{x}{L}\right)_{mN} * G_3\left(\frac{x}{L}\right) d\left(\frac{x}{L}\right) - \left[b_1 \left(\int_{t=0}^{t} G_3\left(\frac{x}{L}\right) d\left(\frac{x}{L}\right) \right) \left(\int_{t=0}^{t} \left(f_3^0\left(\frac{x}{L}\right)_{mN} - f_2^0\left(\frac{x}{L}\right)_{mN} - \frac{1}{3}\left(\frac{h}{a}\right)^2 * a * f_2^1\left(\frac{x}{L}\right)_{mN} \right) d\left(\frac{x}{L}\right) \right) \right] \right\rangle$$
$$* {}^{-1} \left\{ \int_{t=0}^{t} \left(\left(f_1^0\left(\frac{x}{L}\right)^2_{mN} + f_2^0\left(\frac{x}{L}\right)^2_{mN} + f_3^0\left(\frac{x}{L}\right)^2_{mN} \right) + \frac{1}{3} h^2 \left(f_1^1\left(\frac{x}{L}\right)^2 + f_2^1\left(\frac{x}{L}\right)^2 \right) + \frac{2h^2}{3a} \left(f_1^1\left(\frac{x}{L}\right)_{mN} f_1^0\left(\frac{x}{L}\right)_{mN} + f_2^1\left(\frac{x}{L}\right)_{mN} f_2^0\left(\frac{x}{L}\right)_{mN} \right) \right) d\left(\frac{x}{L}\right) \right\}$$

and for the classical model:

(179)
$$A_{mN}(CL) = \left\langle b_m * \int_{t=0}^{t} f_3^0\left(\frac{x}{L}\right)_{mN} * G_3\left(\frac{x}{L}\right) d\left(\frac{x}{L}\right) - \left[b_1 \left(\int_{t=0}^{t} G_3\left(\frac{x}{L}\right) d\left(\frac{x}{L}\right) \right) \left(\int_{t=0}^{t} \left(f_3^0\left(\frac{x}{L}\right)_{mN} - f_2^0\left(\frac{x}{L}\right)_{mN} \right) d\left(\frac{x}{L}\right) \right] * {}^{-1} \left\{ \int_{t=0}^{t} \left(f_1^0\left(\frac{x}{L}\right)^2_{mN} + f_2^0\left(\frac{x}{L}\right)^2_{mN} + f_3^0\left(\frac{x}{L}\right)^2_{mN} \right) d\left(\frac{x}{L}\right) \right\} \right\rangle$$

The term in the [ ] brackets is due to rigid body acceleration of the center of gravity, and is disregarded in the case of the fixed-edge cylinder.

We proceed to consideration of the parameters to be used to evaluate the response of the structure to a forcing function.

According to the Mises-Hencky theory, plastic flow is initiated when the second invariant (I'_2) of the de-

viatoric stress tensor at a point reaches a certain maximum value. The second invariant (I'_2) may be conveniently expressed in terms of the stress components σ_{ik} as follows:

(180) $$I'_2(x,\phi,z,t) = \frac{1}{6}\left[(\sigma_{11}-\sigma_{22})^2+(\sigma_{22}-\sigma_{33})^2+(\sigma_{33}-\sigma_{11})^2+6(\sigma_{12}^2+\sigma_{13}^2+\sigma_{23}^2)\right]$$

The critical value for $I'_2(x,\phi,z,t)$ is determined by σ_o, the yield stress in simple (uniaxial tension:

(181) $$\frac{1}{3}\sigma_o^2 \geq I'_2(x,\phi,z,t)$$

A term called the "stress intensity", σ_r, has been defined as:

(182) $$\sigma_r = \frac{1}{\sqrt{2}}\left[(\sigma_{11}-\sigma_{22})^2+(\sigma_{22}-\sigma_{33})^2+(\sigma_{33}-\sigma_{11})^2+6(\sigma_{12}^2+\sigma_{13}^2+\sigma_{23}^2)\right]^{\frac{1}{2}}$$

Thus, the Mises-Hencky yield criterion may be stated simply as:

(183) $$\sigma_o \geq \sigma_r(x,\phi,z,t)$$

Clearly, then the parameter of interest is σ_r. Equation (183) determines whether or not plastic flow will be initiated, as well as when or where this will happen.

The deformation, stress and strain acting on planes normal to the cylinder surface (σ_{11}, σ_{22}, and σ_{12}) are maximum at either the inner or outer surfaces ($z=\pm h$). The

stress on the surface (σ_{31}, σ_{32}, and σ_{33}) is zero, once the initial impulsive pressure subsides.

For convenience, we examine the stress intensity at the inner and outer surface:

(184) $$\sigma_r(x,\phi,z,t)_{max} = \sigma_r(x,\phi,\pm h,t)$$

The stress intensity becomes:

(185) $$\sigma_r(x,\phi,h,t) = \frac{1}{\sqrt{2}}\left[(\sigma_{11}-\sigma_{22})^2 + \sigma_{22}^2 + \sigma_{11}^2 + 6\sigma_{12}^2\right]^{\frac{1}{2}}$$

Equivalently,

(186) $$\sigma_r(x,\phi,h,t) = \left[\sigma_{11}^2 + \sigma_{22}^2 - \sigma_{11}\sigma_{22} + 3\sigma_{12}^2\right]^{\frac{1}{2}}$$

In expression: C - 1,3 (at the cylinder's surface) :

(187)

a. $$\sigma_{11} = \frac{E}{1-\nu^2}(\epsilon_{11} + \nu\epsilon_{22})$$

b. $$\sigma_{22} = \frac{E}{1-\nu^2}(\epsilon_{22} + \nu\epsilon_{11})$$

c. $$\sigma_{12} = \frac{E}{1-\nu^2} \cdot \frac{1-\nu}{2} \cdot \gamma_{12}$$

The strain-deformation relations have also been previously developed. The pertinent results are repeated below:

(188)

a. $$\epsilon_{11}|_h = \frac{\partial U_1}{\partial x} = \frac{\partial U_1^\circ}{\partial x} + h\frac{\partial U_1'}{\partial x}$$

b. $$\epsilon_{22}|_h = \frac{1}{a+h}\left(\frac{\partial U_2}{\partial \phi} + U_3\right) = \frac{1}{a+h}\left[\frac{\partial U_2^\circ}{\partial \phi} + U_3^\circ + h\frac{\partial U_2'}{\partial \phi}\right]$$

c. $$2\epsilon_{12}|_h = \gamma_{12}|_h = \frac{\partial U_2}{\partial x} + \frac{1}{a+h}\frac{\partial U_1}{\partial \phi} = \frac{\partial U_2^\circ}{\partial x} + h\frac{\partial U_2'}{\partial x} + \frac{1}{a+h}\frac{\partial U_1^\circ}{\partial \phi} + \frac{h}{a+h}\frac{\partial U_1'}{\partial \phi}$$

Substituting into the stress-strain expressions:

(189)

a. $$\sigma_{11} = \frac{E}{1-\nu^2}\left[\frac{\partial U_1^\circ}{\partial x} + h\frac{\partial U_1'}{\partial x} + \frac{\nu}{a+h}\left(\frac{\partial U_2^\circ}{\partial \phi} + U_3^\circ + h\frac{\partial U_2'}{\partial \phi}\right)\right]$$

b. $$\sigma_{22} = \frac{E}{1-\nu^2}\left[\frac{1}{a+h}\left(\frac{\partial U_2^\circ}{\partial \phi} + U_3^\circ + h\frac{\partial U_2'}{\partial \phi}\right) + \nu\left(\frac{\partial U_1^\circ}{\partial x} + h\frac{\partial U_1'}{\partial x}\right)\right]$$

c. $$\sigma_{12} = \frac{E}{1-\nu^2}\left[\left(\frac{1-\nu}{2}\right)\left(\frac{\partial U_2^\circ}{\partial x} + h\frac{\partial U_2'}{\partial x} + \frac{1}{a+h}\frac{\partial U_1^\circ}{\partial \phi} + \frac{h}{a+h}\frac{\partial U_1'}{\partial \phi}\right)\right]$$

The solution to the free vibration problem, with the initial velocity specified, has been found, as equation (175), repeated below for convenience:

(175) $$\left\{U_k^n\right\} = \frac{P_0 \tau (1+\frac{h}{a})}{2\gamma\omega_0 \frac{h}{a}+a} \sum_m \sum_N \left\{f_k^n(x,\phi)_{mN}\right\} * A_{mN} \sin \Omega_{mN} t'$$

We now note that, for any one equation u_k^n,

(190) $$\frac{\partial U_k^n}{\partial x} = \frac{P_o \tau (1+\frac{h}{a})}{a \omega_o 2\gamma \frac{h}{a}} \sum_{mN} \frac{\partial f_{k,mN}^n}{\partial x} \left[A_{mN}\right] \sin \; t' \Omega_{mN}$$

(191) $$\frac{\partial U_k^n}{a \partial \phi} = \frac{P_o \tau (1+\frac{h}{a})}{a \omega_o 2\gamma \frac{h}{a}} \sum_{mN} \frac{\partial f_{k,mN}^n}{a \partial \phi} \left[A_{mN}\right] \sin \; t' \Omega_{mN}$$

The term $f_k^{\,n}(x,\phi)_{mN}$ is defined by equation (99) and (85). We see that, for each mN pair:

(192) $$\frac{\partial f_k^n}{\partial x} = \left(\frac{1}{a}\right) \frac{a}{L} \sum_{i=1}^{10} \mathcal{L}_{kmN;}^{n} \Gamma_{mN;} \lambda_{mN;} e^{\lambda_{mN;} \frac{x}{L}} (\cos m\phi \cup \sin m\phi)$$

(193) $$\frac{\partial f_k^n}{(a+h)\partial \phi} = \frac{m}{(1+\frac{h}{a})} \cdot \left(\frac{1}{a}\right) \sum_{i=1}^{10} \mathcal{L}_{kmN;}^{n} \Gamma_{mN;} e^{\lambda_{mN;} \frac{x}{L}} \frac{\partial(\cos m\phi \cup \sin m\phi)}{\partial(m\phi)}$$

Employing (192) and (193) in (190) and (191), the form of σ_{11}, σ_{22}, σ_{12} (refer to (189)) is seen to be typically:

(194) $$\sigma_{ps} = \frac{E}{1-\nu^2} * \frac{P_o \tau (1+\frac{h}{a})}{2\gamma \frac{h}{a} \omega_o a^2} \left[\sum_{mN} \left[A_{mN}\right] \sin \Omega_{mN} t' * \cos m\phi \cup \sin m\phi * \sum_{i=1}^{10} \Gamma_{mN;} e^{\lambda_{mN;} \frac{x}{L}} \mathcal{F}\left(\mathcal{L}_{kmN;}^{n}, \lambda_{mN;}, m, \frac{h}{a}, \frac{a}{L} \right) \right]_{ps}$$

In (185), the stress intensity σ_r is noted to involve the square root of the sum of several terms, each of which is a product $\sigma_{ps}\, \sigma_{qr}$. Thus:

(195) $$\sigma_r = \sqrt{\Sigma \sigma_{ps} \sigma_{qr}}$$

Examining (176), we now note the equivalent form:

(196) $$\sigma_r = \left(\frac{P_0 c}{2}\left(\frac{a}{h}\right)\left(1+\frac{h}{a}\right)\omega_0\right)\sqrt{\sum\left[\sum_{mn}\ \right]_{ps} * \left[\sum_{mn}\ \right]_{qr}}$$

where the terms in [ ] brackets are obtainable from (194). The dimensionless parameter $\bar{\sigma}_r(x,\phi,h,t)$ becomes:

(197) $$\bar{\sigma}_r\left(x,\phi,h,t,\frac{a}{L},\frac{h}{a}\right) = \sqrt{\quad} = \frac{\sigma_r(x,\phi,h,t)}{\frac{P_0 c}{2}(\omega_0)\left(1+\frac{h}{a}\right)\left(\frac{a}{h}\right)}$$

Equation (196) provides the basic tools necessary for parametric examination.

We expect that the value $\bar{\sigma}_r$ for a free-free cylinder will be greatest at $x = \frac{L}{2}$, $\phi = 0$, and for a clamped cylinder, at $x = 0$, $\phi = 0$. These are the points which have been examined in detail and $\bar{\sigma}_r$ vs t' has been computed and shown in Section X.

For a given cylinder the value of $\bar{\sigma}_r$ found using the five variable theory ($\bar{\sigma}_{r5}$) will be compared with the value of $\bar{\sigma}_{r3}$ found from the three variable theory.

These variables, for fixed and free cylinders, are a function of the cylinder geometry. They are tabulated, for all three forcing functions, at various series truncations.

IX - Computer Program

The preceding equations in Sections II - VIII have been programmed numerically in Fortran IV language and run on an IBM 360 computer. Extensive use of double precision is required and, accordingly, large storage capacity was necessary. The program described below can run for many hours, but has been run segmentally with successive frequency bandwidths.

9.1 Summary of Program Operation

Program Objective:

Evaluation of the total elastic response of a particular cylinder to different forcing functions as an accumulation of normal mode responses. The cylinder is modeled so that its resistance to elastic deformation is first in accordance with a classical shell theory and then in accordance with an SR theory.

Major Input Parameters:

An edge condition (fixed or free), thickness/radius ratio, length/radius.

Three different radially-directed, time impulsive type forcing functions whose spatial characteristics have been tabulated in the axial direction and expanded in a Fourier cosine series in the circumferential direction. This has been incorporated internally and is not necessary as data. The program can be revised to accept other forcing functions as data.

Procedure:

(a) There is an iterative scan to find all the classical model's natural frequencies and associated normal deformation modes which satisfy the boundary conditions. The initial scan is attempted from a low starting value to a pre-determined cut-off frequency. Successive frequency bandwidths are used in later runs. The transmissibility of a normal mode is found with each of the three impulsive velocity inputs whose spatial characteristics differ. The particle stresses developed at a chosen point on the cylinder's surface (fixed edges: x=o, ø=o, $z=+h$; free edges: x=$L/2$, ø=o, $z=+h$) which are associated with this modulated deformation wave are computed. The scan continues and more normal modes are found which are operated upon in the same manner. The cumulative stress from all the normal modes found are finally transposed into a stress intensity acting on this particle. The value of this stress intensity is recorded at 50 intervals during approximately 10 cycles of the lowest natural frequency. Three different sets (one for each of the forcing functions) of time-varying stress intensities are stored.

(b) The above procedure is repeated for the SR model.

(c) The stress intensity history (normalized to the maximum value attained for the Classical model) is tabulated for both the Classical and SR model, for each of the three forcing functions. The percentage difference between the maximum Classical and SR stress intensity developed during the time is recorded.

9.2 Subroutine Operating Details

MAIN: From the starting value of ω, at m = o, iterate ω to

ω_{max}. Then, m is increased and the above is repeated. At a value of m where no further natural frequencies are found, the run terminates.

DOT: Compute coefficients of the frequency/wave length eigenvalue (equation (108-a) for SR or its Classical theory equivalent).

POLROT: This is an IBM subroutine. Scan for roots of eigenvalue equation, i.e. $\lambda_i^2(\omega, m)$ $i = 1, 5U4$. Some of these will be complex.

BJCJ:

Compute $\mathcal{L}^n_{k,i} * [\mathcal{L}^*_{s,i}]^{-1}$ (108 b-e), the relative magnitudes of the axial function components.

Compute the axial function components $\mathcal{L}^n_{k,i} e^{\lambda_i x}$ and their derivatives at the edge. Only the real portion of complex conjugate terms are used. If these are true normal mode functions, (i.e. $\omega = \omega_{mn}$, natural frequency (see DETERM)), the values of the axial function over the cylinder's half length is computed.

Compute the coefficients of the boundary value matrix, (94) U (111) for the free cylinder or (84) U (111) for the fixed edge cylinder.

DETERM:

Compute the determinant of the boundary value matrix. The IBM subroutine MINV is used. This is a Gauss type procedure. For a thin and/or long cylinder an artificial determinant must be formed for the SR model. This is due to the great magnitude of the 5th λ_i^2 root, which causes extremely large and small coefficients in the boundary matrix. Now, there is a return to MAIN to test the magnitude and sign of the

determinant. If the value is not zero, either the forward scan of ω is continued if the sign of the determinant has not changed or the direction of scan is reversed by interval halving, if there was a crossover from plus to minus. When convergence in the crossover region is ascertained, we have a natural frequency and a normal deformation mode.

Compute the eigenvector $\Gamma_i = \Gamma_i^* [\Gamma_{10} U \Gamma_8]^{-1}$.
A set of non-homogeneous equations are formed when the last equation is extracted and $\Gamma_{10} U \Gamma_8$ is set equal to one .
An inversion of the left-hand matrix is done through MINV.
After Γ_i is computed, a test is made on all the original equations, including the extracted one. The total non-dimensional natural deformation function, $f_k^n(x,o) = (\sum_i \Gamma_i \chi_{ki}^n e^{\lambda_i t})$ (cos m ϕ U sinmϕ), is now available (see (77) and (99)).

RMN: The transmissibility factor, Amn, (see (178), (179)) is computed for each of the three forcing functions. The Generalized Force and Mass are computed with an integration procedure implementing the trapezoidal Rule.

SIA: The particle stresses due to the modulated normal deformation mode are computed at the proper spatial location, using (109) These stresses will vary in a sinusoidal manner determined by the natural frequency.

SIB: The total particle stresses from this and all normal modes are accumulated at 50 discrete time intervals. When the frequency scan cut-off is reached for both the SR and Classical models, the stress intensity history at this location is computed for both theories and tabulated. The percentage differences between the models are recorded.

SECTION X - COMPUTER RESULTS

The computational procedure described in the previous section was used to record the response of a free-free cylinder and a clamped cylinder to the three impulsive type forcing functions described in Section VIII, namely, the cosine frontal, triangular and exponential loadings. These are shown in (figure 14 (Section XI). In both cases, the cylinders examined were short, (a/L = .5), moderately thick, ($^h/_a$ = .025) with a Poisson's ratio (ν =.3) applicable to Steel or Aluminum. The response of the cylinder, with a particular forcing function, was first obtained with the restraint to elastic deformation considered as due to my Classical model and then a different response was obtained when my SR model determined this restraint. These responses were compared. The primary comparison parameter was the normalized stress intensity developed at a critical point on the cylinder's surface. For the free-free cylinder, this point was at x = $^L/_2$, ϕ = 0, z = + h, and for the clamped cylinder, x = 0, ϕ=0, z=+h . The comparison was conducted over approximately 10 cycles of the lowest natural frequency oscillation.

As stated previously, the method of analysis was the normal mode procedure. It is the accumulation of the normal mode deformations, whose amplitude directions are changing at an associated natural frequency, which creates a total stress pattern at a given time. The maximum amplitude of any modal deformation is determined by the congruence of its spatial characteristics to that of the impulsive forcing functions. In the sequence of computational events, it is necessary to first determine the normal deformation modes and their associated natural frequencies of oscillation. This was done by an iteration procedure through successive bandwidths of trial fre-

quencies. A partial listing of the natural frequencies discovered with the clamped cylinder, for both the SR model and the Classical model, in conjunction with the nodal pattern they are associated with, is shown in Table I. These results are presented graphically in figures 5 a-b. The significance of these findings is discussed in Section XI. The modes listed are those associated with frequencies found in a lower iteration bandwidth, $0 < \Omega < 5.00$, and are seen to be associated with the longest structural waves (m, N small). Table I and figures 5 a-b are concerned with only first branch frequencies, i.e. the first frequency found for a particular nodal deformation pattern.* Some higher branch frequencies were uncovered in this frequency bandwidth and are listed in Table II. Similar information was obtained for the free-free cylinder, within the frequency bandwidth, $0 < \Omega < 5.0$ and is presented in Table III, figures 6 a-b, and Table IV. A compilation of the higher natural frequencies and their associated mode shapes, uncovered in succeeding frequency bandwidth searches, for both cylinders, is available from the computer printouts but is not presented here.

As the frequency search bandwidth is extended, more normal modes, and modes of a different nature, i.e. those associated with shorter structural waves, are uncovered. The results of using a limited number of deformation modes to construct the stress intensity at the critical point, when a very low frequency bandwidth was investigated, are seen in

---

*Note: There are five frequencies associated with each nodal pattern for the SR model and three for the classical model.

figures 7 and 8. The stress history of both cylinders, according to the SR model and the Classical model, for the three different functions are presented. The percentage difference between the maximum stress intensities achieved by the Classical and SR models during this time, $\frac{\bar{\sigma}_r(CL)_{max} - \bar{\sigma}_r(SR)_{max}}{\bar{\sigma}_r(CL)_{max}}$, is noted. An extension of the bandwidth to an intermediate level permits the inclusion of shorter structural waves in the deformation pattern. The resulting stress intensity histories are presented in figures 9 and 10. A further extension of the bandwidth to a higher level will incorporate yet more terms in the stress series. The effect of this is shown in figures 11 and 12. All these curves are discussed in section XI.

TABLE I

TABULATION OF FIRST BRANCH NATURAL FREQUENCIES

FIXED, SHORT, THICK CYLINDERS

FREQUENCY BANDWIDTH 0.0-5.0

SR THEORY
CL THEORY

AXIAL WAVE NUMBER N	1	2	3	4	5	6
CIRCUMBERENTIAL WAVE NUMBERS m						
0	.9413206	.9615661	1.054321	1.172950	1.405679	1.730199
	.9423107	*.9620972*	*1.055481*	*1.183073*	*1.432106*	*1.781108*
1	.5882228	.8738103	1.001704	1.158125	1.388555	1.704712
	.5884256	*.8754699*	*1.007269*	*1.173783*	*1.423492*	*1.774696*
2	.3949330	.7022034	.9204603	1.128390	1.387477	1.713612
	.3957091	*.7045150*	*.9272837*	*1.165394*	*1.426591*	*1.789436*
3	.3097141	.5848122	.8457765	1.101724	1.393019	1.738719
	.3112829	*.5852178*	*.8549937*	*1.123138*	*1.437217*	*1.820515*
4	.3185976	.5251021	.8160527	1.101521	1.419151	1.782873
	.3211099	*.5263043*	*.8290813*	*1.128580*	*1.471039*	*1.874301*
5	.4041968	.6020311	.8456828	1.141494	1.474896	1.851769
	.4092459	*.6080998*	*.8642770*	*1.176383*	*1.537052*	*1.956052*
6	.5407767	.6959557	.9327559	1.225917.	1.564992	1.948942
	.5503199	*.7112410*	*.9591328*	*1.271222*	*1.640482*	*2.069684*
7	.7128448	.8495336	1.068548	1.352860	1.690410	2.075975
	.7295713	*.8733178*	*1.105615*	*1.417715*	*1.782847*	*2.217345*
8	.9137881	1.039092	1.244058	1.517845	1.849743	2.232870
	.9412368	*1.075017*	*1.295604*	*1.594339*	*1.963452*	*2.399569*
9	1.140535	1.258362	1.452593	1.7.6.92	2.040523	2.418515
	1.183183	*1.310981*	*1.523291*	*1.815140*	*2.18065*	
10	1.391247	1.503693	1.689543	1.943933	2.260116	
	1.454572	*1.578569*	*1.785068*	*2.071172*	*2.432773*	*2.866308*

TABLE I - (CONTINUED)

TABULATION OF FIRST BRANCH NATURAL FREQUENCIES

FIXED, SHORT, THICK CYLINDERS

FREQUENCY BANDWIDTH 0.0-5.0

SR THEORY
CL THEORY

AXIAL WAVE NUMBER N	1	2	3	4	5	6
CIRCUMFERENTIAL WAVE NUMBERS m						
11	1.664513	1.772744	1.951764	2.198007		2.869823
	1.755042	*11876471*	*2.078812*	*2.360312*	*2.718066*	*3.149159*
12	1.959087	2.063780	2.237069	2.475780	2.775780	3.131874
	2.084421	*2.204062*	*2.403319*	*2.681151*	*3.035487*	*3.460125*
13	2.273788	2.375390	2.543448		3.067773	3.415956
	2.442636			*3.032714*	*3.384120*	*3.810155*
14		2.706249		3.095351	3.380268	3.720605
		2.946776	*3.141835*	*3.414421*	*3.763280*	*4.186952*
15	2.959081		3.214003	3.433865	3.711816	4.044374
	3.243125	*3.361562*	*3.555189*	*3.825780*	*4.172401*	*4.594099*
16	3.327441	3.420937	3.576655	3.789940	4.061073	4.385894
	3.3689745	*3.805312*	*3.997633*	*4.266561*		
17	3.711523	3.802577	3.95338	4.162175	4.426685	4.744140
	4.162890	*4.277731*	*4.469072*	*4.736620*		
18	4.110312	4.199124	4.345983	4.549640	4.807812	
	4.664687	*4.778968*	*4.969421*			
19	4.522890	4.609436	4.752655	4.951233		
20	4.948388					

TABLE I - (CONTINUED)

TABULATION OF FIRST BRANCH NATURAL FREQUENCIES

FIXED, SHORT, THICK CYLINDERS

FREQUENCY BANDWIDTH 0.0-5.0

SR THEORY
CL THEORY

AXIAL WAVE NUMBER N	7	8	9	10	11	12
CIRCUMFERENTIAL WAVE NUMBERS m						
0	2.105402 *2.203218*	2.566073 *2.728258*	3.074218 *3.150856*	3.658007 *4.016033*	4.279823	4.719530
1	2.08807	2.538085 *2.738671*	3.037011 *3.324244*	 *4.028163*	4.184374 *4.688866*	
2	2.104521	2.557323	3.065526		4.213085	
3	2.142480 *2.283962*		3.111094 *3.455956*	3.665624 *4.120116*	4.299843 *4.887499*	4.889940
4	2.197909	2.664745 *2.894237*	 *3.514452*	3.731737	4.328397 *4.976464*	4.958397
5	2.275741 *2.443892*	2.746581	 *3.677929*	3.819335	4.414100	
6	2.378476 *2.568219*	2.852831 *3.125097*	3.370058 *3.756581*	3.927772 *4.458943*	4.521936	
7	2.507480 *2.716894*	2.983105 *3.283730*	3.500526 *3.919335*		4.658788	
8	2.663183 *2.902343*	3.137733 *3.472597*	3.653710 *4.111523*	4.208291 *4.855077*		
9	2.845214 *3.120019*	3.316640 *3.692284*	3.829589 *4.333437*	4.380897	4.967577	
10	3.052636 *3.369960*	3.519276 *3.942968*	4.027815	4.574843		

TABLE I - (CONTINUED)

TABULATION OF FIRST BRANCH NATURAL FREQUENCIES

FIXED, SHORT, THICK CYLINDERS

FREQUENCY BANDWIDTH 0.0-5.0

SR THEORY
CL THEORY

AXIAL WAVE NUMBER N	7	8	9	10	11	12
CIRCUMFERENTIAL WAVE NUMBERS m						
11	3.284316 *3.651515*	3.745019 *4.224648*	4.247987 *4.867480*	4.789550		
12	3.539002 *3.965038*	3.992870 *4.537148*	4.489198			
13	3.815331 *4.309316*	4.261659 *4.880370*	4.750683			
14	4.111952 *4.684276*	4.550275				
15	4.427609	4.857714				
16	4.761034					
17						
18						
19						
20						

First Branch Natural Frequencies - Fixed, Short, Thick, Cylinder

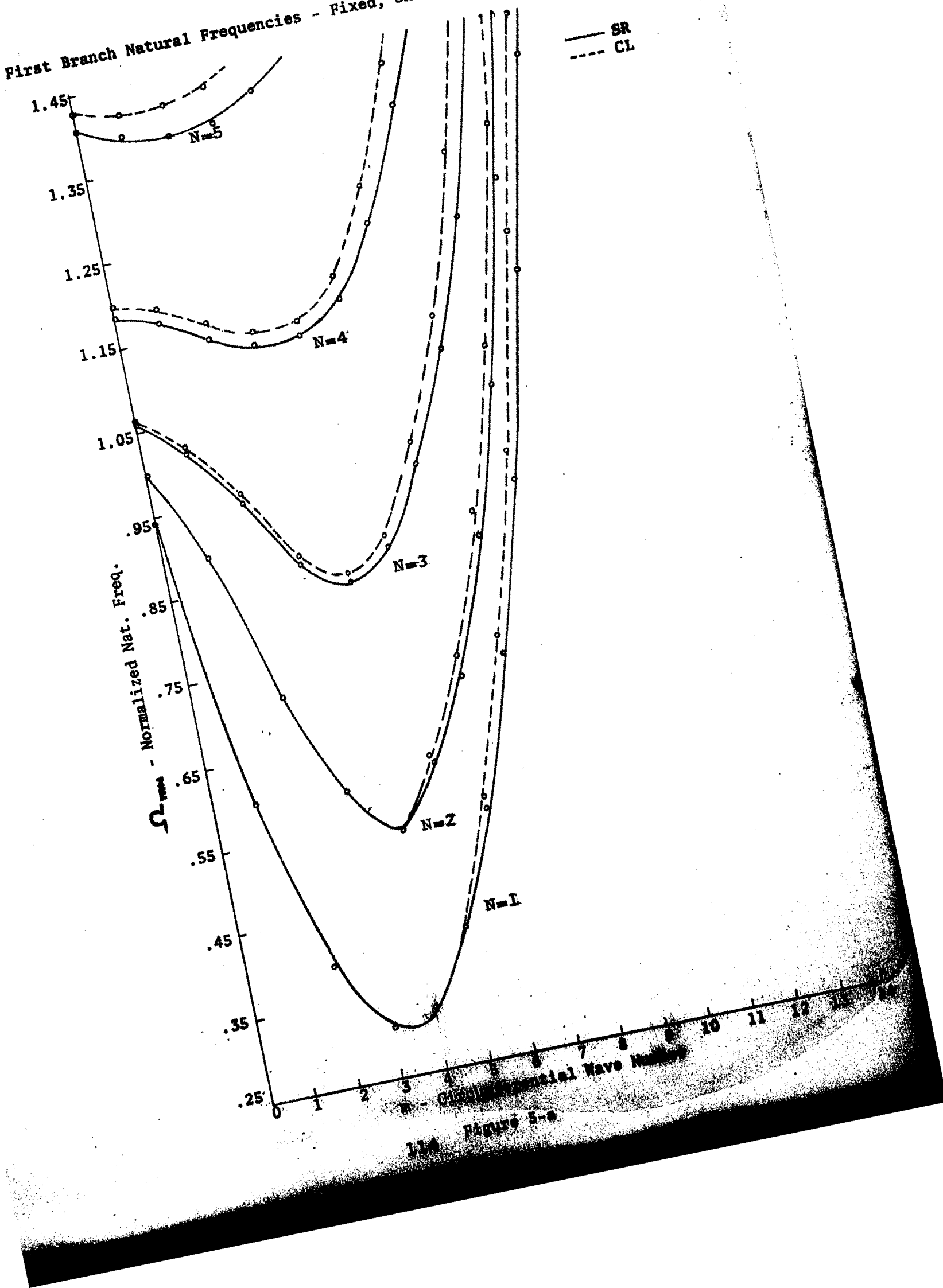

Figure 5-a

First Branch Natural Frequencies - Continued

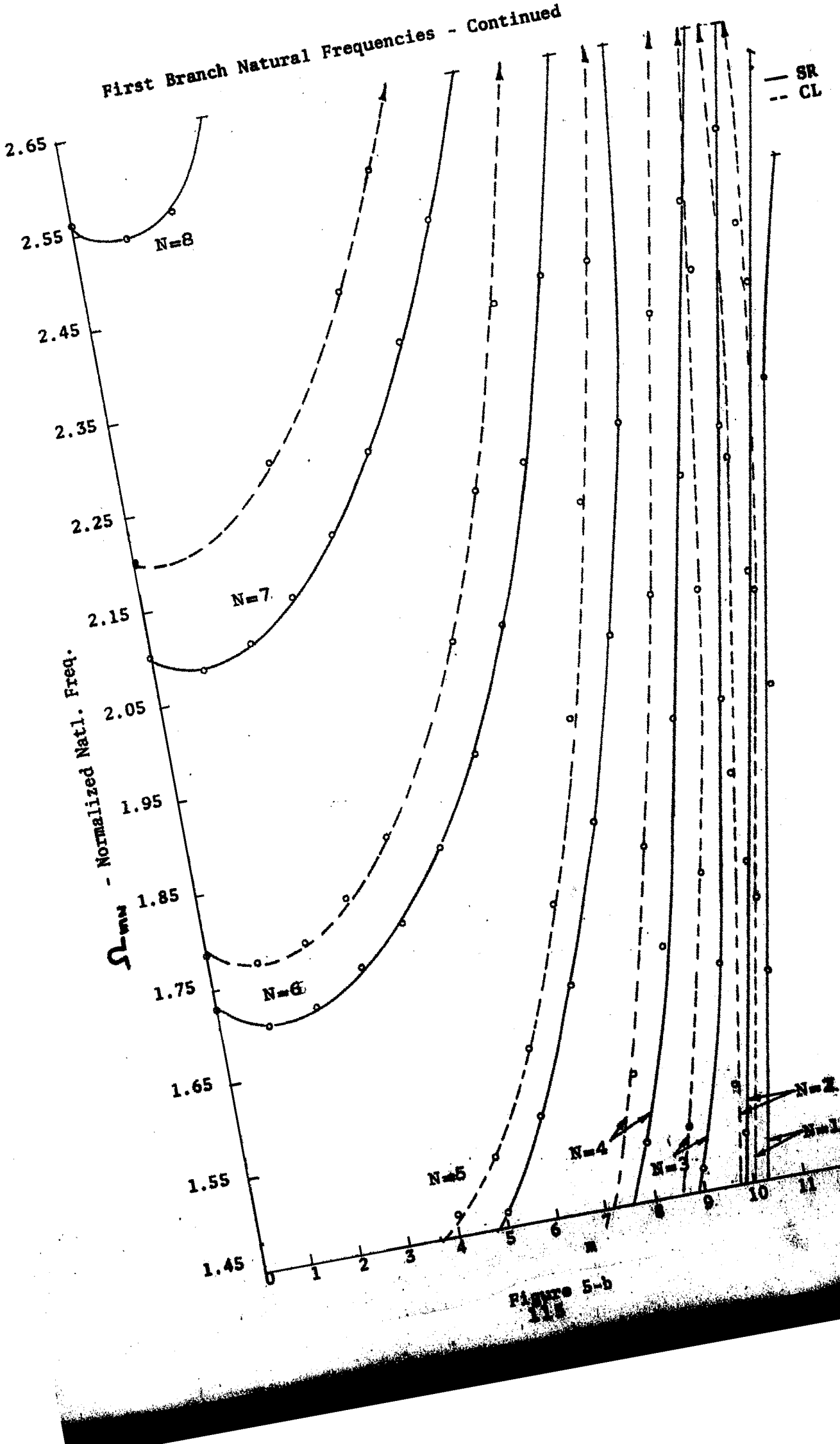

Figure 5-b

TABLE II

TABULATION OF HIGHER BRANCH NATURAL FREQUENCIES

FIXED, SHORT, THICK CYLINDERS

FREQUENCY BANDWIDTH 0.0-6.0

SR THEORY
CL THEORY

AXIAL WAVE NUMBER N	1	2	3	4	5	6
CIRCUMFERENTIAL WAVE NUMBERS m						
0	3.165956					
	3.337223			*3.755566*		*4.721666*
1	1.031983	2.225155				
	1.032169		*3.383752*		*2.779140*	
			3.799413			
2		1.769577	2.225142			
		1.769010	*2.931347*			
3	1.775826	2.162123	2.818652			
	1.775835	*2.163294*	*4.294781*	*3.897753*		*4.223183*
4			4.225917			
	3.240468					
5						
		3.168546			*4.921679*	
6		3.717089				
			4.199425	*4.734081*		
				3.717480		
7						4.280663
			4.651366	*4.280413*		

TABLE III

TABULATION OF FIRST BRANCH NATURAL FREQUENCIES

FREE, SHORT, THICK CYLINDERS

FREQUENCY BANDWIDTH 0.0-5.0

SR THEORY
CL THEORY

AXIAL WAVE NUMBER N	1	2	3	4	5	6
CIRCUMFERENTIAL WAVE NUMBERS m						
0	.9286233			.9750750	1.042047	1.181628
	.9286188			*.9764170*	*1.045221*	*1.190442*
1		.0084358	.8412119	.9424426	1.030774	1.180931
			.8395546	*.9391896*	*1.029425*	*1.187571*
2		.0865702	.6138657	.8241521	1.007369	1.087153
		.0507866	*.6035942*	*.8123505*	*.9896801*	*1.088228*
3		.1736945	.4734239	.7493637	.9864024	1.220427
		.1288002	*.4420542*	*.7177870*	*.9498333*	*1.088228*
4		.2764208	.4649198	.7280065	.9969982	1.220427
		.2315641	*.4102197*	*.6747337*	*.9404554*	*1.187822*
5	.3437369	.4019967	.5489328	.7810563	1.055863	1.356669
	.3350977	*.3612658*	*.4860213*	*.7123273*	*.9844017*	*1.287445*
6	.4984192	.5544369	.6853738	.8952364	1.163903	1.473880
	.4918690	*.5188380*	*.6258263*	*.8225726*	*1.086248*	*1.287445*
7	.6792147	.7341237	.8572091	1.053827	1.314195	1.625142
	.6774304	*.7046830*	*.8062055*	*.9869550*	*1.240139*	*1.553340*
8	.8851662	.9398466	1.052828	1.246553	1.499473	1.807714
	.8917329	*.9189775*	*1.019090*	*1.192286*	*1.437744*	*1.748729*
9	1.111528	1.170200	1.285577	1.467943	1.714532	2.018554
	1.134744	*1.161804*	*1.261903*	*1.431820*	*1.672685*	*1.981152*
10	1.368534	1.423890	1.537057	1.714815	1.955859	
	1.406447	*1.433205*	*1.533784*	*1.702464*	*1.940820*	

TABLE III - (CONTINUED)

TABULATION OF FIRST BRANCH NATURAL FREQUENCIES

FREE, SHORT, THICK CYLINDERS

FREQUENCY BANDWIDTH 0.0-5.0

SR THEORY
CL THEORY

AXIAL WAVE NUMBER N	1	2	3	4	5	6
CIRCUMFERENTIAL WAVE NUMBERS m						
11	1.643867	1.699706	1.811230	1.985097		
	1.706827	*1.733206*	*1.834472*	*2.002871*		*2.545703*
12	1.940234	1.996546	2.106531	2.276953	2.508046	2.796927
	2.035937	*2.061859*	*2.163762*	*2.332324*		*2.874355*
13	2.256484	2.313187	2.421843	2.589093	2.815640	3.099140
	2.393593		*2.521703*	*2.690593*	*2.927609*	*3.232749*
14	2.591562	2.648499	2.755906		3.142296	3.420507
	2.779999		*2.908265*	*3.077546*	*3.314941*	*3.620253*
15	2.944296	3.001468	3.107702	3.269042	3.486855	3.759708
	3.194999	*3.219437*	*3.323437*	*3.493203*	*3.730911*	*4.036643*
16	3.313749	3.370999	3.476062	3.634562	3.848140	4.115702
	3.638670	*3.662562*	*3.767150*	*3.937351*	*4.175544*	*4.481738*
17	3.698906	3.756078	3.859968	4.015734	4.225093	4.487402
	4.110937	*4.134281*	*4.239507*	*4.410156*	*4.648769*	*4.955404*
18	4.098671	4.155765	4.258398	4.411464	4.616684	4.873280
			4.740524	*4.911464*		

TABLE III - (CONTINUED)

TABULATION OF FIRST BRANCH NATURAL FREQUENCIES

FREE, SHORT, THICK CYLINDERS

FREQUENCY BANDWIDTH 0.0-5.0

SR THEORY
CL THEORY

AXIAL WAVE NUMBER N	7	8	9	10	11	12
CIRCUMFERENTIAL WAVE NUMBERS m						
0	1.409564	1.726055		3.705370	4.339550	
	1.143119	*1.771124*	*3.332643*	*4.016665*	*4.777659*	
1	1.411788	1.725346	3.080055	3.640956		
	1.436011	*1.780468*				
2	1.445433	1.770117	3.128066	3.687402	4.289746	4.929960
	1.452611	*1.809570*		*4.074454*		
3	1.503397	1.852315		3.764550		
	1.487122	*1.865327*		*4.146777*	*4.900039*	
4	1.584365	1.935546	3.317578	3.871523	4.466894	
	1.546080	*1.936230*				
5	1.689653	2.061230	2.475585	4.006347	4.597558	
	1.635932	*2.043359*	*2.800330*	*4.379296*		
6	1.820996	2.206288	2.631542		4.753808	
	1.761035	*2.160597*				
7	1.979101	2.373046	2.806048	4.344921	4.926183	
	1.927389	*2.351171*		*4.730120*		
8	2.163417	2.561718	2.999843	4.559118	4.377578	
	2.120996	*2.554394*		*4.943984*		
9	2.372949	2.772402	3.247392	4.734667		
	2.354101	*2.790371*	*4.489160*	*4.897207*		
10	2.606347	3.004433	3.444628	3.923476	4.437304	
	2.620312	*3.058242*	*4.765624*			

TABLE III - (CONTINUED)

TABULATION OF FIRST BRANCH NATURAL FREQUENCIES

FREE, SHORT, THICK CYLINDERS

FREQUENCY BANDWIDTH 0.0-5.0

SR THEORY
CL THEORY

AXIAL WAVE NUMBER N	7	8	9	10	11	12
CIRCUMFERENTIAL WAVE NUMBERS m						
11	2.862109	3.257128	3.695449	4.173027	4.686230	
	2.918398	*3.357226*	*3.862050*			
12	3.139121	3.529882	3.964784	4.439648		
		3.686621	*4.192714*			
13	3.436035	3.821718	4.252050	4.722988		
	3.605566	*4.045742*	*4.552832*			
14	3.751601	4.131737	4.556738			
	3.993483	*4.434179*	*4.942226*			
15	4.084970	4.458984	4.877968			
	4.410351	*4.851699*				
16	4.434960	4.458984				
	4.855898					
17	4.800527					
18						

First Branch Natural Frequencies - Free, Short, Thick, Cylinder

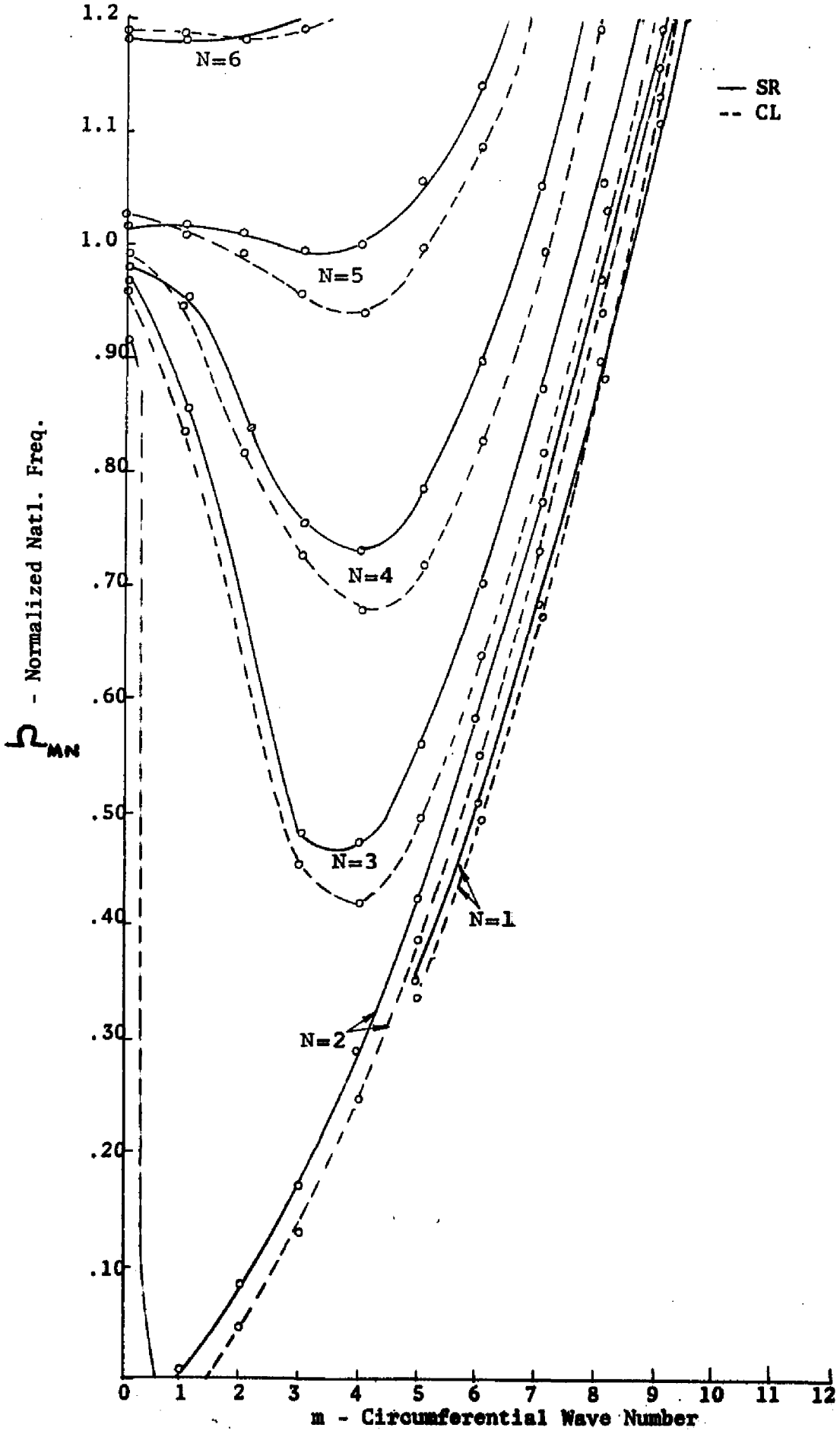

Figure 6-a

First Branch Natural Frequencies - Continued

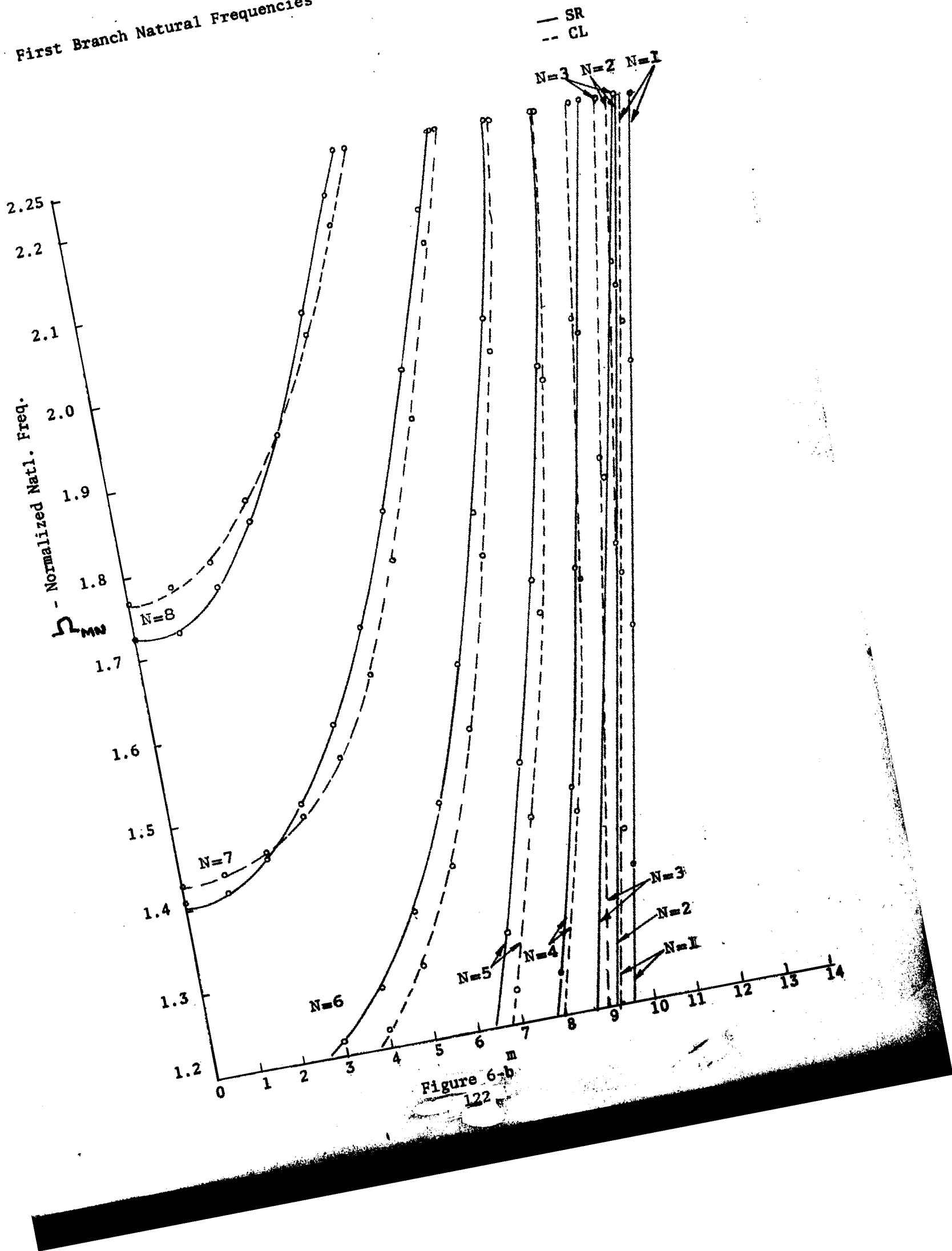

Figure 6-b

TABLE II

TABULATION OF HIGHER BRANCH NATURAL FREQUENCIES

FREE, SHORT, THICK CYLINDERS

FREQUENCY BANDWIDTH 0.0 - 5.0

SR THEORY
CL THEORY

AXIAL WAVE NUMBER N	1	2	3	4	5	6
CIRCUMFERENTIAL WAVE NUMBERS m			1.614382			4.689941
		3.157830	*1.614285*		*3.750961*	*4.690039*
			2.250195			
0			4.722695			
			4.722637			
	.5916865	.736975	3.378808			
	.5916865	*.736909*	*2.250488*			
1	1.238423	1.522940				
	1.238633	*1.523183*				
	1.601309					
	1.601231					
	1.183707		1.537880	1.087453		
2	*1.775292*	*2.164687*	*1.536083*	*1.088228*	*3.829271*	
				2.911171		
				3.80869		
3	3.074804					1.60557
	3.075273	*4.279882*				*1.604365*
4		4.760976				
		3.028789	*3.688281*			
				4.735781		
5	*2.913051*			*3.452124*		
				4.736757		
6	*3.553320*					
7	*4.14588*					
8	*4.730312*					

Fixed, Short, Thick Cylinder
Stress Intensity History at x=o, ϕ=o

Cut-off frequency, 0.9

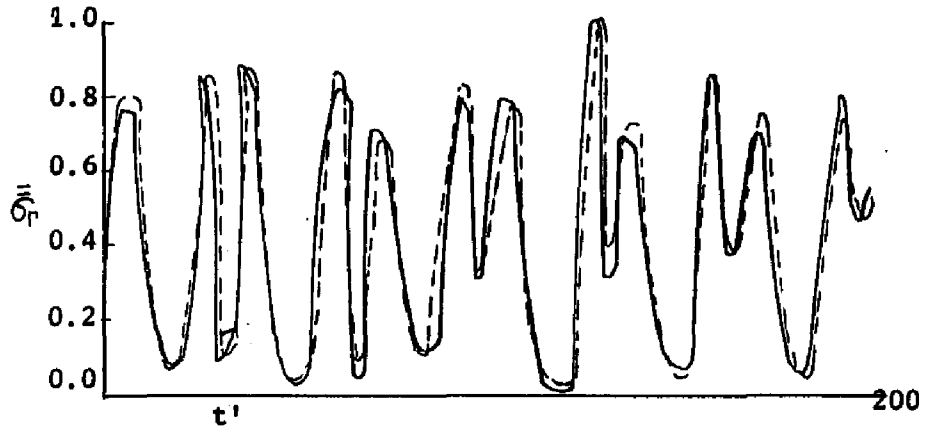

Cosine Frontal Impulse

%Difference + 1.96

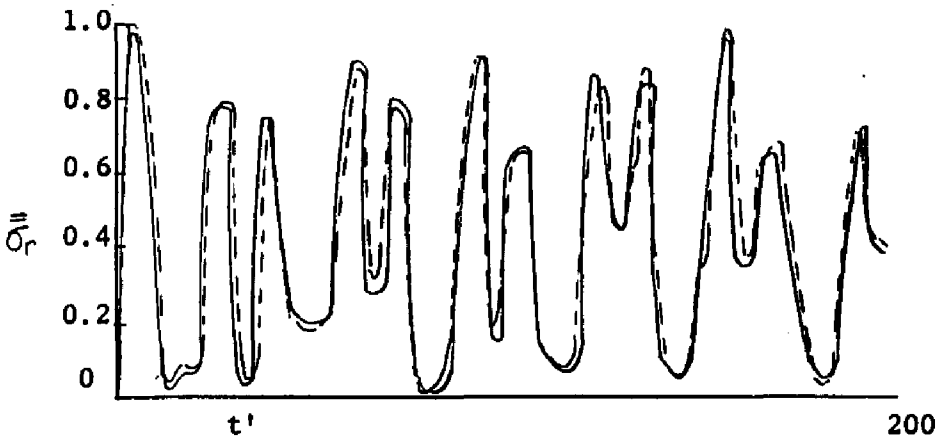

Triangular Impulse

% Difference + 2.71

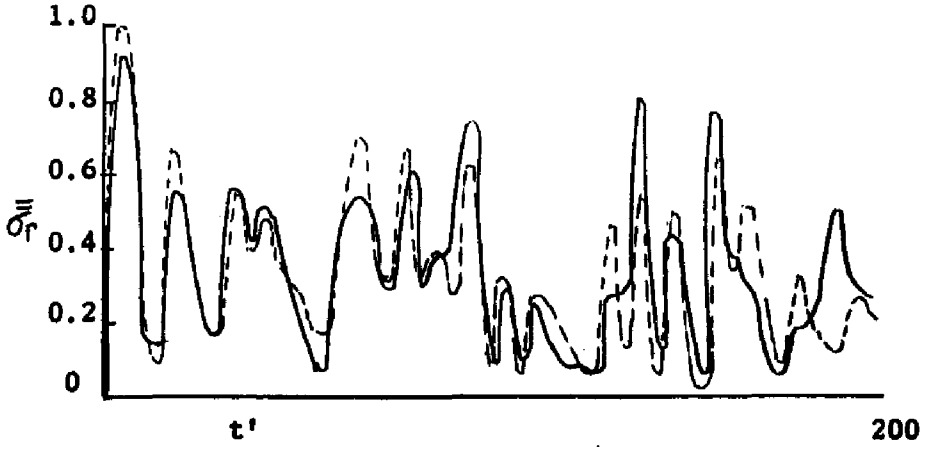

Exponential Impulse

% Difference + 5.36

Figure 7

Free, Short, Thick Cylinder Cut-Off frequency, 0.7
Stress Intensity History at $x=L/_2, \phi=o$

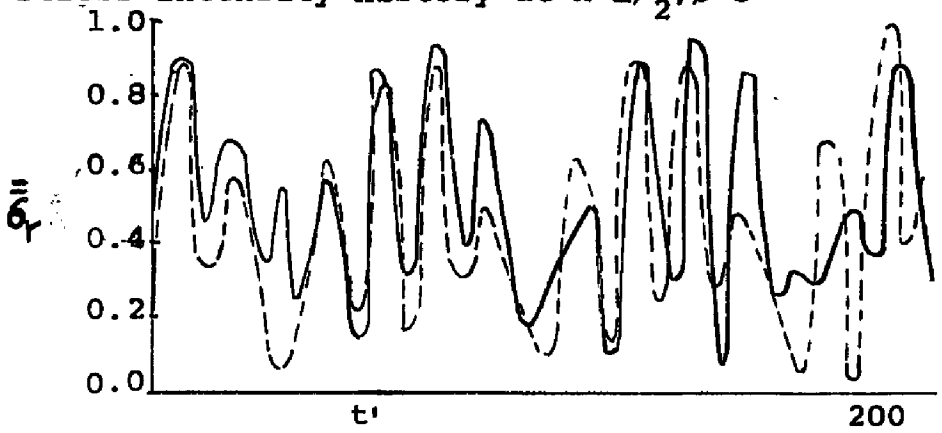

% Difference (of Maximum Stress Intensity)

$$= \left[\frac{\bar{\sigma}_{r(CL)_{max}} - \bar{\sigma}_{r(SR)_{max}}}{\bar{\sigma}_{r(CL)_{max}}}\right] \times 100$$

Cosine Frontal Impulse

% Difference + 4.234

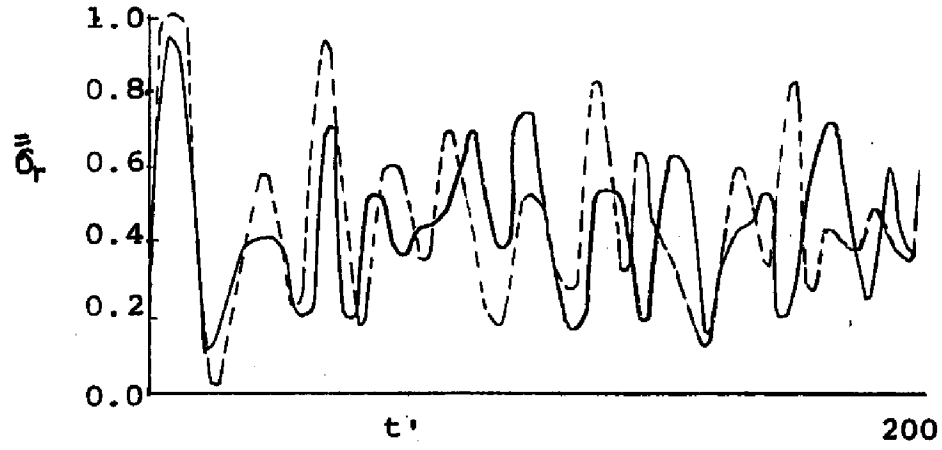

Triangular Impulse

% Difference + 5.31

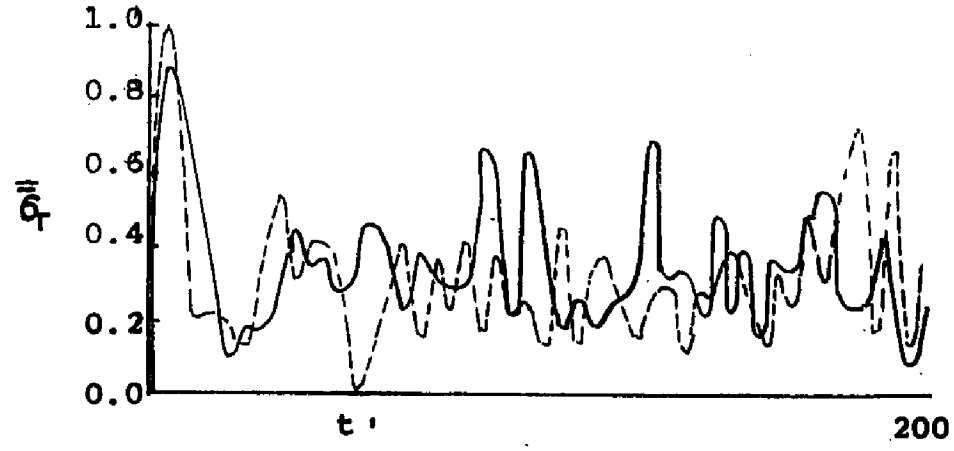

Exponential Impulse

% Difference + 12.17

Figure 8

Fixed, Short, Thick Cylinder
Stress Intensity History at x=0, ø=0

Cut-Off frequency 16.0

—SR
---CL

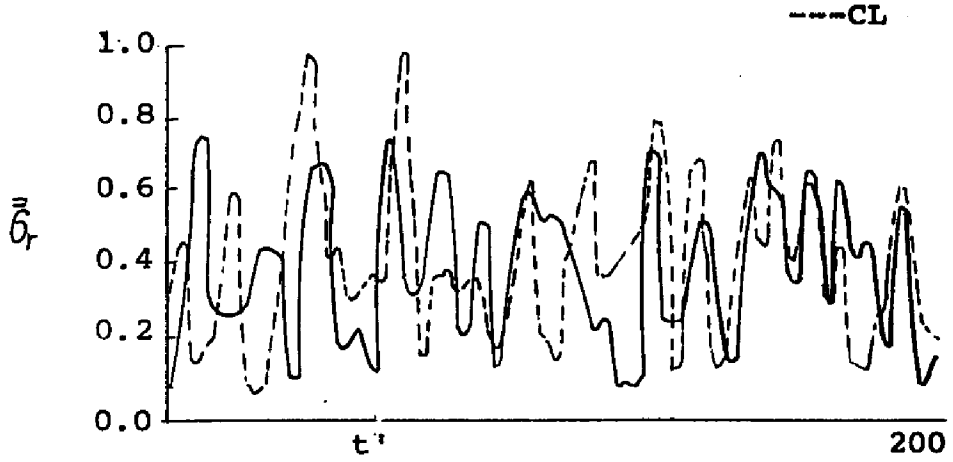

Cosine Frontal Impulse
% Difference + 22.9

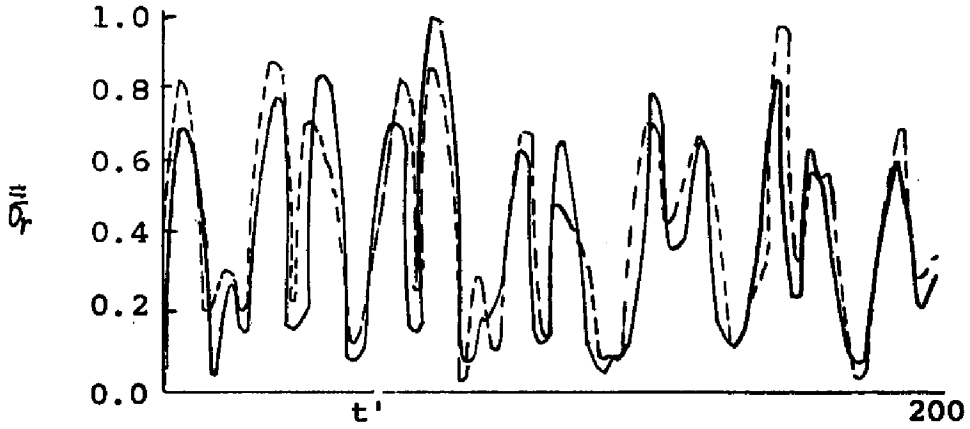

Triangular Impulse
% Difference - 1.95

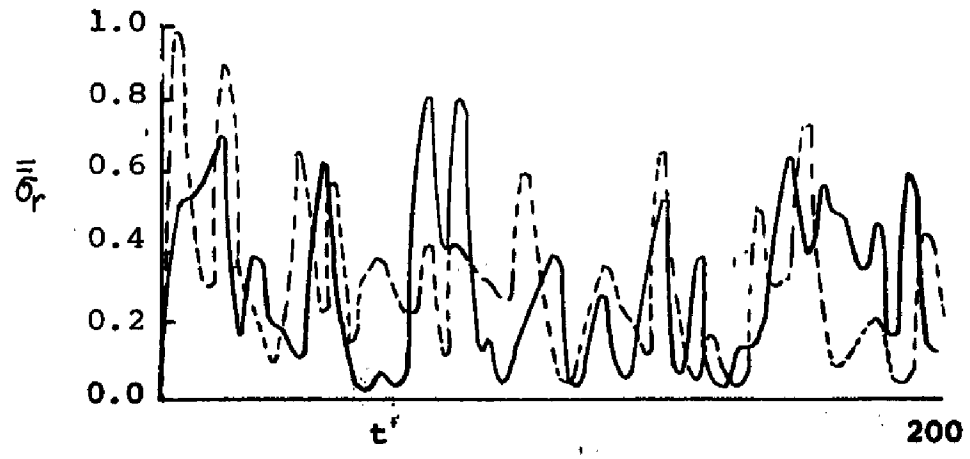

Exponential Impulse
% Difference + 16.4

Figure 9

Free short, thick cylinder stress intensity history
at x = L/2, ϕ = 0

Cut-Off Frequency, 16.0

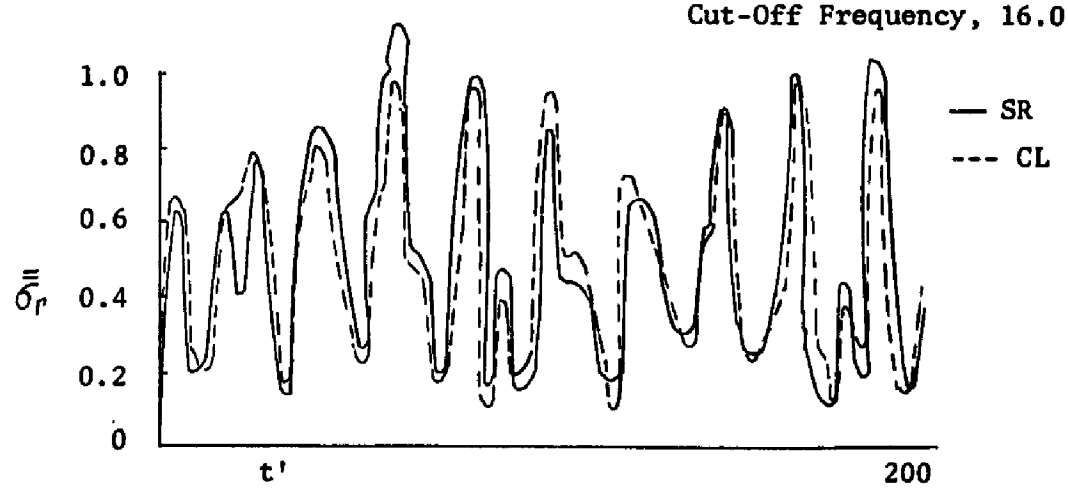

Cosine Frontal Impulse

% Difference - 15.2%

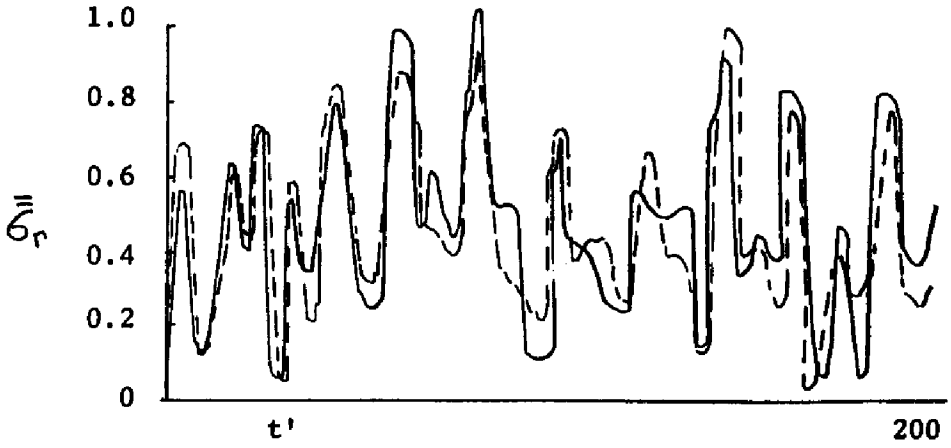

Triangular Impulse

% Difference - 5.6%

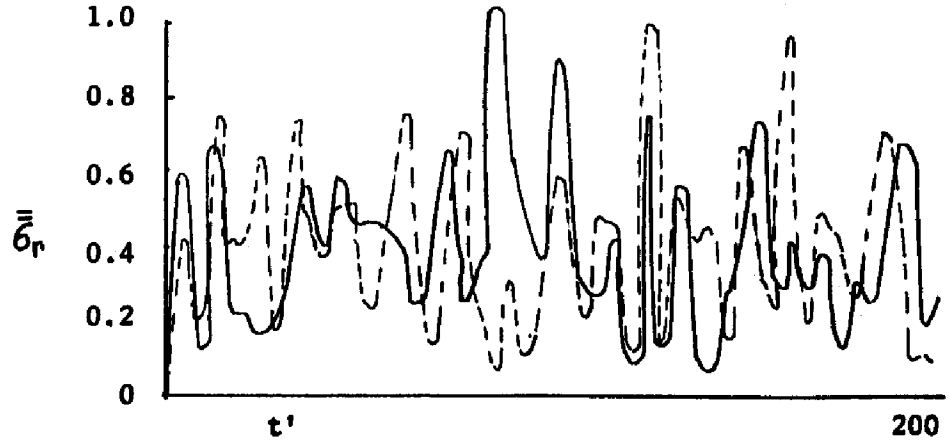

Exponential Impulse

% Difference - 6.94%

Figure 10

Fixed, short, thick, cylinder stress intensity history
at x = 0, ϕ = 0

Cut-off frequency, 30.0

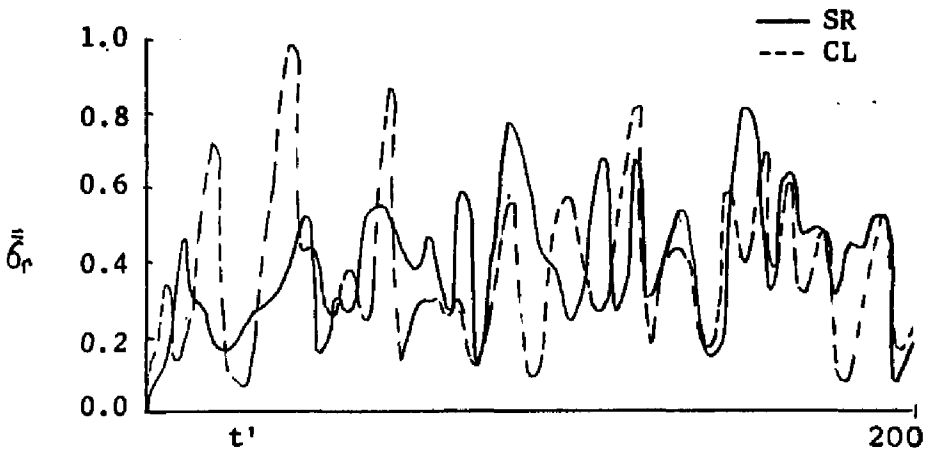

Cosine Frontal Impulse

% Difference 17.822

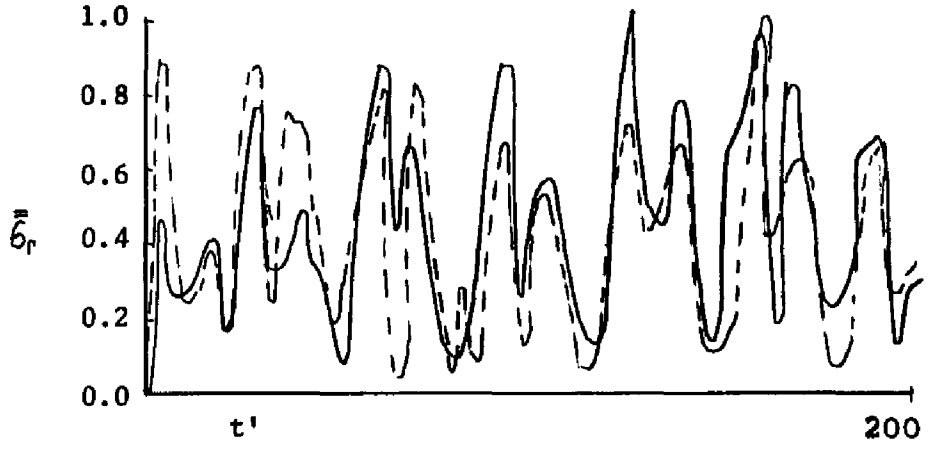

Triangular Impulse

% Difference - 5.838

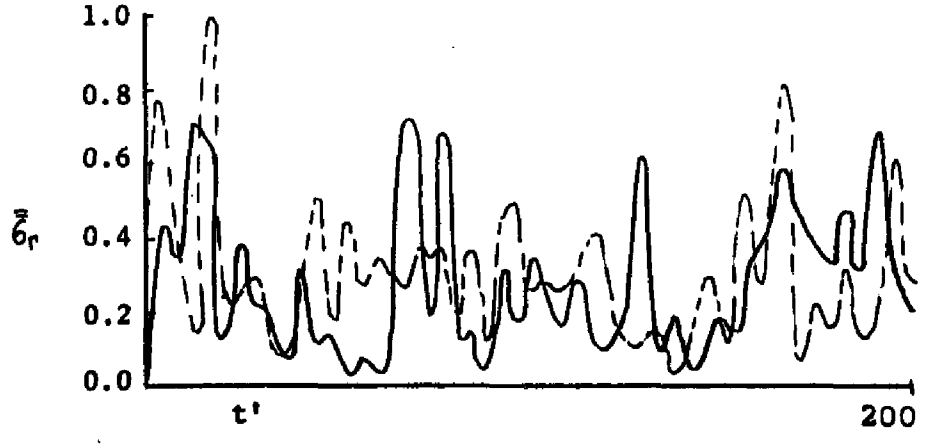

Exponential Impulse

% Difference 27.05

Figure 11

Free, short, thick, cylinder stress intensity history
at x = L/2, ϕ = 0

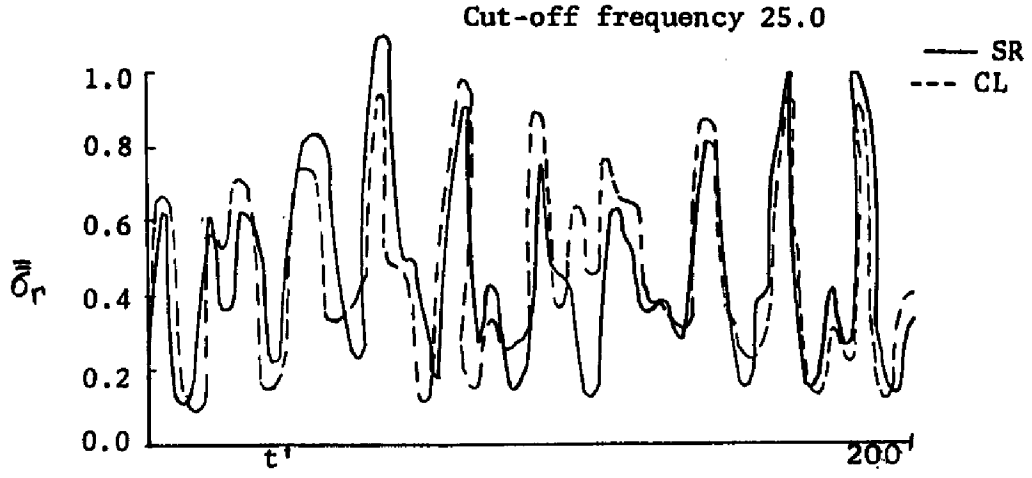

Cosine Frontal Impulse

% Difference - 11.02

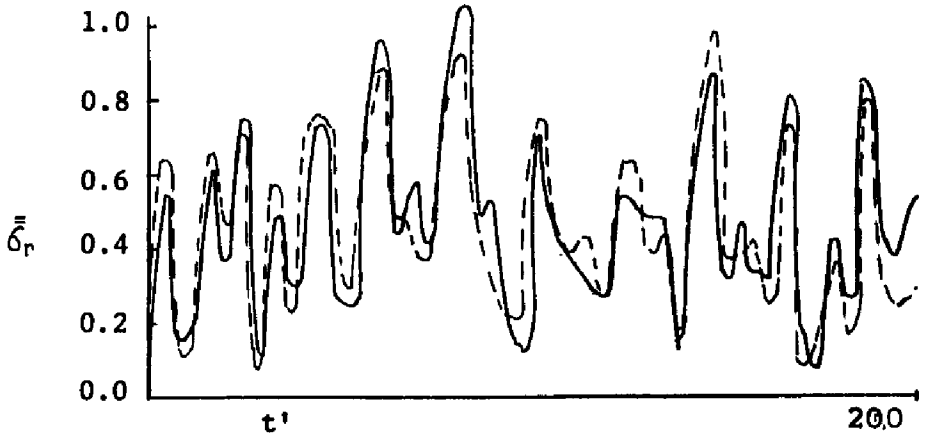

Triangular Impulse

% Difference - 5.14

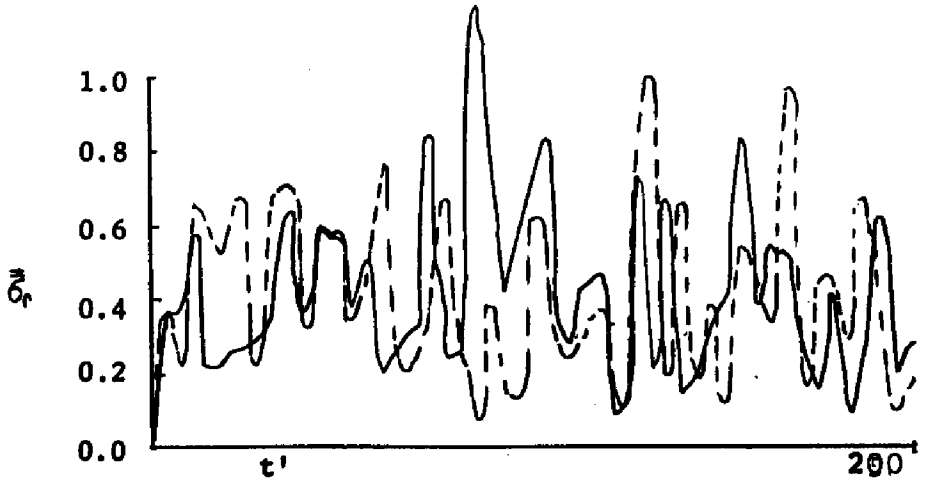

Exponential Impulse

% Difference - 19.92

Figure 12

SECTION XI
COMPARISON OF SR AND CLASSICAL MODELS

11.1 Introduction

The method of numerical computation has been described in Section IX. Natural frequencies actually found by this procedure for particular cases of interest are presented in Section X, in both tabular and graphical fashion. Also shown in Section X are values for the stress intensity, computed for the three types of impulsive loading previously selected.

In this Section, the fundamental differences in the models are explored at some length. The effects of these differences are illustrated by an examination of particular results in depth. Comments are offered as to the utility and applicability of each model.

To facilitate the discussion, the symbol CL will be used to denote the classical model, and the symbol SR the model which permits transverse shear deformation and includes rotary inertia.

11.2 The Pliancy Effect

The major expected source of any differences in deformation and stress, when comparing the alternative elastic models for the cylinders, as they respond to the same loading, is that due to the inclusion of transverse shear strain (as transverse stress is developed) in the SR model. This motion is prevented in the CL model. The added freedom makes the SR model more pliant or flexible. This pliancy effect (valid at all spatial locations through the cylindrical shell) is shown

graphically in Figure 13 for deformation in an axial plane.

The rotation (u_1') of a plane originally normal to the median surface depends on the existence of a flexural moment resultant (σ_{11}') at that spatial location. The existence of such a moment usually implies the existence of a transverse force resultant ($\sigma_{13}^{\bullet}$). In the CL theory the strain associated with this transverse force is suppressed by imposing an infinite shear modulus. The result of this is the continuous orthogonality of the transverse plane and the median surface (See Figure 13-a). The relaxation of the constraint on transverse shear in the SR model (Figure 13-b) permits the same rotation of the transverse surface associated with the flexural moment, but with a steeper radial deformation gradient ($\frac{\partial u_3^{\bullet}}{\partial x}$)of the median surface. The difference in gradient is due to the permitted shear strain (γ_{13}).

Of course, a similar illustration could be offered for deformations in a plane perpendicular to the cylinder axis. In this case:

u_2' = Rotation of a plane originally normal to the median surface

σ_{22}' = Flexural moment resultant

$\sigma_{12}^{\bullet}$ = Transverse force resultant

$\frac{\partial u_3^{\bullet}}{\partial \phi}$ = Radial deformation gradient in the circumferential direction

The foregoing implies that there would be generally larger deformations when an SR model cylinder responds to a given loading than would be the case when a CL model cylinder responds to the same loading pattern.

PLIANCY EFFECT

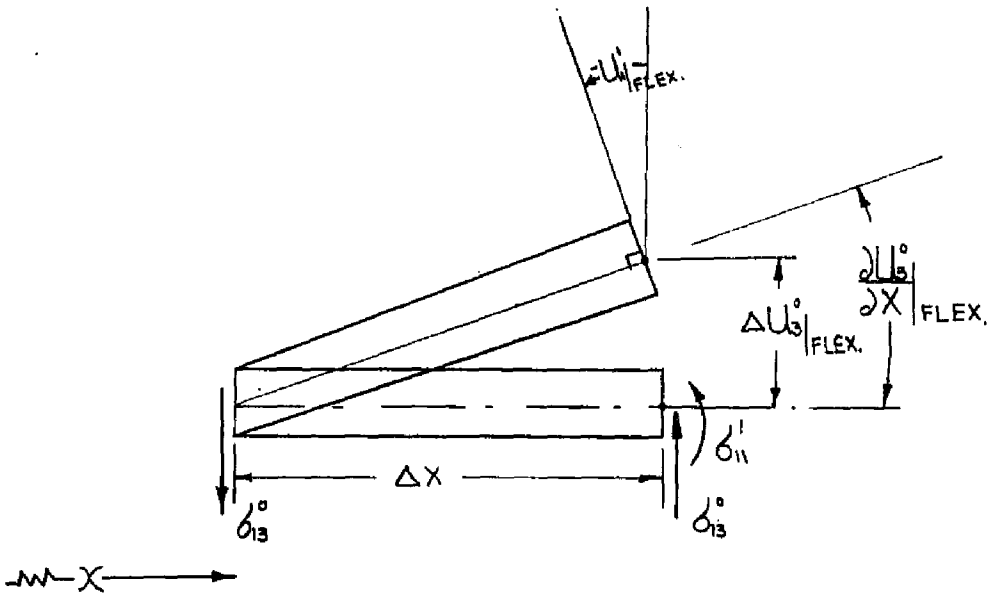

(a) Classical Model

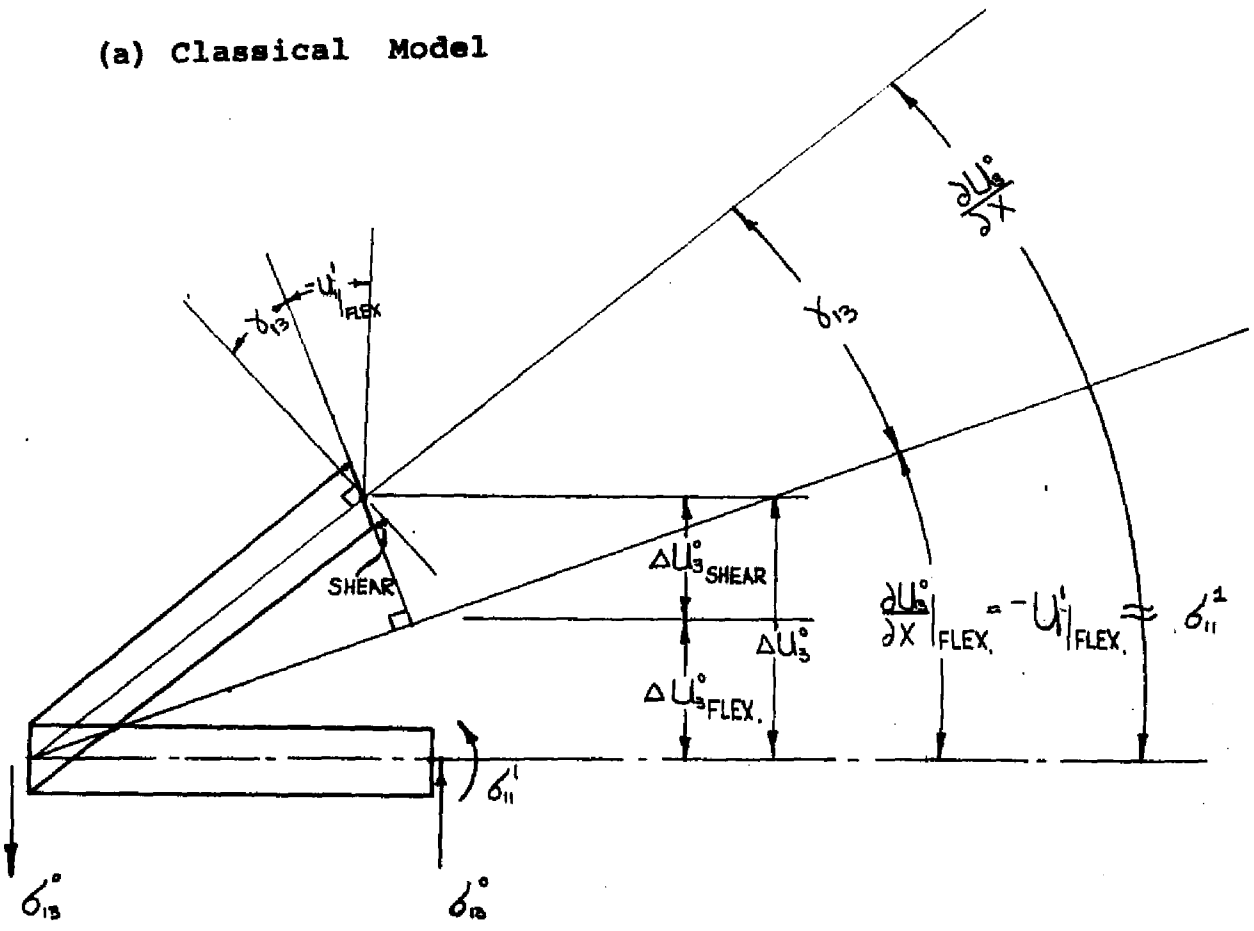

(b) SR Model

FIGURE 13

11.2.1 Implications of the Pliancy Effect

When the flexural moments (and associated transverse forces) are large, the magnitude of the permissible SR model shear strains are correspondingly large. This high stress condition would be expected to accentuate any difference in the radial deformation gradient at any spatial location. The total deformation patterns for the two alternative models would then diverge.

This high stress condition will also be associated with a particular type of deformation pattern. As the number of nodal points on the cylinder's median surface increases (i.e., points where $U_3^{\bullet}(x,\phi,t) = 0$), the structural waves get shorter. This is true in both axial and circumferential directions. These shorter structural waves (with a smaller radius of curvature of the median surface) are implicitly due to large flexural moments and transverse forces. Therefore, these types of waves should differ more in form (as the SR and CL models are compared), than should the longer waves.

The deformation pattern at any time is considered as the summation of a series of natural mode responses. From the preceding discussion, differences in natural modal frequencies and stresses between the two models, reflecting the differences in deformation patterns, should begin to become more pronounced when the natural short structural waves are excited. The more short, high frequency waves that are included in the truncated infinite deformation (or stresses) series, the more the results obtained for each model should diverge from each other. An awareness of this fact has influenced my choice of the dynamic force imputs for which the response of the elastic cylinder models are to be examined and compared.

11.2.2 Dynamic Loading

A physical environment which stimulates phenomena to which the models respond differently seems most appropriate to this model comparison study. Therefore, dynamic inputs were chosen which are composed in sufficient quantity of large amplitude forces varying with steep gradients along the surface of the cylinder, and rapidly changing in time. These inputs will excite short structural waves, oscillating at high frequencies. As previously explained, the excitation of these waves was taken to be necessary to elicit different responses from the two models.

Three inputs were chosen. They are all time impulsive forces, applied in the radial direction on the top half surface (i.e., non-axisymmetric). They are symmetric about the crown point ($\phi = 0$) and longitudinally symmetric about $x = L/2$. They are termed:

a) Cosine frontal
b) Triangular
c) Exponential

These are shown qualitatively on Figure 14.

The time impulsive character was chosen to ensure no attenuation of force input at the high time frequencies in its Fourier spectrum. It is at these higher frequencies that the multi-noded short structural waves naturally oscillate. The exponential load has the highest proportion of significant short spatial force waves. Therefore, the differences in the dynamic response of the SR and CL models with exponential input should be more pronounced than with the other two inputs.

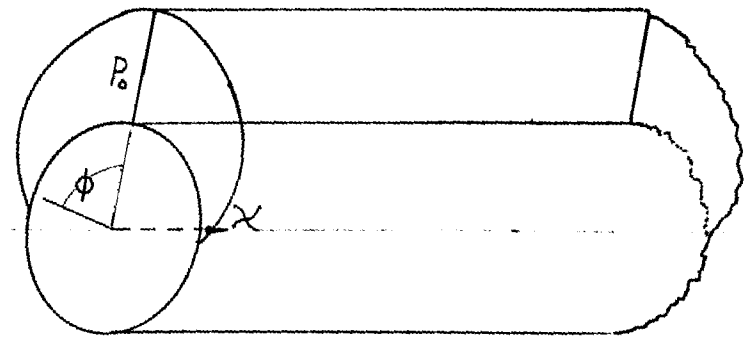

(a) Cosine Frontal

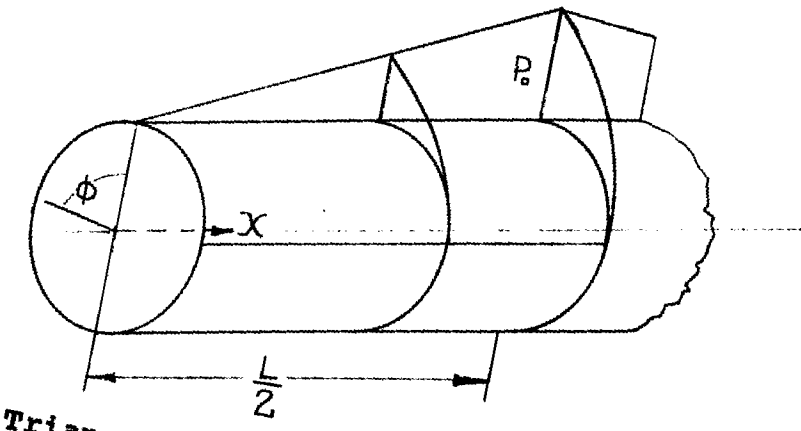

(b) Triangular

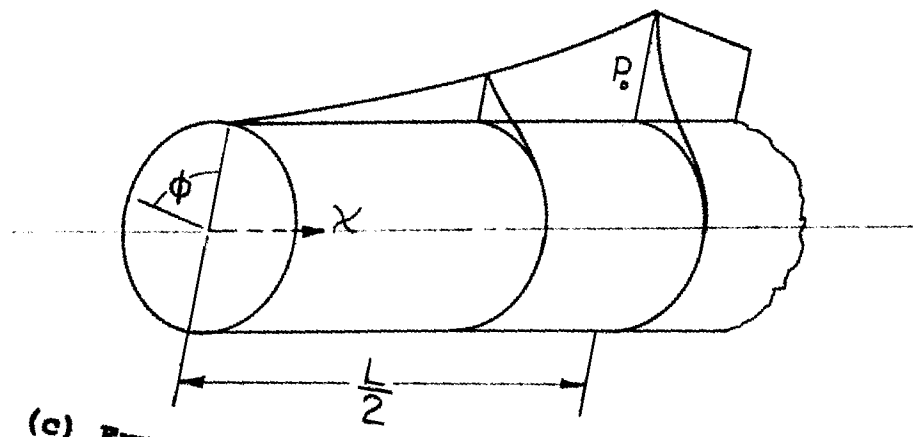

(c) Exponential

FIGURE 14

11.3 Natural Boundary Conditions

Another possible source of variation in dynamic response may be attributed to the different formulation (for each model) of what constitutes a given edge condition. The number of variables constrained, and which ones they are, is a direct consequence of modeling. For example, because the natural mode/frequency (eigenvalue) determinant for the classical theory is eighth order, only four shell variables need be prescribed at each edge of the cylinder. This will ensure a unique solution for the inter-relationship of the eight terms of the axial normal mode function. Any more coordinates prescribed at the edges would be redundant; any less would be insufficient. The SR eigenvalue determinant is of tenth order (equation 79) . Consequently, five variables are prescribed at each edge. In both cases the variables are "shell" variables. Shell variables are developed when the median surface motion coordinates are assumed to function in such a manner as to generate a particular deformation pattern throughout the thickness of the shell.

My natural boundary conditions were developed within the Hamilton Integral but are in no way extraordinary. They satisfy the above requirements with regard to number and perhaps could have been developed intuitively. For example, they are identical (after manipulation) to those used by Timoshenko (28) in his Classical Theory for fixed and for free edges. The following will analyze, for these edge conditions, how differences in the variables constrained for each model could influence the theoretical dynamic response of the cylinders.

11.3.1 Fixed Edge

For the CL theory, the four boundary constraints at each edge are (Refer to equations 67):

$$\frac{\partial u_3^\circ}{\partial x} = u_3^\circ = u_2^\circ = u_1^\circ = 0 \qquad *$$

For the SR theory, the five boundary constraints are (Refer to equations 83):

$$u_1' = u_2' = u_3^\circ = u_2^\circ = u_1^\circ = 0$$

The significant strain displacement equations (from Appendix C) are:

C-14.e $$\gamma_{13} = u_1' + \frac{\partial u_3^\circ}{\partial x}$$

C-14.f $$\gamma_{23}(1+z/a) = u_2' + \frac{1}{a}\left(\frac{\partial u_3^\circ}{\partial \phi} - u_2^\circ\right)$$

For the CL model at all locations, the transverse strain (γ_{13} , γ_{23}) is suppressed. Continuing for the CL model, since $\frac{\partial u_3^\circ}{\partial x}$ = 0 at x = 0,L, then from C14e, u_1' = 0. It is also evident, from C14f (because $\frac{\partial u_3^\circ}{\partial \phi}$ = 0 is implied in the condition u_3° = 0 for all Ø at x = 0 and L) that u_2' = 0.

Thus, in effect, the boundary conditions for the CL theory also imply $u_1^1 = u_2^1 = 0$, as in the SR theory. For the

---

* Note: The deformation coordinate for the fixed-edge cylinder are actually the inertially referenced displacement coordinates, r_k^n . The equations containing u_k^n in Appendix C would also have been transposed to r_k^n for a fixed-edge cylinder.

Natural Boundary Conditions-Fixed-Ended Cylinder

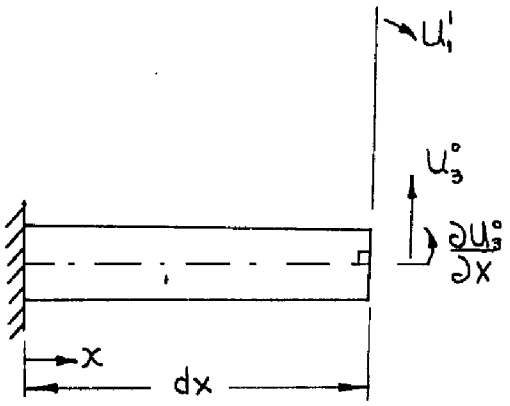

B.C.

$$\frac{\partial u_3^\circ(0)}{\partial x} = u_3^\circ(0) = 0$$

$$u_1^\circ = 0$$

$$u_2^\circ = 0$$

(a) Classical Theory

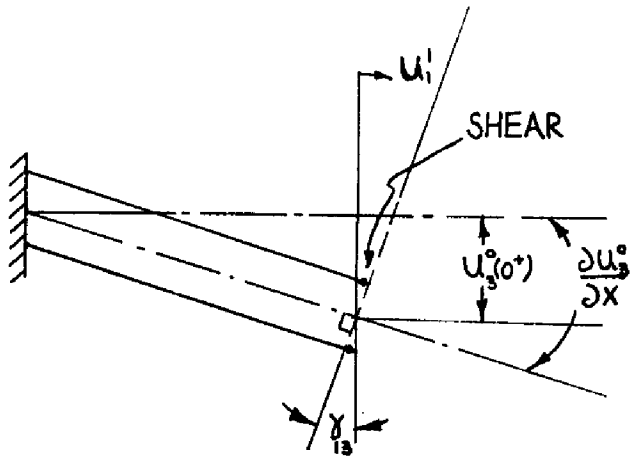

B.C.

$$u_1'(0) = u_3^\circ(0) = 0$$

$$u_1^\circ = 0$$

$$u_2^\circ = 0$$

$$u_3^\circ = 0$$

(b) SR Theory

FIGURE 15

SR theory, however, $\gamma_{13} \neq 0$ and $\gamma_{23} \neq 0$. From C14e:

C-14.e $$\gamma_{13} = \frac{\partial u_3^0}{\partial x} \neq 0$$

i.e., the gradient of the radial deformation coordinate in the axial direction is not constrained in the SR model, and will be produced at the edge, by the pure shear strain γ_{13}, which is permitted in the SR model. The deformation near the edges in the axial plane is shown in Figure 15 for both models.

As an aside, we briefly note from equation C14f that γ_{23} at the very edge is required to be zero. (All terms on the right hand side are equal to zero). Thus, there must be a "transition" between a circular cross section at the ends, and some circumferential wave pattern not far from the ends. This must be true for both models and does not by itself constitute a reason for a difference in response.

Thus the difference between the two models is just that illustrated in Figure 15. It is clear that this is no more than the general pliancy effect which is valid at all spatial locations in an SR-CL comparison. Therefore, the differences in the fixed-edge boundary conditions for the models are not expected to have any unique effect in the dynamic response comparison. The situation is somewhat different for the free-edged cylinder, discussed below.

11.3.2 Free-Edge

The SR model boundary conditions for the "free" edge, developed within the Hamilton Integral, are quite clear. It is that all shell stress resultants on the edges should vanish: (See equations 90)

$$\sigma_{11}^0 = \sigma_{12}^0 = \sigma_{13}^0 = \sigma_{11}^1 = \sigma_{12}^1 = 0$$

The case of the CL model, where only four shell parameters are constrained, has been handled intuitively by Timoshenko, on the basis of force balance considerations, by postulating an ersatz transverse shear stress resultant and an ersatz membrane shear stress resultant. The four boundary conditions are:

(198) a. $\sigma_{11}^{\circ} = 0$

b. $\sigma_{11}^{1} = 0$

c. $" \sigma_{13}^{\circ} " = \sigma_{13}^{\circ} + \frac{1}{a}\frac{\partial \sigma_{12}^{1}}{\partial \phi} = 0$

d. $" \sigma_{12}^{\circ} " = \sigma_{12}^{\circ} + \frac{1}{a}\sigma_{12}^{1} = 0$

The boundary conditions I used, developed within the Hamilton Integral are identical (equation 68) except for the ersatz transverse shear (198-c), which has the following form when there are only radial input forces on the cylinder's surface:

(199) $$\frac{\partial \sigma_{11}^{1}}{\partial x} + \frac{\partial \sigma_{21}^{1}}{a\partial \phi} + \frac{1}{a}\frac{\partial \sigma_{12}^{1}}{\partial \phi} = " \sigma_{13}^{\circ} " = 0$$

The actual transverse shear stress, σ_{13}°, has been absorbed within the Hamilton Integral in my development. It can be obtained, though, by a force balance or by a direct reduction of the SR equilibrium equations (equation 42), when the rotary inertia is neglected and only radial forces are present on the cylinder's surface. The transverse shear is seen to be:

(200) $$\sigma_{13}^{\circ} = \frac{\partial \sigma_{11}^{1}}{\partial x} + \frac{1}{a}\frac{\partial \sigma_{21}^{1}}{\partial \phi}$$

Therefore, equation 199 is identical to 198c. The free edge boundary conditions for SR and CL models are shown graphically in Figure 16. What is significant is that the free cylinder, as a consequence of classical modeling, permits the existence on its so-called "free" surface of the following stress resultants: a membrane shear σ_{12}°, a transverse shear σ_{13}°, and a twisting moment σ_{12}^{1}, where:

(201)

a. $\sigma_{12}^{1} \neq 0$

b. $\sigma_{12}^{\circ} = -\sigma_{12}^{1}/a$

c. $\sigma_{13}^{\circ} = -\frac{1}{a}\frac{\partial \sigma_{12}^{1}}{\partial \phi}$

This is in no way theoretically untenable, according to St. Venant's hypothesis, especially as the stress intensities I am investigating in detail are those at the axial midplane of the cylinder, much removed from the edge.

It is of interest, though, to examine the ways in which the natural boundary conditions associated with each model affect stress distributions, deformation patterns etc. For this purpose it is desirable to consider these effects on the response of separate normal modes. We note initially that for the deformation pattern formed by short axial waves, boundary condition effects become increasingly localized, especially with respect to stress. The influence of these effects at the axial midplane, where I have computed the stress

Natural Boundary Conditions-Free-Ended Cylinder

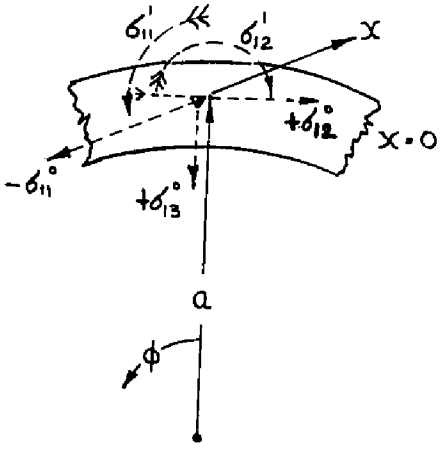

B.C.

$\sigma_{11}^0(0) = 0$

$\sigma_{12}^0(0) = 0$

$\sigma_{13}^0(0) = 0$

$\sigma_{11}^1(0) = 0$

$\sigma_{12}^1(0) = 0$

(a) SR Theory

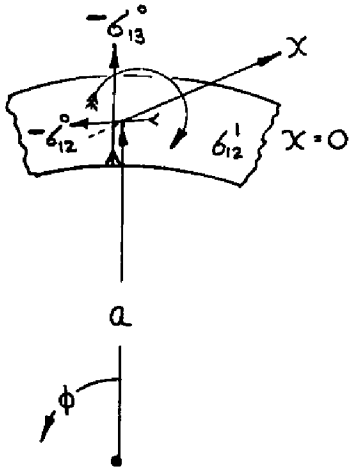

B.C.

$\sigma_{11}^0(0) = 0$

$\sigma_{11}^1(0) = 0$

$$0 = \left[\left(\frac{\partial \sigma_{11}^1}{\partial x} + \frac{1}{a}\frac{\partial \sigma_{21}^1}{\partial \phi}\right) + \frac{\partial \sigma_{12}^1}{a\partial \phi}\right]_{x=0} = \left(\sigma_{13}^0(0)\right) + \left.\frac{\partial \sigma_{12}^1}{a\partial \phi}\right|_{x=0}$$

$$\sigma_{12}^0(0) + \frac{\sigma_{12}^1(0)}{a} = 0$$

(b) Classical Theory

FIGURE 16

intensities, are minimal. Any differences between the response of the two models for these modes should be due to the general pliancy effect. If these short, axial waves are also associated with short, circumferential waves, the preceding statement may be somewhat modified. This is because the difference in magnitude (for the two models) of stresses developed at the edge region is considerably influenced by the shape of the cylinder in the circumferential direction. The absolute magnitude of the stresses in one of the models may be sufficient to influence regions beyond the edge. The source of this differing influence of the circumferential deformation shape for each model is analyzed below.

The rate of change of the axial flexural moment resultant ($\frac{\partial \sigma_{11}'}{\partial x}$) is an informative parameter. At the edge, for both models, the axial moment resultant (σ_{11}') is zero. From the general equilibrium equations (42) for the SR model, taking into account that the axial transverse shear stress (and therefore strain) are required to be zero at the edge, the following expression is obtained:

$$(202) \qquad \left.\frac{\partial \sigma_{11}'}{\partial x}\right|_{x=0,L} = f(h^3, \ddot{u}_1', \ddot{u}_1^\circ, \ddot{\gamma}_\circ) - \frac{1}{a}\frac{\partial \sigma_{21}'}{\partial \phi}$$

For the classical model, the natural boundary condition (199) requires:

$$(203) \qquad \left.\frac{\partial \sigma_{11}'}{\partial x}\right|_{x=0,L} = -\frac{1}{a}\frac{\partial \sigma_{21}'}{\partial \phi} - \frac{1}{a}\frac{\partial \sigma_{12}'}{\partial \phi}$$

The difference between these equations are more readily seen in terms of the displacement coordinates.

Differentiating C20g with respect to x, the change in the axial flexural moment at the edge for the SR model is (with no axial transverse shear strain):

$$(204) \qquad \left.\frac{\partial \sigma_{11}^{1}}{\partial x}\right|_{x=0,L} \sim \nu a^2 \frac{\partial^2 u_2^1}{\partial \phi \partial x} - a^3 \frac{\partial^3 u_3^0}{\partial x^3} + a^2 \frac{\partial u_1^0}{\partial x^2}$$

Differentiating the terms for the twisting moments in D-30h and D30j as required by 203 leads to the corresponding formulation for the CL model:

$$(205) \qquad \left.\frac{\partial \sigma_{11}^{1}}{\partial x}\right|_{x=0,L} \sim -\frac{3(1-\nu)}{2} a^2 \frac{\partial^2 u_2^1(CL)}{\partial \phi \partial x} + a^3 \frac{(1-\nu)}{2a^2} \frac{\partial^2 u_3^0}{\partial \phi^2 \partial x} + \frac{(1-\nu)a^2}{2a^2} \frac{\partial^2 u_1^0}{\partial \phi^2}$$

where the symbol $u_2^1(CL)$ refers to the rotation of the circumferential transverse plane for the classical model. From equation D-14:

$$(D\text{-}14) \qquad u_2^1(CL) = \frac{1}{a}\left(u_2^0 - \frac{\partial u_3^0}{\partial \phi}\right)$$

Equation D-14 is, of course, applicable only when the transverse shear strain γ_{23} is suppressed. The other rotation $u_1^1(CL)$ for the classical model is given by equation D-13:

$$(D\text{-}13) \qquad u_1^1(CL) = -\frac{\partial u_3^0}{\partial x}$$

We note that equations 204 (SR) and 205 (CL) are basically concerned with the same mid-surface coordinates: u_2^1, u_3^0 and u_1^0. But in the CL model (for the latter two terms) a dependence on variation in the circumferential direction

replaces what in the SR model appears as a variation in the axial direction. Thus, we may expect, for the term $\frac{\partial \sigma_{ij}'}{\partial x}$ in the region of the edge a difference in the model behavior which will be accentuated as the circumferential waves get shorter, and the rate of variation of the displacement coordinates in the circumferential direction increases.

Beyond the edge region, the form of this variable is found by differentiating C-20g and D-30g. For the SR and CL models respectively:

(206) $$\left.\frac{\partial \sigma_{ij}'}{\partial x}\right|_{x>0} \approx a^2 \frac{\partial^2 u_i^\circ}{\partial x^2} + a^3 \frac{\partial^2 u_i'}{\partial x^2} + \nu a^2 \frac{\partial u_2'}{\partial \phi \partial x}$$

(207) $$\left.\frac{\partial \sigma_{ij}'}{\partial x}\right|_{x>0} \approx a^2 \frac{\partial^2 u_i^\circ}{\partial x^2} + a^3 \frac{\partial^2 u_i'(CL)}{\partial x^2} + \nu a^2 \frac{\partial u_2'(CL)}{\partial \phi \partial x}$$

Thus, beyond the edge region, the expressions differ only in terms concerned with the general pliancy effect. What importance the alternate boundary conditions will assume in determining extensive response difference will depend on the magnitudes of the differences between terms like equation 204 and equation 205, developed in the edge regions only.

It has been my experience, catalogued in the sections below on modal response, that the boundary conditions have played a significant role in free cylinders, even for long wave lengths at low natural frequency. The numerical results show that the total dynamic response of the SR and CL models diverge more for the free-edged cylinder than for the fixed-edged cylinder when these waves are excited. The results seem to have been more influenced by differences in the form of the

natural boundary conditions for the free cylinder than I had initially expected.

11.4 Natural Mode Response

11.4.1 Fixed Cylinders

11.4.1.1 Introduction

An extensive examination was made of the dynamic response of a short, thick cylinder with fixed edges for the CL and SR models. The total response of the cylinder is composed of the cumulative response of each natural mode to the given input. It was, of course, therefore necessary to identify the shape of the natural modes and their associated natural frequency of oscillation. The natural modes are of the following form:

$$(208)\quad U_k^n(x,\phi,t)_{mN} = f_k^{(n)}(x,m)_N * \cos m\phi \; U \sin m\phi * \sin \omega_{mN} t$$

and are dependent upon the edge conditions (e.g., for fixed edge cylinder, $(f_k^{(n)}(x,m)_N = 0)$. They are categorized according to increasing order of nodal points ($U_3^0(x,\phi,t) = 0$. The general form of some natural mode shapes for fixed ended cylinders are shown in Figure 17. For a mode shape identified by the subscripts m, N, the circumferential pattern has 2m nodes, and the axial pattern has N + 1 nodes. (The free cylinder has N-1 axial nodes. See Figure 28). The natural frequencies, axial deformation patterns, stress resultants and potential energy distributions were examined. A general discussion of the results of this examination is presented

NODAL PATTERNS - FIXED CYLINDER

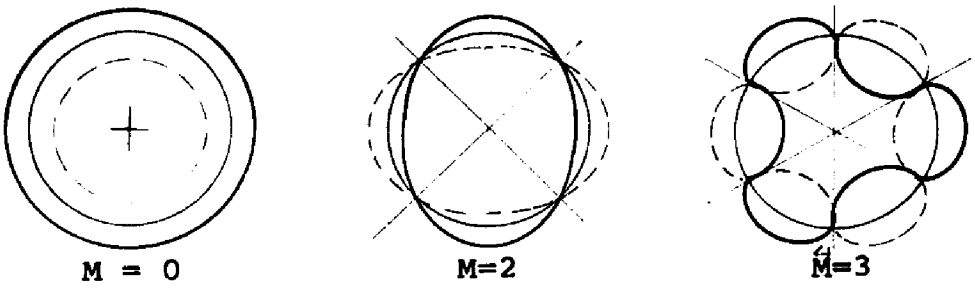

CIRCUMFERENTIAL NODAL PATTERN

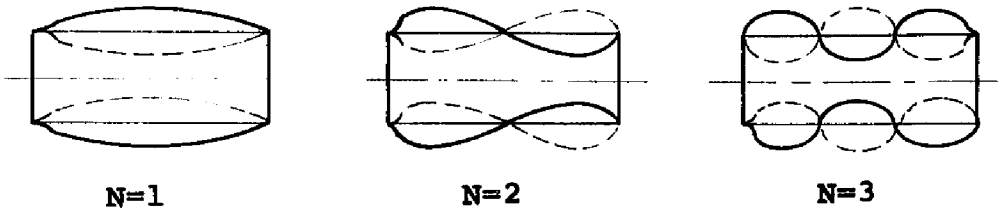

AXIAL NODAL PATTERN

NODAL ARRANGEMENT FOR M=3, N=4

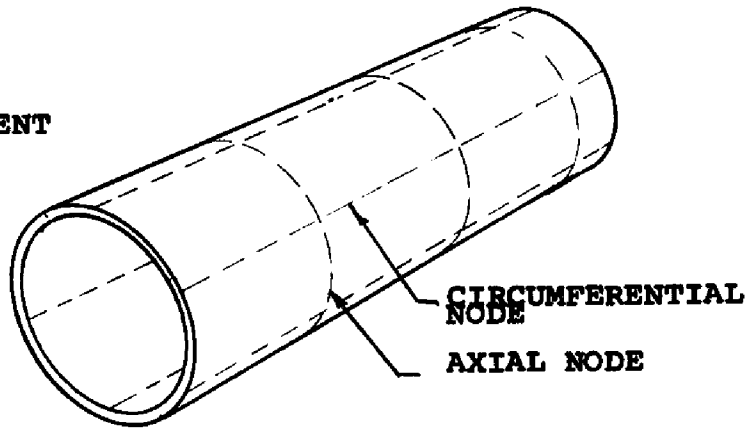

FIGURE 17

below.

11.4.1.2 Natural Frequencies (Fixed-ended cylinder)

The natural frequencies of the short, thick, fixed-ended cylinder and their associated various modal patterns are shown in Table I (Section X), for both the SR and CL models. The data for Table I is presented graphically in Figure 5 a-b. The lowest frequency * found at each circumferential wave number, m, is that associated with one axial half-wave. For a given axial nodal pattern, N, the lowest frequency is found at that circumferential nodal pattern, m, where the deformation strain energy is minimum. Generally, the higher frequencies are associated with short structural wave lengths (m, N are larger). This may be seen from Table I and from Figure 5 a-b. We note that as the waves get shorter, the natural frequencies for the SR and CL model diverge more. This phenomenon has been noted in free vibration investigations of simply supported and infinite cylinders (References 6, 40, and 63). The phenomenon is an apparent consequence of the pliancy effect. The SR model becomes increasingly pliant, compared to the classical model, as the shorter structural waves are examined. Other parameters affected are the axial deformation pattern, stress resultants and elastic strain energy. These are presented below for some representative

---

* What are shown here are the first (lowest) branch of the natural frequency curves. For each nodal pattern there are five natural frequencies for the SR model. There are three natural frequencies associated with each nodal pattern for the CL model. Higher branch frequencies identified during the run are shown in Table II (Section X)

natural modes.

11.4.1.3 Deformation Patterns, Stress Resultants, Elastic Strain Energy

The axial deformation patterns for both the SR and CL models, for the natural modes of m = 5, N = 1 and m = 2, N = 1 are shown in Figure 18. The mode shapes have been normalized to the same maximum amplitude. A detailed comparison was made of these two modes. They both have the same axial nodal pattern but a different circumferential nodal pattern. (m = 5, of course, has shorter circumferential waves). Both modes oscillate at approximately the same natural frequency (Figure 5-a) and therefore have accumulated the same elastic strain energy. The energy distributions, however, do differ as well as the relative importance of the three different types of strain energy (for the axial direction), associated with each nodal pattern.

Figure 18 indicates that the radial deformation patterns in the axial direction, comparing the CL and SR models, differ only slightly in both these modes.* The difference in natural frequency between the models is greater for the case of five circumferential waves than for two waves. The reasons for this, though, are not apparent from an examination of the deformation pattern, and it is necessary to examine the energy distributions.

---

* A radial deformation during free vibration of 1" is assumed at the axial half-length for fixed cylinder natural modes which are symmetrical. Anti-symmetrical modes have a maximum 1" deformation elsewhere.

THICK, SHORT, FIXED CYLINDER
AXIAL WAVE PATTERN, SR AND CL

For M=2, N=1
NAT. FREQ SR = .394933
NAT. FREQ CL = .395709

For M=5, N=1
NAT. FREQ SR = .404198
NAT. FREQ CL = .409246

For M=2, N=2
NAT. FREQ SR = .702203
NAT. FREQ CL = .704515

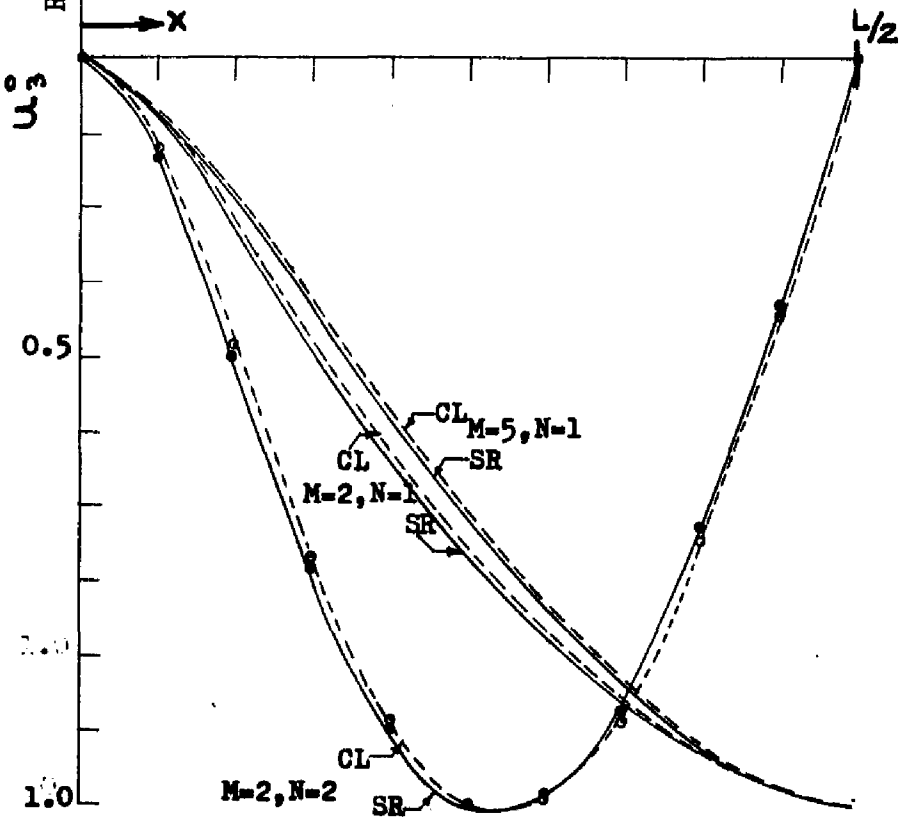

FIGURE 18

The radius of curvature of the axial median surface of both models for m = 5 is greater than for m = 2 at the fixed edge and less than that of m = 2 at the half-length. The stress resultants (Figures 19 and 20) in the axial direction, especially the flexural moment resultant, σ_{11}^{1} *, reflect this particular variation in the deformation pattern. The moment for m = 5 compared to m = 2 is lower at the edges but greater at the center. It is also seen that the membrane stress, σ_{11}^{o}, is generally lower for m = 5 than for m = 2. A striking difference is that the transverse shear stress resultant on the face normal to the axial median surface σ_{13}^{o},** diverges significantly, when the CL model is compared to the SR model, with the shorter circumferential waves (Figure 20). The combined influence of these stresses and deformations are shown in the elastic strain energy distribution, Figures 21 and 22.

For a given axial wave length (N = 1) as the circumferential waves become shorter (m = 5 compared to m = 2), the axial strain energy distribution exhibits the following tendencies:

- The membrane energy (U_{memb}) diminishes in importance in relation to the flexural energy (U_{mom}), for both models.
- The difference between flexural energy for the two models is more pronounced.
- The difference between shear energy (U_{shear}) for the two models is more pronounced.

---

* Stress Resultants and Strain Energy in the following graphs have been normalized. See "Nomenclature"

** The ersatz transverse shear is plotted for the classical model

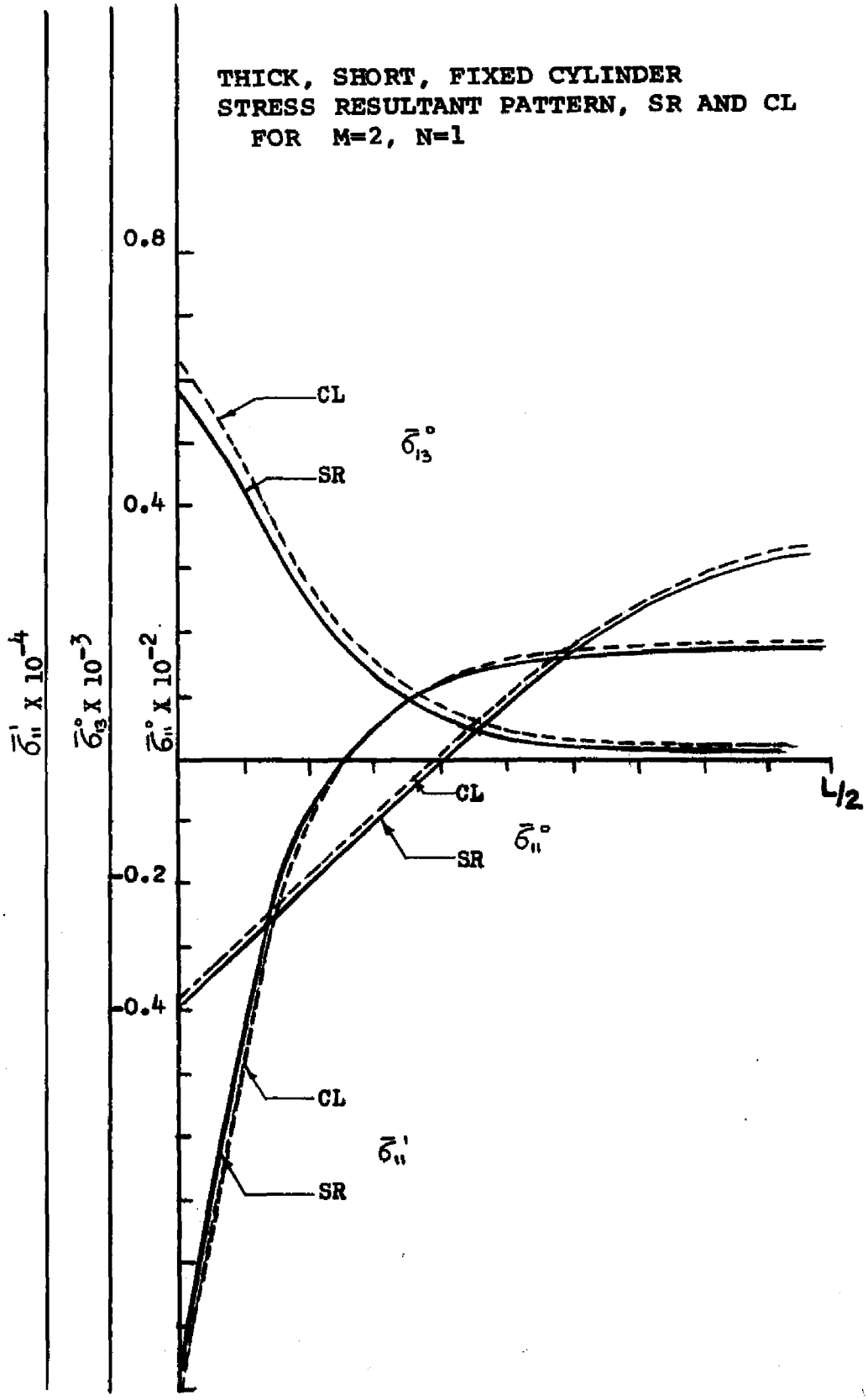
THICK, SHORT, FIXED CYLINDER
STRESS RESULTANT PATTERN, SR AND CL
FOR M=2, N=1
0.8
0.4
-0.2
-0.4
CL
SR
$\bar{\sigma}_{13}^{\circ}$
$\bar{\sigma}_{11}^{\circ}$
$\bar{\sigma}_{11}'$
$\bar{\sigma}_{11}'$ X 10^{-4}
$\bar{\sigma}_{13}^{\circ}$ X 10^{-3}
$\bar{\sigma}_{11}^{\circ}$ X 10^{-2}
L/2

FIGURE 19

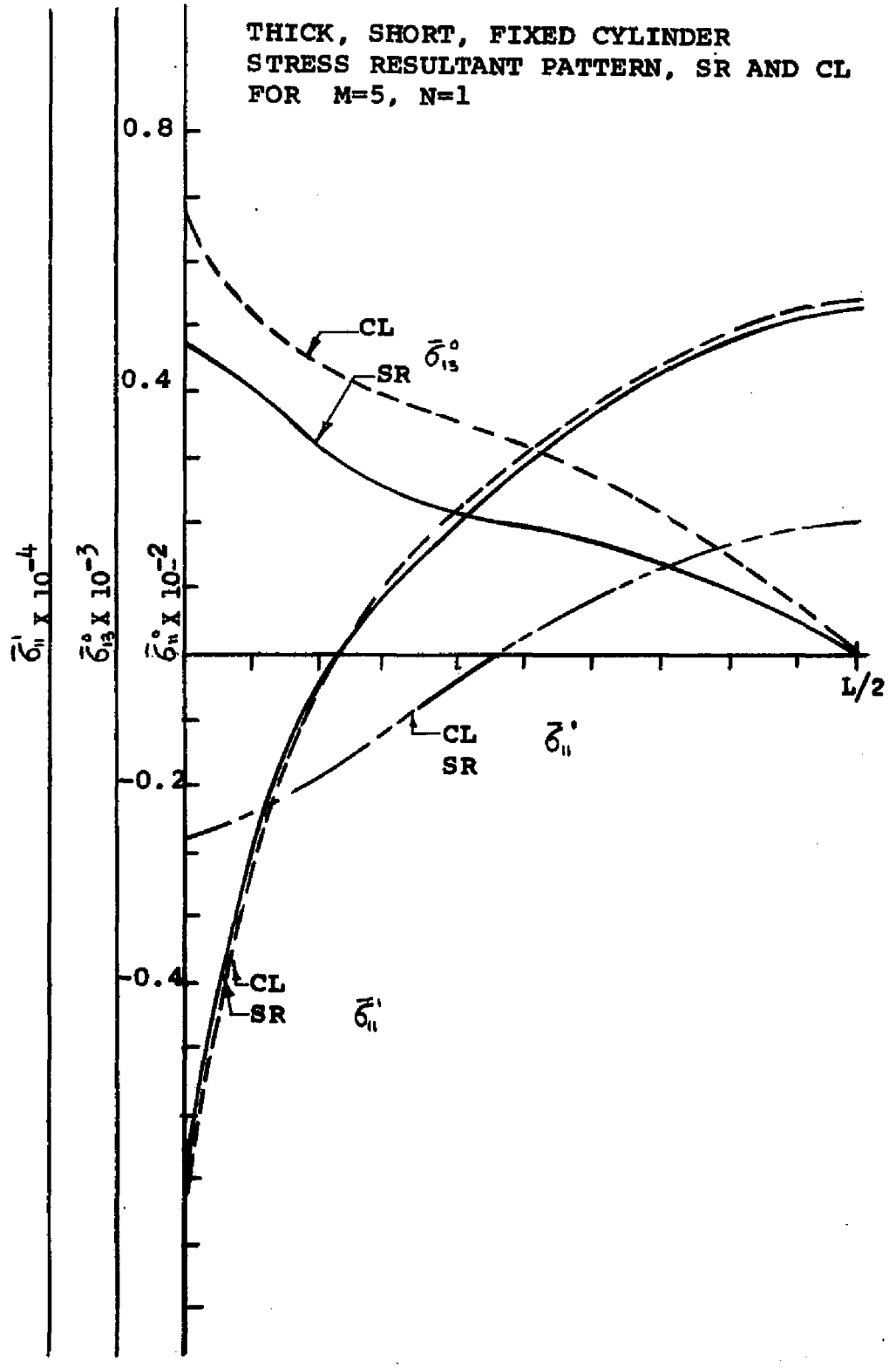
THICK, SHORT, FIXED CYLINDER
STRESS RESULTANT PATTERN, SR AND CL
FOR M=5, N=1
0.8
0.4
-0.2
-0.4
CL
SR
CL
SR
CL
SR
L/2

FIGURE 20

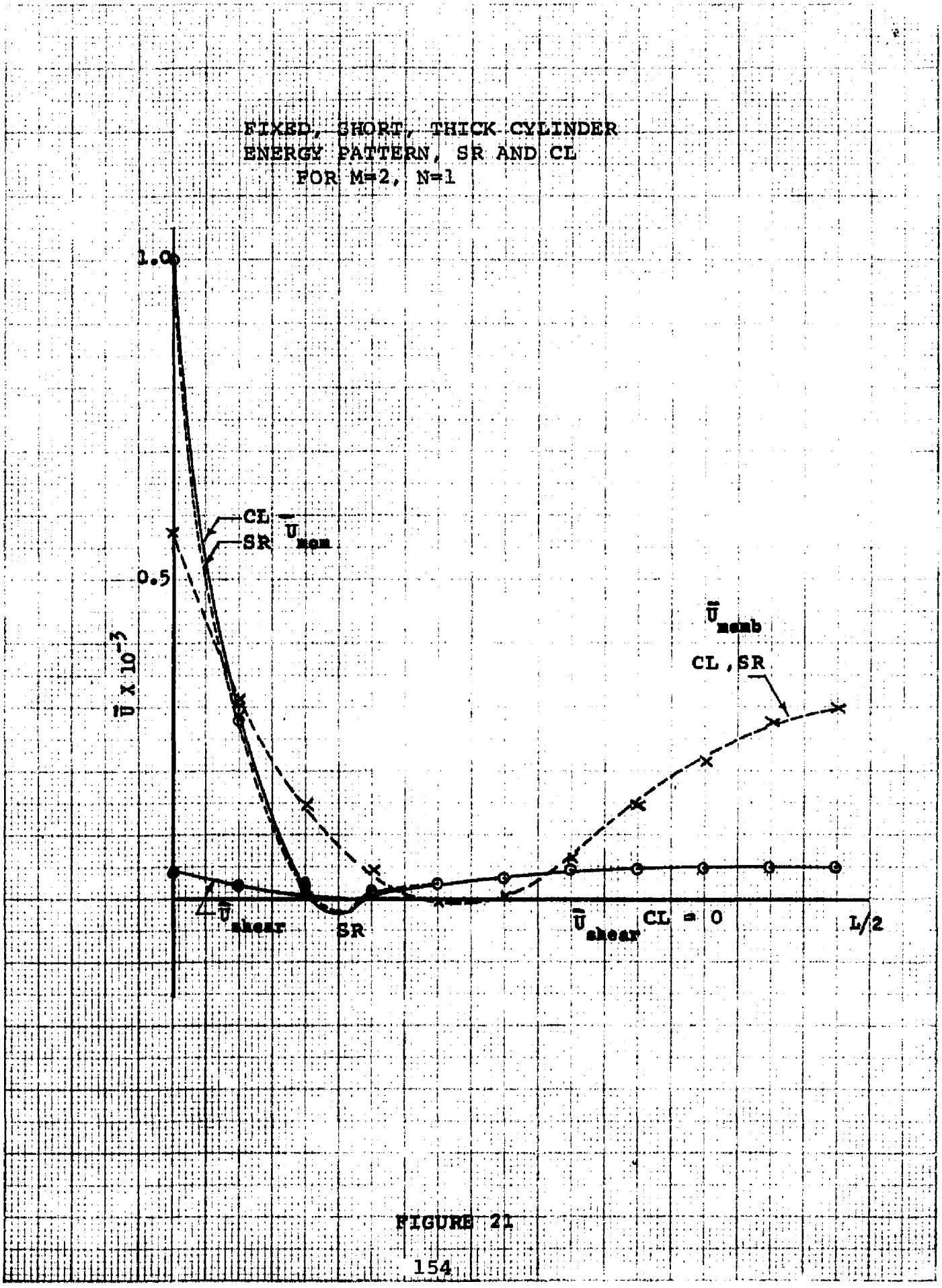
FIXED, SHORT, THICK CYLINDER
ENERGY PATTERN, SR AND CL
FOR M=2, N=1
1.0
0.5
$\bar{U} \times 10^{-3}$
CL
SR
$\bar{U}_{nom}$
$\bar{U}_{membr}$
CL, SR
$\bar{U}_{shear}$
SR
$\bar{U}_{shear}$
CL = 0
L/2

FIGURE 21

THICK, SHORT, FIXED CYLINDER
ENERGY PATTERN, SR AND CL
FOR M=5, N=1

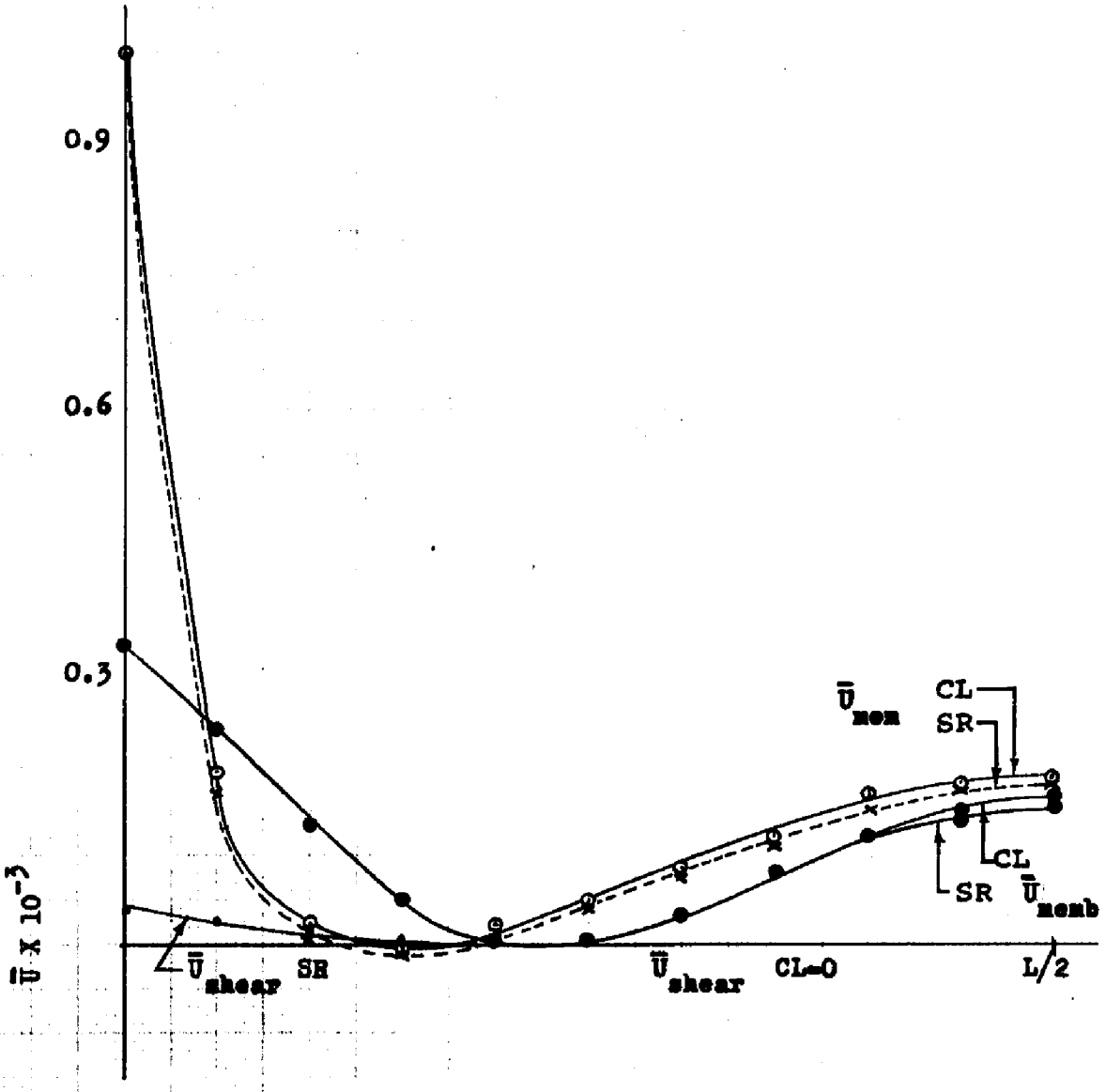

FIGURE 22

The latter two items are direct consequences of the first.

Model differences are related to transverse strains and flexural moments, and would not generally be in evidence when extensional (membrane) energy is predominant in the deformation patterns of the cylinder. The former parameters are related to variation in strain throughout the cross-section, the latter to the average of these strains. These differences between models, in the energy distribution with the shorter circumferential waves, account for the greater difference between the natural frequencies. These tendencies: i.e., divergence of energies, stress and frequencies between models as the circumferential waves get shorter (and membrane energy decreases in significance) verify my initial expectations as regards the pliancy/wave length effect.

The parameters in the axial direction have been examined to indicate the effects of circumferential wave shortening. An even more striking example of this manifestation of the pliancy effect occurs as the axial waves themselves are shortened. Figures 18, 23 and 24 are for the condition of two axial half waves (N=2) with the circumferential pattern m=2, and should be compared to N=1, m=2 (Figures 18-20, respectively). The tendencies noted before are even more pronounced, as the membrane energy is of relatively little importance, and greater differences are noted between the models in frequencies, stresses and energies.

The stress intensities generated in each model for the short, thick, fixed ended cylinder are discussed in Section 11.5. They indicate that as more high frequency, short wave length modes are included in the deformation series the differences between the models increase as expected. With these modes included, the tendencies noted above are shown in

THICK, SHORT, FIXED CYLINDER
STRESS RESULTANT PATTERN, SR AND CL
FOR M=2, N=2

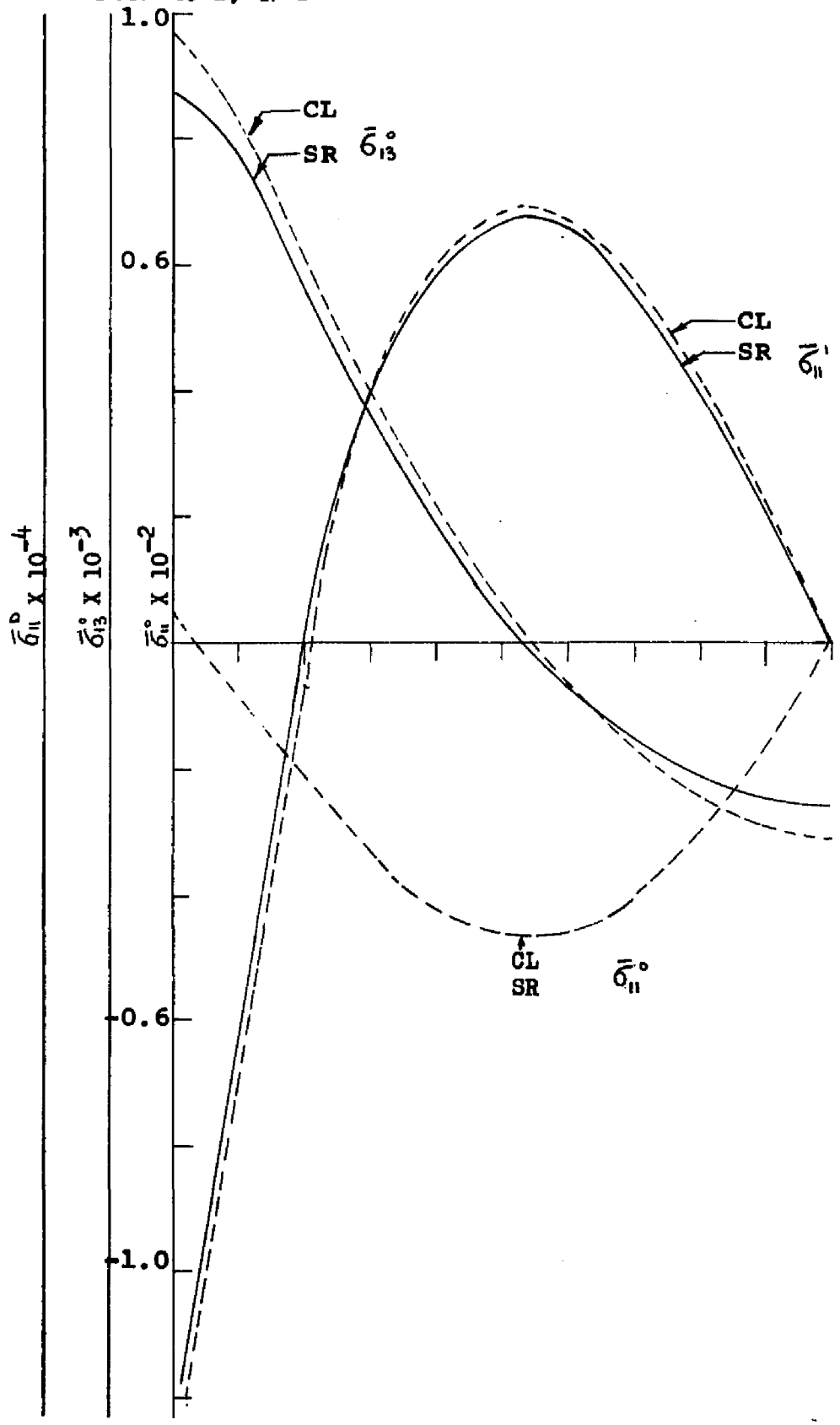

FIGURE 23

THICK, SHORT, FIXED CYLINDER
ENERGY PATTERN, SR AND CL
FOR M=2, N=2

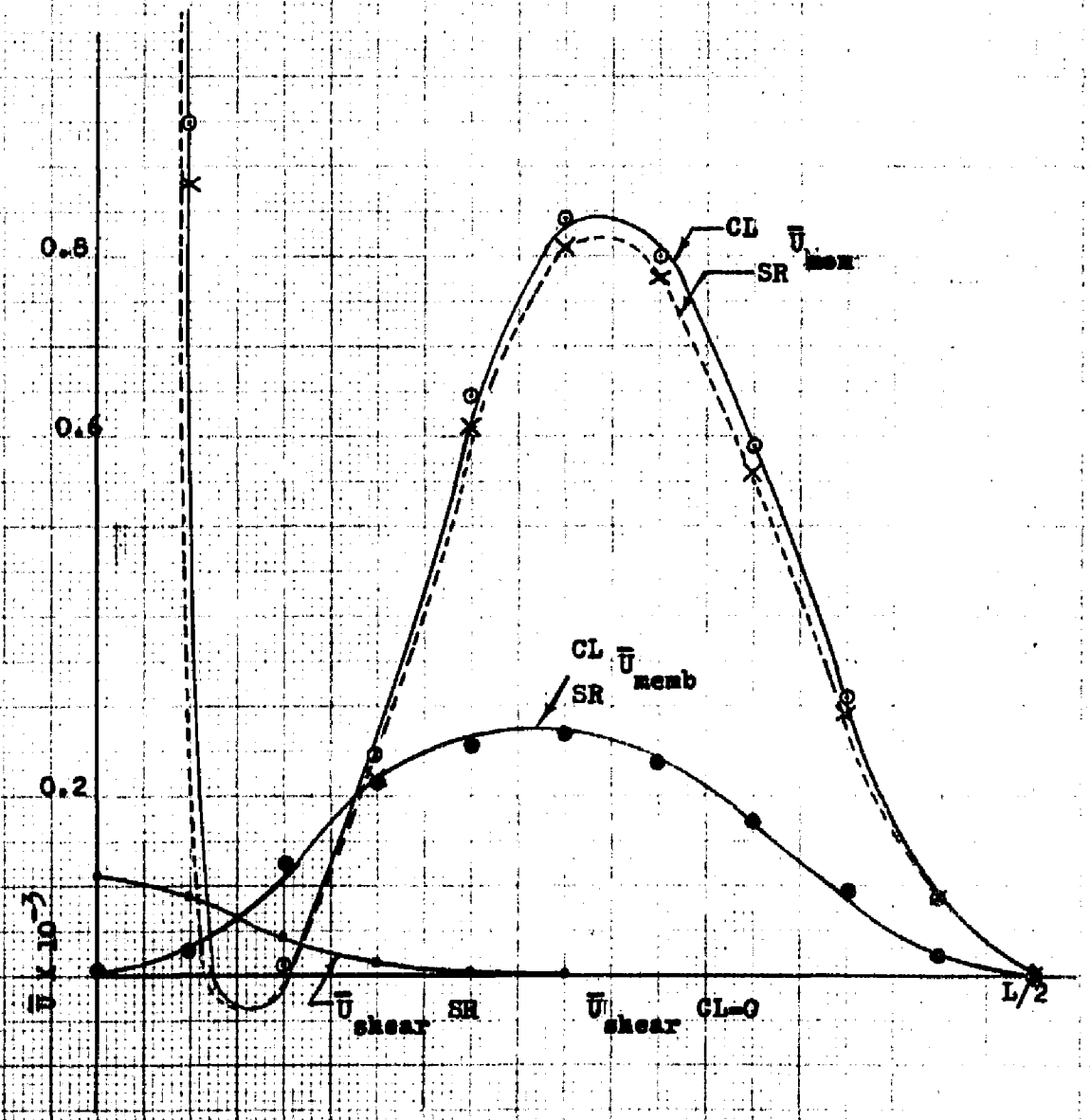

FIGURE 24

a greater proportion of the total number of terms included in this series. As stated before, for the fixed-ended cylinder, all differences are attributable to the pliancy effect.

11.4.1.4 Effects of Length and Thickness

The energy distribution for the CL and SR natural modes for m=2, N=1, for short-thin, long-thin and long-thick cylinders are shown in Figures 25, 26 and 27. They all show membrane energy decidedly more prominent, and flexural energy less so, than the similar mode shape in the short, thick cylinder. The thin cylinder demonstrates less flexural and less transverse shear energy for a given median surface deformation pattern because these energies are developed from variations in strain throughout the cross-section which are related to the distance from the mid-surface. The waves of a long cylinder (for a 1" maximum deformation with a given nodal pattern) require relatively little change in the curvature of the median surface, thereby also demonstrating only little flexural and shear energy.

Therefore, the pliancy effect will appear only after a great number of modes are accumulated in the deformation series. The modeling difference will be less important than in the short thick cylinder. Accordingly, a more extensive examination has been made only of the latter geometry.

11.4.2 Free Cylinders

11.4.2.1 Mode Shapes

The general form of some of the natural mode shapes developed during dynamic deformation are shown in Figure 28.

THIN, SHORT, FIXED CYLINDER
ENERGY PATTERN, SR AND CL
FOR M=2, N=1

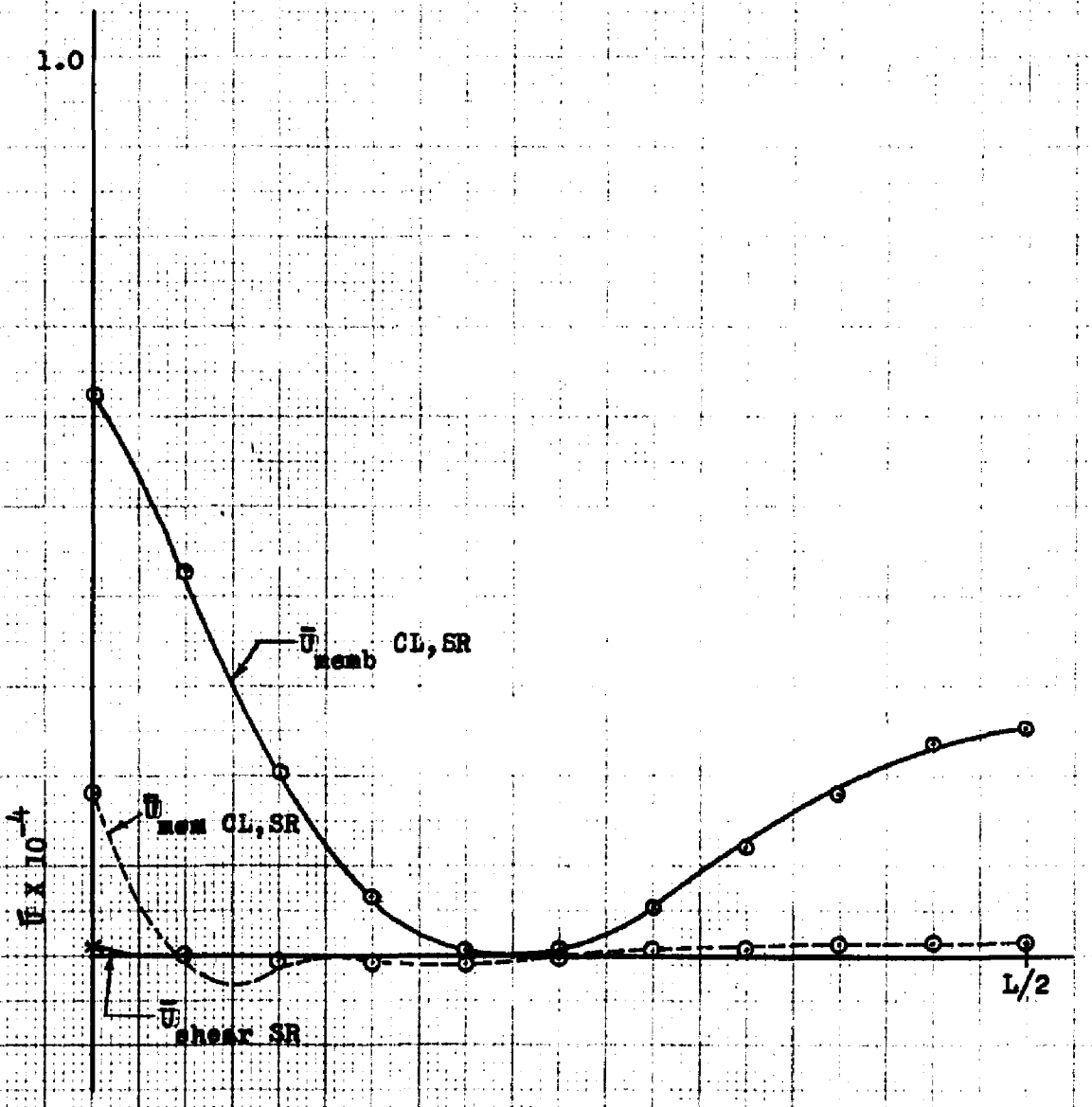

FIGURE 25

THIN, LONG, FIXED CYLINDER
ENERGY PATTERN, SR AND CL
FOR M=2, N=1

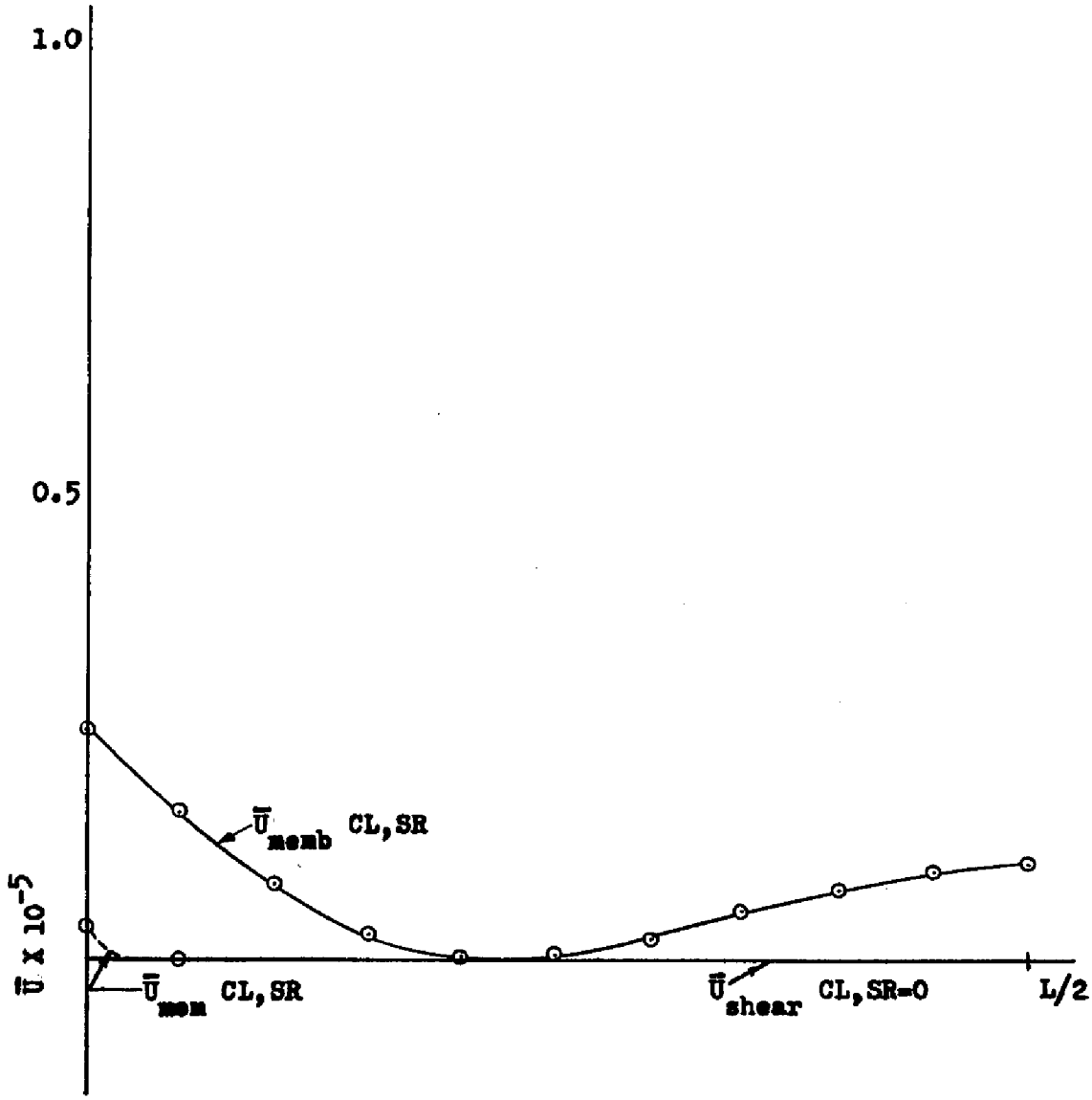

FIGURE 26

THICK, LONG, FIXED CYLINDER
ENERGY PATTERN
FOR M=2, N=1

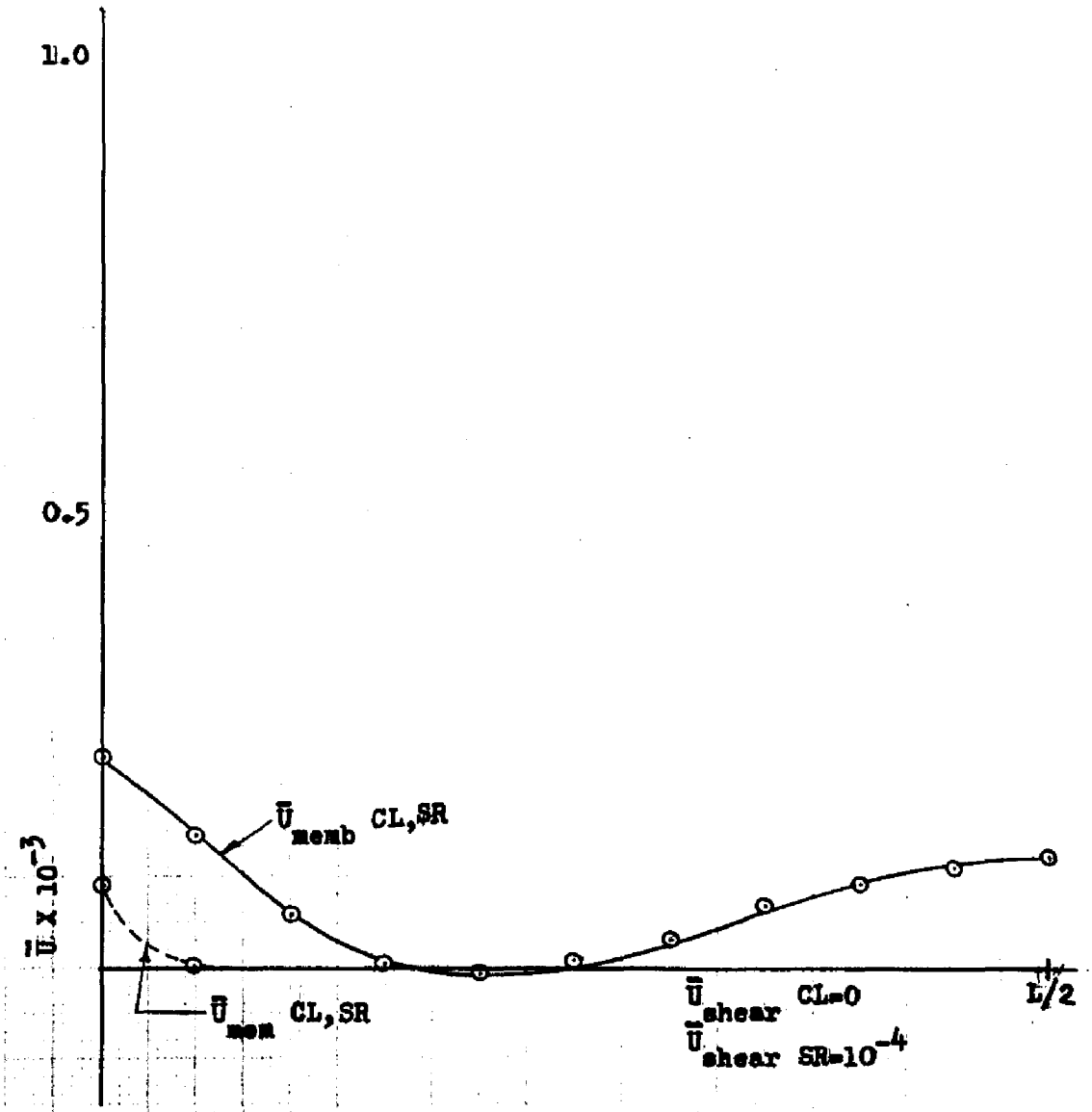

FIGURE 27

NODAL PATTERNS - FREE-EDGE CYLINDER

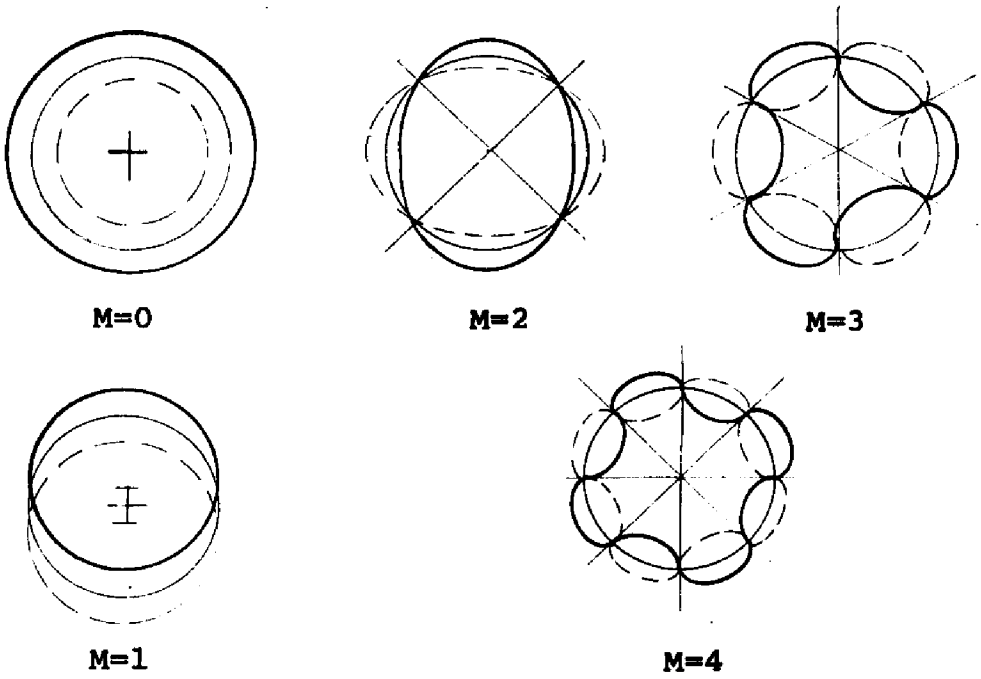

CIRCUMFERENTIAL NODAL PATTERN

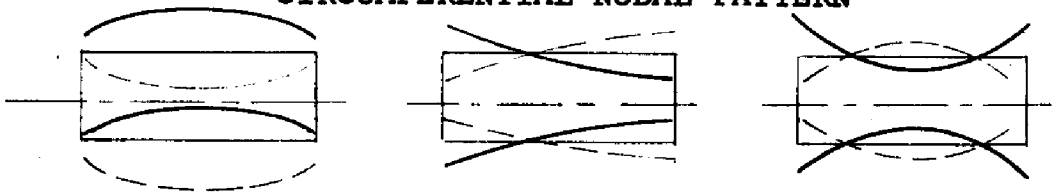

AXIAL NODAL PATTERN

NODAL ARRANGEMENT
FOR M=3, N=4

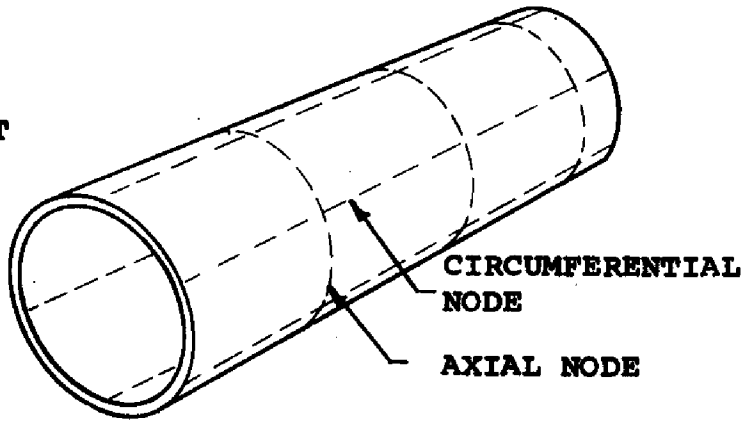

FIGURE 28

They are categorized according to an axial and circumferential nodal pattern (N, m). Information derived from a detailed study of the actual natural modes of the short, thick, free-ended cylinder is shown below. Special attention is paid to longer waves where the effects of boundary modeling is exhibited.

11.4.2.2 Natural Frequencies

The natural frequencies of oscillation for the cylinder, for both the CL and SR models, are recorded in Table III (Section X) and shown graphically in Figure 6 a-b. Differences in the natural frequencies, of given modal pattern, as the SR model is compared to the CL, do exist. These differences are tabulated in Table V. We note that for certain modal deformation patterns (m,N) the natural frequencies of oscillation for the SR model are higher than those for the CL model, while for other m,N combinations the situation is reversed* This phenomenon is shown schematically in Figure 29. Regions are defined, according to m,N nodal combinations, where either the CL natural frequency or the SR natural frequency may be higher.

We recall that with the fixed-ended cylinder, the natural frequency was always higher when the CL model was excited than when the SR model was excited. This was due to the pliancy effect, as previously discussed. The enhanced ease of deformation of the SR model accounts for its longer period of oscillation. The pliancy effect becomes more pronounced as the natural modal waves become shorter in both the axial and circumferential directions. This phenomenon is apparently also the controlling factor for the free cylinder in Region I (Figure 29) where the frequency of the CL model is higher than that of the SR model. In segment a of Region I,

*See note p. 193

N	1	2	3	4	5	6	7	8	9	10	11	12
m= 0	+.0000			-.0014	-.0030	-.0090	-.0800	-.0450		-.3160	-.4400	
1	+	+.0080	+.0017	+.0030	+.0010	-.0066	-.0200	-.0550				
2		+.0358	+.0100	+.0118	+.0180	-.0010	-.0070	-.0300		-.3900		
3		+.0448	+.0310	+.0310	+.0370	+.0320	+.0160	-.0110		-.3900		
4		+.0451	+.0547	+.0530	+.0560	+.0540	+.0380	-.0007			-.5400	
5	+.0087	+.0407	+.0629	+.0687	+.0700	+.0690	+.0540	+.0180	-.3300	-.5500		
6	+.0078	+.0358	+.0595	+.0728	+.0770	+.0750	+.0590	+.0360			-.5500	
7	+.0018	+.0295	+.0510	+.0670	+.0720	+.0720	+.0520	+.0220		-.3900	-.5800	
8	-.0060	+.0210	+.0400	+.0540	+.0620	+.0590	+.0420	+.0070		-.3900		
9	-.0230	+.0090	+.0240	+.0360	+.0380	+.0370	+.0180	-.0170	-.1600	-.4600		
10	-.0380	-.0100	+.0033	+.0080	+.0015	+.0020	-.0140	-.0540				
11	-.0630	-.0340	-.0230	-.0150	-.0080	-.0300	-.0560	-.1000	-.1700			
12	-.0900	-.0650	-.0570	-.0570	-.0400	-.0800	-.1000	-.1600	-.2300			
13	-.1400		-.1000	-.1100	-.1120	-.1130	-.1700	-.2300	-.3000			
14	-.1800		-.1500		-.1700	-.2000	-.2400	-.3000	-.4400			
15	-.2500	-.2200	-.2250	-.2300	-.2400	-.2800	-.3300	-.4000	-.5900			
16	-.3200	-.2900	-.2900	-.3000	-.3300	-.3700	-.4200	-.4900				
17	-.4200	-.3800	-.3800	-.4000	-.4200	-.4700	-.5300					
18			-.4900	-.5000	-.5400	-.5900						

TABLE V

TABULATION OF DIFFERENCES BETWEEN FIRST BRANCH

NATURAL FREQUENCIES ($\omega_{sr} - \omega_{c1}$)

FREE, SHORT, THICK CYLINDERS FREQUENCY BANDWIDTH 0.0-6.0

MAP OF NATURAL FREQUENCY DIFFERENCE - SR vrs. CL - FREE CYLINDER

N - Axial Wave Number

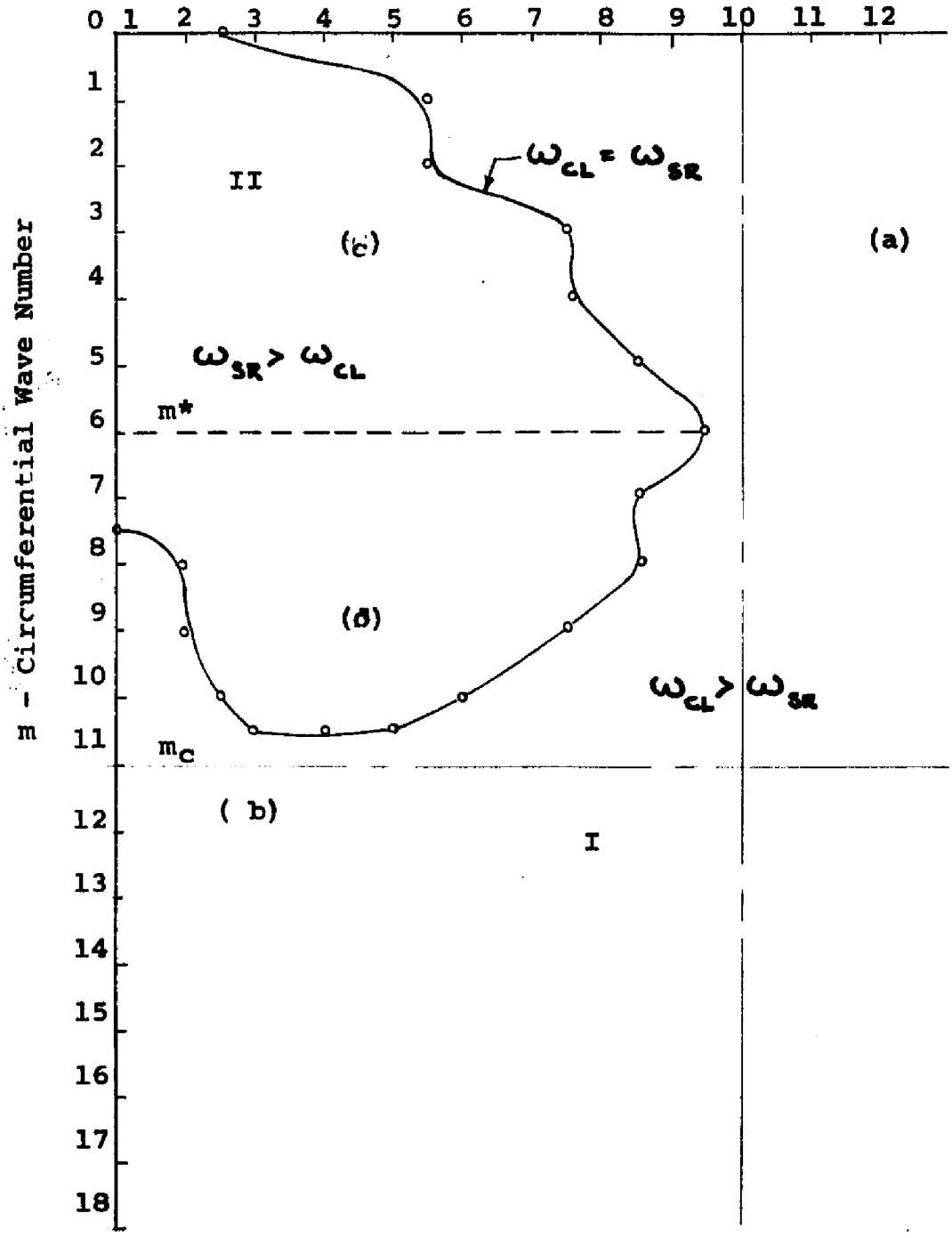

Figure 29

where the axial wave lengths are all shorter than some critical length ($N \geq N_c$), the deformation in the middle section is sufficiently isolated from any constraints at the edges. Here, the CL frequency is greater than the SR frequency as a consequence of axial pliancy difference.

In Region II, where the SR frequencies are greater than the CL, the waves are relatively long (m,N smaller) with lower natural frequencies. In this region, the importance of the state of the boundary appears to supersede the factor of pliancy. It is this boundary modeling effect which operates to raise the SR frequency over the classical. The source of this boundary effect lies in the necessary development of different SR and CL axial deformation forms, these differences originating at the boundary. This difference in deformation is in turn caused by necessary differences in the stress developed near the boundary for each model (equations 204,205) for a given axial nodal pattern. These stress differences increase as the rate of deformation in the circumferential (Ø) direction increases (m gets higher). In comparing natural frequencies, the boundary modeling effect must also manifest itself increasingly as the circumferential waves are shortened. This is seen in segment c of Region II. In this area, when a given circumferential deformation pattern has shorter waves, it must be associated with shorter axial deformation waves before the CL frequency exceeds that for SR. This prominence of boundary conditions, in determining differences in dynamic responses, is ineffectively challenged only till a certain point (m*). Beyond that point, the effects of greater flexural energy in the middle section of the cylinder (implied by the small radii of curvature in the circumferential direction) make themselves felt. The models deform differently under flexure. This circumferential

pliancy effect, of course, increases the natural frequency of the CL model relative to the SR model. In segment d of Region II, as m increases, the increased circumferential pliancy effect is beginning to substantially counteract the less rapidly increasing influence of the boundary modeling effect. Eventually, beyond m_c, in segment b of Region I, the CL frequency is always higher with any axial nodal pattern.

11.4.2.3 Deformation Patterns-Long Waves

The deformation patterns for some relatively long axial waves are shown in Figure 30. These modal shapes differ (as the CL and SR model is compared) more than those with the same nodal sequence in fixed-ended cylinders. The source of this deformation difference over the total length is found in the region of the boundary. This is more clearly seen in Figure 31, which illustrates the cylinder deformation near the edge. The deformation gradients ($\frac{\partial u_3^*}{\partial x}$) for the models are noticeably different right at the boundary. The gradients become parallel at a short distance from the edge and remain so. The effective length between the outer nodes is shortened for the SR form. This increases its natural frequency, which is higher than for the CL model. Deformation differences generated at the boundary increase as m increases (for a given N) implying the dependence of this axial phenomenon on the circumferential deformation at the boundary. As the axial wave lengths shorten (N increases), for the same m, the effect on the edge region deformation gradient is not as pronounced. The total deformation patterns (compared to longer axial waves) are such that the percentage difference of the effective lengths of the two models is less (the absolute effective length is greater between the outer nodes). Therefore, in most

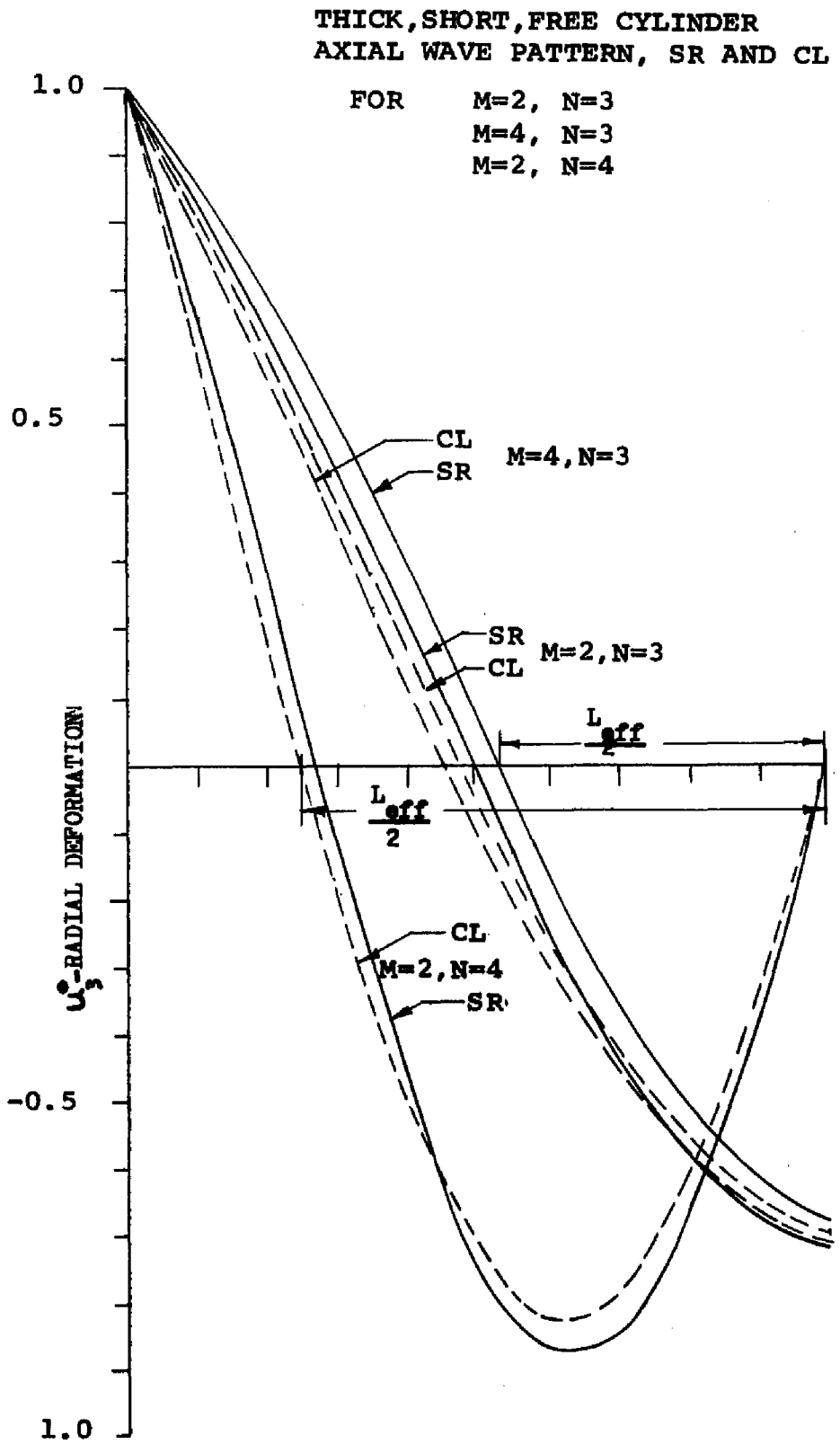
THICK, SHORT, FREE CYLINDER
AXIAL WAVE PATTERN, SR AND CL
FOR M=2, N=3
M=4, N=3
M=2, N=4
1.0
0.5
-0.5
1.0
CL
SR
M=4, N=3
SR
CL
M=2, N=3
CL
M=2, N=4
SR
$L_{\frac{eff}{2}}$
$L_{\frac{eff}{2}}$
u_3^*-RADIAL DEFORMATION

FIGURE 30

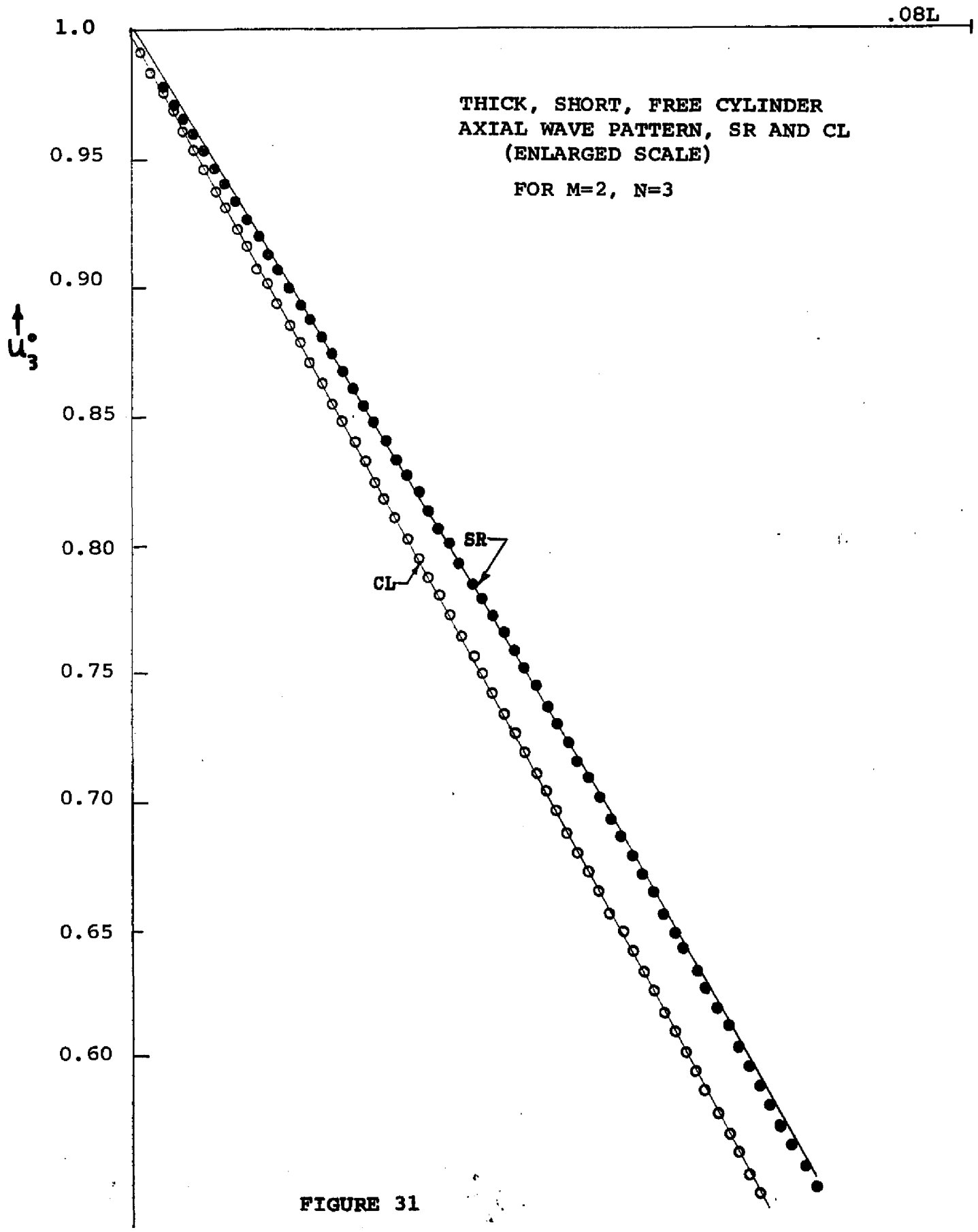
THICK, SHORT, FREE CYLINDER
AXIAL WAVE PATTERN, SR AND CL
(ENLARGED SCALE)
FOR M=2, N=3
1.0
0.95
0.90
0.85
0.80
0.75
0.70
0.65
0.60
.08L
u_3^*
SR
CL

FIGURE 31

cases the difference between the SR frequency and the CL frequency is decreased. The effect of this boundary phenomenon (deformation gradient divergence) is indicated in the graphs of the axial stress resultants (Figures 32, 33, and 34). Discussion of these figures is contained in the next section.

11.4.2.4 Axial Stress Resultants-Long Waves

For the CL and SR models, the different rates of change of the flexural moment resultant, $\frac{\partial \sigma_{11}'}{\partial x}$, near the region of the boundary, is evident in Figures 32, 33 and 34. For a given axial nodal pattern, as the circumferential waves shorten, (Figures 32 and 33) there is an increase in the absolute difference of the moment, σ_{11}', and of the transverse shear, σ_{13}°, between the models, causing the differing axial deformation patterns seen in Figure 30. Circumferential stresses near the boundary, associated with a required circumferential deformation, imply the existence of stress resultants in the axial plane due to Poisson's cross-coupling. The fictitious forces postulated for the CL model on the end faces permit a smoother force transition near the edge. This is esthetically pleasing but not necessarily more realistic. Nevertheless, the ultimate effect is to cause decidedly different stress (and deformation) patterns near the edge.

A change in the axial nodal pattern (Figures 32,34) for a given circumferential shape, produces less significant divergences.

In these curves for long, axial waves, the boundary effect, increasing as the circumferential waves shorten, is still a significant factor in determining the total stress

THICK, SHORT, FREE CYLINDER
STRESS RESULTANT PATTERN, SR, CL
FOR M=2, N=3

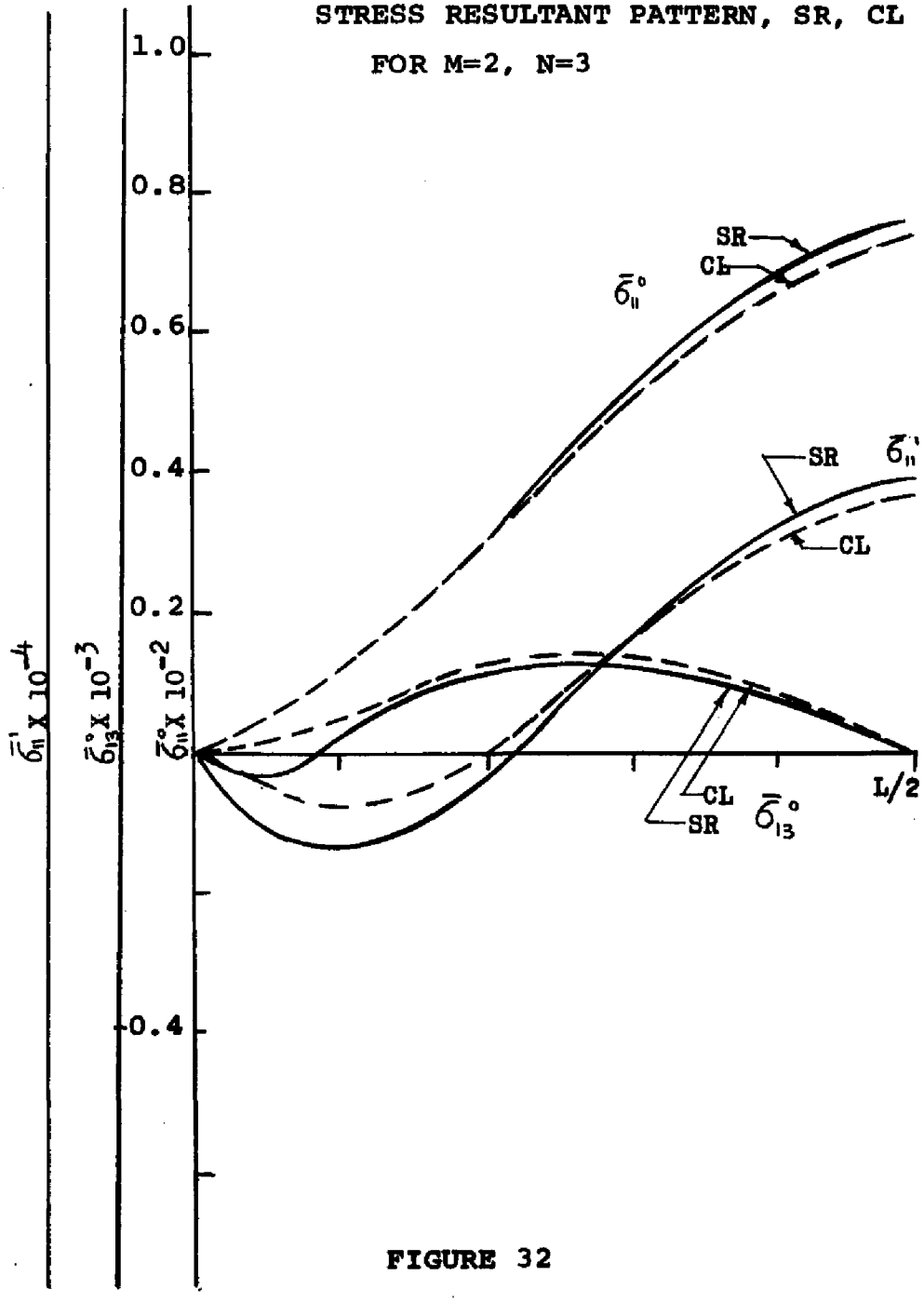

FIGURE 32

THICK, SHORT, FREE CYLINDER
STRESS RESULTANT PATTERN SR, CL
FOR M=4, N=3

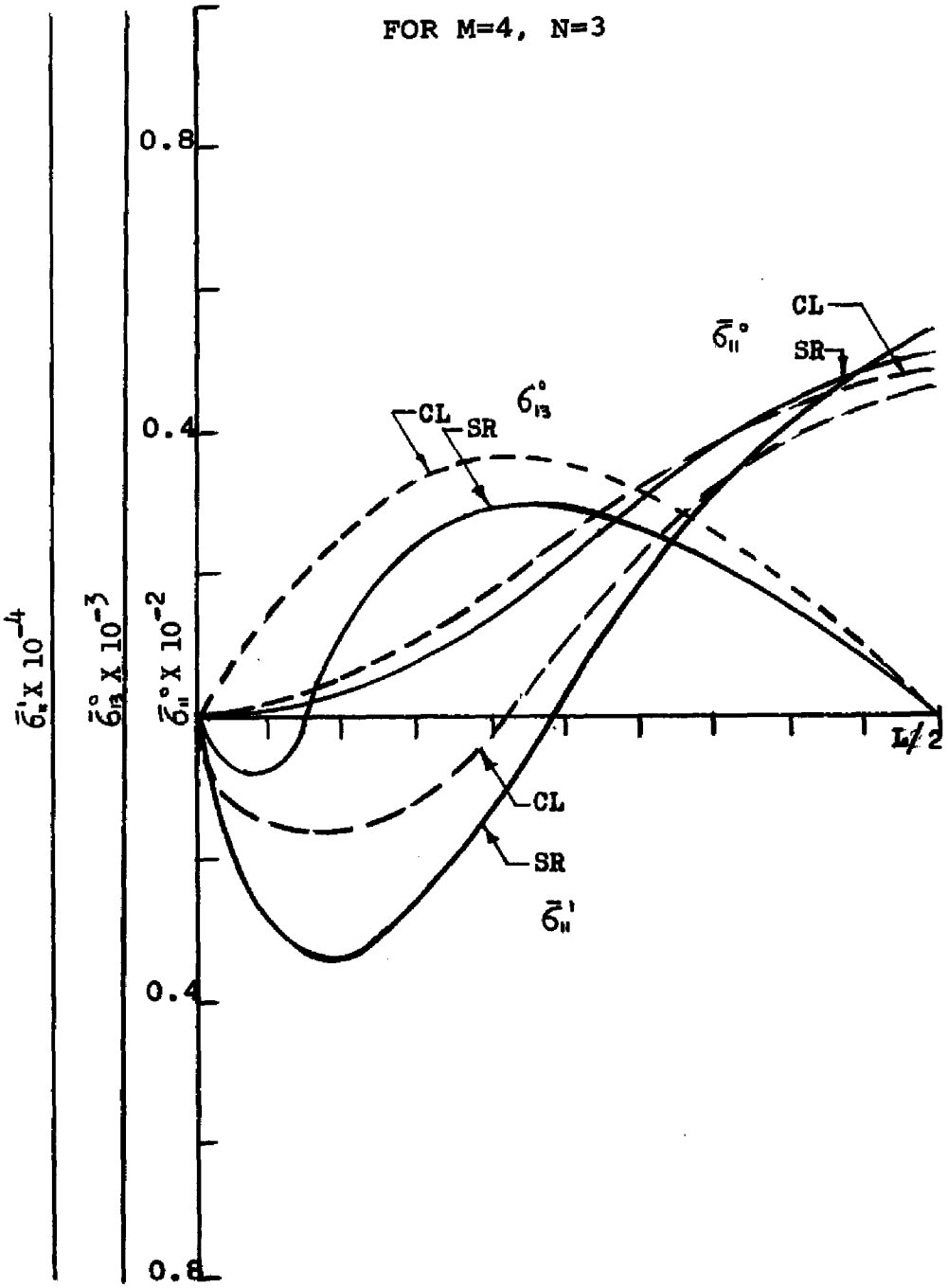

FIGURE 33

THICK, SHORT, FREE CYLINDER
STRESS RESULTANT PATTERN, SR, CL
FOR M=2, N=4

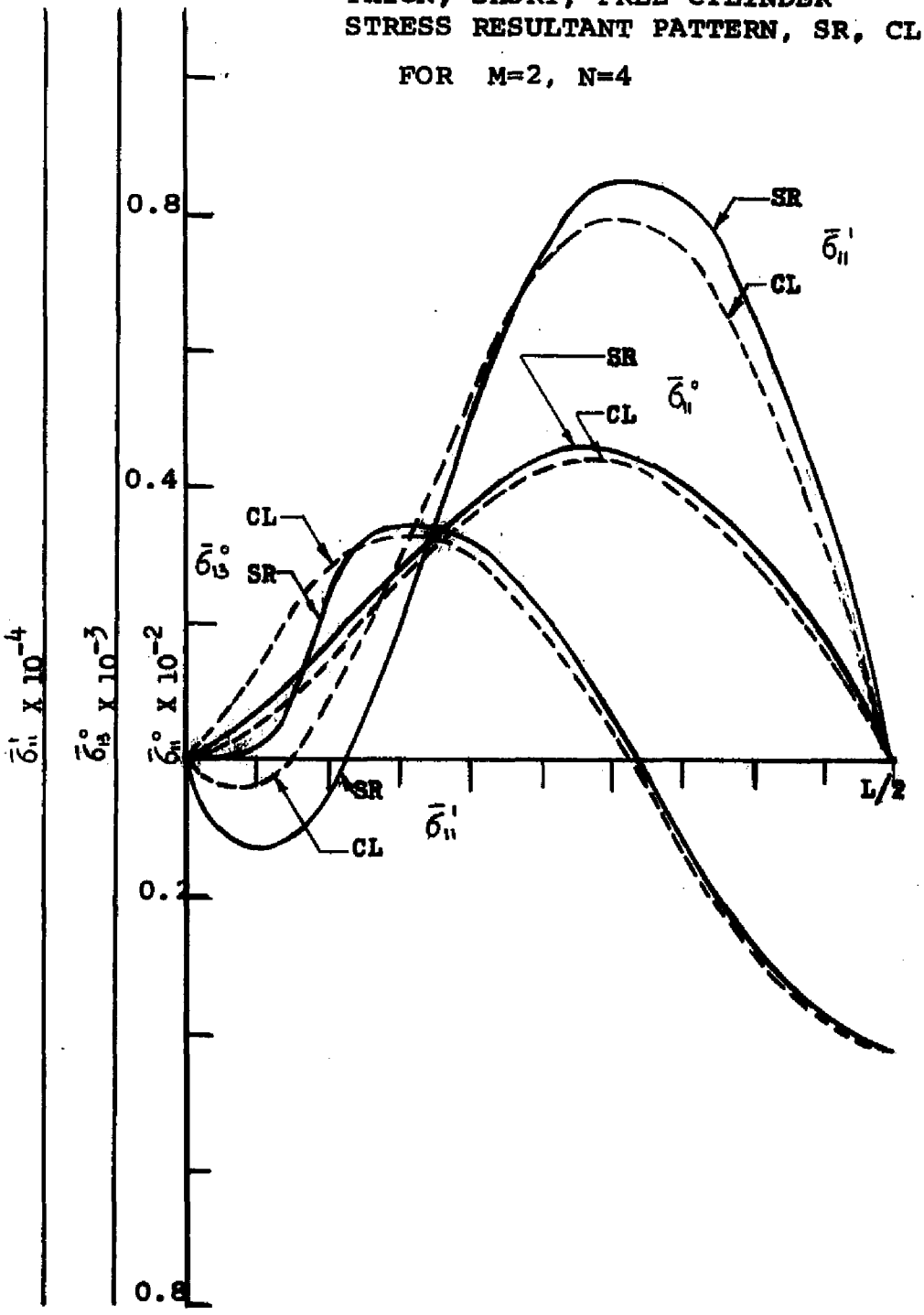

FIGURE 34

distribution throughout the length. These boundary differences in stress are the critical factor in developing the different deformation patterns seen in Figure 30 and ultimately accounting for the placement of these modes in Region II of Figure 29 where the frequency of the SR model is higher than that of the CL model.

The combined influence of the stresses and deformations are shown in the elastic strain energy distribution, Figures 35, 36, and 37. These Figures are discussed in the next section.

11.4.2.5 Axial Strain Energy Distribution-Long Waves

These Figures (35, 36, 37) for the free cylinder show different characteristics from the fixed-ended cylinder with the equivalent nodal pattern. The membrane energy is greater with the free cylinder and the differences between the energy in the SR and CL model is greater than with the fixed-ended cylinder. The existence of significant, and different, membrane energies, indicates that something more than the pliancy effect, which is associated with flexural and shear energy alone, is operative in causing these differences.

As the circumferential waves shorten, with a given axial nodal pattern (Figures 35, 36) the absolute value of the flexural energies increase and that of the membrane energies decrease. The percentage difference between the models for both these energies increase. A variation of this sort in the axial energy shows the influence of the boundary effect, with its dependence on the circumferential deformation. If the circumferential pliancy effect were important, the classical flexural energy at the half-length would be greater than the SR flexural energy.

FREE, THICK, SHORT CYLINDER
ENERGY DISTRIBUTION FOR M=2, N=3

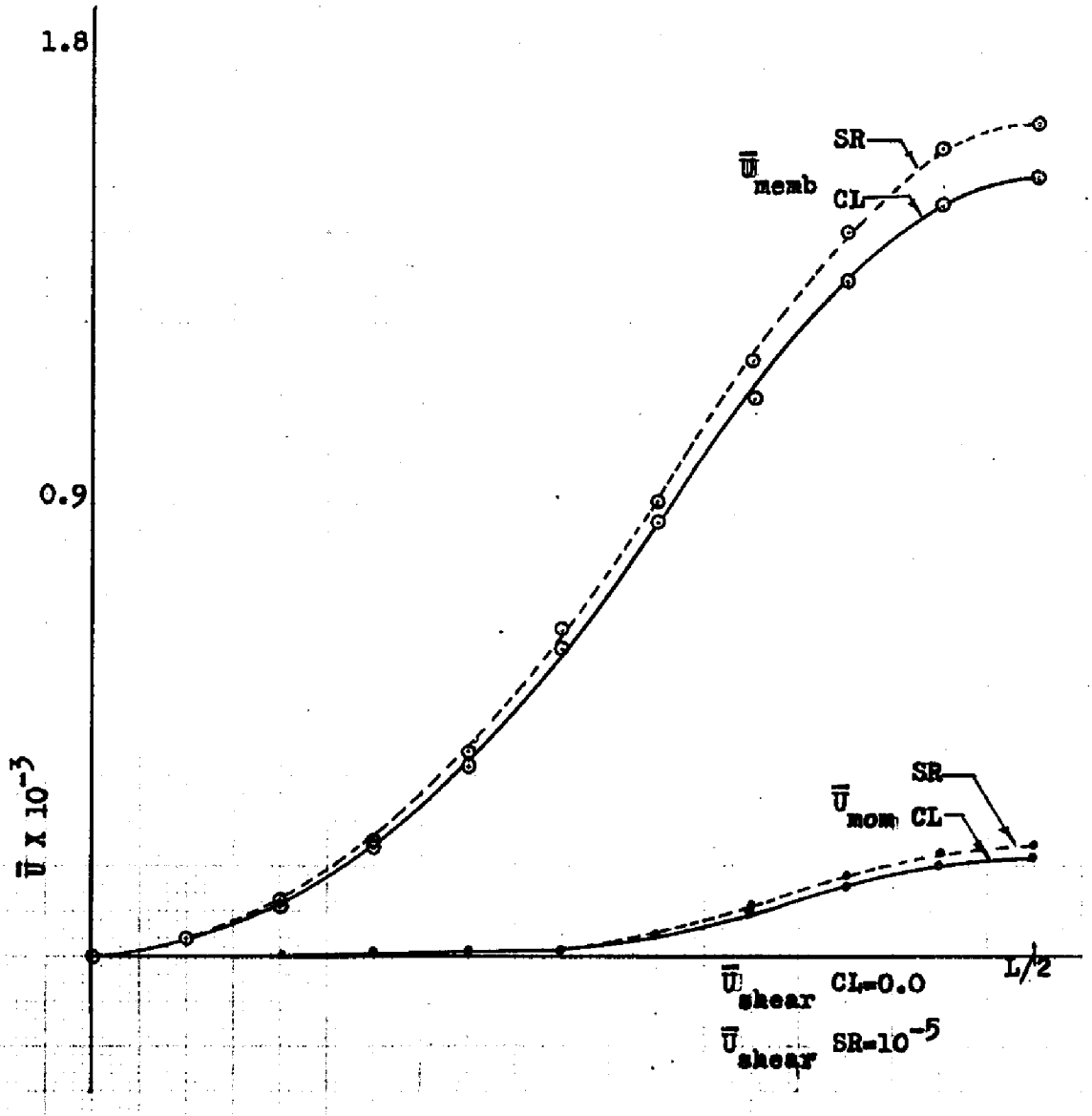

FIGURE 35

FREE, SHORT, THICK CYLINDER
ENERGY PATTERNS
FOR M=4, N=3

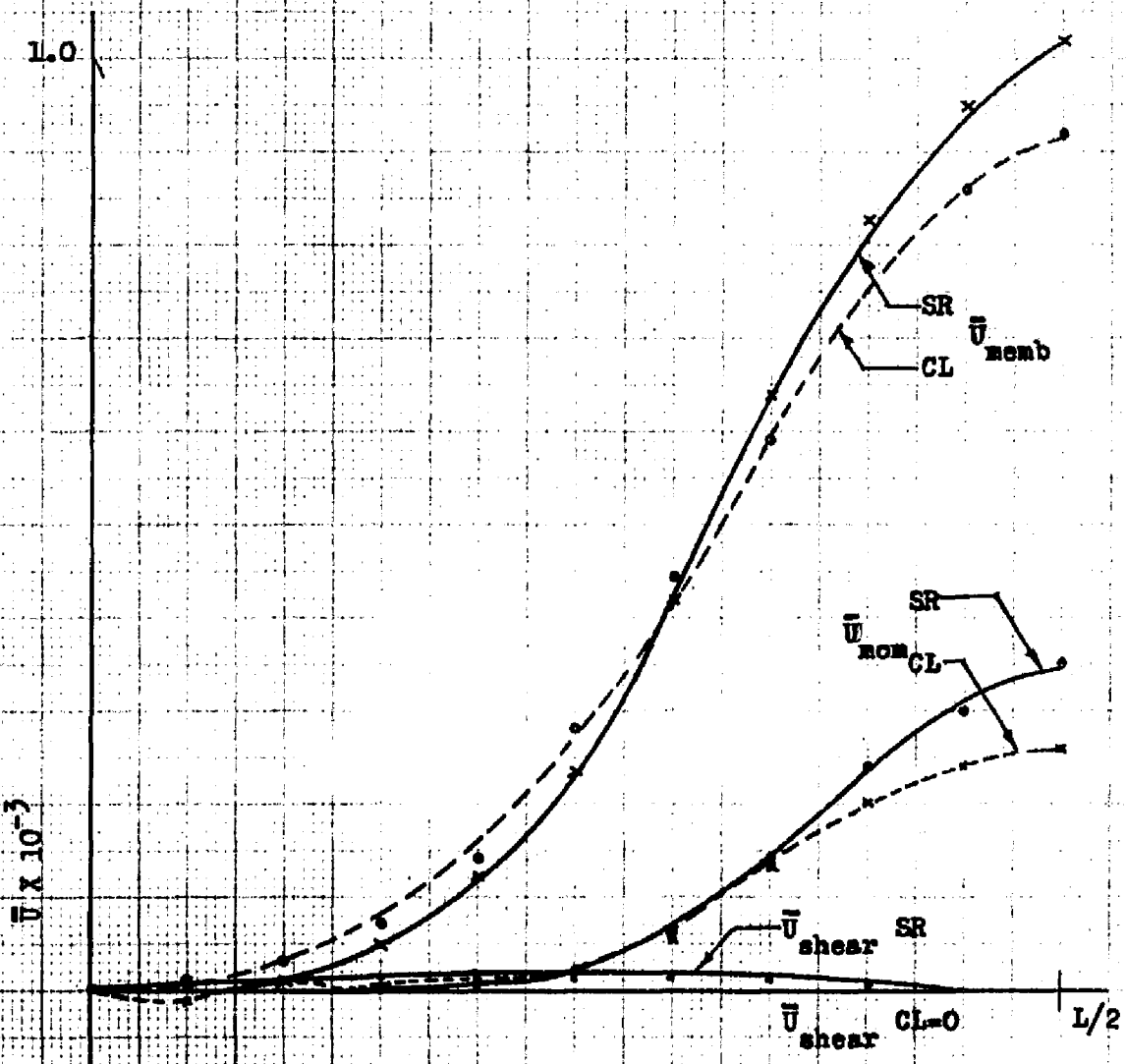

FIGURE 36

FREE, SHORT, THICK CYLINDER
ENERGY PATTERNS
FOR M=2, N=4

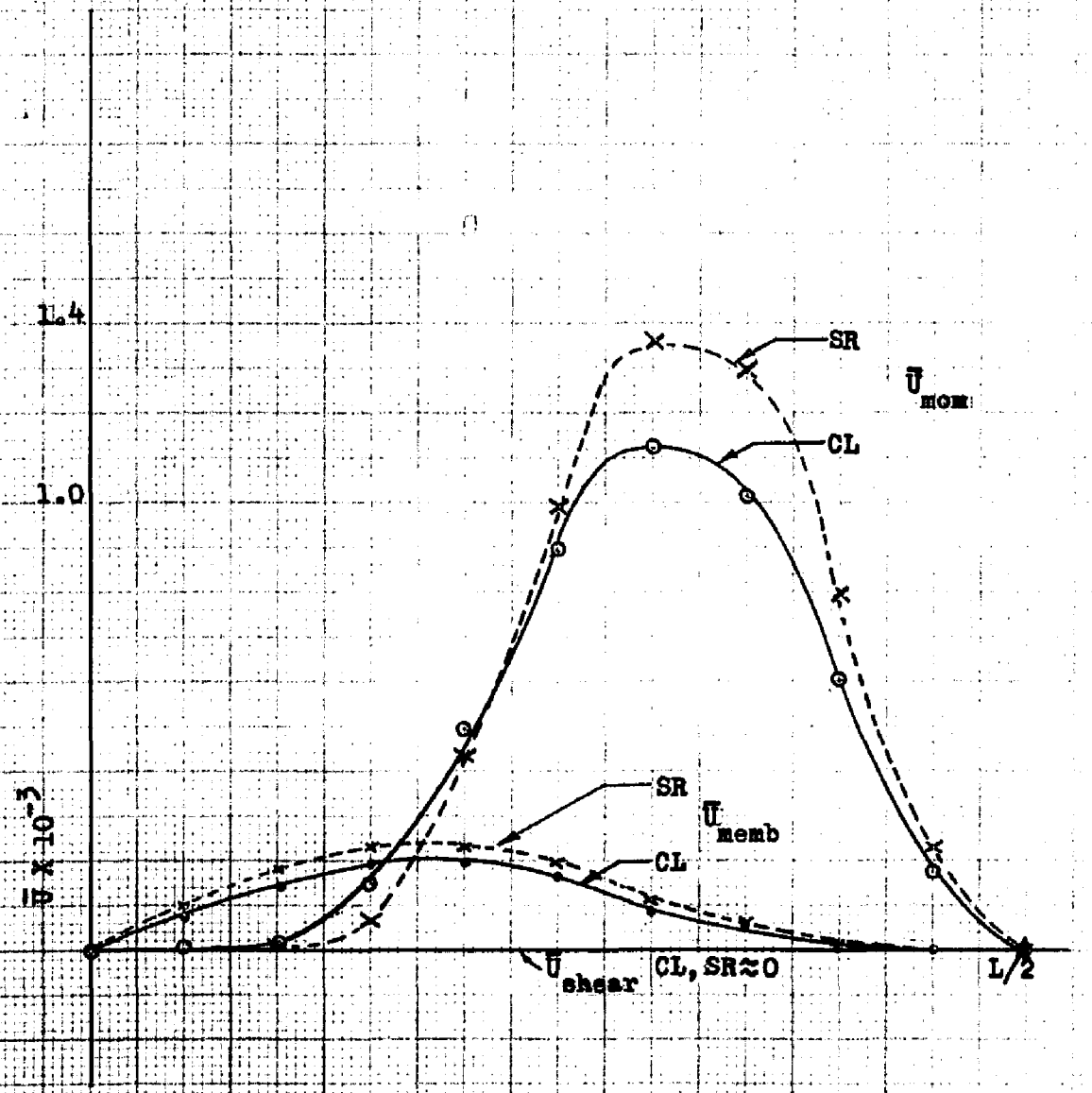

FIGURE 37

As the axial waves shorten (Figures 35,37) for a given circumferential shape, the absolute value of the flexural energies increase and the membrane energies decrease, proportionately more than when just the circumferential waves were shortened. This is to be expected, as we are examining axial strain energy, which is dependent upon median-surface deformation curvature in the axial direction. The percentage differences in the energies between the models, though, have not increased as much. As the number of axial half waves increase, the boundary effects are more isolated. Therefore, the axial (and circumferential) pliancy effect, as well as the boundary effect, is an important factor in producing the energy distribution throughout the half-length, shown in Figure 37.

11.4.2.6 Effects of Length and Thickness

The energy distribution of short-thin and long-thin cylinders are seen in Figures 38 and 39. Greater differences exist between the models for the free cylinder than with the same nodal pattern for the fixed-ended cylinder. These differences, for these waves, are primarily in membrane energy. As with the fixed cylinders, a modeling comparison for short-thick cylinders was chosen to be most informative.

11.5 Stress Histories

FREE, SHORT, THIN CYLINDER
ENERGY PATTERNS, SR AND CL

FOR M=2, N=3

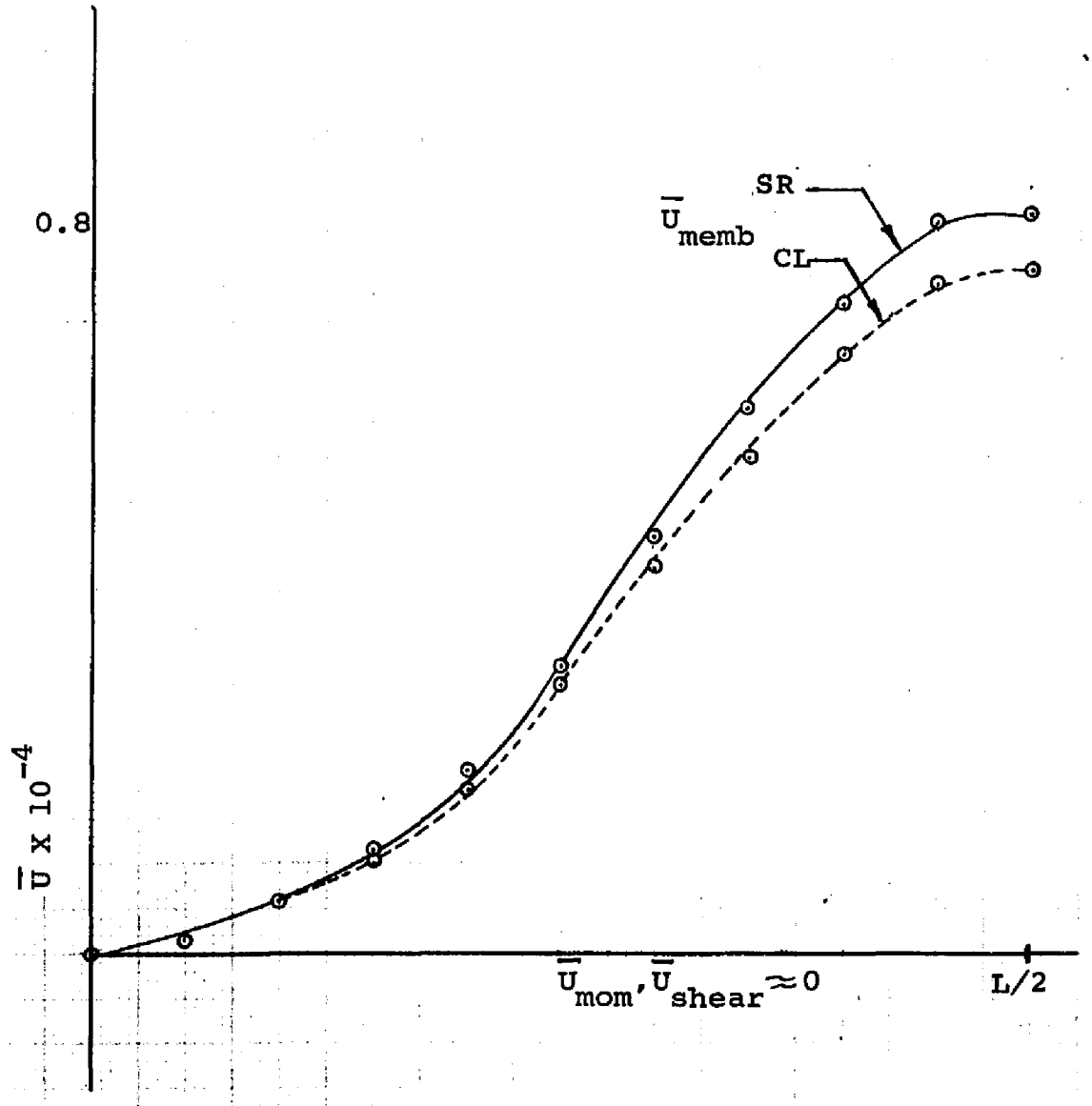

FIGURE 38

FREE, LONG, THIN CYLINDER
ENERGY PATTERN, SR AND CL
FOR M=2, N=3

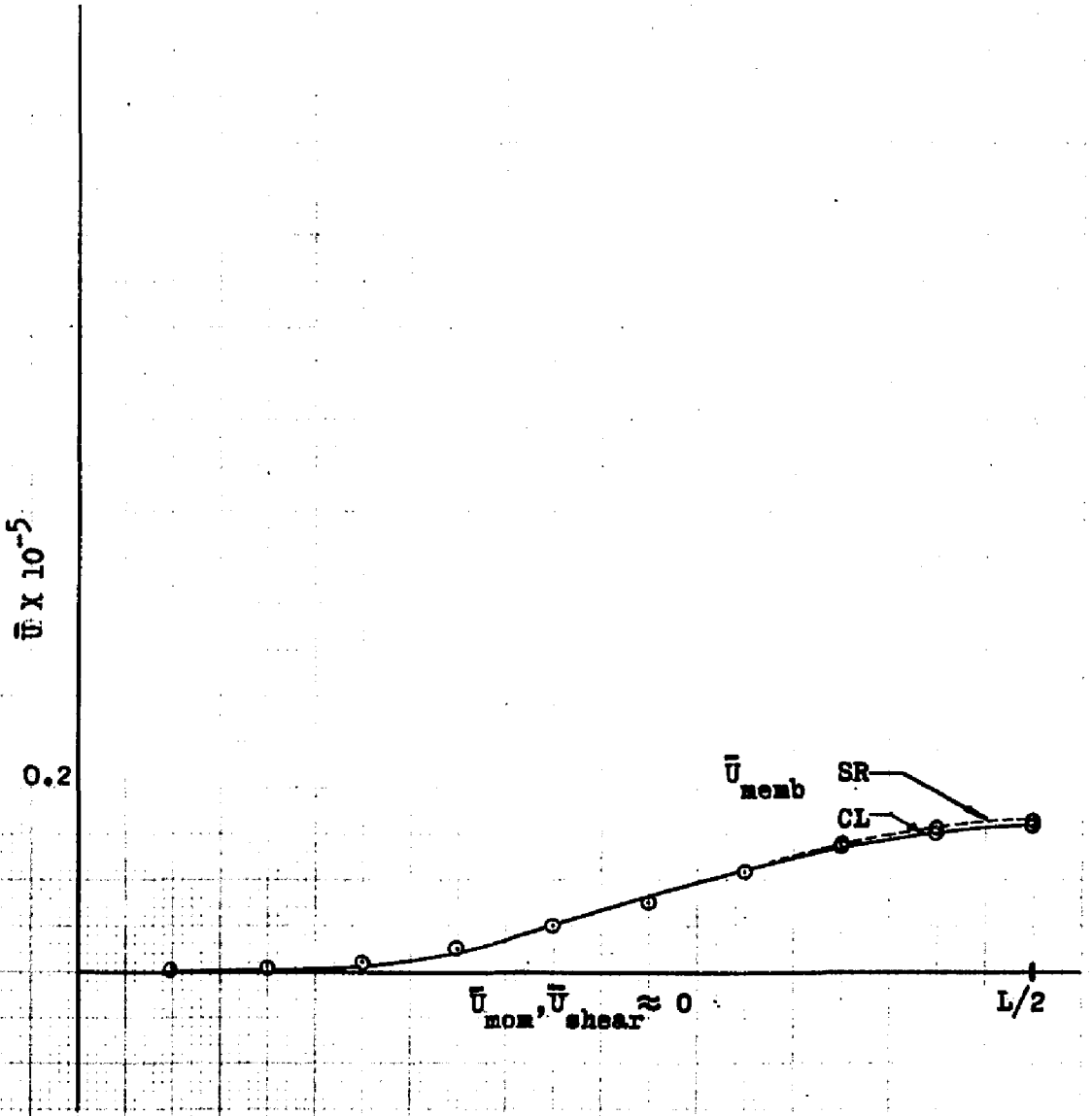

FIGURE 39

11.5.1 Fixed Cylinders

As previously explained, differences are encountered for the SR and CL models of fixed cylinders in the natural frequencies found, the stresses, and energy storage. These differences are accentuated as the structural waves become shorter, and they may be directly attributed to the pliancy effect.

In the normal mode solution to a forced vibration problem, the deformation series may be composed of as many terms as desired, as additional natural frequency elements are incorporated. The stresses, and stress intensity are direct function of the deformation series. Therefore, as more high frequency, short wave length modes are included in the deformation series, differences in the stress intensity histories between the models may be expected also to increase. When the higher order modes are included, a greater proportion of the total number of terms in the series are significantly different from equivalent terms in the deformation series for the alternate model.

There is no prior method by which one can determine how many terms should be included in the deformation series. A scan of natural frequencies was made, starting from zero. Stress intensity histories for the three loadings examined (cosine frontal, triangular, and exponential) are presented in Figures 7, 9 and 11. In Figure 7 the bandwidth is from 0 to 0.9. In Figure 9 the bandwidth has been extended, and now includes 0.0 to 16.0.

Again, in Figure 11, the bandwidth includes from 0 to 30.0. Units for the bandwidth are in terms of normalized natural frequency.

In examining these stress intensity curves, as well as those for the free cylinder (Figures 8, 10 and 12), we could compare the SR and CL results for a particular loading for the three proposed values of cutoff frequency. Alternately, we could compare the SR and CL results at a particular cutoff frequency for the three different loads.

Several parameters may be chosen as an index of comparison: the general appearance of the curves, the occurrence of maxima and minima, their values, the range between extremes, the mean value of the curve, and the standard deviation of the values from the mean. In examining the stress intensity history, it should be noted that the values are normalized for each pair of curves to the maximum stress intensity for the CL theory.

The history of stress intensity can be viewed in two ways: either as an approximation to the actual history, or as a statistical sampling of the stress intensity in time. Either attitude is useful.

First, examine Figure 7. The bandwidth is from 0.0 to 0.9 units of normalized natural frequency. The history is presented for 10 cycles of the lowest frequency found. As will be seen, this bandwidth includes only a small number of the actual natural frequencies for the cylinder.

They are also all relatively low, and the structural waves are relatively long.

In Figure 7, the differences in stress intensity history are relatively small. In fact, for the Cosine Frontal Impulse and the Triangular Impulse, the SR and CL curves are essentially duplicates of each other. Only the result for the Exponential Impulse shows any difference at all. This loading has clearly excited whatever short structural waves exist in this bandwidth.

Continuing in Figure 7, we have noted that the whole bandwidth consists of fairly long structural waves. For this bandwidth, this group of longer structural waves may be subdivided further into two groups. In the first group membrane energy is prominent and in the other group flexural energy is prominent. The membrane energy waves have a higher frequency of oscillation and a higher velocity of wave propagation. This is related to an apparent anomaly in Figure 7c. A high stress intensity peak is noted (for both CL and SR theories) which occurs almost immediately after application of the impulse, which is not repeated within the time span examined. I believe that this is because the flexural waves, with a slower wave propagation velocity, dominate the response curve for the exponential load initially. In the cosine frontal and triangular pulses, the short waves are not as important, proportionally, in the stress series at any time. It may be expected that in higher frequency bandwidths the normal modes with short structural (flexural) waves that are disclosed by the scan will have a higher frequency of oscillation and a greater wave propagation velocity.

In Figure 7a, comparing the CL and SR curves for the cosine frontal loading, the differences between the maximum values of stress intensity encountered is 1.96 percent. The difference in the average value for this case was computed to be 3.2 percent. For both figures, the maxima, and the averages, the CL response is slightly higher. In Figure 7b, the difference in maximum values is 2.71 percent, and the difference in averages 3.0 percent. Again, the CL values are higher. For 7c, the difference in maximum values is 5.36 percent, while the difference in average values is - 7.5 percent. (The negative sign is used to denote the fact that the calculation results in a higher value for the SR theory than the CL theory).

It was expected that the CL theory would give higher values for the stress intensity than the SR, with the greatest effect being noted for the exponential impulse. A comparison of the maximum value differences, i.e., 1.96, 2.71 and 5.36 show the result is as expected. On the basis of further experience, however, I believe the sampling is too small to be reliable.

Now, consider Figure 9. The bandwidth is from 0.0 to 16.0 cycles of normalized natural frequency. From the general appearance of the curves, there are now significant differences to be noted between the SR and the CL models for all loads. It is evident that more short waves have been incorporated into the deformation and stress intensity series.

Examine first Figure 9c. Note that for the exponential impulse, high stress intensities are found in greater abundance at times later than just directly after the application of the impulse.

This is because of the inclusion of the new modes. They have a high frequency and wave propagation velocity, and their influence is repeated during the time span examined.

These new waves also effect the stress intensity history shortly after the cosine frontal impulse is applied. See Figure 9a. The effect is opposite to the values found previously, which had been traced to the influence of membrane energy terms.

The differences between maxima are shown on graphs 9a, 9b and 9c respectively to be 22.9, - 1.95 and 16.4 percent. These are not in the order expected. My interpretation is that the cosine frontal response is being affected earlier than the other two loads. The differences in the mean values (not shown on the graphs) are 3.8, 8.2 and -6.3 percent.

Now, examine Figure 11. The calculations were carried forward to include a bandwidth from 0.0 to 30.0. Many more short waves have been incorporated, and the tendencies previously noted are accentuated.

Significant differences in the SR and CL models exist for three loads. In comparing the CL stress intensities between Figure 9 and Figure 11, I note that they have not changed significantly, while the SR stress intensities have changed slightly. The least change in SR stresses has been with the cosine frontal impulse, where because of its spatial distribution, the short waves are least excited.

In comparing Figures 11a, 11b and 11c, the differences between maximum values are 17.8, - 5.84 and 27.5 percent. The differences in average values are (again not shown) - 4.4, -1.92 and + 5.14 percent. These latter are ordered in the proper manner, but I would expect the SR to be consistently lower in value than the CL. (All positive).

Now, an attempt must be made to answer the question as to whether or not the situation has stabilized or is close to stabilization. Additional computation is extremely expensive and is not warranted unless there is a clear reason for pursuing it.

Figure 40 is a comparison of the maximum stress intensities for these bandwidths. Although from the graph, it is not conclusively apparent that intensities are stabilized for all loadings, certain other tendencies, though, may be definitely identified now. The SR model responds more slowly initially, with respect to time, to <u>any</u> impulse. The <u>total</u> stress-time pattern differs significantly between the models for all three loads. The percentage difference between the maximum stress intensities is already 27 percent for the exponential impulse. This parameter (the difference between maxima) is somewhat fragile, though, as the point where the maximum stress is achieved varies as additional terms are included.

In view of two facts: the significant differences in the total stress intensity history, through the time span investigated, between the SR and CL models, for all inputs, and the differences between maxima as exemplified in Figure 40, <u>it is concluded that the choice of the SR</u>

model is warranted for fixed cylinders undergoing transient loadings. For the actual case, it is further recommended that enough normal modes be included so that the stress intensity history becomes stable for higher cutoff points. This will have to remain as a matter of engineering judgement for the particular case where an answer is required.

11.5.2 Free Cylinders

Again, differences are encountered for the SR and CL models of free cylinders in the natural frequencies found, the stresses and energy storage. These differences are accentuated as structural waves become shorter, but there are now two influences at work. In addition to the pliancy effect, the end conditions are also important. This has been discussed earlier in this chapter.

For the free cylinder, a scan of natural frequencies was also made, starting from 0.0. Stress intensity histories are presented for the three loadings being investigated in Figures 8, 10 and 12. In Figure 8, the bandwidth is from 0 to 0.7. In Figure 10, the bandwidth has been extended to 16.0, and subsequently in Figure 12, to 25.0.

First, examine Figure 8. At this low truncation bandwidth, long normal mode waves are uncovered. The differences in stress intensities for the SR and CL model are much greater than was the case with the fixed cylinder. The effect is due to the different natural boundary conditions developed within Hamilton's Integral.

Very different wave shapes and internal stresses are induced, with the same nodal conditions. It is this effect that is predominant in this region.

The differences in the maxima for the three loadings are 4.2, 5.3 and 12.2 percent respectively, as shown in Figure 8a, 8b and 8c. These are properly ordered.

Now, examine Figure 10, which includes the bandwidth from 0.0 to 16.0. The situation has been altered considerably. The stress intensity histories of both models are very similar, more so than with the fixed cylinder at the same truncation of the search frequency. These new modes (included in the band are from 0.7 to 16.0) short, flexural waves, where the boundary effects are isolated in the edge regions. The pliancy effect is primarily operative in producing model differences, but is not as critical here as with the fixed cylinder. The small differences that do exist are noticeably evident only for 10c, the case of the exponential impulse.

The differences in maxima are shown on Figure 41, but are considered to be less important in evaluating the results than the fact that the stress history curves are very similar.

Now, proceed to Figure 12, which covers a bandwidth from 0.0 to 25.0. The differences between models are now more evident, although the patterns in time of the stress intensities have not been much altered. The stress intensities now, compared to the intermediate region shown in Figure 10, are at least as close to stabilization as for the fixed cylinder at this truncation frequency.

Differences between the models are not as great as they were for the fixed cylinder. We note, however, that the exponential impulse has produced a percentage difference (in maxima) for the models of 20 percent.

Certain conclusion can be reached concerning the applicability of the SR or CL model from these findings. The most important, perhaps, is that no general rule can be formulated about the influence of the SR and CL model in a structure with arbitrary edge supports. The unexpected effect of the different natural boundary conditions for the two models with the free cylinder is a case in point. Specifically, for the free cylinder, the effect of a transient dynamic load in producing different response from the models is not as evident as with the fixed cylinder. A more gradually applied load, though which might primarily excite longer structural waves, would produce a difference in response, according to the alternate models, greater than in a fixed cylinder.

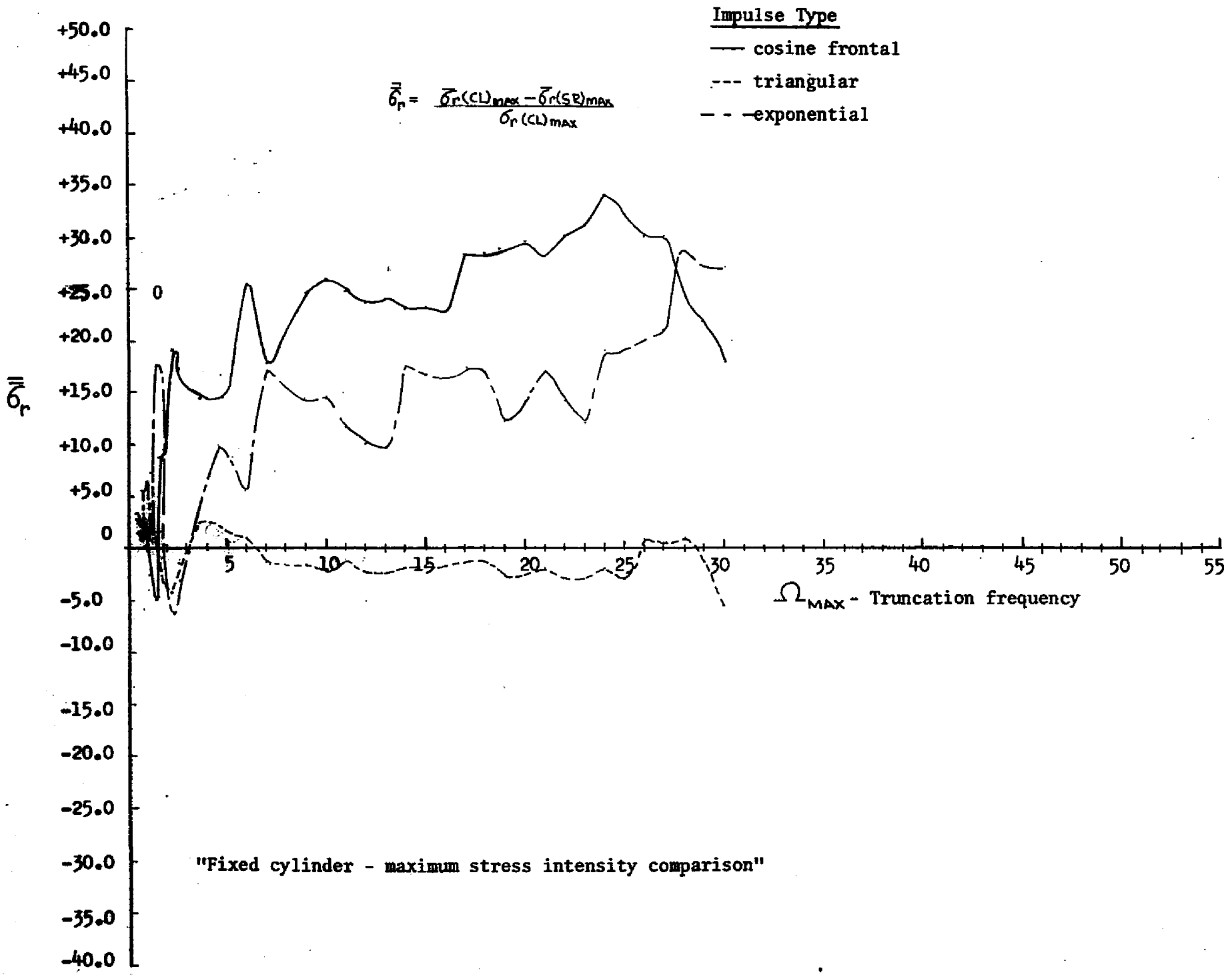

"Fixed cylinder - maximum stress intensity comparison"

Figure 40

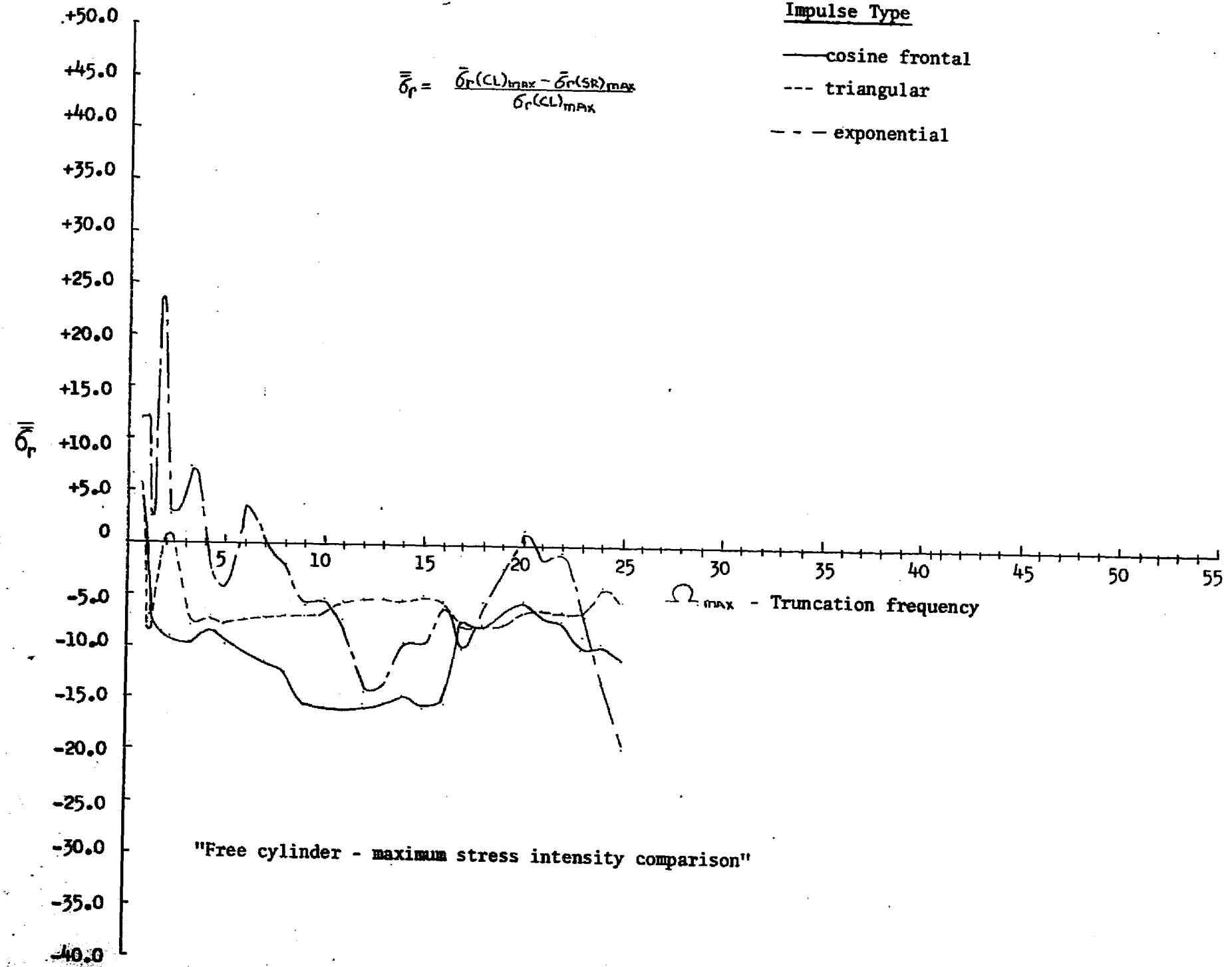

"Free cylinder - maximum stress intensity comparison"

Figure 41

Footnote to 11.4.2.2, Free Cylinder Natural Frequencies

Reismann and Padlog, (63) compared the CL theory of Timoshenko-Love with the SR theory of Hermann-Mirsky (36), for the axisymmetric response of a finite length, simply supported cylinder. They published first branch phase velocities for both theories which showed a greater value for the CL theory with the longest axial waves. In their original work, Hermann and Mirsky (12), working with a CL model reduced from their SR theory, did not note this phenomena with an infinite cylinder. When Hermann and Mirsky (12) consider nonaxially symmetric motion of the infinite cylinder, where circumferential deformation is influential, their SR theory did exhibit what they considered a peculiar effect with the first branch phase velocities. A double minimum was noted in the region of the longer axial waves (implying an unexpected increase in the natural modal frequencies). This occurred only with the longer circumferential waves. Yu (6) noted similar results for his SR theory with the infinite cylinder.

APPENDIX A

VARIATION OF THE LAGRANGIAN DENSITY

The application of Hamilton's principle requires that:

$$\text{(A-1)} \qquad \int_t \int_V \delta\left(\tfrac{1}{2}\rho \dot{\bar{r}}\cdot\dot{\bar{r}}\right) dV dt - \int_t \int_V \delta\left(\tfrac{1}{2}\sigma_{ik}\epsilon_{ik}\right) dV dt + \int_t \int_\Sigma \bar{P}\cdot\delta\bar{r}\, d\Sigma\, dt = 0$$

We evaluate these, term by term, starting with the second term, which relates to the strain energy.

STRAIN ENERGY

The strain-displacement equations in curvilinear coordinates for a linear infinitesimal strain theory are represented by the tensor:

$$\text{(A-2)} \qquad \epsilon_{ik} = \frac{1}{2}\left[\frac{\partial u_i}{\partial s_k} + \frac{\partial u_k}{\partial s_i} + \left(\bar{e}_i\cdot\frac{\partial \bar{e}_t}{\partial s_k} + \bar{e}_k\cdot\frac{\partial \bar{e}_t}{\partial s_i}\right)u_t\right]$$

The constitutive equations of an isotropic material are:

$$\text{(A-3)} \qquad \sigma_{ik} = \mathcal{L}\,\epsilon_{tt}\,\delta_{ik} + 2G\epsilon_{ik}$$

in which ϵ_{tt} is the dilatation and $\mathcal{L}$, G are Lame's constants. For a homogeneous material, $\mathcal{L}$ and G do not vary. (δ_{ik} is the Kronecker delta, which vanishes for $i \neq k$, and is equal to 1 for $i = k$).

Both σ_{ik} and ϵ_{ik} are thus functions of the deformation coordinates u_k and their space derivatives. We have already indicated that u_k is taken as a function containing the parameter α (refer to equation 17). Thus:

(A-4)

$$-\delta\left(\tfrac{1}{2}\sigma_{ik}\epsilon_{ik}\right) = -\frac{\partial}{\partial\alpha_\ell}\left(\tfrac{1}{2}\sigma_{ik}\epsilon_{ik}\right)d\alpha_\ell$$

Before proceeding, we shall demonstrate that:

(A-5) $$-\delta U = -\delta\left(\tfrac{1}{2}\sigma_{ik}\epsilon_{ik}\right) = -\sigma_{ik}\delta(\epsilon_{ik}) = -\frac{\partial U}{\partial\epsilon_{ik}}\delta(\epsilon_{ik})$$

where $\sigma_{ik} = \partial U/\partial\epsilon_{ik}$ for an elastic material with no dissipative properties. This may be done as follows. First, expand $-\delta(1/2\,\sigma_{ik}\epsilon_{ik})$

(A-6) $$-\delta\left(\tfrac{1}{2}\sigma_{ik}\epsilon_{ik}\right) = -\frac{\partial}{\partial\sigma_{ik}}(\quad)\delta\sigma_{ik} - \frac{\partial}{\partial\epsilon_{ik}}(\quad)\delta\epsilon_{ik}$$

(A-7) $$-\delta\left(\tfrac{1}{2}\sigma_{ik}\epsilon_{ik}\right) = -\tfrac{1}{2}\epsilon_{ik}\delta\sigma_{ik} - \tfrac{1}{2}\sigma_{ik}\delta\epsilon_{ik}$$

The expression for σ_{ik} is available from (A-3). We rewrite (A-3) below:

(A-3) $$\sigma_{ik} = \mathcal{L}\epsilon_{\ell\ell}\delta_{ik} + 2G\epsilon_{ik}$$

Introducing an equivalent form,

(A-8) $$\sigma_{ik} = \mathcal{L}(\epsilon_{\ell j}\delta_{\ell j})\delta_{ik} + 2G\epsilon_{ik}$$

Taking $\delta\sigma_{ik}$:

(A-9) $$\delta\sigma_{ik} = \frac{\partial\sigma_{ik}}{\partial\epsilon_{\ell j}}\delta(\epsilon_{\ell j}) + \frac{\partial\sigma_{ik}}{\partial\epsilon_{ik}}\delta(\epsilon_{ik})$$

This reduces to:

(A-10) $$\delta\sigma_{ik} = \mathcal{L}\delta_{\ell j}\delta_{ik}\delta(\epsilon_{\ell j}) + 2G\delta(\epsilon_{ik})$$

Now, substitute (A-10) in (A-7):

$$(A\text{-}11) \qquad -\delta\left(\tfrac{1}{2}\sigma_{ik}\epsilon_{ik}\right) = -\tfrac{1}{2}\sigma_{ik}\delta(\epsilon_{ik}) - \tfrac{1}{2}\epsilon_{ik}\left\{\lambda\delta_{tj}\delta_{ik}\delta(\epsilon_{tj}) + 2G\delta(\epsilon_{ik})\right\}$$

Factor out the ½ to obtain:

$$(A\text{-}12) \qquad -\delta\left(\tfrac{1}{2}\sigma_{ik}\epsilon_{ik}\right) = -\tfrac{1}{2}\left\{\sigma_{ik}\delta(\epsilon_{ik}) + \lambda\epsilon_{ik}\delta_{tj}\delta_{ik}\delta(\epsilon_{tj}) + 2G\epsilon_{ik}\delta(\epsilon_{ik})\right\}$$

In the second term, $\epsilon_{ik}\delta_{ik} \rightarrow \epsilon_{tt}$

$$(A\text{-}13) \qquad -\delta\left(\tfrac{1}{2}\sigma_{ik}\epsilon_{ik}\right) = -\tfrac{1}{2}\left\{\sigma_{ik}\delta(\epsilon_{ik}) + \lambda\epsilon_{tt}\delta_{tj}\delta(\epsilon_{tj}) + 2G\epsilon_{ik}\delta(\epsilon_{ik})\right\}$$

Now change the indices so that $\delta_{tj}\delta(\epsilon_{tj}) \rightarrow \delta_{ik}\delta(\epsilon_{ik})$

$$(A\text{-}14) \qquad -\delta\left(\tfrac{1}{2}\sigma_{ik}\epsilon_{ik}\right) = -\tfrac{1}{2}\left\{\sigma_{ik}\delta(\epsilon_{ik}) + \lambda\epsilon_{tt}\delta_{ik}\delta(\epsilon_{ik}) + 2G\epsilon_{ik}\delta(\epsilon_{ik})\right\}$$

Factor out $\delta(\epsilon_{ik})$

$$(A\text{-}15) \qquad -\delta\left(\tfrac{1}{2}\sigma_{ik}\epsilon_{ik}\right) = -\tfrac{1}{2}\left\{\sigma_{ik} + \lambda\epsilon_{tt}\delta_{ik} + 2G\epsilon_{ik}\right\}\delta(\epsilon_{ik})$$

Note that the last two terms are equal to σ_{ik} by equation (A-3), so that (A-15) reduces to:

$$(A\text{-}5) \qquad -\delta\left(\tfrac{1}{2}\sigma_{ik}\epsilon_{ik}\right) = -\sigma_{ik}\delta(\epsilon_{ik})$$

(This is what we set out to demonstrate).

To proceed with the actual variation of the strain energy term, use (A-2) and (A-5) in (A-1):

$$(A\text{-}16) \qquad -\int_t\int_V \delta\left(\tfrac{1}{2}\sigma_{ik}\epsilon_{ik}\right)dVdt = -\int_t\int_V \frac{\sigma_{ik}}{2}\delta\left\{\frac{\partial u_i}{\partial s_k} + \frac{\partial u_k}{\partial s_i} + \right.$$

$$\left. + \left(\bar{e}_i \cdot \frac{\partial \bar{e}_t}{\partial s_k} + \bar{e}_k \cdot \frac{\partial \bar{e}_t}{\partial s_i}\right)u_t\right\}dVdt$$

Consider the first two terms on the right side of (A-16):

$$(A\text{-}17) \qquad -\int_t\int_V \frac{\sigma_{ik}}{2}\delta\left\{\frac{\partial u_i}{\partial S_k}+\frac{\partial u_k}{\partial S_i}\right\} = -\int_t\int_V\left\{\frac{\sigma_{ik}}{2}\delta\frac{\partial u_i}{\partial S_k}+\frac{\sigma_{ik}}{2}\delta\frac{\partial u_k}{\partial S_i}\right\}dV\,dt$$

Since k and i now become dummy indices, interchange them in the first term:

$$(A\text{-}18) \qquad = -\int\int\left(\frac{\sigma_{ki}}{2}\delta\frac{\partial u_k}{\partial S_i}+\frac{\sigma_{ik}}{2}\delta\frac{\partial u_k}{\partial S_i}\right)dV\,dt$$

In general, because the stress tensor is symmetric,

$$(A\text{-}19) \qquad \sigma_{ki} = \sigma_{ik}$$

Using (A-19), and interchanging the operators δ and $\frac{\partial}{\partial S_i}$

$$(A\text{-}20) \qquad -\int_t\int_V \frac{\sigma_{ik}}{2}\delta\left\{\frac{\partial u_i}{\partial S_k}+\frac{\partial u_k}{\partial S_i}\right\}dV\,dt = -\int_t\int_V \sigma_{ik}\frac{\partial}{\partial S_i}\delta u_k\,dV\,dt$$

We now employ the definition of dV (equation (12) to yield:

$$(A\text{-}21) \qquad = -\int_t\int_{S_1}\int_{S_2}\int_{S_3}\sigma_{ik}\frac{\partial}{\partial S_i}\delta u_k\,dS_1\,dS_2\,dS_3\,dt$$

It is understood that i can take on in succession the values 1, 2, 3. Using equation (15), we rewrite (A-21) to:

$$(A\text{-}22) \qquad = -\int_t\int_{\lambda_1}\int_{\lambda_2}\int_{\lambda_3}\sigma_{ik}\frac{\partial}{\partial S_i}(\delta u_k)h_1\,d\lambda_1\,h_2\,d\lambda_2\,h_3\,d\lambda_3\,dt$$

In general,

$$\frac{\partial}{\partial S_i} = \frac{\partial}{\partial \lambda_i} \cdot \frac{\partial \lambda_i}{\partial S_i} = \frac{1}{h_i} \frac{\partial}{\partial \lambda_i} \tag{A-23}$$

The form of (A-22) when i = 1 is:

$$= -\int_t \int_{\lambda_1} \int_{\lambda_2} \int_{\lambda_3} \sigma_{1K} \frac{\partial}{\partial \lambda_1} (\delta u_K) d\lambda_1 \, h_2 d\lambda_2 \, h_3 d\lambda_3 \, dt \tag{A-24}$$

Integrating (A-24) by parts with respect to λ_1

$$= -\int_t \int_{\lambda_2} \int_{\lambda_3} (\sigma_{1K} h_2 h_3) \delta u_K \Big|_{\lambda_1(MIN)}^{\lambda_1(MAX)} d\lambda_2 \, d\lambda_3 \, dt + \int_t \int_{\lambda_1} \int_{\lambda_2} \int_{\lambda_3} \delta u_K \frac{\partial}{\partial \lambda_1} (\sigma_{1K} h_2 h_3) d\lambda_1 d\lambda_2 d\lambda_3 dt \tag{A-25}$$

Similarly, i can = 2 or 3, so that equation (A-25) can serve as the model for the complete expression of the result of (A-22). We can thus write that (A-22) becomes:

$$\begin{aligned} = & -\int_t \int_{\lambda_2} \int_{\lambda_3} (\sigma_{1K} \delta u_K h_2 h_3) \Big|_{\lambda_1(MIN)}^{\lambda_1(MAX)} d\lambda_2 \, d\lambda_3 \, dt \\ & -\int_t \int_{\lambda_1} \int_{\lambda_3} (\sigma_{2K} \delta u_K h_1 h_3) \Big|_{\lambda_2(MIN)}^{\lambda_2(MAX)} d\lambda_1 d\lambda_3 \, dt \\ & -\int_t \int_{\lambda_1} \int_{\lambda_2} (\sigma_{3K} \delta u_K h_1 h_2) \Big|_{\lambda_3(MIN)}^{\lambda_3(MAX)} d\lambda_1 d\lambda_2 dt \\ & + \int_t \int_{\lambda_1} \int_{\lambda_2} \int_{\lambda_3} \delta u_K \left[\frac{\partial}{\partial \lambda_1} (\sigma_{1K} h_2 h_3) + \frac{\partial}{\partial \lambda_2} (\sigma_{2K} h_1 h_3) \right. \\ & \left. + \frac{\partial}{\partial \lambda_3} (\sigma_{3K} h_1 h_2) \right] d\lambda_1 d\lambda_2 d\lambda_3 dt \end{aligned} \tag{A-26}$$

In each of the first three terms, ($\sigma_{ik}\ \delta u_k$) be evaluated at the surface, at the extreme positions taken by the direction coordinates λ_i. Examine the first term and designate $d\Sigma_1$ to represent the surface element encountered. We may now use equation (14) to write, for the first term only:

$$= -\int_t \int_{\Sigma_1} (\sigma_{ik}\delta u_k)\bar{n}\cdot\bar{e}_i \Big|_{\lambda_i(MIN)}^{\lambda_i(MAX)} d\Sigma_1\, dt \tag{A-27}$$

Expand (A-27) to find:

$$= -\int_t \int_{\Sigma_1} (\sigma_{ik}\delta u_k)\bar{n}\cdot\bar{e}_i \Big|^{\lambda_i(MAX)} d\Sigma_1 dt + \int_t \int_{\Sigma_1} (\sigma_{ik}\delta u_k)\bar{n}\cdot(-\bar{e}_i)\Big|^{\lambda_i(MIN)} d\Sigma_1 dt \tag{A-28}$$

To find:

$$= -\int_t \int_{\Sigma_1} \bar{n}\cdot\bar{e}_i \left\{(\sigma_{ik}\delta u_k)^{\lambda_i(MAX)} + (\sigma_{ik}\delta u_k)^{\lambda_i(MIN)}\right\} d\Sigma_1\, dt \tag{A-29}$$

The first three terms of (A-26) thus become

$$-\int_t \int_{\Sigma_i} \bar{n}\cdot\bar{e}_i \left\{(\sigma_{ik}\delta u_k)^{\lambda_i(MAX)} + (\sigma_{ik}\delta u_k)^{\lambda_i(MIN)}\right\} d\Sigma_i\, dt \tag{A-30}$$

Consider now the fourth term of (A-26) and letting ℓ, m, n represent the subscripts of λ, we summarize it as follows:

$$= +\int_t \int_{\lambda_\ell} \int_{\lambda_m} \int_{\lambda_n} \frac{\partial}{\partial \lambda_\ell}(\sigma_{\ell k} h_m h_n)\delta u_k\, d\lambda_\ell\, d\lambda_m\, d\lambda_n\, dt \tag{A-31}$$

with $\ell \neq m \neq n$.

Expanding under the integral sign:

(A-32)

$$= + \int_t \int_{\lambda_\ell} \int_{\lambda_m} \int_{\lambda_n} \frac{\partial \sigma_{\ell k}}{\partial \lambda_\ell} (h_m h_n) \delta u_k \, d\lambda_\ell \, d\lambda_m \, d\lambda_n \, dt$$

$$+ \int_t \int_{\lambda_\ell} \int_{\lambda_m} \int_{\lambda_n} \sigma_{\ell k} \frac{\partial}{\partial \lambda_\ell} (h_m h_n) \delta u_k \, d\lambda_\ell \, d\lambda_m \, d\lambda_n \, dt$$

Rewrite (A-32) as follows:

(A-33)

$$= + \int_t \int_{\lambda_\ell} \int_{\lambda_m} \int_{\lambda_n} \left(\frac{1}{h_\ell} \frac{\partial \sigma_{\ell k}}{\partial \lambda_\ell} \right) \delta u_k \, h_\ell \, d\lambda_\ell \, h_m d\lambda_m \, h_n d\lambda_n \, dt$$

$$+ \int_t \int_{\lambda_\ell} \int_{\lambda_m} \int_{\lambda_n} \frac{\sigma_{\ell k}}{h_\ell h_m h_n} \frac{\partial}{\partial \lambda_\ell} (h_m h_n) \delta u_k \, h_\ell \, d\lambda_\ell \, h_m d\lambda_m \, h_n d\lambda_n \, dt$$

Simplifying,

(A-34) $$= + \int_t \int_V \left\{ \frac{1}{h_\ell} \frac{\partial \sigma_{\ell k}}{\partial \lambda_\ell} + \sigma_{\ell k} \left[\frac{1}{h_\ell h_n} \frac{\partial h_n}{\partial \lambda_\ell} + \frac{1}{h_\ell h_m} \frac{\partial h_m}{\partial \lambda_\ell} \right] \right\} \delta U_k \, dV dt$$

Since we know that $\partial h_\ell / \partial \lambda = 0$, we can add $1/h_\ell h_\ell \; \partial h_\ell / \partial \lambda_\ell$ to the second term without changing anything. Noting that $h_\ell \partial \lambda_\ell = \partial s_\ell$ we write:

(A-35) $$= + \int_t \int_V \left\{ \frac{\partial \sigma_{\ell k}}{\partial s_\ell} + \sigma_{\ell k} \left[\frac{1}{h_\ell h_n} \frac{\partial h_n}{\partial \lambda_\ell} + \frac{1}{h_\ell h_m} \frac{\partial h_m}{\partial \lambda_\ell} + \frac{1}{h_\ell h_\ell} \frac{\partial h_\ell}{\partial \lambda_\ell} \right] \right\} \delta U_k \, dV dt$$

The second term can be replaced by a tensor:

$$= + \int_t \int_V \left\{ \frac{\partial \sigma_{\ell k}}{\partial s_\ell} + \sigma_{\ell k} \frac{\partial h_t}{\partial \lambda_\ell} \cdot \frac{1}{h_\ell h_t} \right\} \delta U_k \, dV dt \tag{A-36}$$

Replace the index ℓ by i to obtain:

$$= + \int_t \int_V \left\{ \left[\frac{\partial \sigma_{ik}}{\partial s_i} + \sigma_{ik} \frac{\partial h_t}{\partial \lambda_i} \frac{1}{h_i h_t} \right] \right\} \delta U_k \, dV dt \tag{A-37}$$

It may be shown that

$$\bar{e}_t \cdot \frac{\partial \bar{e}_i}{\partial \lambda_t} = \frac{1}{h_i} \frac{\partial h_t}{\partial \lambda_i} \tag{A-38}$$

Multiply both sides of (A-38) by $1/h_t$

$$\bar{e}_t \cdot \frac{1}{h_t} \frac{\partial \bar{e}_i}{\partial \lambda_t} = \frac{1}{h_i} \frac{1}{h_t} \frac{\partial h_t}{\partial \lambda_i} = \bar{e}_t \cdot \frac{\partial \bar{e}_i}{\partial s_t} \tag{A-39}$$

Thus, equation (37) becomes:

$$= + \int_t \int_V \left\{ \left[\frac{\partial \sigma_{ik}}{\partial s_i} + \sigma_{ik} \left(\bar{e}_t \cdot \frac{\partial \bar{e}_i}{\partial s_t} \right) \right] \right\} \delta u_k \, dV dt \tag{A-40}$$

We return now to the third and fourth terms of (A-16):

$$= - \int_t \int_V \frac{\sigma_{ik}}{2} \delta \left\{ \left(\bar{e}_i \cdot \frac{\partial \bar{e}_t}{\partial s_k} + \bar{e}_k \cdot \frac{\partial \bar{e}_t}{\partial s_i} \right) u_t \right\} dV dt \tag{A-41}$$

This equals:

$$= - \int_t \int_V \left(\frac{\sigma_{ik}}{2} \bar{e}_i \cdot \frac{\partial \bar{e}_t}{\partial s_k} \delta u_t - \frac{\sigma_{ik}}{2} \bar{e}_k \cdot \frac{\partial \bar{e}_t}{\partial s_i} \delta u_t \right) dV dt \tag{A-42}$$

In the second term, interchange i and k, to yield

$$(A\text{-}43) \qquad = -\int_t \int_V \left(\frac{\sigma_{ik}}{2} \bar{e}_i \cdot \frac{\partial \bar{e}_t}{\partial s_k} \delta u_t + \frac{\sigma_{ki}}{2} \bar{e}_i \cdot \frac{\partial \bar{e}_t}{\partial s_k} \delta u_t \right) dV dt$$

Again, using $\sigma_{ik} = \sigma_{ki}$, this reduces to:

$$(A\text{-}44) \qquad -\int_t \int_V \left(\sigma_{ik} \bar{e}_i \cdot \frac{\partial \bar{e}_t}{\partial s_k} \delta u_t \right) dV dt$$

Interchange t and k to obtain:

$$(A\text{-}45) \qquad -\int_t \int_V \left(\sigma_{ti} \bar{e}_i \cdot \frac{\partial \bar{e}_k}{\partial s_t} \delta u_k \right) dV dt$$

Now, noting that:

$$(A\text{-}46) \qquad \bar{e}_i \cdot \frac{\partial \bar{e}_k}{\partial s_t} = - \bar{e}_k \cdot \frac{\partial \bar{e}_i}{\partial s_t}$$

Equation (A-45) becomes:

$$(A\text{-}47) \qquad +\int_t \int_V \left(\sigma_{ti} \bar{e}_k \cdot \frac{\partial \bar{e}_i}{\partial s_t} \right) \delta u_k \, dV dt$$

Thus, all the terms resulting from the variation in strain energy have been found. They are specifically contained in equations (A-30), (A-40) and (A-47).

The terms resulting from strain energy variation are summarized below:

$$(A\text{-}48) \qquad \int_t \int_V \left[\frac{\partial \sigma_{ik}}{\partial s_i} + \sigma_{ik} \left(\bar{e}_t \cdot \frac{\partial \bar{e}_i}{\partial s_t} \right) + \sigma_{ti} \left(\bar{e}_k \cdot \frac{\partial \bar{e}_i}{\partial s_t} \right) \delta u_k \, dV dt \right.$$

$$-\int_t \int_{\Sigma_i} \bar{n}\cdot\bar{e}_i \left\{ (\sigma_{ik}\delta u_k)^{\lambda_i\,MAX} + (\sigma_{ik}\delta u_k)^{\lambda_i\,MIN} \right\} d\Sigma_i\, dt$$

We now proceed to the variation of kinetic energy.

KINETIC ENERGY

The variation in kinetic energy is expressed:

(A-49) $$\delta\int_t T\,dt = \int_t\int_V \delta\left(\tfrac{1}{2}\gamma\dot{\bar{r}}\cdot\dot{\bar{r}}\right)dV\,dt$$

But, from equation (6):

(A-50) $$\dot{\bar{r}} = \dot{\bar{Y}}_B + \dot{\bar{u}}$$

Substitute (A-50) in (A-49) to obtain:

(A-51) $$\delta(K.E.) = \int_t\int_V \frac{\gamma}{2}\,\delta\left\{\left[\dot{\bar{Y}}_B + \dot{\bar{u}}\right]\cdot\left[\dot{\bar{Y}}_B + \dot{\bar{u}}\right]\right\} dV\,dt$$

Expanding:

(A-52) $$\delta(K.E.) = \int_t\int_V \frac{\gamma}{2}\,\delta\left[\dot{\bar{Y}}_B\cdot\dot{\bar{Y}}_B + 2\dot{\bar{u}}\cdot\dot{\bar{Y}}_B + \dot{\bar{u}}\cdot\dot{\bar{u}}\right] dV\,dt$$

But:

(A-53) $$\dot{\bar{Y}}_B = \dot{\bar{Y}}_B(t)_p\,\tilde{\bar{\omega}}_p$$

$$\dot{\bar{u}} = \dot{u}_k\bar{e}_k$$

Also, from equations (17) and (18),

(A-54) $$U_K = (U_K)_{MIN} + \alpha\, \eta_K(x,\phi,z,t)$$
$$Y_B(t)_P = (Y_B(t)_P)_{MIN} + \beta\, \chi_P(t)$$

Since $\delta(\frac{1}{2}\dot{\bar{r}}\cdot\dot{\bar{r}})$ ultimately depends on the two parameters α and β, we must take:

(A-55) $$\delta\left(\frac{\gamma}{2}\dot{\bar{r}}\cdot\dot{\bar{r}}\right) = \frac{\partial}{\partial\alpha}\left(\frac{\gamma}{2}\dot{\bar{r}}\cdot\dot{\bar{r}}\right)d\alpha + \frac{\partial}{\partial\beta}\left(\frac{\gamma}{2}\dot{\bar{r}}\cdot\dot{\bar{r}}\right)d\beta$$

Performing the operations indicated in (A-55):

(A-56) $$\delta\left(\frac{\gamma}{2}\dot{\bar{r}}\cdot\dot{\bar{r}}\right) = \frac{\gamma}{2}\dot{\bar{r}}\cdot\frac{\partial\dot{\bar{r}}}{\partial\alpha}\,d\alpha + \frac{\gamma}{2}\dot{\bar{r}}\cdot\frac{\partial\dot{\bar{r}}}{\partial\alpha}\,d\alpha + \gamma\dot{\bar{r}}\cdot\frac{\partial\dot{\bar{r}}}{\partial\beta}\,d\beta.$$

or, noting that $\frac{\partial\dot{\bar{r}}}{\partial\alpha}\,d\alpha = \delta\dot{\bar{u}}$ and $\frac{\partial\dot{\bar{r}}}{\partial\beta}\,d\beta = \delta\dot{\bar{Y}}_B$

(A-57) $$\delta\left(\frac{\gamma}{2}\dot{\bar{r}}\cdot\dot{\bar{r}}\right) = \gamma\left[(\dot{\bar{Y}}_B + \dot{\bar{U}})\cdot\delta\dot{\bar{U}}\right] + \gamma\left[(\dot{\bar{Y}}_B + \dot{\bar{U}})\cdot\delta\dot{\bar{Y}}_B\right]$$

(A-58) $$\delta\left(\frac{\gamma}{2}\dot{\bar{r}}\cdot\dot{\bar{r}}\right) = \gamma\left[\dot{\bar{Y}}_B\cdot\delta\dot{\bar{U}} + \dot{\bar{U}}\cdot\delta\dot{\bar{Y}}_B + \dot{\bar{Y}}_B\cdot\delta\dot{\bar{Y}}_B + \dot{\bar{U}}\cdot\delta\dot{\bar{U}}\right]$$

(Equation (58) could have been derived directly from (A-52)). Note that $\delta\dot{\bar{Y}}_B = \delta\left(\frac{\partial\bar{Y}_B}{\partial t}\right)$ and that δ and $\partial/\partial t$ operators may be interchanged. Substitute (A-58) in (A-52):

(A-59) $$\delta(K.E.) = \int_t \dot{\bar{Y}}_B\cdot\delta\dot{\bar{Y}}_B\int_V \gamma\,dV\,dt + \int_t\left[\frac{\partial}{\partial t}\int_V \gamma\bar{U}\,dV\right]\cdot\delta\dot{\bar{Y}}_B\,dt$$
$$+\int_t\int_V \delta\dot{\bar{Y}}_B\cdot\frac{\partial}{\partial t}(\delta\bar{U})\,dV\,dt + \int_t\int_V \gamma\dot{\bar{U}}\cdot\frac{\partial}{\partial t}(\delta\bar{U})\,dV\,dt$$

The second term vanishes, because of the definition of center of gravity, and the remaining terms are integrated by parts. The result is:

(A-60)

$$\delta(K.E.) = M\dot{\bar{Y}}_B \cdot \delta\bar{Y}_B\Big|_{t_1}^{t_2} - \int_t M\ddot{\bar{Y}}_B \cdot \delta\bar{Y}_B\, dt$$
$$+\int_V \gamma\dot{\bar{Y}}_B \cdot \delta\bar{U}\Big|_{t_1}^{t_2} - \int_t\int_V \gamma\ddot{\bar{Y}}_B \cdot \delta\bar{U}\, dV dt$$
$$+\int_V \gamma\dot{\bar{U}} \cdot \delta\bar{U}\Big|_{t_1}^{t_2} - \int_t\int_V \gamma\ddot{\bar{U}} \cdot \delta\bar{U}\, dV dt$$

Since $\delta\bar{Y}_B$ and $\delta\bar{u}$ vanish at the time boundaries, equation (60) reduces to:

(A-61) $$\delta(K.E.) = -\int_t M\ddot{\bar{Y}}_B \cdot \delta\bar{Y}_B\, dt - \int_t\int_V \gamma\left[\ddot{\bar{Y}}_B + \ddot{\bar{U}}\right] \cdot \delta\bar{U}\, dV dt$$

M is used to represent body mass. We replace the vector dot products by the appropriate scalar tensor forms:

(A-62) $$\delta\int_t\int_V T\, dV dt = -\left\{\int_t M Y_B(t)_p\, \delta Y_B(t)_p\, dt + \int_t\int_V \gamma\left[\ddot{Y}_B(t)_K + \ddot{U}_K\right]\delta U_K\, dV dt\right\}$$

We now proceed to the variation in the work term:

(A-63) $$\delta\int_t W dt = \delta\int_t\int_\Sigma \bar{P}\cdot\bar{r}\, d\Sigma\, dt$$

This may be written:

(A-64) $$\delta\int_t W dt = \int_t\int_\Sigma \bar{P}\cdot\delta\bar{Y}_B(t)\, d\Sigma dt + \int_t\int_\Sigma \bar{P}\cdot\delta\bar{u}\, d\Sigma\, dt$$

Rearranging slightly:

$$\text{(A-65)} \qquad \delta\int_t W\,dt = \int_t \left\{\int_\Sigma \bar{P}\,d\Sigma\right\}\cdot \delta\bar{Y}_B(t)\,dt + \int_t\int_\Sigma \bar{P}\cdot\delta\bar{U}\,d\Sigma\,dt$$

The term $\int_\Sigma \bar{P}\,d\Sigma$ may be replaced by $\bar{F}(t)$, the resultant force on the body. Using appropriate subscripts:

$$\text{(A-66)} \qquad \delta\int_t W\,dt = \int_t F(t)_p\,\delta Y_B(t)_p\,dt + \int_t\int_\Sigma P_K\,\delta U_K\,d\Sigma\,dt$$

(It should be noted that the integration with respect to $d\Sigma$ must proceed over $d\Sigma_1$, $d\Sigma_2$, and $d\Sigma_3$, as previously discussed).

The final result is available from equations (A-48), (A-62) and (A-66), and is shown below:

(A-67)

$$\delta\int_t L\,dt = \int_t\int_V \left\{\left[\frac{\partial\sigma_{iK}}{\partial S_i} + \sigma_{iK}\left(\bar{e}_t\cdot\frac{\partial\bar{e}_i}{\partial S_t}\right) + \sigma_{ti}\left(\bar{e}_K\cdot\frac{\partial\bar{e}_i}{\partial S_t}\right)\right] - \gamma\left[\ddot{Y}_B(t)_K + \ddot{U}_K\right]\right\}\delta U_K\,dV\,dt$$

$$+\int_t\int_{\Sigma_i}\left[F_t\delta u_K - \bar{n}\cdot\bar{e}_i\left\{(\sigma_{iK}\delta U_K)^{A_i\,MAX} + (\sigma_{iK}\delta U_K)^{A_i\,MIN}\right\}\right]d\Sigma_i\,dt$$

$$+\int_t\left[F(t)_p - M\ddot{Y}_B(t)_p\right]\delta Y_B(t)_p\,dt = 0$$

The first integral provides the equilibrium equations, the second provides the boundary conditions, and the third shows the conditions for rigid body motion.

APPENDIX B

DERIVATION OF SHELL EQUATIONS

As we examine equation (39) prior to integration, we recognize the need to find the values of such terms as $\partial \bar{e}_i / \partial s_t$ in cylindrical coordinates. It may be shown that:

(B-1) $$\frac{\partial \bar{e}_3}{\partial s_2} = \frac{1}{R}\bar{e}_2 \quad \text{and} \quad \frac{\partial \bar{e}_2}{\partial s_2} = -\frac{1}{R}\bar{e}_3$$

and that all other values of the indices yield 0. This, of course, considerably simplifies the problem.

We turn our attention first to the equilibrium equations themselves. Two forms may be isolated, one to do with δu_K^0 and the other with δu_K^1. In each case, the coefficients of these arbitrary variations must be identically zero:

(B-2) $$\int_{-h}^{+h} \left[\frac{\partial \sigma_{jK}}{\partial s_j} + \sigma_{ik}\left(\bar{e}_t \cdot \frac{\partial \bar{e}_i}{\partial s_t}\right) + \sigma_{ti}\left(\bar{e}_K \cdot \frac{\partial \bar{e}_i}{\partial s_t}\right) - \gamma\left(\ddot{Y}_{B,K} + \ddot{U}_K^{(0)} + z\ddot{U}_K^{(1)}\right)\right]\left(1 + \frac{z}{a}\right)\delta U_K^{(0)}\, dz = 0$$

(B-3) $$\int_{-h}^{+h} \left[\frac{\partial \sigma_{jK}}{\partial s_j} + \sigma_{ik}\left(\bar{e}_t \cdot \frac{\partial \bar{e}_i}{\partial s_t}\right) + \sigma_{ti}\left(\bar{e}_K \cdot \frac{\partial \bar{e}_i}{\partial s_t}\right) - \gamma\left(\ddot{Y}_{B,K} + \ddot{U}_K^{(0)} + z\ddot{U}_K^{(1)}\right)\right](z)\left(1 + \frac{z}{a}\right)\delta U_K^{(1)}\, dz = 0$$

As k assumes successively the values 1, 2, 3,

there will be three equations from (B-2) and two from (B-3). For k = 1, equation (B-2) becomes:

(B-4) $$\int_{-h}^{+h}\left[\frac{\partial\sigma_{11}}{\partial S_1}+\frac{\partial\sigma_{21}}{\partial S_2}+\frac{\partial\sigma_{31}}{\partial S_3}+\left(\frac{1}{a+z}\right)\sigma_{31}-\rho\left(\ddot{Y}_{31}+\ddot{U}_1^{(0)}+z\ddot{U}_1^{(1)}\right)\right]\left(\frac{a+z}{a}\right)dz = 0$$

Using the curvilinear values for S_1, S_2, S_3, we write (B-4) as:

(B-5)

$$\frac{\partial}{\partial x}\int_{-h}^{h}\sigma_{11}\left(1+\frac{z}{a}\right)dz+\frac{1}{(a+z)}\frac{\partial}{\partial\varphi}\int_{-h}^{h}\sigma_{21}\left(1+\frac{z}{a}\right)dz$$
$$+\int_{-h}^{h}\frac{\partial\sigma_{31}}{\partial z}\left(1+\frac{z}{a}\right)dz+\frac{1}{a}\int_{-h}^{h}\sigma_{31}\,dz$$
$$-\rho\int_{-h}^{h}\left(\ddot{Y}_{31}+\ddot{U}_1^{(0)}+z\ddot{U}_1^{(1)}\right)\left(1+\frac{z}{a}\right)dz = 0$$

The third term is expanded and then integrated by parts to yield:

(B-6) $$\sigma_{31}\Big|_{-h}^{+h}+z\frac{\sigma_{31}}{a}\Big|_{-h}^{+h}-\int_{-h}^{h}\frac{\sigma_{31}}{a}dz$$

We confine our attention to the case of surface traction on the outer surface ($^+$h) only. Further, we define:

(B-7) $$\sigma_{11}^{(0)} = N_{xx} = \int_{-h}^{h}\sigma_{11}\left(1+\frac{z}{a}\right)dz$$

(B-8) $$\sigma_{21}^{(0)} = N_{\phi x} = \int_{-h}^{h}\sigma_{21}\,dz$$

Utilizing (B-6), (B-7) and (B-8), with the restriction cited for surface traction, equation (B-5) becomes:

(B-9) $$\frac{\partial \sigma_{11}^{(0)}}{\partial x} + \frac{1}{a}\frac{\partial \sigma_{21}^{(0)}}{\partial \phi} + P_1^+\left(1+\frac{h}{a}\right) - 2\gamma h \ddot{Y}_B(t)\cdot \bar{e}_1 - 2\gamma \ddot{u}_1^{(0)} h - \frac{2}{3a}\gamma h^3 \ddot{u}_1^{(1)} = 0$$

We retain equation (B-9), and continue for k = 2 to explore what happens to (B-2):

(B-10) $$\int_{-h}^{h}\left[\frac{\partial \sigma_{12}}{\partial s_1} + \frac{\partial \sigma_{22}}{\partial s_2} + \frac{\partial \sigma_{32}}{\partial s_3} + \frac{\sigma_{32}}{a+z} + \frac{\sigma_{23}}{a+z} - \gamma\left(\ddot{Y}_{B_2} + \ddot{u}_2^{(0)} + z\ddot{u}_2^{(1)}\right)\right]\left(1+\frac{z}{a}\right)\delta u_2^0\, dz = 0$$

Again, using the curvilinear values for S_1, S_2 and S_3:

(B-11)

$$\frac{\partial}{\partial x}\int_{-h}^{h}\sigma_{12}\left(1+\frac{z}{a}\right)dz + \frac{1}{a}\frac{\partial}{\partial \phi}\int_{-h}^{h}\sigma_{22}\,dz + \int_{-h}^{h}\frac{\partial \sigma_{32}}{\partial z}\left(1+\frac{z}{a}\right)dz + \frac{2}{a}\int_{-h}^{h}\sigma_{32}\,dz - \int_{-h}^{h}\gamma\left(\ddot{Y}_{B2} + \ddot{u}_2^{(0)} + z\ddot{u}_2^{(1)}\right)\left(1+\frac{z}{a}\right)dz = 0$$

Now, defining:

(B-12)

$$\sigma_{12}^{(0)} = \int_{-h}^{h}\sigma_{12}\left(1+\frac{z}{a}\right)dz = N_{x\phi}$$

$$\sigma_{22}^{(0)} = \int_{-h}^{h}\sigma_{22}\,dz = N_{\phi\phi}$$

$$\sigma_{23}^{(0)} = \int_{-h}^{h}\sigma_{32}\,dz = Q_\phi$$

Using (B-12) and integrating the third term of (B-11) by parts, and confining our interest to outside surface traction only, equation (B-11) reduces to:

$$(B\text{-}13)\qquad \frac{\partial \sigma_{12}^{(0)}}{\partial x}+\frac{1}{a}\frac{\partial \sigma_{22}^{0}}{\partial \phi}+\frac{\sigma_{32}^{(0)}}{a}+P_2^{+}\left(1+\frac{h}{a}\right)-2\gamma h\ddot{Y}_B(t)\cdot\bar{e}_2-2\gamma h\ddot{U}_2^{(0)}-\frac{2\gamma h^3}{3a}\ddot{U}_2^{(1)}\equiv 0$$

We retain equation (B-13), and continue to examine (B-2) when k = 3:

$$(B\text{-}14)\int_{-h}^{h}\left[\frac{\partial \sigma_{13}}{\partial S_1}+\frac{\partial \sigma_{23}}{\partial S_2}+\frac{\partial \sigma_{33}}{\partial S_3}+\frac{\sigma_{32}}{(a+z)}-\frac{\sigma_{22}}{(a+z)}-\gamma\left(\ddot{Y}_{B3}+\ddot{U}_3^{(0)}+z\ddot{U}_3^{(1)}\right)\right]\left(1+\frac{z}{a}\right)dz\equiv 0$$

Again, using the curvilinear values for S_1, S_2, and S_3:

(B-15)

$$\frac{\partial}{\partial x}\int_{-h}^{h}\sigma_{13}\left(1+\frac{z}{a}\right)dz+\frac{1}{a}\frac{\partial}{\partial \phi}\int_{-h}^{h}\sigma_{23}\,dz+\int_{-h}^{h}\frac{\partial \sigma_{33}}{\partial z}\left(1+\frac{z}{a}\right)dz$$

$$+\frac{1}{a}\int_{-h}^{h}\sigma_{33}\,dz-\frac{1}{a}\int_{-h}^{h}\sigma_{22}\,dz-\int_{-h}^{h}\gamma\left(\ddot{Y}_{B3}+\ddot{U}_3^{(0)}+z\ddot{U}_3^{(1)}\right)\left(1+\frac{z}{a}\right)dz\equiv 0$$

The third term is integrated by parts. We define

$$(B\text{-}16)\qquad \sigma_{13}^{(0)}=Q_x=\int_{-h}^{h}\sigma_{13}\left(1+\frac{z}{a}\right)dz$$

Note that $\sigma_{23}=\sigma_{32}$, and finally obtain:

(B-17)

$$\frac{\partial \sigma_{13}^{(0)}}{\partial x}+\frac{1}{a}\frac{\partial \sigma_{23}^{(0)}}{\partial \phi}+P_3^{+}\left(1+\frac{h}{a}\right)-\frac{\sigma_{22}^{(0)}}{a}$$

$$-2\gamma h\ddot{Y}_B(t)\cdot\bar{e}_3-2\gamma h\ddot{U}_3^{(0)}-\frac{2\gamma h^3}{3a}\ddot{U}_3^{(1)}\equiv 0$$

To summarize (B-9), (B-13) and (B-17) are the equations that derive from (B-2) for k = 1, 2 and 3 respectively. They represent equilibrium equations in the x, ϕ and z directions, and must be viewed as being multiplied by the arbitrary variations δu_1^o, δu_2^o and δu_3^o.

We now return to (B-3) and evaluate it for $k = 1$ and $k = 2$. First, for $k = 1$, (B-3) becomes:

(B-18)

$$\int_{-h}^{h} \left[\frac{\partial \sigma_{11}}{\partial S_1} + \frac{\partial \sigma_{21}}{\partial S_2} + \frac{\partial \sigma_{31}}{\partial S_3} + \frac{1}{(a+z)} \sigma_{31} - \gamma \left(\ddot{Y}_{B1} + \ddot{U}_1^{(0)} + z \ddot{U}_1^{(1)} \right) \right] z \left(1 + \frac{z}{a}\right) dz = 0$$

Using the curvilinear coordinates for S_1, S_2, and S_3, we write:

(B-19)

$$\frac{\partial}{\partial x} \int_{-h}^{h} z \sigma_{11} \left(1 + \frac{z}{a}\right) dz + \frac{1}{a} \frac{\partial}{\partial \phi} \int_{-h}^{h} z \sigma_{21} dz + \int_{-h}^{h} z \frac{\partial \sigma_{31}}{\partial z} \left(1 + \frac{z}{a}\right) dz + \frac{1}{a} \int_{-h}^{h} z \sigma_{31} dz - \gamma \int_{-h}^{h} \left(\ddot{Y}_{B1} + \ddot{U}_1^{(0)} + z \ddot{U}_1^{(1)} \right) z \left(1 + \frac{z}{a}\right) dz = 0$$

We define

(B-20)

$$\sigma_{11}^{(1)} = M_x = \int_{-h}^{h} z \sigma_{11} \left(1 + \frac{z}{a}\right) dz$$

$$\sigma_{21}^{(1)} = M_{\phi x} = \int_{-h}^{h} z \sigma_{21} dz$$

and obtain:

(B-21)

$$\frac{\partial}{\partial x} \sigma_{11}^{(1)} + \frac{1}{a} \frac{\partial \sigma_{21}}{\partial \varphi} + P_1^+ h \left(1 + \frac{h}{a}\right) - \sigma_{13}^{(0)} - \frac{2\gamma h^3}{a} \ddot{Y}_B(t) \cdot \bar{e}_1 - \frac{2\gamma h^3}{a} \ddot{U}_1^{(0)} - 2\gamma h^3 \ddot{U}_1^{(1)} = 0$$

Last, we return to (B-2) and evaluate it for $k = 2$ to find:

(B-22)

$$\int_{-h}^{h}\Big[\frac{\partial\sigma_{12}}{\partial s_1}+\frac{\partial\sigma_{22}}{\partial s_2}+\frac{\partial\sigma_{32}}{\partial s_3}\frac{\sigma_{32}}{a+z}+\frac{\sigma_{32}}{a+z}$$

$$-\gamma(\ddot{Y}_{B_2}+\ddot{U}_2^{(0)}+z\ddot{U}_2^{(1)})\Big](z)(1+\frac{z}{a})dz = 0$$

and this may be written as:

(B-23)

$$\frac{\partial}{\partial x}\int_{-h}^{h}z\sigma_{12}(1+\frac{z}{a})dz+\frac{1}{a}\frac{\partial}{\partial\varphi}\int_{-h}^{h}z\sigma_{22}dz$$

$$+\int_{-h}^{h}z\frac{\partial\sigma_{32}}{\partial z}(1+\frac{z}{a})dz+\frac{z}{a}\int_{-h}^{h}z\sigma_{32}dz$$

$$-\int_{-h}^{h}\gamma(\ddot{Y}_{B_2}+\ddot{U}_2^{(0)}+z\ddot{U}_2^{(1)})(z)(1+\frac{z}{a})dz = 0$$

Define:

(B-24)

$$\sigma_{12}^{(1)} = M_{x\varphi} = \int_{-h}^{h}z\sigma_{12}(1+\frac{z}{a})dz$$

$$\sigma_{22}^{(1)} = M_{\varphi} = \int_{-h}^{h}z\sigma_{22}dz$$

Equation (B-22) becomes:

(B-25)

$$\frac{\partial\sigma_{12}^{(1)}}{\partial x}+\frac{1}{a}\frac{\partial\sigma_{22}^{(1)}}{\partial\varphi}+P_2^{+}h(1+\frac{h}{a})-\sigma_{32}^{(0)}$$

$$-\frac{2\gamma h^3}{a}\ddot{Y}_B(t)\cdot\bar{e}_2-\frac{2\gamma h^2}{a}\ddot{U}_2^{(0)}-2h^3\gamma\ddot{U}_2^{(1)} = 0$$

The additional equations required are (B-21) and (B-25).*

Equation (39) may also be used to provide the boundary conditions. For each boundary, namely $x = 0$, $x = L$, $z = \pm h$, there are five equations, obtained by iterating through the arbitrary variations δu_k^o and δu_k^1. We consider them in the order in which they are given in equation (39).

In general, for clamped end cylinders the displacements will be prescribed at $x = 0$ and $x = L$. For free ends, the stress and moment resultants will be specified at $x = 0$ and $x = L$. In each case, the surface tractions will govern the boundary conditions at $z = \pm h$.

---

*NOTE: In the several equations (B-9), (B-13), (B-17), (B-21) and (B-25), the substitutions:

$$P_1^+ = \sigma_{31})_h$$

$$P_2^+ = \sigma_{32})_h$$

$$P_3^+ = \sigma_{33})_h$$

have actually been made before a rigorous demonstration supports the notation. These follow logically from the boundary conditions equations (B-26). When $\delta u_k^n \neq o$, being not fixed at the free outside boundary, it is necessary that $P_1^+ = \sigma_{31}^+$, etc.

In order to preserve maximum generality, we will retain the multipliers δu_k^0 and δu_k^1 for each case.

At z = h

(B-26)

$$\int_t \int_x \int_\phi \Big[(P_1^+ - \sigma_{31})_{z=h} (a+h) \delta U_1^{(0)} + (P_1^+ - \sigma_{31})_{z=h} (a+h) h (\delta U_1^{(1)}) + (P_2^+ - \sigma_{32})_{z=h} (a+h) \delta U_2^{(0)} + (P_2^+ - \sigma_{32})_{z=h} (a+h) h (\delta U_2^{(1)}) + (P_3^+ - \sigma_{33})_{z=h} (a+h) \delta U_3^{(0)} \Big] dx\, d\phi\, dt = 0$$

At z = -h

(B-27)

$$\int_t \int_x \int_\phi \Big[(P_1^- + \sigma_{31})_{z=-h} (a-h) \delta U_1^{(0)} + (P_1^- + \sigma_{31})_{z=-h} (a-h)(-h) \delta U_1^{(1)} + (P_2^- + \sigma_{32})_{z=-h} (a-h) \delta U_2^{(0)} + (P_2^- + \sigma_{32})_{z=-h} (a-h)(-h) \delta U_2^{(1)} + (P_3^- + \sigma_{33})_{z=-h} (a-h) \delta U_3^{(0)} \Big] dx\, d\phi\, dt = 0$$

At x = 0

(B-28)

$$\int_t \int_\phi \Big\{ \Big[\sigma_{11}^{(0)} + \int_{-h}^{h} P_1 \Big(1 + \frac{z}{a}\Big) dz \Big]_{x=0} \delta U_1^{(0)} + \Big[\sigma_{11}^{(1)} + \int_{-h}^{h} P_1 z \Big(1 + \frac{z}{a}\Big) dz \Big]_{x=0} \delta U_1^{(1)} + \Big[\sigma_{12}^{(0)} + \int_{-h}^{h} P_2 \Big(1 + \frac{z}{a}\Big) dz \Big]_{x=0} \delta U_2^{(0)} + \Big[\sigma_{12}^{(1)} + \int_{-h}^{h} P_2 z \Big(1 + \frac{z}{a}\Big) dz \Big]_{x=0} \delta U_2^{(1)} + \Big[\sigma_{13}^{(0)} + \int_{-h}^{h} P_3 \Big(1 + \frac{z}{a}\Big) dz \Big]_{x=0} \delta U_3^{(0)} \Big\} a\, d\phi\, dt = 0$$

In expressions (B-28), P_1, P_2 and P_3 refer to values of surface traction at $x = 0$.

Finally,

At $x = L$

(B-29)

$$\int_t \int_\phi \left\{ \left[\sigma_{11}^{(0)} - \int_{-h}^{h} P_1 \left(1 + \frac{z}{a}\right) dz \right]_{x=L} \delta u_1^{(0)} \right.$$
$$+ \left[\sigma_{11}^{(1)} - \int_{-h}^{h} P_1(z) \left(1 + \frac{z}{a}\right) dz \right]_{x=L} \delta u_1^{(1)}$$
$$+ \left[\sigma_{12}^{(0)} - \int_{-h}^{h} P_2 \left(1 + \frac{z}{a}\right) dz \right]_{x=L} \delta u_2^{(0)}$$
$$+ \left[\sigma_{12}^{(1)} - \int_{-h}^{h} P_2(z) \left(1 + \frac{z}{a}\right) dz \right]_{x=L} \delta u_2^{(1)}$$
$$\left. + \left[\sigma_{13}^{(0)} - \int_{-h}^{h} P_3 \left(1 + \frac{z}{a}\right) dz \right]_{x=L} \delta u_3^{(0)} \right\} a \, d\phi \, dt = 0$$

Again, in these equations, P_1, P_2 and P_3 represent the surface tractions at the face $x = L$.

APPENDIX C

TRANSFORMATION OF EQUATIONS INTO DEFORMATION COORDINATES

Our task is to transform the set of equilibrium equations, (42), as well as the boundary condition equations (45-48), into ones that involve the deformation coordinates u_K^n.

The sequence of steps are planned as follows:

- Express the stresses in terms of the strains
- Write the strain-displacement relations
- Transform the strain-displacement relations into the deformation coordinates u_K^n of the mid-surface.
- Derive the stresses in terms of u_K^n
- Integrate over z to find the stress-resultants in terms of u_K^n
- Substitute these equations for the stress-resultants into equations (42) and (45-48).

The Stress-Strain Relations

To begin, we reiterate that the constitutive equations for a homogeneous, isotropic material are specified as in equation (A-3), repeated below for convenience:

(A-3) $$\sigma_{ik} = \lambda \epsilon_{rr} \delta_{ik} + 2G\epsilon_{ik}$$

When this is true, the individual stress-strain relations may be written:

(C-1) $$\sigma_{11} = \frac{E}{1-\nu^2}\left[\epsilon_{11} + \nu\epsilon_{22}\right] + \frac{\nu}{1-\nu}\sigma_{33}$$

(C-2) $$\sigma_{22} = \frac{E}{1-\nu^2}\left[\epsilon_{22} + \nu\epsilon_{11}\right] + \frac{\nu}{1-\nu}\sigma_{33}$$

(C-3) $$\sigma_{12} = 2G\epsilon_{12} = \frac{E}{1-\nu^2}(1-\nu)\epsilon_{12}$$

(C-4) $$\sigma_{13} = 2G\epsilon_{13} = \frac{E}{1-\nu^2}(1-\nu)\epsilon_{13}$$

(C-5) $$\sigma_{23} = 2G\epsilon_{23} = \frac{E}{1-\nu^2}(1-\nu)\epsilon_{23}$$

In order to prepare a path for the eventual neglect of transverse shear, we create what might be termed a pseudo-isotropic material by using $G' = \kappa G$ for the last two equations, (C-4). κ is known as Mindlin's constant, as he suggested this device in another connection. κ is a constant which may be chosen at a particular value for a particular purpose. In our case, at the appropriate time, κ will be permitted to approach ∞ in the limit.

We thus replace equations (C-4) and (C-5) with:

(C-6) $$\sigma_{13} = 2G'\epsilon_{13} = \frac{\kappa E}{1-\nu^2}(1-\nu)\epsilon_{13}$$

(C-7) $$\sigma_{23} = 2G'\epsilon_{23} = \frac{\kappa E}{1-\nu^2}(1-\nu)\epsilon_{23}$$

The Strain-Displacement Relations

In Appendix A, the strain-displacement equations for curvilinear coordinates in infinitesimal strain are shown as:

(A-2)

$$\epsilon_{ik}(x,\phi,z,t) \equiv \frac{1}{2}\left[\frac{\partial u_i}{\partial s_k} + \frac{\partial u_k}{\partial s_i} + \left(\bar{e}_i \cdot \frac{\partial e_t}{\partial s_k} + \bar{e}_k \cdot \frac{\partial e_t}{\partial s_i}\right) u_t\right]$$

In equation (A-2) $\bar{e}_k$ is the body-referenced orthogonal triad shown in Figure 1. Each of the terms u_i, u_k and u_t are the deformation coordinates of the point. We reiterate that $\bar{e}_k$ is a function of ϕ, while u_i, etc. are dependent on x, ϕ, z and t.

The dS_k set has also been defined, and is repeated below for convenience: (Refer to equations (14) and (15)).

$$dS_1 = dx$$

$$dS_2 = (a)\ (1 + \frac{z}{a})\ d\phi = Rd\phi$$

$$dS_3 = dz$$

Using this information, the strain-displacement relations for an arbitrary point become (see reference (27)).

(C-8) $$\epsilon_{11} = \frac{\partial u_1}{\partial x}$$

(C-9) $$\epsilon_{22} = \left(\frac{1}{a+z}\right)\left(\frac{\partial u_2}{\partial \phi} + u_3\right)$$

(C-10) $$\epsilon_{33} = \frac{\partial u_3}{\partial z}$$

(C-11) $$\epsilon_{12} = \frac{1}{2}\gamma_{12} = \frac{1}{2}\left[\frac{\partial u_2}{\partial x} + \frac{1}{a+z}\frac{\partial u_1}{\partial \phi}\right]$$

(C-12) $$\epsilon_{13} = \frac{1}{2}\gamma_{13} = \frac{1}{2}\left[\frac{\partial u_1}{\partial z} + \frac{\partial u_3}{\partial x}\right]$$

(C-13) $$\epsilon_{23} = \frac{1}{2}\gamma_{23} = \frac{1}{2}\left[\frac{\partial u_2}{\partial z} + \frac{1}{a+z}\frac{\partial u_3}{\partial \phi} - \frac{u_2}{a+z}\right]$$

We have also adopted the following truncated series expansion so as to be able to express the deformations of a point in terms of the deformations and rotations of a mid-surface:

(30) $$u_1 = u_1^{(0)} + z u_1^{(1)}$$

$$u_2 = u_2^{(0)} + z u_2^{(1)}$$

$$u_3 = u_3^{(0)}$$

In these equations, for clarity, we note once again that:

u_k = Deformation components of arbitrary point

$u_k^{\,o}$ = Deformation components of the middle surface of the shell

$u_k^{\,1}$ = Changes in slope of normal to mid-surface in the $-\bar{e}_1$ and $\bar{e}_2$ directions.

Transformation of the Strain-Displacement Relations

Substitution of equations (30) into equations (C-8) through (C-13) yields:

(C-14)

a. $\epsilon_{11} = \frac{\partial u_1^o}{\partial x} + z\frac{\partial u_1^1}{\partial x}$

b. $\epsilon_{22} = \frac{1}{a+z}\left[\frac{\partial u_2^o}{\partial \phi} + z\frac{\partial u_2^1}{\partial \phi} + u_3^o\right]$

c. $\epsilon_{33} = \frac{\partial u_3^o}{\partial z} = 0$

d. $\epsilon_{12} = \frac{1}{2}\gamma_{12} = \frac{1}{2}\left\{\frac{\partial u_2^o}{\partial x} + z\frac{\partial u_2^1}{\partial x} + \frac{1}{a+z}\frac{\partial u_1^o}{\partial \phi} + \frac{z}{a+z}\frac{\partial u_1^1}{\partial \phi}\right\}$

e. $\epsilon_{13} = \frac{1}{2}\gamma_{13} = \frac{1}{2}\left[\frac{\partial u_1^o}{\partial z} + z\frac{\partial u_1^1}{\partial z} + u_1 + \frac{\partial u_3^o}{\partial x}\right]$

f. $\epsilon_{23} = \frac{1}{2}\gamma_{23} = \frac{1}{2}\left\{\frac{\partial u_2^o}{\partial z} + z\frac{\partial u_2^1}{\partial z} + u_2^1 + \frac{1}{a+z}\frac{\partial u_3^o}{\partial \phi} - \frac{1}{a+z}(u_2^o + z u_2^1)\right\}$

Equations (C-14e) and (C-14f) are further simplified by noting that $\frac{\partial u_i^o}{\partial z}$ and $\frac{\partial u_i^1}{\partial z} = 0$, etc. These become:

e. $\epsilon_{13} = \frac{1}{2}\gamma_{13} = \frac{1}{2}\left[u_1^1 + \frac{\partial u_3^o}{\partial x}\right]$

f. $\epsilon_{23} = \frac{1}{2}\gamma_{23} = \frac{1}{2}\left[\frac{a}{a+z}\cdot\left(u_2^1 + \frac{1}{a}\frac{\partial u_3^o}{\partial \phi} - \frac{1}{a}u_2^o\right)\right]$

We note, in passing that ϵ_{13} is a function of x and ϕ alone, (constant throughout the thickness), and that ϵ_{23} is equal to $\frac{a}{a+z}$ multiplied by a function of x and ϕ.

Stresses in Terms of u_k^n

Equations (C-14) are now substituted into equations (C-1) through (C-5) to obtain the point stresses in terms of the mid-surface displacements u_k^n:

(C-15)

a. $$\sigma_{11} = \frac{E}{1-\nu^2}\left[\frac{\partial u_1^0}{\partial x} + z\frac{\partial u_1^1}{\partial x} + \frac{\nu}{a+z}\left[\frac{\partial u_2^0}{\partial \phi} + z\frac{\partial u_2^1}{\partial \phi} + u_3^0\right]\right] + \frac{\nu}{1-\nu}\sigma_{33}$$

b. $$\sigma_{22} = \frac{E}{1-\nu^2}\left[\frac{1}{a+z}\left[\frac{\partial u_2^0}{\partial \phi} + z\frac{\partial u_2^1}{\partial \phi} + u_3^0\right] + \nu\left[\frac{\partial u_1^0}{\partial x} + z\frac{\partial u_1^1}{\partial x}\right]\right] + \frac{\nu}{1-\nu}\sigma_{33}$$

c. $$\sigma_{12} = \frac{E}{1-\nu^2}\frac{(1-\nu)}{2}\left[\frac{\partial u_2^0}{\partial x} + z\frac{\partial u_2^1}{\partial x} + \frac{1}{a+z}\frac{\partial u_1^0}{\partial \phi} + \frac{z}{a+z}\frac{\partial u_1^1}{\partial \phi}\right]$$

d. $$\sigma_{13} = \frac{KE}{1-\nu^2}\frac{(1-\nu)}{2}\left[u_1^1 + \frac{\partial u_3^0}{\partial x}\right]$$

e. $$\sigma_{23} = \frac{KE}{1-\nu^2}\frac{(1-\nu)}{2}\left[\frac{a}{a+z}\cdot\left(u_2^1 + \frac{1}{a}\frac{\partial u_3^0}{\partial \phi} - \frac{1}{a}u_2^0\right)\right]$$

Integration Over z To Get Stress Resultants

The shell stress resultants are defined in Appendix B as follows, and are repeated below for convenience:

(C-16)

a. $$\sigma_{11}^{(0)} = N_x = \int_{-h}^{h}\sigma_{11}\left(1+\frac{z}{a}\right)dz$$

b. $$\sigma_{12}^{(0)} = N_{x\phi} = \int_{-h}^{h}\sigma_{12}\left(1+\frac{z}{a}\right)dz$$

c. $$\sigma_{13}^{(0)} = Q_x = \int_{-h}^{h}\sigma_{13}\left(1+\frac{z}{a}\right)dz$$

d. $$\sigma_{21}^{(0)} = N_{\phi x} = \int_{-h}^{h}\sigma_{12}\,dz$$

e. $$\sigma_{22}^{(o)} = N_\phi = \int_{-h}^{h} \sigma_{22}\, dz$$

f. $$\sigma_{23}^{(o)} = Q_\phi = \int_{-h}^{h} \sigma_{23}\, dz$$

g. $$\sigma_{11}^{(1)} = M_x = \int_{-h}^{h} (z)\left(1+\frac{z}{a}\right)\sigma_{11}\, dz$$

h. $$\sigma_{12}^{(1)} = M_{x\phi} = \int_{-h}^{h} (z)\left(1+\frac{z}{a}\right)\sigma_{12}\, dz$$

i. $$\sigma_{22}^{(1)} = M_\phi = \int_{-h}^{h} z\,\sigma_{22}\, dz$$

j. $$\sigma_{21}^{(1)} = M_{\phi x} = \int_{-h}^{h} z\,\sigma_{21}\, dz$$

It is now necessary to compute each of the expressions (C-16), with the assistance of equations (C-15). This is done on a term by term basis:

a. $$\sigma_{11}^{(o)} = N_x = \frac{E}{1-\nu^2}\int_{-h}^{h}\left[1+\frac{z}{a}\right]\left[\frac{\partial u_1^{(o)}}{\partial x} + z\frac{\partial u_1^{(1)}}{\partial x} + \frac{\nu}{a+z}\left(\frac{\partial u_2^{(o)}}{\partial \phi} + z\frac{\partial u_2^{(1)}}{\partial \phi} + u_3^{(o)}\right) + \frac{(1+\nu)}{E}\sigma_{33}\right] dz$$

(C-17)

b. $$\sigma_{12}^{(o)} = N_{x\phi} = \frac{E}{1-\nu^2}\cdot\frac{1-\nu}{2}\int_{-h}^{h}\left[1+\frac{z}{a}\right]\left[\left[\frac{\partial u_2^{(o)}}{\partial x} + z\frac{\partial u_2^{(1)}}{\partial x} + \frac{1}{a+z}\frac{\partial u_1^{(o)}}{\partial \phi} + \left(\frac{z}{a+z}\right)\frac{\partial u_1^{(1)}}{\partial \phi}\right]\right] dz$$

c. $$\sigma_{13}^{(o)} = Q_x = \frac{KE(1-\nu)}{(1-\nu^2)(2)}\int_{-h}^{h}\left(1+\frac{z}{a}\right)\left(u_1' + \frac{\partial u_3^o}{\partial x}\right) dz$$

d. $$\sigma_{21}^{(o)} = N_{\phi x} = \frac{E(1-\nu)}{(1-\nu^2)(2)}\int_{-h}^{h}\left[\frac{\partial u_2^o}{\partial x} + z\frac{\partial u_2'}{\partial \phi} + \frac{1}{a+z}\frac{\partial u_1^o}{\partial \phi} + \frac{z}{a+z}\frac{\partial u_1'}{\partial \phi}\right] dz$$

e. $$\sigma_{22}^{o} = N_\phi = \frac{E}{1-\nu^2}\int_{-h}^{h}\left[\frac{1}{a+z}\left[\frac{\partial u_2^o}{\partial \phi} + z\frac{\partial u_2'}{\partial \phi} + u_3^o\right] + \nu\left[\frac{\partial u_1^o}{\partial x} + z\frac{\partial u_1'}{\partial x}\right] + \frac{(1+\nu)(\nu)}{E(1-\nu)}\sigma_{33}\right] dz$$

f. $$\sigma_{23}^{o} = Q_\phi = \frac{KE(1-\nu)}{(1-\nu^2)(2)}\int_{-h}^{h}\frac{a}{a+z}\left(u_2' + \frac{1}{a}\frac{\partial u_3^o}{\partial \phi} - \frac{1}{a}u_2^o\right) dz$$

g. $$\sigma_{11}^{1} = M_x = \frac{E}{1-\nu^2}\int_{-h}^{h}(z)\left(1+\frac{z}{a}\right)\left\{\frac{\partial u_1^o}{\partial x} + z\frac{\partial u_1'}{\partial x} + \frac{\nu}{a+z}\left[\frac{\partial u_2^o}{\partial \phi} + z\frac{\partial u_2'}{\partial \phi} + u_3^o\right] + \frac{\nu(1+\nu)}{E(1-\nu)}\sigma_{33}\right\} dz$$

h. $$\sigma_{12}^1 = M_{x\phi} = \frac{E(1-\nu)}{(1-\nu^2)(2)}\int_{-h}^{h}(z)\left(1+\frac{z}{a}\right)\left[\frac{\partial u_2^0}{\partial x} + z\frac{\partial u_2^1}{\partial x} + \frac{1}{a+z}\frac{\partial u_1^0}{\partial \phi} + \frac{z}{a+z}\frac{\partial u_1^1}{\partial \phi}\right] dz$$

i. $$\sigma_{22}^1 = M_{\phi} = \frac{E}{1-\nu^2}\int_{-h}^{h}(z)\left[\frac{1}{a+z}\left\{\frac{\partial u_2^0}{\partial \phi} + z\frac{\partial u_2^1}{\partial \phi} + u_3^0\right\} + \nu\left\{\frac{\partial u_1^0}{\partial x} + z\frac{\partial u_1^1}{\partial x}\right\} + \frac{(\nu)(1+\nu)}{E(1-\nu)}\sigma_{33}\right] dz$$

j. $$\sigma_{21}^1 = M_{\phi x} = \frac{E(1-\nu)}{(1-\nu^2)(2)}\int_{-h}^{h} z\left[\frac{\partial u_2^0}{\partial x} + z\frac{\partial u_2^1}{\partial x} + \frac{1}{a+z}\frac{\partial u_1^0}{\partial \phi} + \frac{z}{a+z}\frac{\partial u_1^1}{\partial \phi}\right] dz$$

The integration of equations (17a-j) is straightforward, although laborious. It is worth noting that after the integration, only terms containing odd powers of z survive.

We also pause to note the presence of the factor K in (17c) and (17f), which define the transverse shear resultants. These are the specific terms which will eventually be affected by the assumption of no transverse shear.

In the integration of equations (17), we shall make the following assumptions:

(C-18)

$$\int_{-h}^{h}\left(1+\frac{z}{a}\right)(\sigma_{33})\,dz = 0$$

$$\int_{-h}^{h}\sigma_{33}\,dz = 0$$

$$\int_{-h}^{h}(z)\left(1+\frac{z}{a}\right)\sigma_{33}\,dz = 0$$

$$\int_{-h}^{h} z\,\sigma_{33}\,dz = 0$$

Wherever, in the integration it occurs, we take

(C-19) $$\frac{1}{a+z} = \frac{1}{a} - \frac{z}{a^2} + \frac{z^2}{a^3} - \ldots$$

In the results of the integration, use is made of the "thin shell requirement" that h^2/a^2 may be neglected compared to 1.

Proceeding with the integration, we obtain:

(C-20) a. $$\sigma_{11}^0 = N_x = \frac{2Eh}{1-\nu^2}\left[\frac{\partial u_1^0}{\partial x} + \frac{h^2}{3a}\frac{\partial u_1^1}{\partial x} + \frac{\nu}{a}\frac{\partial u_2^0}{\partial \phi} + \frac{\nu}{a}u_3^0\right]$$

b. $$\sigma_{12}^0 = N_{x\phi} = \frac{E}{1-\nu^2}\cdot\frac{1-\nu}{2}\cdot 2h\left\{\frac{\partial u_2^0}{\partial x} + \frac{1}{a}\frac{\partial u_1^0}{\partial \phi} + \frac{h^2}{3a}\frac{\partial u_2^1}{\partial x}\right\}$$

c. $$\sigma_{13}^0 = Q_x = \frac{KE}{1-\nu^2}\cdot\frac{1-\nu}{2}\cdot 2h\left[u_1^1 + \frac{\partial u_3^0}{\partial x}\right]$$

d. $$\sigma_{21}^0 = N_{\phi x} = \frac{2Eh}{1-\nu^2}\cdot\frac{1-\nu}{2}\left\{\frac{\partial u_2^0}{\partial x} + \frac{1}{a}\frac{\partial u_1^0}{\partial \phi} - \frac{h^2}{3a^2}\frac{\partial u_1^1}{\partial \phi}\right\}$$

e. $$\sigma_{22}^0 = N_\phi = \frac{2Eh}{1-\nu^2}\left\{\frac{1}{a}\frac{\partial u_2^0}{\partial \phi} + \frac{u_3^0}{a} + \frac{\nu}{\partial x}\frac{\partial u_1^0}{\partial x} - \frac{h^2}{3a^2}\frac{\partial u_2^1}{\partial \phi}\right\}$$

f. $$\sigma_{23}^0 = Q_\phi = \frac{2KEh}{1-\nu^2}\cdot\frac{1-\nu}{2}\left\{u_2^1 + \frac{1}{a}\frac{\partial u_3^0}{\partial \phi} - \frac{1}{a}u_2^0\right\}$$

g. $$\sigma_{11}^1 = M_x = \frac{E}{1-\nu^2}\cdot\frac{2h^3}{3}\left[\frac{1}{a}\frac{\partial u_1^0}{\partial x} + \frac{\partial u_1^1}{\partial x} + \frac{\nu}{a}\frac{\partial u_2^1}{\partial \phi}\right]$$

h. $$\sigma_{12}^1 = M_{x\phi} = \frac{2Eh^3}{3(1-\nu^2)}\cdot\frac{1-\nu}{2}\left\{\frac{1}{a}\frac{\partial u_2^0}{\partial x} + \frac{\partial u_2^1}{\partial x} + \frac{1}{a}\frac{\partial u_1^1}{\partial \phi}\right\}$$

i. $$\sigma_{22}^1 = M_\phi = \frac{2Eh^3}{3(1-\nu^2)}\left\{\frac{1}{a}\frac{\partial u_2^1}{\partial \phi} - \frac{1}{a^2}\frac{\partial u_2^0}{\partial \phi} - \frac{1}{a^2}u_3^0 + \nu\frac{\partial u_1^1}{\partial x}\right\}$$

j. $$\sigma_{21}^1 = M_{\phi x} = \frac{2Eh^3}{3(1-\nu^2)}\cdot\frac{1-\nu}{2}\left\{\frac{\partial u_2^1}{\partial x} - \frac{1}{a^2}\frac{\partial u_1^0}{\partial \phi} + \frac{1}{a}\frac{\partial u_1^1}{\partial \phi}\right\}$$

Equations (C-20) were obtained by Yu in 1958 (Reference 1). They will now be substituted in equations (42) and (45-48).

Substitution into Equation 42

Equation 42 becomes, after substitution:

(C-21)

$$\int_t \int_x \int_\phi \Bigg\{ \Bigg[\frac{2Eh}{1-\nu^2} \Big[\frac{\partial^2 u_1^0}{\partial x^2} + \frac{1-\nu}{2a^2} \frac{\partial^2 u_1^0}{\partial \phi^2} + \frac{1+\nu}{2a} \frac{\partial^2 u_2^0}{\partial x \partial \phi} + \frac{\nu}{a} \frac{\partial u_3^0}{\partial x}$$

$$+ ka \Big[\frac{\partial^2 u_1'}{\partial x^2} - \Big(\frac{1-\nu}{2a^2}\Big) \frac{\partial^2 u_1'}{\partial \phi^2} \Big] \Big\} + P_1^+ \Big(1 + \frac{h}{a}\Big) - 2\gamma h \ddot{Y}_B(t) \cdot \bar{e}_1$$

$$- 2\gamma h \frac{\partial^2 u_1^0}{\partial t^2} - \frac{2\gamma h^3}{3a} \frac{\partial^2 u_1'}{\partial t_1^2} \Big] \delta u_1^0$$

$$+ \Bigg[\frac{2Eh^3}{3a(1-\nu^2)} \Big\{ \frac{\partial^2 u_1^0}{\partial x^2} - \frac{(1-\nu)}{2a^2} \frac{\partial^2 u_1^0}{\partial \phi^2} + a \frac{\partial^2 u_1'}{\partial x^2} + \frac{(1-\nu)}{2a} \frac{\partial^2 u_1'}{\partial \phi^2} + \frac{(1+\nu)}{2} \frac{\partial^2 u_2'}{\partial x \partial \phi}$$

$$- \frac{K}{ka} \Big(u_1' + \frac{\partial u_3}{\partial x} \Big) \Big\} + P_1^+ h \Big(1 + \frac{h}{a}\Big) - \frac{2\gamma h^3}{3a} \ddot{Y}_B(t) \cdot \bar{e}_1$$

$$- \frac{2\gamma h^3}{3} \Big[\frac{\partial^2 u_1^0}{a \partial t_1^2} + \frac{\partial^2 u_1'}{\partial t_1^2} \Big] \Bigg] \delta u_1'$$

$$+ \Bigg[\frac{2Eh}{1-\nu^2} \Big\{ \Big(\frac{1+\nu}{2a}\Big) \frac{\partial^2 u_1^0}{\partial x \partial \phi} + \frac{(1-\nu)}{2} \frac{\partial^2 u_2^0}{\partial x^2} + \frac{1}{a^2} \frac{\partial^2 u_2^0}{\partial \phi^2} + \frac{1}{a^2} \frac{\partial u_3^0}{\partial \phi}$$

$$+ ka \Big[\frac{(1-\nu)}{2} \cdot \frac{\partial^2 u_2'}{\partial^2 x} - \frac{1}{a^2} \frac{\partial^2 u_2'}{\partial \phi^2} \Big] - K \Big[\frac{u_2^0}{a^2} - \frac{1}{a^2} \frac{\partial u_3^0}{\partial \phi} - \frac{u_2'}{a^2} \Big] \Big\}$$

$$+ P_2^+ \Big(1 + \frac{h}{a}\Big) - 2h\gamma \frac{\partial^2 u_2^0}{\partial t^2} - \frac{2\gamma h^3}{3a} \frac{\partial^2 u_2'}{\partial t_1^2} - 2\gamma h \ddot{Y}_B(t) \cdot \bar{e}_2 \Big] \delta u_2^0$$

$$+ \Bigg[\frac{2Eh^3}{3a(1-\nu^2)} \Big[\Big(\frac{1-\nu}{2}\Big) \frac{\partial^2 u_2^0}{\partial x^2} - \frac{\partial^2 u_2^0}{a^2 \partial \phi^2} - \frac{1}{a} \frac{\partial u_3^0}{\partial \phi} + \Big(\frac{1+\nu}{2}\Big) \frac{\partial^2 u_1'}{\partial x \partial \phi} + \frac{(1-\nu)}{2} a \frac{\partial^2 u_2'}{\partial x^2}$$

$$+\frac{1}{a}\frac{\partial^2 u_2'}{\partial\phi^2}+\frac{K}{k}\left(\frac{u_2^0}{a^2}-\frac{1}{a^2}\frac{\partial u_3^0}{\partial\phi}-\frac{u_2'}{a}\right)\Big\}$$

$$+P_2^+h\left(1+\frac{h}{a}\right)-\frac{2\gamma h^3}{3a}\ddot{Y}_B(t)\cdot\bar{e}_2-\frac{2\gamma h^3}{3}\left[\frac{\partial^2 u_2^0}{\partial t_1^2}\cdot\frac{1}{a}+\frac{\partial^2 u_2'}{\partial t_1^2}\right]\Big]\delta u_2'$$

$$+\Big[\frac{-h2E}{1-\nu^2}\Big\{\frac{\nu}{a}\frac{\partial u_1^0}{\partial x}+\frac{1}{a^2}\frac{\partial u_2^0}{\partial\phi}+\frac{u_3^0}{a^2}-\frac{k}{a}\frac{\partial u_2'}{\partial\phi}+K\left(\frac{1}{a^2}\frac{\partial u_2^0}{\partial\phi}-\nabla^2 u_3^0-\frac{\partial u_1'}{\partial x}-\frac{1}{a}\frac{\partial u_2'}{\partial\phi}\right\}$$

$$+P_3^+\left(1+\frac{h}{a}\right)-2h\gamma\frac{\partial^2 u_3^0}{\partial t^2}-2\gamma h\ddot{Y}_B(t)\cdot\bar{e}_3\Big]\delta u_3^0\Big\}a\,dx\,d\phi\,dt\;=0$$

In equation (C-21), the following notations are used:

(C-22)
$$k=\frac{1}{3}\frac{h^2}{a^2}$$
$$K=\frac{\kappa(1-\nu)}{2}$$

Also, the subscript 1 is used on t for time to identify those terms which are associated with rotary inertia.

Equation (C-21) was also obtained by Yu in Reference 6, although not by the Variational Principle.

Substitution into Equations (45-48) (Boundary Conditions)

In much the same manner, we now substitute equations (C-20) in equations (45-48), which become:

(C-23) Same as (45) (see text)

(C-24) Same as (46) (see text)

(C-25)

$$\int_t\int_\phi \Bigg\{\Bigg[\frac{2Eh}{1-\nu^2}\left(\frac{\partial u_1^\circ}{\partial x}+\frac{h^2}{3a}\frac{\partial u_1'}{\partial x}+\frac{\nu}{a}\frac{\partial u_2^\circ}{\partial\phi}+\frac{\nu}{a}u_3^\circ\right)+\int_{-h}^{h}P_1\left(1+\frac{z}{a}\right)dz\Bigg]_{x=0}\delta u_1^\circ$$

$$+\Bigg[\frac{E}{1-\nu^2}\cdot\frac{2h^3}{3}\left\{\frac{1}{a}\frac{\partial u_1^\circ}{\partial x}+\frac{\partial u_1'}{\partial x}+\frac{\nu}{a}\frac{\partial u_2'}{\partial\phi}\right\}+\int_{-h}^{h}P_1(z)\left(1+\frac{z}{a}\right)dz\Bigg]_{x=0}\delta u_1'$$

$$+\Bigg[\frac{E}{1-\nu^2}\cdot\frac{1-\nu}{2}\cdot 2h\left\{\frac{\partial u_2^\circ}{\partial x}+\frac{1}{a}\frac{\partial u_1^\circ}{\partial\phi}+\frac{h^2}{3a}\frac{\partial u_1'}{\partial x}\right\}+\int_{-h}^{h}P_2\left(1+\frac{z}{a}\right)dz\Bigg]_{x=0}\delta u_2^\circ$$

$$+\Bigg[\frac{2Eh^3}{3(1-\nu^2)}\cdot\frac{1-\nu}{2}\left\{\frac{1}{a}\frac{\partial u_2^\circ}{\partial x}+\frac{\partial u_2'}{\partial x}+\frac{1}{a}\frac{\partial u_1'}{\partial\phi}\right\}+\int_{-h}^{h}P_2 z\left(1+\frac{z}{a}\right)dz\Bigg]_{x=0}\delta u_2'$$

$$+\Bigg[\frac{KE}{1-\nu^2}\cdot\frac{1-\nu}{2}\cdot 2h\left\{u_1'+\frac{\partial u_3^\circ}{\partial x}\right\}+\int_{-h}^{h}P_3\left(1+\frac{z}{a}\right)dz\Bigg]_{x=0}\delta u_3^\circ\Bigg\}\,a\,d\phi\,dt=0$$

(C-26)

$$\int_t\int_\phi \Bigg\{\Bigg[\frac{2Eh}{1-\nu^2}\left(\frac{\partial u_1^\circ}{\partial x}+\frac{h^2}{3a}\frac{\partial u_1'}{\partial x}+\frac{\nu}{a}\frac{\partial u_2^\circ}{\partial\phi}+\frac{\nu}{a}u_3^\circ\right)-\int_{-h}^{h}P_1\left(1+\frac{z}{a}\right)dz\Bigg]_{x=L}\delta u_1^\circ$$

$$+\Bigg[\frac{E}{1-\nu^2}\cdot\frac{2h^3}{3}\left(\frac{1}{a}\frac{\partial u_1^\circ}{\partial x}+\frac{\partial u_1'}{\partial x}+\frac{\nu}{a}\frac{\partial u_2'}{\partial\phi}\right)-\int_{-h}^{h}P_1 z\left(1+\frac{z}{a}\right)dz\Bigg]_{x=L}\delta u_1'$$

$$+\Bigg[\frac{E}{1-\nu^2}\cdot\frac{1-\nu}{2}\cdot 2h\left(\frac{\partial u_2^\circ}{\partial x}+\frac{1}{a}\frac{\partial u_1^\circ}{\partial\phi}+\frac{h^2}{3a}\frac{\partial u_1'}{\partial x}\right)-\int_{-h}^{h}P_2\left(1+\frac{z}{a}\right)dz\Bigg]_{x=L}\delta u_2^\circ$$

$$+\Bigg[\frac{2Eh^3}{3(1-\nu^2)}\cdot\frac{1-\nu}{2}\left(\frac{1}{a}\frac{\partial u_2^\circ}{\partial x}+\frac{\partial u_2'}{\partial x}+\frac{1}{a}\frac{\partial u_1'}{\partial\phi}\right)-\int_{-h}^{h}P_2 z\left(1+\frac{z}{a}\right)dz\Bigg]_{x=L}\delta u_2'$$

$$+\Bigg[\frac{KE}{1-\nu^2}\cdot\frac{1-\nu}{2}\cdot 2h\left\{u_1'+\frac{\partial u_3^\circ}{\partial x}\right\}-\int_{-h}^{h}P_3\left(1+\frac{z}{a}\right)dz\Bigg]_{x=L}\delta u_3^\circ\Bigg\}\,a\,d\phi\,dt=0$$

APPENDIX D

EFFECT OF DISREGARDING ROTARY INERTIA AND TRANSVERSE SHEAR

The effect of disregarding rotary inertia in equations 42 is considered first. By rotary inertia we mean the inertia deriving from the kinetic energy of rotation of the plane normal to the mid-surface.

The total kinetic energy of the body has been given in Appendix A as:

(A-49) $$K.E. = \int_V \frac{\gamma}{2}(\dot{\vec{r}}\cdot\dot{\vec{r}})\,dV$$

Expanding by the definition of $\dot{\vec{r}}$,

(D-1) $$K.E. = \int_V \frac{\gamma}{2}\left[\dot{\vec{Y}}_\beta\cdot\dot{\vec{Y}}_\beta + 2\dot{\vec{u}}\cdot\dot{\vec{Y}}_\beta + \dot{\vec{u}}\cdot\dot{\vec{u}}\right] dV$$

We note that:

(D-2) $$\dot{\vec{u}} = (\dot{u}_K^\circ + z\dot{u}_K')\vec{e}_K$$

and

(D-3) $$\dot{\vec{Y}}_\beta = \dot{\vec{Y}}_{\beta_K}\dot{\vec{e}}_K$$

Using the volume coordinates dS_K, and expressions (D-2) and (D-2) in (D-1), we obtain:

(D-4)

$$K.E. = \int_x \int_\phi \sum_{k=1}^{3} \int_z \frac{\gamma}{2} \left\{ \left[\dot{Y}_{B_k} \right]^2 + 2 \left[\dot{Y}_{B_k} \right] \left[\dot{u}_k^o + z \dot{u}_k^1 \right] + \left[u_k^o + z u_k^1 \right]^2 \right\} R \, d\phi \, dx \, dz$$

Expanding (D-4), and taking R = a+z,

(D-5)

$$K.E. = \int_x \int_\phi \sum_{k=1}^{3} \int_{-h}^{h} \frac{\gamma}{2} \left\{ \left[\dot{Y}_{B_k} \right]^2 + 2 \dot{Y}_{B_k} \dot{u}_k^o + 2z \dot{Y}_B \dot{u}_k^1 + \dot{u}_k^{o\,2} + 2 \dot{u}_k^o z \dot{u}_k^1 + z^2 \dot{u}_k^{1\,2} \right\} \left(1 + \frac{z}{a} \right) dz \, a \, d\phi \, dx$$

We examine the results of the integration in z, to the extent that it affects the terms containing $\dot{u}_k^n$ and $\ddot{Y}_{B,k}$. Such terms are;

(D-6) $$R.I.\ terms = \frac{\gamma}{2} \int_x \int_\phi \ldots \frac{4}{3a} h^3 Y_{B_k} \dot{u}_k^1 + \ldots \frac{4 \dot{u}_k^o \dot{u}_k^1}{3a} h^3 + \ldots \frac{2h^3}{3} \dot{u}_k^{1\,2}$$

We may thus conclude that in equations (42), the R. I. terms are those that contain $\underline{h^3}$. These terms may be identified by calling the time t_1 rather than t. (This is done in the development of the system of five equations in deformation coordinates, equations (53-57)).

If these terms due to rotary inertia are eliminated from the stree-motion equations, (42), they become; ($\delta u_k^n \neq o$):

(D-7)

$$\int_t\int_x\int_\phi \Big\{\Big[\frac{\partial\sigma_{11}^\circ}{\partial x}+\frac{1}{a}\frac{\partial\sigma_{21}^\circ}{\partial\phi}+P_1^+(1+\frac{h}{a})-2\gamma h\ddot{Y}_B(t)\cdot\bar{e}_1-2\gamma\ddot{u}_1^\circ h\Big]\delta u_1^\circ$$
$$+\Big[\frac{\partial\sigma_{11}^1}{\partial x}+\frac{1}{a}\frac{\partial\sigma_{21}^1}{\partial\phi}+P_1^+(h)(1+\frac{h}{a})-\sigma_{13}^\circ\Big]\delta u_1^1$$
$$+\Big[\frac{\partial\sigma_{12}^\circ}{\partial x}+\frac{1}{a}\frac{\partial\sigma_{22}^\circ}{\partial\phi}+\frac{\sigma_{23}^\circ}{a}+P_2^+(1+\frac{h}{a})-2\gamma h\ddot{Y}_B(t)\cdot\bar{e}_1-2\gamma h\ddot{u}_2^\circ\Big]\delta u_2^\circ$$
$$+\Big[\frac{\partial\sigma_{12}^1}{\partial x}+\frac{1}{a}\frac{\partial\sigma_{22}^1}{\partial\phi}+P_2^+h(1+\frac{h}{a})-\sigma_{23}^\circ\Big]\delta u_2^1$$
$$+\Big[\frac{\partial\sigma_{13}^\circ}{\partial x}+\frac{1}{a}\frac{\partial\sigma_{23}^\circ}{\partial\phi}+P_3^+(1+\frac{h}{a})-\frac{\sigma_{22}^\circ}{a}-2\gamma h\ddot{Y}_B(t)\cdot\bar{e}_3-2\gamma\ddot{u}_3^\circ h\Big]\delta u_3^\circ\Big\}a\,d\phi\,dx\,dt=0$$

We now turn our attention to the neglect of transverse shear.

From Appendix C, equations (C-14):

(C-14) e. $$\epsilon_{13}=\frac{1}{2}\gamma_{13}=\frac{1}{2}\Big\{u_1^1+\frac{\partial u_3^\circ}{\partial x}\Big\}$$

f. $$\epsilon_{23}=\frac{1}{2}\gamma_{23}=\frac{1}{2}\Big\{\frac{a}{a+z}\Big[u_2^1+\frac{1}{a}\frac{\partial u_3^\circ}{\partial\phi}-\frac{1}{a}u_2^\circ\Big]\Big\}$$

and also:

(C-17) e. $$\sigma_{13}^\circ=Q_x=\frac{KE(1-\nu)}{(1-\nu^2)2}\int_{-h}^{h}(1+\frac{z}{a})(u_1^1+\frac{\partial u_3^\circ}{\partial x})\,dz$$

f. $$\sigma_{23}^\circ=Q_\phi=\frac{KE(1-\nu)}{(1-\nu^2)(2)}\int_{-h}^{h}\frac{a}{a+z}(u_2^1+\frac{1}{a}\frac{\partial u_3^\circ}{\partial\phi}-\frac{1}{a}u_2^\circ)\,dz$$

We now combine equations (C-14e) and (C-17e), as well as (C-14f) and (C-17f), to yield:

$$\frac{1}{2}\left[u_1' + \frac{\partial u_3^\circ}{\partial x}\right] = \frac{\sigma_{13}^\circ}{\frac{KE(1-\nu)}{1-\nu^2}\int_{-h}^{h}\left(1+\frac{z}{a}\right)dz} \tag{D-8}$$

$$\frac{1}{2}\left[u_2' + \frac{1}{a}\frac{\partial u_3^\circ}{\partial \phi} - \frac{1}{a}u_2^\circ\right] = \frac{\sigma_{23}^\circ}{\frac{KE(1-\nu)}{1-\nu^2}\int_{-h}^{h}\left(\frac{a}{a+z}\right)dz} \tag{D-9}$$

In order to require that the transverse deformation go to zero:

$$\begin{aligned} \epsilon_{13} &= 0 \\ \epsilon_{23} &= 0 \end{aligned} \tag{D-10}$$

This is the same as requiring:

$$u_1' + \frac{\partial u_3^\circ}{\partial x} = 0 \tag{D-11}$$

$$u_2' + \frac{1}{a}\frac{\partial u_3^\circ}{\partial \phi} - \frac{1}{a}u_2^\circ = 0 \tag{D-12}$$

This can be accomplished by letting $K \to \infty$ in (D-8) and (D-9), so long as σ_{13}° and σ_{23}° remain finite, although undefined.

As $K \to \infty$, conclude, from (D-11) and (D-12), that:

$$u_1' = -\frac{\partial u_3^\circ}{\partial x} \tag{D-13}$$

$$u_2' = \frac{1}{a}u_2^\circ - \frac{1}{a}\frac{\partial u_3^\circ}{\partial \phi} \tag{D-14}$$

We consider now the variations in u_1^1 and u_2^1:

(D-15) $$\delta u_1^1 = -\delta \frac{\partial u_3^0}{\partial x} = -\frac{\partial}{\partial x}\delta u_3^0$$

(D-16) $$\delta u_2^1 = \frac{1}{a}\delta u_2^0 - \frac{1}{a}\frac{\partial}{\partial \phi}\delta u_3^0$$

In equation (D-15), one must evaluate the integration with respect to x, and a similar operation is involved in (D-16) with respect to ϕ. We substitute (D-15) and (D-16) in (D-7);

(D-17)

$$\int_t\int_x\int_\phi \Big\{\Big[\frac{\partial \sigma_{11}^0}{\partial x} + \frac{1}{a}\frac{\partial \sigma_{21}^0}{\partial \phi} + P_1^+\Big(1+\frac{h}{a}\Big) - 2\gamma h \ddot{Y}_B(t)\cdot\bar{e}_1 - 2\gamma \ddot{u}_1^0 h\Big]\delta u_1^0$$

$$+\Big[\frac{\partial \sigma_{11}^1}{\partial x} + \frac{1}{a}\frac{\partial \sigma_{21}^1}{\partial \phi} + P_1^+ h\Big(1+\frac{h}{a}\Big) - \sigma_{13}^0\Big]\Big[-\frac{\partial}{\partial x}\delta u_3^0\Big]$$

$$+\Big[\frac{\partial \sigma_{12}^0}{\partial x} + \frac{1}{a}\frac{\partial \sigma_{22}^0}{\partial \phi} + \frac{\sigma_{23}^0}{a} + P_2^+\Big(1+\frac{h}{a}\Big) - 2\gamma h \ddot{Y}_B(t)\cdot\bar{e}_1 - 2\gamma h \ddot{u}_2\Big]\delta u_2^0$$

$$+\Big[\frac{\partial \sigma_{12}^1}{\partial x} + \frac{1}{a}\frac{\partial \sigma_{22}^1}{\partial \phi} + P_2^+ h\Big(1+\frac{h}{a}\Big) - \sigma_{23}^0\Big]\Big[\frac{1}{a}\delta u_2^0 - \frac{1}{a}\frac{\partial}{\partial \phi}\delta u_3^0\Big]$$

$$+\Big[\frac{\partial \sigma_{13}^0}{\partial x} + \frac{1}{a}\frac{\partial \sigma_{23}^0}{\partial \phi} + P_3^+\Big(1+\frac{h}{a}\Big) - \frac{\sigma_{22}^0}{a} - 2\gamma h \ddot{Y}_B(t)\cdot\bar{e}_3 - 2\gamma \ddot{u}_3^0 h\Big]\delta u_3^0\Big\}\, a\, d\phi\, dx\, dt = 0$$

In equation (D-17), the terms may now be regrouped as coefficents of δu_1^0, δu_2^0 and δu_3^0 to form new equilibrium equations. The terms which are coefficients of $\frac{\partial}{\partial x}\delta u_3^0$ and $\frac{\partial}{\partial \phi}\delta u_3^0$ must be integrated with respect to x and ϕ respectively.

The term that combine to contribute initially to the equilibrium equations become:

(D-18)

$$\int_t\int_x\int_\phi \Big\{\Big[\frac{\partial\sigma_{11}^\circ}{\partial x}+\frac{1}{a}\frac{\partial\sigma_{21}^\circ}{\partial\phi}+P_1^+\Big(1+\frac{h}{a}\Big)-2\gamma h\ddot{Y}_B(t)\cdot\bar{e}_1-2\gamma\ddot{u}_1^\circ h\Big]\delta u_1^\circ$$
$$+\Big[\frac{\partial\sigma_{12}^\circ}{\partial x}+\frac{1}{a}\frac{\partial\sigma_{22}^\circ}{\partial\phi}+P_2^+\Big(1+\frac{h}{a}\Big)-2\gamma h\ddot{Y}_B(t)\cdot\bar{e}_1-2\gamma h\ddot{u}_2^\circ+\frac{1}{a}\frac{\partial\sigma_{12}^1}{\partial x}+\frac{1}{a^2}\frac{\partial\sigma_{22}^1}{\partial\phi}+\frac{P_2^+}{a}h\Big(1+\frac{h}{a}\Big)\Big]\delta u_2^\circ$$
$$+\Big[\frac{\partial\sigma_{13}^\circ}{\partial x}+\frac{1}{a}\frac{\partial\sigma_{23}^\circ}{\partial\phi}+P_3^+\Big(1+\frac{h}{a}\Big)-\frac{\sigma_{22}^\circ}{a}-2\gamma h\ddot{Y}_B(t)\cdot\bar{e}_3-2\gamma\ddot{u}_3^\circ h\Big]\delta u_3^\circ\Big\}\,a\,d\phi\,dx\,dt$$

We note, in the coefficient of δu_2°, that $\frac{\sigma_{23}(o)}{a}-\frac{\sigma_{23}(o)}{a}=o$ has disappeared.

The additional terms are:

(D-19)
$$\int_t\int_x\int_\phi \Big\{\Big[\frac{\partial\sigma_{11}^1}{\partial x}+\frac{1}{a}\frac{\partial\sigma_{21}^1}{\partial\phi}+P_1^+h\Big(1+\frac{h}{a}\Big)-\sigma_{13}^\circ\Big]\Big(-\frac{\partial}{\partial x}\delta u_3^\circ\Big)$$
$$+\Big[\frac{\partial\sigma_{12}^1}{\partial x}+\frac{1}{a}\frac{\partial\sigma_{22}^1}{\partial\phi}+P_2^+h\Big(1+\frac{h}{a}\Big)-\sigma_{23}^\circ\Big]\Big(-\frac{1}{a}\frac{\partial}{\partial\phi}\delta u_3^\circ\Big)\Big\}\,a\,dx\,d\phi\,dt$$

Integrate term by term of equation (D-19), by parts:

(D-20) a. $$\int_x\Big(\frac{\partial\sigma_{11}^1}{\partial x}\Big)\Big(-\frac{\partial}{\partial x}\delta u_3^\circ\Big)dx=-\frac{\partial\sigma_{11}^1}{\partial x}\delta u_3^\circ\Big|_o^L+\int_x\frac{\partial^2\sigma_{11}^1}{\partial x^2}\delta u_3^\circ\,dx$$

b. $$\int_x\frac{1}{a}\frac{\partial\sigma_{21}^1}{\partial\phi}\Big(-\frac{\partial}{\partial x}\delta u_3^\circ\Big)dx=-\frac{\partial\sigma_{21}^1}{a\partial\phi}\delta u_3^\circ\Big|_o^L+\int_x\frac{1}{a}\frac{\partial^2\sigma_{21}^1}{\partial\phi\partial x}\delta u_3^\circ\,dx$$

c. $$\int_x P_1^+h\Big(1+\frac{h}{a}\Big)\Big(-\frac{\partial}{\partial x}\delta u_3^\circ\Big)dx=-P_1^+h\Big(1+\frac{h}{a}\Big)\delta u_3^\circ\Big|_o^L+\int_x\frac{\partial P_1^+}{\partial x}(h)\Big(1+\frac{h}{a}\Big)\delta u_3^\circ\,dx$$

d. $$\int_x+\sigma_{13}^\circ\frac{\partial}{\partial x}(\delta u_3^\circ)dx=\sigma_{13}^\circ\delta u_3^\circ\Big|_o^L-\int_x\frac{\partial\sigma_{13}^\circ}{\partial x}\delta u_3^\circ\,dx$$

(D-21) a. $$\int_\phi \frac{\partial \sigma_{12}^1}{\partial x}\left(-\frac{1}{a}\frac{\partial}{\partial \phi}\delta u_3^o\right)a\,d\phi = -\frac{\partial \sigma_{12}^1}{\partial x}\delta u_3^o\Big|_0^{2\pi} + \int_\phi \frac{1}{a}\frac{\partial^2 \sigma_{12}^1}{\partial x\,\partial \phi}\delta u_3^o\,d\phi$$

b. $$\int_\phi \left(\frac{1}{a}\frac{\partial \sigma_{22}^1}{\partial \phi}\right)\left(-\frac{1}{a}\frac{\partial}{\partial \phi}\delta u_3^o\right)a\,d\phi = -\frac{1}{a}\frac{\partial \sigma_{22}^1}{\partial \phi}\delta u_3^o\Big|_0^{2\pi} + \int_\phi \frac{1}{a^2}\frac{\partial^2 \sigma_{22}^1}{\partial \phi^2}\delta u_3^o\,a\,d\phi$$

c. $$\int_\phi P_2^+ h\left(1+\frac{h}{a}\right)\left(-\frac{1}{a}\frac{\partial}{\partial \phi}\delta u_3^o\right)a\,d\phi = -P_2^+ h\left(1+\frac{h}{a}\right)\delta u_3^o\Big|_0^{2\pi} + \int_\phi \frac{\partial P_2^+}{\partial \phi}\frac{h}{a}\left(1+\frac{h}{a}\right)\delta u_3^o\,a\,d\phi$$

d. $$\int_\phi +\frac{\sigma_{23}^o}{a}\frac{\partial}{\partial \phi}\left(\delta u_3^o\right)a\,d\phi = \sigma_{23}^o\,\delta u_3^o\Big|_0^{2\pi} - \int_\phi \frac{1}{a}\frac{\partial \sigma_{23}^o}{\partial \phi}\delta u_3^o\,a\,d\phi$$

In equations (D-20 (a-d)) the left hand terms add to the boundary conditions and the right hand terms to the coefficient of δu_3^o. In equations (D-21 (a-d)) the left hand terms are identically zero, and the right hand terms contribute to the coefficient of δu_3^o. In the process, the terms $\frac{\partial \sigma_{13}^o}{\partial x}$ and $\frac{\partial \sigma_{23}^o}{a\,\partial \phi}$ vanish.

The final result, which involves a combination of (D-18), (D-20) and (D-21), form the equilibrium equation set: (Since δu_1^o, δu_2^o and δu_3^o are arbitrary):

(D-22) $$\left[\frac{\partial \sigma_{11}^o}{\partial x} + \frac{1}{a}\frac{\partial \sigma_{21}^o}{\partial \phi} + P_1^+\left(1+\frac{h}{a}\right) - 2\gamma h \ddot{Y}_B(t)\cdot \bar{e}_1 - 2\gamma h \ddot{u}_1^o\right]\delta u_1^o = 0$$

(D-23) $$\left[\frac{\partial \sigma_{12}^o}{\partial x} + \frac{1}{a}\frac{\partial \sigma_{22}^o}{\partial \phi} + P_2^+\left(1+\frac{h}{a}\right) - 2\gamma h \ddot{Y}_B(t)\cdot \bar{e}_1 - 2\gamma h u_2^o + \frac{1}{a}\frac{\partial \sigma_{12}^1}{\partial x} + \frac{1}{a^2}\frac{\partial \sigma_{22}^1}{\partial \phi} + P_2^+\frac{h}{a}\left(1+\frac{h}{a}\right)\right]\delta u_2^o = 0$$

(D-24) $$\left[+P_3^+\left(1+\frac{h}{a}\right) - \frac{\sigma_{22}^o}{a} - 2\gamma h \ddot{Y}_B(t)\cdot \bar{e}_3 - 2\gamma h \ddot{u}_3^o + \frac{\partial^2 \sigma_{11}^1}{\partial x^2} + \frac{1}{a}\frac{\partial^2 \sigma_{21}^1}{\partial \phi\,\partial x} + \frac{\partial P_1^+}{\partial x}(h)\left(1+\frac{h}{a}\right) + \frac{1}{a}\frac{\partial^2 \sigma_{21}^1}{\partial x\,\partial \phi} + \frac{1}{a^2}\frac{\partial^2 \sigma_{22}^1}{\partial \phi^2} + \frac{\partial P_2^+}{\partial \phi}\frac{h}{a}\left(1+\frac{h}{a}\right)\right]\delta u_3^o = 0$$

Equations (D-22), (D-23) and (D-24) are the forms of the stress-motion equations when rotary inertia and transverse shear deformation are neglected. We note:

- Only three equations are necessary
- All terms containing σ_{13}° and σ_{32}° have vanished. (These corresponded to the shear stress resultants Qx and Qø).

The second condition is particularly important, because in our assumption $\kappa \to \infty$ (refer to equations (D-12) and (D-13)). Qx and Qø remained undefined.

Now, we proceed to the boundary conditions, shown both in Appendix B and as equations (45 - 48) in the text. Again, we must make use of (D-15), and (D-16) repeated below for convenience:

(D-15) $$\delta u_1' = -\frac{\partial}{\partial x}\delta u_3^{\circ}$$

(D-16) $$\delta u_2' = \frac{1}{a}\delta u_2^{\circ} - \frac{1}{a}\frac{\partial}{\partial \phi}\delta u_3^{\circ}$$

In the boundary conditions on z, at $\pm h$, equations (45) and (46) are not affected by the manipulations of this section.

First, we reconstitute the boundary conditions at x = 0, by using equation (47) and parts of (D-20).

At x = 0

(D-25) $$\int_t\int_{\phi}\Big\{\Big[\sigma_{11}^{\circ} + \int_{-h}^{h} P_1\left(1+\frac{z}{a}\right)dz\Big]\delta u_1 + \Big[\sigma_{11}' + \int_{-h}^{h} P_1 z\left(1+\frac{z}{a}\right)dz\Big]\delta u_1'$$
$$+\Big[\sigma_{12}^{\circ} + \int_{-h}^{h} P_2\left(1+\frac{z}{a}\right)dz\Big]\delta u_2^{\circ} + \Big[\sigma_{12}' + \int_{-h}^{h} P_2 z\left(1+\frac{z}{a}\right)dz\Big]\delta u_2'$$

$$+\left[\sigma_{13}^{\circ}+\int_{-h}^{h}P_3\left(1+\frac{z}{a}\right)dz\right]\delta u_3^{\circ}+\left[\frac{\partial\sigma_{11}^{1}}{\partial x}+\frac{\partial\sigma_{21}^{1}}{a\partial\phi}+P_1^{+}h\left(1+\frac{h}{a}\right)-\sigma_{13}^{\circ}\right]\delta u_3^{\circ}\Bigg\}a\,d\phi\,dt=0$$

First, note that the σ_{13}° terms may be cancelled. Then, substitute (D-15) and (D-16), and regroup:

At x = 0

(D-26)

$$\int_t\int_\phi\Bigg\{\left[\left[\sigma_{11}^{\circ}+\int_{-h}^{h}P_1\left(1+\frac{z}{a}\right)dz\right]_{x=0}\delta u_1^{\circ}\right.$$

$$-\left[\sigma_{11}^{1}+\int_{-h}^{h}P_1 z\left(1+\frac{z}{a}\right)dz\right]_{x=0}\delta\left(\frac{\partial u_2^{\circ}}{\partial x}\right)$$

$$+\left[\sigma_{12}^{\circ}+\int_{-h}^{h}P_2\left(1+\frac{z}{a}\right)dz+\frac{\sigma_{12}^{1}}{a}+\frac{1}{a}\int_{-h}^{h}P_2 z\left(1+\frac{z}{a}\right)dz\right]\delta u_2^{\circ}$$

$$+\left[\int_{-h}^{h}P_3\left(1+\frac{z}{a}\right)dz+P_1^{+}h\left(1+\frac{h}{a}\right)+\frac{\partial\sigma_{11}^{1}}{\partial x}+\frac{\partial\sigma_{21}^{1}}{\partial\phi}\right]_{x=0}\delta u_3^{\circ}$$

$$\left.-\frac{1}{a}\left[\sigma_{12}^{1}+\int_{-h}^{h}P_2 z\left(1+\frac{z}{a}\right)dz\right]_{x=0}\frac{\partial}{\partial\phi}\delta u_3^{\circ}\right\}a\,d\phi\,dt=0$$

The last term may be integrated by parts with respect to ø, and the final result is:

At x = 0

(D-27)

$$\int_t \int_\phi \Big\{ \Big[\sigma_{11}^\circ + \int_{-h}^{h} P_1 \left(1 + \frac{z}{a}\right) dz \Big]_{x=0} \delta u_1^\circ$$

$$- \Big[\sigma_{11}^1 + \int_{-h}^{h} P_1 z \left(1 + \frac{z}{a}\right) dz \Big]_{x=0} \frac{\partial}{\partial x} (\delta u_3^\circ)$$

$$+ \Big[\sigma_{12}^\circ + \int_{-h}^{h} P_2 \left(1 + \frac{z}{a}\right) dz + \frac{\sigma_{12}^1}{a} + \frac{1}{a} \int_{-h}^{h} P_2 z \left(1 + \frac{z}{a}\right) dz \Big]_{x=0} \delta u_2^\circ$$

$$+ \Big[\int_{-h}^{h} P_3 \left(1 + \frac{z}{a}\right) dz + P_1^+ h \left(1 + \frac{h}{a}\right) + \frac{\partial \sigma_{11}^1}{\partial x} + \frac{\partial \sigma_{21}^1}{\partial \phi}$$

$$+ \frac{1}{a} \frac{\partial \sigma_{12}^1}{\partial \phi} + \frac{1}{a} \frac{\partial}{\partial \phi} \int_{-h}^{h} P_2 z \left(1 + \frac{z}{a}\right) dz \Big]_{x=0} \delta u_3^\circ \Big\} a \, d\phi \, dt = 0$$

For a fixed-end cylinder, the end conditions must clearly be prescribed: (at both x = 0 and x = L)

(D-28)

$$u_1 = 0$$

$$u_2 = 0$$

$$u_3 = 0$$

$$\frac{\partial}{\partial x} u_3 = 0$$

For a free-ended cylinder, $P_1 = P_2 = P_3 = 0$, and for arbitrary δu_1°, etc., the boundary conditions at x = 0 and also x = L become:

(D-29)

$$\sigma_{11}^\circ = N_x = 0$$

$$\sigma_{11}^1 = M_x = 0$$

$$\sigma_{12}^\circ + \frac{1}{a}\sigma_{12}^1 = N_{x\phi} + \frac{1}{a}M_{x\phi} = 0 \qquad \text{ERSATZ SHEAR}$$

$$\frac{\partial \sigma_{11}^1}{\partial x} + \frac{\partial \sigma_{21}^1}{\partial \phi} + P_1^+(h)\left(1+\frac{h}{a}\right) + \frac{1}{a}\frac{\partial \sigma_{12}^1}{\partial \phi}$$

$$= \frac{\partial M_x}{\partial x} + \frac{\partial M_{\phi x}}{a\partial x} + P_1^+(h)\left(1+\frac{h}{a}\right) + \frac{1}{a}\frac{\partial M_{x\phi}}{\partial \phi} = 0 \quad \text{ERSATZ TRANSVERSE SHEAR}$$

where the first 3 terms of the last equation define $Q_x\big|_{x=o,L}$, with no rotary inertia considered.

We may now obtain the corresponding expressions in terms of deformation coordinates. Starting with the equation set (C-20 a through j), we substitute for

$$u_1^1\Big|_{K\to\infty} = -\frac{\partial u_3^\circ}{\partial x}$$

and

$$u_2^1\Big|_{K\to\infty} = \frac{1}{a}u_2^\circ - \frac{1}{a}\frac{\partial u_3^\circ}{\partial \phi}$$

to obtain:

(D-30)

a. $$\sigma_{11}^\circ = N_x = \frac{2Eh}{1-\nu^2}\left[\frac{\partial u_1^\circ}{\partial x} + \frac{h^2}{3a}\left(-\frac{\partial^2 u_3^\circ}{\partial x^2}\right) + \frac{\nu}{a}\frac{\partial u_2^\circ}{\partial \phi} + \frac{\nu}{a}u_3^\circ\right]$$

b. $$\sigma_{12}^\circ = N_{x\phi} = \frac{E}{1-\nu^2}\cdot\frac{1-\nu}{2}\cdot 2h\left[\left(1+\frac{h^2}{3a^2}\right)\frac{\partial u_2^\circ}{\partial x} + \frac{1}{a}\frac{\partial u_1^\circ}{\partial \phi} - \frac{h^2}{3a^2}\frac{\partial^2 u_2^\circ}{\partial \phi \partial x}\right]$$

c. $$\sigma_{13}^\circ = Q_x = \frac{\kappa E}{1-\nu^2}\cdot\frac{1-\nu}{2}\cdot 2h\left[0\right] = \infty\cdot 0$$

d. $$\sigma_{21}^\circ = N_{\phi x} = \frac{2Eh}{1-\nu^2}\cdot\frac{1-\nu}{2}\left[\frac{\partial u_2^\circ}{\partial x} + \frac{1}{a}\frac{\partial u_1^\circ}{\partial \phi} + \frac{h^2}{3a^2}\frac{\partial^2 u_3^\circ}{\partial \phi \partial x}\right]$$

e. $$\sigma_{22}^\circ = N_\phi = \frac{2Eh}{1-\nu^2}\left[\left(\frac{1}{a}-\frac{h^2}{3a^3}\right)\frac{\partial u_2^\circ}{\partial \phi} + \frac{u_3^\circ}{a} + \frac{h^2}{3a^3}\frac{\partial^2 u_3^\circ}{\partial \phi^2} + \nu\frac{\partial u_1^\circ}{\partial x}\right]$$

f. $\sigma_{23}^{\circ} = Q_{\phi} = \frac{2KEh}{1-\nu^2} \cdot \frac{1-\nu}{2} \left[0\right] = \infty \cdot 0$

g. $\sigma_{11}^{1} = M_x = \frac{E}{1-\nu^2} \cdot \frac{2h^3}{3} \left[\frac{1}{a} \frac{\partial u_1^{\circ}}{\partial x} - \frac{\partial^2 u_3^{\circ}}{\partial x^2} - \frac{\nu}{a^2} \frac{\partial^2 u_3^{\circ}}{\partial \phi^2} + \frac{\nu}{a^2} \frac{\partial u_2^{\circ}}{\partial \phi} \right]$

h. $\sigma_{12}^{1} = M_{x\phi} = \frac{2Eh^3}{3(1-\nu^2)} \cdot \frac{1-\nu}{2} \left\{ \frac{2}{a} \cdot \frac{\partial u_2^{\circ}}{\partial x} - \frac{2}{a} \frac{\partial^2 u_3^{\circ}}{\partial \phi \partial x} \right\}$

i. $\sigma_{22}^{1} = M_{\phi} = \frac{2Eh^3}{3(1-\nu^2)} \left\{ \frac{1}{a^2} \frac{\partial u_2^{\circ}}{\partial \phi} - \frac{1}{a^2} \frac{\partial^2 u_3^{\circ}}{\partial \phi^2} - \frac{1}{a^2} \frac{\partial u_2^{\circ}}{\partial \phi} - \frac{1}{a^2} u_3^{\circ} - \nu \frac{\partial^2 u_3^{\circ}}{\partial x^2} \right\}$

j. $\sigma_{21}^{1} = M_{\phi x} = \frac{2Eh^3}{3(1-\nu^2)} \cdot \frac{1-\nu}{2} \left\{ \frac{1}{a} \frac{\partial u_1^{\circ}}{\partial x} - \frac{2}{a} \frac{\partial^2 u_3^{\circ}}{\partial \phi \partial x} - \frac{1}{a^2} \frac{\partial u_1^{\circ}}{\partial \phi} \right\}$

We can now make use of these expressions for the stress resultants in terms of deformation coordinates by appropriate substitution in (D-22), (D-23) and (D-24). This becomes the Hamilton Integral as $K \to \infty$. The results are: (for δu_1°, δu_2° and δu_3° all $\neq 0$)

(D-31) $$\frac{2Eh}{1-\nu^2} \left[\frac{\partial^2 u_1^{\circ}}{\partial x^2} + \frac{(1-\nu)}{2a^2} \frac{\partial^2 u_1^{\circ}}{\partial \phi^2} + \frac{1+\nu}{2a} \frac{\partial^2 u_2^{\circ}}{\partial x \partial \phi} + \frac{\nu}{a} \frac{\partial u_3^{\circ}}{\partial x} + k \left(\frac{1-\nu}{2a} \cdot \frac{\partial^3 u_2^{\circ}}{\partial \phi^2 \partial x} - a \frac{\partial^3 u_3^{\circ}}{\partial x^3} \right) \right] - \left\{ 2\gamma h \ddot{Y}_B(t) \cdot \bar{e}_1 + 2\gamma h \ddot{u}_1^{\circ} - P_1^{+} \left(1 - \frac{h}{a}\right) \right\} = 0$$

(D-32) $$\frac{2Eh}{1-\nu^2} \left\{ \frac{1+\nu}{2a} \frac{\partial^2 u_1^{\circ}}{\partial \phi \partial x} + \frac{1-\nu}{2} \frac{\partial^2 u_2^{\circ}}{\partial x^2} + \frac{1}{a^2} \frac{\partial^2 u_2^{\circ}}{\partial \phi^2} + \frac{1}{a^2} \frac{\partial u_3^{\circ}}{\partial \phi} + k \left[\frac{3}{2} (1-\nu) \frac{\partial^2 u_2^{\circ}}{\partial x^2} - \frac{1}{a^2} \frac{\partial^2 u_2^{\circ}}{\partial \phi^2} - \frac{1}{a^2} \frac{\partial u_3^{\circ}}{\partial \phi} - \left(\frac{3-\nu}{2}\right) \frac{\partial^3 u_3^{\circ}}{\partial x^2 \partial \phi} \right] \right\}$$
$$- \left\{ 2\gamma h \ddot{Y}_B(t) \cdot \bar{e}_1 + 2\gamma h \ddot{u}_2^{\circ} - P_2^{+} \left(1 + \frac{h}{a}\right) - \frac{P_2^{+}}{a} h \left(1 + \frac{h}{a}\right) \right\} = 0$$

(D-33) $$- \frac{2Eh}{1-\nu^2} \left[\frac{1}{a^2} \frac{\partial u_2^{\circ}}{\partial \phi} + \frac{u_3^{\circ}}{a^2} + \frac{\nu}{a} \frac{\partial u_1^{\circ}}{\partial x} - ka^2 \left[\frac{1}{a} \frac{\partial^3 u_1^{\circ}}{\partial x^3} - \frac{(1-\nu)}{2a^3} \frac{\partial^3 u_1^{\circ}}{\partial \phi^2 \partial x} + \frac{(3-\nu)}{2a^2} \frac{\partial^3 u_2^{\circ}}{\partial x^2 \partial \phi} + \frac{1}{a^4} \frac{\partial u_2^{\circ}}{\partial \phi} - \frac{2}{a^4} \frac{\partial^2 u_3^{\circ}}{\partial \phi^2} - \nabla^4 u_3^{\circ} \right] \right]$$
$$- \left\{ 2\gamma h \ddot{Y}_B(t) \cdot \bar{e}_3 + 2\gamma h \ddot{u}_3^{\circ} - P_3^{+} \left(1 + \frac{h}{a}\right) - \frac{\partial P_1^{+}}{\partial x} h \left(1 + \frac{h}{a}\right) - \frac{\partial P_2^{+}}{\partial \phi} \frac{h}{a} \left(1 + \frac{h}{a}\right) \right\} = 0$$

Equations (D-31) through (D-33) are essentially the same as those obtained by Yu in Reference 6, except of course for the terms containing the external load and the $Y_B(t)$ terms. They differ from the well-known Flugge equations only in terms with the coefficient k. (Yu used a force balance method to obtain his equations).

We contend that this system of three equations, derived directly from Hamilton's Principle, is inherently consistent with the basic (correct) system of five equations, and will use them instead of the Flugge equations.

APPENDIX E

DEMONSTRATION OF ORTHOGONALITY OF THE NORMAL MODES

In section VII, we indicated (equation 127) that it would be necessary to satisfy the following orthogonality requirement:

$$(E\text{-}1) \qquad \int_x \int_\phi F_K^n(x,\phi)_{ps} f_K^n(x,\phi)_{mN}\, a\, d\phi\, dx \begin{cases} =0 & m \neq p \\ =0 & s \neq N \\ \neq 0 & m=p,\ s=N \end{cases}$$

The term $F_k^n(x,\phi)_{ps}$ is identified in equation (104) as being associated with the variation in kinetic energy, and the $f_k^n(x,\phi)_{mN}$ are the normal modes in free vibration. (Refer to equations (80), (85) and (99)).

This condition (E-1) is essential to the solution of the forced vibration problem, in that it ensures that it is possible to develop the Lagrange equilibrium equations for prinicpal (separable) time coordinates.

This type of orthogonality requirement is commonly encountered whenever the solution to a forced vibration problem is attempted by the classical "normal mode method". The usual practice is to demonstrate that the necessary orthogonality conditions are met by manipulating the actual expressions for the normal modes. In this appendix, the verification is taken directly from Hamilton's equations.

There are three major assumptions in the proof:

- The system must be linearly elastic, without energy dissipation
- The normal mode functions must satisfy the equilibrium equations for free vibration

- The normal mode functions must satisfy the boundary conditions

(These will be cited as needed).

We begin by restating Hamilton's principle (Refer to equations (8), (15), and (16)):

$$\delta\int_0^t (T-U+W)\,dt = 0 \tag{E-2}$$

For the case of free vibration, there are no surface tractions $\overline{P}$, hence no term W, and no acceleration of the center of gravity $\ddot{Y}_B(t)$.*

Thus, for free vibration, Hamilton's principle reduces to:

$$\delta\int_0^t (T-U)\,dt = 0 \tag{E-3}$$

the kinetic energy variation is expressed (see Appendix A)

$$\int_0^t \delta T\,dt = \int_0^t \int_V \delta\left(\tfrac{1}{2}\gamma\dot{\overline{r}}\cdot\dot{\overline{r}}\right)\Big|_{\dot{Y}_B = \text{CONST (FREE CYL.)}} dV\,dt \tag{E-4}$$

---

*NOTE: Here, we are of course glossing over certain subtleties that have been adequately discussed elsewhere in this analysis. For a free-ended cylinder $\overline{P} = 0$, while in a constrained end situation, no work is done by the constraint. Again, were this simply a question of free vibration, no use of the center of gravity as the origin of a bodyfixed coordinate system would even have been considered for a constrained end (i.e. $\overline{u} \rightarrow \overline{r}$).

Since we are now dealing with an inertial system ($\dot{\bar{V}}_B$ = constant), (E-4) reduces to:

$$\text{(E-5)} \qquad \int_0^t \delta T dt = \int^t \int_v \gamma \delta\left(\tfrac{1}{2}\dot{\bar{U}}\cdot\dot{\bar{U}}\right) dV dt = \int_t \int_v -\gamma \ddot{U}_K \delta U_K dV dt$$

In equation (E-5), u_k are deformation coordinates and indicial notation is of course implied.

We proceed to the variation of the strain-energy term. For a linearly elastic material, we showed in Appendix A (Equations A1-A15) that:

$$\text{(E-6)} \qquad -\int_0^t \delta U dt = -\int_t \int_v \frac{\partial U_{VOL}}{\partial \epsilon_{ij}} \delta\epsilon_{ij} dV dt = \int_t \int_v \sigma_{ij} \delta\epsilon_{ij} dV dt$$

In Appendix A (Refer to (A-20) and (A-47)), this expression was shown to be:

$$\text{(E-7)} \qquad -\int_0^t \delta U dt = -\int_t \int_v \sigma_{ik} \frac{\partial}{\partial S_i} \delta U_k dV dt + \int_t \int_v \left(\sigma_{ti} \bar{e}_k \cdot \frac{\partial \bar{e}_i}{\partial S_t}\right) \delta U_k dV dt$$

We have shown, in Appendix A, that the right hand side is equal to:

$$\text{(E-8)} \qquad -\int_0^t \delta U dt = -\int_t \int_{\Sigma_i} \bar{n}\cdot\bar{e}_i \left[(\sigma_{ik}\delta U_k)^{\lambda_i\,MAX} + (\sigma_{ik}\delta U_k)^{\lambda_i\,MIN}\right] d\Sigma_i dt$$
$$+ \int_t \int_v (\nabla\cdot\tau)_K \delta U_K dV dt$$

in which it was understood that the subscript i refers to the direction of traversal. During the subsequent manipulation of (E-8), we have utilized (see equations (30) and (37):

$$\text{(E-9)} \qquad u_K = U_K^{(0)} + \varepsilon U_K^{(1)} \qquad \delta U_K = \delta U_K^{(0)} + \varepsilon \delta U_K^{(1)}$$

and used a slightly different form to emphasize the boundary surface in the direction of z as contrasted with the boundary surface normal to the mid-surface.

Using all of the above information, we may write (E-3) as:

$$(E\text{-}10)\quad \delta\int_0^t (T-U)\,dt = \int_t\int_x\int_\phi \left[\int_{-h}^{h} \left[(\nabla\cdot\tau)_K\left(1+\frac{z}{a}\right)z^n - \rho\left(z^0\ddot{U}_K^{(\phi)} + z^1 U_K^{(\phi)}\right)z^n\right] dz\, a\,d\phi\, dx\, dt$$

$$-\int_t\oint_c \left(\left[\sigma_{ik}^{(m)}\bar{n}\cdot\bar{e}_i\right]\delta U_K^{(m)}\right)_c dC\, dt$$

$$-\int_t\int_{\Sigma_3} \sigma_{3K}(\pm h)\,\bar{n}\cdot\bar{e}_3\,\delta U_K(\pm h)\,d\Sigma_3\,dt \equiv 0$$

For free vibration with homogeneous conditions the solutions have been developed (which of course satisfy Hamilton's integral (E-10) in the form:

$$(E\text{-}11)\quad \left\{U_K^n\right\} = \sum_p\sum_s \left\{f_K^n(x,\phi)_{ps}\right\} q(t)_{ps} = \sum_p\sum_s \left\{f_K^n(x,\phi)_{ps}\right\} C_{ps}\, e^{i\omega_{ps}t}$$

As has been explained (Refer to equation (121)) we want to distinguish the modal pairs in terms δu_K^n from those used elsewhere in the equations. We retain the choice adopted there, employing m, N subscripts for any terms involving δu_K^n. We thus write, for use in equation (E-10):

$$(E\text{-}12)\quad \delta U_K^n = \sum_m\sum_N f_K^n(x,\phi)_{mN}\,\delta q(t)_{mN}$$

$$(E\text{-}13)\quad \delta U_K(h) = \sum_m\sum_N \left[f_K^0(x,\phi)_{mN} + h f_K^1(x,\phi)_{mN}\right]\delta q(t)_{mN}$$

(E-14) $$\bar{n}\cdot\bar{e}_i\,\sigma^n_{ik} = \sum_p \sum_s \bar{n}\cdot\bar{e}_i\, S^n_{ik}(x,\phi)_{ps}\, q(t)_{ps}$$

(where $\bar{n}\cdot\bar{e}_1\ S^n_{1k}\ (x,\phi)ps = 0$ for a free-ended cylinder

(E-15) $$\bar{n}\cdot\bar{e}_3\,\sigma_{3k}(h) = \sum_p \sum_s \bar{n}\cdot\bar{e}_3\, S_{3k}(x,\phi,h)_{ps}\, q(t)_{ps}$$

and this equals zero for no traction.

(E-16) $$-\int_{-h}^{h} \gamma\left(z^o \ddot{U}^{(o)}_k + z^1 U^{(1)}_k\right) z^n \left(1+\frac{z}{a}\right) dz = \sum_p \sum_s F^n_k(x,\phi)_{ps}\, \omega^2_{ps}\, q(t)_{ps}$$

(E-17) $$-\int_{-h}^{h} (\nabla\cdot\tau)_k \left(1+\frac{z}{a}\right) z^n\, dz = \sum_p \sum_s \Lambda^n_k\left(\left\{f^n_k(x,\phi)_{ps}\right\}\right)_{ps}\, q(t)_{ps}$$

If we now substitute equations (E-12) through (E-17) in (E-10), the result becomes:

(E-18)

$$0 = \int_t \sum_m \sum_N \delta q(t)_{mN} \left[\sum_p \sum_s q(t)_{ps} \left(\int_x \int_\phi \left(\Lambda^n_k\left(\left\{f^n_k(x,\phi)_{ps}\right\}\right)_{ps} + F^n_k(x,\phi)_{ps}\,\omega^2_{ps}\right) f^n_k(x,\phi)_{mN}\, a\, d\phi\, dx\right)\right] dt$$

$$-\int_t \sum_m \sum_N \delta q(t)_{mN} \left[\sum_p \sum_s q(t)_{ps} \left(\oint_c \bar{n}\cdot\bar{e}_i\, S^n_{ik}(x,\phi)_{ps} f^n_k(x,\phi)_{mN}\, dC\right)\right] dt$$

$$-\int_t \sum_m \sum_N \delta q(t)_{mN} \left[\sum_p \sum_s q(t)_{ps} \left(\int_{z_3} \bar{n}\cdot\bar{e}_3\, S_{3k}(x,\phi,\pm h)_{ps} \left(f^o_k(x,\phi)_{mN} + h f^1_k(x,\phi)_{mN}\right) d\Sigma_3\right)\right] dt$$

Equation (18) can also be written in the form:

(E-19) $$0 = \int_t \sum_m \sum_N \delta q(t)_{mN} \left[\overset{[M]}{Q}(t)_{mN} + \overset{[K]}{Q}(t)_{mN}\right] dt = \int_t \sum_m \sum_N \delta q(t)_{mN} \left[Q(t)_{mN}\right] dt$$

in which:

$\overset{[U]}{Q}(t)_{mN}$ is the generalized force associated with the conservative work due to the increase in strain energy.

$\overset{[T]}{Q}(t)_{mN}$ is the generalized d'Alembert force associated with the work done by the variation of kinetic energy.

Thus:

$$\int_t -(\delta U)\,dt = \int_t \left(\sum_m \sum_N \delta q(t)_{mN}\, \overset{[U]}{Q}(t)_{mN}\right) dt \tag{E-20}$$

$$\int_t (\delta T)\,dt = \int_t \left(\sum_m \sum_N \delta q(t)_{mN}\, \overset{[T]}{Q}(t)_{mN}\right) dt \tag{E-21}$$

We write:

$$\overset{[U]}{Q}(t)_{mN} = \sum_p \sum_s q(t)_{ps}\, K_{mN\text{-}ps} = \sum_p \sum_s \overset{[U]}{Q}(t)^{ps}_{mN} \tag{E-22}$$

$$\overset{[T]}{Q}(t)_{mN} = \sum_p \sum_s q(t)_{ps} \int_x \int_\phi \omega^2_{ps} F^n_K(x,\phi)_{ps} f^n_K(x,\phi)_{mN}\, a\,d\phi\,dt = \sum_p \sum_s \overset{[T]}{Q}(t)^{ps}_{mN} \tag{E-23}$$

From equation (E-18), it is apparent that:

$$\begin{aligned} K_{mN\text{-}ps} = {} & \int_x \int_\phi \Lambda^n_K \left(\left\{f^n_K(x,\phi)_{ps}\right\}\right) f^n_K(x,\phi)_{mN}\, a\,d\phi\,dx \\ & - \oint_c \bar{n}\cdot\bar{e}_i\, S^n_{iK}(x,\phi)_{ps} \Big|_c f^n_K(x,\phi)\Big|_c dC \\ & - \int_{\Sigma_3} \bar{n}\cdot\bar{e}_3\, S_{3K}(x,\phi,\pm h)\Big|_{\Sigma_3} \left(f^o_K(x,\phi)_{mN} + h f^1_K(x,\phi)_{mN}\right)\Big|_{\Sigma_3} d\Sigma_3 \end{aligned} \tag{E-24}$$

Now for any function satisfying the boundary conditions, (either free or clamped ends) the latter two integrals vanish, and K_{mN-ps} reduces to:

$$K_{mN-ps} = \int_x \int_\phi \Lambda_K^n \left(\left[f_K^n(x,\phi)_{ps} \right] \right)_{ps} f_K^n(x,\phi)_{mN} \, a \, d\phi \, dx \tag{E-25}$$

We retain (E-25), and rewrite (E-19), substituting (E-22) and (E-23):

$$0 = \int_t \sum_m \sum_N \delta q(t)_{mN} \left[\sum_p \sum_s \left\{ {}^{[v]}Q(t)_{mN}^{ps} + {}^{[r]}Q(t)_{mN}^{ps} \right\} \right] dt \tag{E-26}$$

Since the term $\delta q(t)_{mN}$ is arbitrary, the interior brackets must equal zero, which leads to all and any:

$${}^{[v]}Q(t)_{mN}^{ps} + {}^{[r]}Q(t)_{mN}^{ps} = 0 \tag{E-27}$$

Equation (E-27) holds for all terms in (E-26), and the ps sum should be considered as the coefficient of $\delta q(t)_{mN}$.

Now consider a particular term of (E-26), identified as including $\delta q(t)_{\underline{mN}}$. Associated with this term is the doubly infinite series:

$$\sum_p \sum_s \left\{ {}^{[v]}Q(t)_{\underline{mN}}^{ps} + {}^{[r]}Q(t)_{\underline{mN}}^{ps} \right\} \tag{E-28}$$

In (E-28), isolate one term, corresponding to ps. This coefficient of $\delta q(t)_{\underline{mN}}$ is thus:

$${}^{[v]}Q(t)_{\underline{mN}}^{\underline{ps}} + {}^{[r]}Q(t)_{\underline{mN}}^{\underline{ps}} = 0 \tag{E-29}$$

Multiply this coefficient by $q(t)_{\underline{mN}}$ (this is still equal to zero).

(E-30) $$[u]\underline{Q(t)}^{\underline{ps}}_{\underline{mN}}\, q(t)_{\underline{mN}} + [r]\underline{Q(t)}^{\underline{ps}}_{\underline{mN}}\, q(t)_{\underline{mN}} = 0$$

In a parallel way, we can invert the values of $\underline{mN}$ and $\underline{ps}$, and multiply the corresponding coefficient by $q(t)\underline{ps}$ to obtain:

(E-31) $$[u]\underline{Q(t)}^{\underline{mN}}_{\underline{ps}}\, q(t)_{\underline{ps}} + [r]\underline{Q(t)}^{\underline{mN}}_{\underline{ps}}\, q(t)_{\underline{ps}} = 0$$

We now substract (E-31) from (E-30) to obtain:

(E-32) $$\left[[u]\underline{Q(t)}^{\underline{ps}}_{\underline{mN}}\, q(t)_{\underline{mN}} - [u]\underline{Q(t)}^{\underline{mN}}_{\underline{ps}}\, q(t)_{\underline{ps}}\right] + \left[[r]\underline{Q(t)}^{\underline{ps}}_{\underline{mN}}\, q(t)_{\underline{mN}} - [r]\underline{Q(t)}^{\underline{mN}}_{\underline{ps}}\, q(t)_{\underline{ps}}\right] = 0$$

Now by Betti's Law the first bracket is equal to zero.*

Also note, by reference to equations (100) and (104), (E-32) is exactly;

---

*NOTE: Betti's Law applies to linear, elastic systems. In this case:

$$[u]\underline{Q(t)}^{\underline{ps}}_{\underline{mN}}\, q(t)_{\underline{mN}} - [u]\underline{Q(t)}^{\underline{mN}}_{\underline{ps}}\, q(t)_{\underline{ps}} = 0 \quad +$$

which may be written:

$$(q(t)_{\underline{ps}} K_{\underline{mN}-\underline{ps}})\, q(t)_{\underline{mN}} - (q(t)_{\underline{mN}} K_{\underline{ps}-\underline{mN}})\, q(t)_{\underline{ps}} = 0$$

This is then seen to be a generalized statement of Maxwell's reciprocity theory.

$$K_{\underline{mN}-\underline{ps}} = K_{\underline{ps}-\underline{mN}}$$

Maxwell's Theorem can be verified in the following manner:

'A linear stress-strain relationship, $\sigma_{ij} = C_{ijk\ell}\epsilon_{k\ell}$ is

'+ Bibliography, No. 34

(E-33) $$0=\int_x\int_\phi^{2\pi}\left(H^n_{\kappa,ps}\,u^n_{\kappa,mN}-H^n_{\kappa,mN}\,u^n_{\kappa,ps}\right)a\,d\phi\,dx$$

which is the equivalent* Sturm-Liouville orthogonality scheme for a set of partial differential equations with homogeneous boundary conditions which will be satisfied by any mode shape. This proof is attempted by a detailed evaluation of (E-33), utilizing the boundary conditions. What remains of (E-32) is therefore:

(E-34) $$\overset{[M]}{Q}(t)^{ps}_{mN}\,q_i(t)_{mN}-\overset{[T]}{Q}(t)^{mN}_{ps}\,q_i(t)_{ps}=0$$

Using equation (E-23) this may be written as:

(E-35) $$q(t)_{mN}q(t)_{ps}\left(\omega^2_{ps}-\omega^2_{mN}\right)\int_x\int_\phi F^n_\kappa(x,\phi)_{ps}\,f^n_\kappa(x,\phi)_{mN}\,a\,d\phi\,dx=0$$

because it can be shown that (See (162), (164))

(E-36) $$F^n_\kappa(x,\phi)_{mN}\,f^n_\kappa(x,\phi)_{ps}=F^n_\kappa(x,\phi)_{ps}\,f^n_\kappa(x,\phi)_{mN}$$

Since, in general, unless m,N = p,s, $\omega^2_{ps}\neq\omega^2_{mN}$, equation (E-35) demonstrates the desired orthogonality relation.

Continuation of Note on Preceding Page

formed for an elastic system whose strain energy density is a symmetric quadratic function of the strains, $U_{vol}=\frac{1}{2}C_{ijk\ell}\,\epsilon_{k\ell}\,\epsilon_{ij}$, (higher order strain products are disregarded with infinitesimal strain).
For a system in free vibration with homogeneous boundary conditions, the strain, which is composed of the separable deformation coordinates (100) and their space derivatives

* Bibliography, No. 61

Continuation of Note on Preceding Page

(A-2) is;

$$(1) \qquad \epsilon_{ij} = \sum_{mN}^{\infty\infty\infty} h_{ij}(x,\phi,z)_{mN}\, q(t)_{mN}$$

$$(2) \qquad \epsilon_{kl} = \sum_{ps}^{\infty\infty\infty} h_{kl}(x,\phi,z)_{ps}\, q(t)_{ps}$$

This develops a strain energy variation

(E-6)

$$-\int_{t_o}^{t_1} \delta U dt = -\delta \int_t \int_V \sum_{mN}^{\infty\infty\infty} \sum_{ps}^{\infty\infty\infty} \tfrac{1}{2} C_{ijkl} h_{kl}(x,\phi,z)_{ps} q(t)_{ps} h_{ij}(x,\phi,z)_{mN} q(t)_{mN} dV dt$$

and in terms of the generalized force associated with the increase in strain energy;

$$-\delta \int_{t_o}^{t_1} U dt = -\int_t \sum_{mN}^{\infty\infty\infty} \left[\frac{\partial U}{\delta q(t)_{mN}}\right] \delta q_{mN} dt = +\int_t \sum_{mN}^{\infty\infty\infty} \left[\overset{[u]}{Q}(t)_{mN}\right] \delta q(t)_{mN}$$

$$= -\int_t \int_V \frac{\partial U_{vol}}{\partial \epsilon_{ij}} \delta \epsilon_{ij} dV dt = -\int_t \int_V \sigma_{ij} \sum_{mN}^{\infty\infty\infty} \frac{\partial \epsilon_{ij}}{\delta q(t)_{mN}} \delta q_{mN} dV dt$$

$$(3) \qquad -\int_{t_o}^{t_1} \delta U dt = -\int_{t_o}^{t_1} \sum_{mN}^{\infty\infty\infty} \delta q(t)_{mN} \left[\sum_{ps}^{\infty\infty\infty} q(t)_{ps} \int C_{ijkl} h_{kl,ps}\, h_{ij,mN} dV\right] dt$$

The term within the integral is the stiffness coefficient equivalent to E-24;

Continuation of Note on preceding page

(4) $$K_{mN-ps} = \frac{\partial Q(t)_{mN}^{(v)}}{\partial q(t)_{ps}} = \frac{\partial\left(\frac{\partial U}{\partial q(t)_{mN}}\right)}{\partial q(t)_{ps}} = -\int_v C_{ijkl}\, h_{ij,mN}\, h_{kl,ps}\, dV$$

By the same token:

(5) $$K_{ps-mN} = \frac{\partial Q(t)_{ps}^{(v)}}{\partial q(t)_{mN}} = -\frac{\partial\left(\frac{\partial U}{\partial q(t)_{ps}}\right)}{\partial q(t)_{mN}} = -\int_v C_{ijkl}\, h_{ij,ps}\, h_{kl,mN}\, dV = -\int_v C_{klij}\, h_{kl,ps}\, h_{ij,mN}\, dV$$

The latter equivalency is due to an interchange of the dummy variables ij and kl in the summation.
Due to the symmetry of the elastic constants
$C_{ijk} = C_{kl}$ ij;

(6) $$K_{mN-ps} = K_{ps-mN} = -\int_v C_{ijkl}\, h_{ij,mN}\, h_{kl,ps}\, dV$$

This quarantees the proper usage of Betti's Law for this system.

Bibliography

1. Rayleigh, J.W.S., "The Theory of Sound" Volume 1, Dover Publications, New York, Second Edition, 1945.

2. Baron, M.L., Bleich, H.H., "Tables for Frequencies and Modes of Free Vibration of Infinitely Long, Thin, Cylindrical Shells", Journal of Applied Mechanics, Vol. 76, 1954.

3. Arnold, R.N., Warburton, G.B., "Flexural Vibrations of the Walls of Thin Cylindrical Shells Having Freely Supported Ends", Proceedings of the Royal Society of London, England, series A, Vol. 197, 1949.

4. Arnold, R.N., Warburton, G.B., "The Flexural Vibrations of Thin Cylinders" Proceedings of the Institution of Mechanical Engineers, Vol. 167, 1963.

5. Yu, Y.Y., "Free Vibrations of Thin Cylindrical Shells Having Finite Lengths With Freely Supported and Clamped Ends", Journal of Applied Mechanics, December, 1955.

6. Yu, Y.Y., "Vibrations of Thin Cylindrical Shells Analyzed by Means of Donnell-Type Equations", Journal of the AERO/SPACE SCIENCES, Vol. 25 No. 11, Nov. 1958.

7. Forsberg, K., "Influence of Boundary Conditions on the Modal Characteristics of Thin Cylindrical Shells",AIAA Journal, Vol. 2, No. 12, Dec. 1964.

8. Forsberg, K., "Review of Analytical Methods Used to Determine the Modal Characteristics of Cylindrical Shells", NASA CR-613, Sept. 1966.

9. Warburton, G.B., "Vibrations of Thin Cylindrical Shells", Journal of Mechanical Engineering Science, Vol. 7, No. 4, Dec. 1965.

10. Weingarten, V.I., "Free Vibrations of a Thin-Walled Cylindrical Shell Subjected to a Bending Moment",AIAA Journal, Vol. 3, No. 1, Jan. 1965.

11. Weingarten, V.I., "Free Vibration of Thin Cylindrical Shells", AIAA Journal, Vol. 2, No. 4, Apr. 1964.

12. Mirsky, I., Herrmann, G., "Nonaxially Symmetric Motions of Cylindrical Shells", The Journal of the Acoustical Society of America, Vol. 29, No. 10, Oct. 1957.

13. Mirsky, I., "Vibrations of Orthotropic, Thick Cylindrical Shells", The Journal of the Acoustical Society of America, Vol. 36, No. 1, Jan. 1964.

14. Payton, R.G., "Dynamic Membrane Stresses in a Circular Elastic Shell", Journal of Applied Mechanics, Sept. 1961.

15. Humphreys, J., Winter, R., "Dynamic Response of a Cylinder to a Side Pressure Pulse", AIAA Journal, Vol. 3, No. 1, Jan. 1965.

16. Sheng, J., "The Response of a Thin Cylindrical Shell to Transient Surface Loading", AIAA Journal, Vol. 3, No. 4, April 1965.

17. Bushnell, D., "Dynamic Response of Two-Layered Cylindrical Shells to Time-Dependent Loads", AIAA Journal, Vol. 3, No. 9, September 1965.

18. Yao, J.C., "Analytical and Experimental Study of Cylinders under Localized Impact Loads", Aeronautical Quarterly, Vol. 17 pt. 1, Feb. 1966.

19. Flugge, W., "Statik und Dynamik der Schalen", Julius Springer, Berlin, 1934.

20. Wah, T. et al, "Respnse of Missile Structures to Impulse Loading", Technical Documentary Report ASD-TDR-62-475, Wright-Patterson Airforce Base, Ohio, March 1963.

21. Johnson, D., Greif, R., "Dynamic Response of a Cylindrical Shell: Two Numerical Methods", AIAA Journal, Vol. 4, No. 3, March 1966.

22. Sanders, J.L. Jr., "An Improved First Approximation Theory for Thin Shells", NASA Rept. 24 (June 1959).

23. Mehta, P., Davids, N., "A Direct Numerical Analysis Method for Cylindrical and Spherical Elastic Waves", AIAA Journal, Vol. 4, No. 1, Jan. 1966.

24. Witmer, E.A., et al, "Large Dynamic Deformations of Beams, Rings, Plates and Shells", AIAA Journal, Vol. 1, No. 8, Aug. 1963.

25. Pian, T.H.H., "On Large Dynamic Deformations of General Shells", Technical Documentary Report RTD-TDR-63-4271, Jan. 1964.

26. Leech, J.W., "Finite Difference Calculation Method for Large Elastic-Plastic Dynamically Induced Deformation of General Shells", AFFDL-TR-66-171, Dec. 1966.

27. Love, A.E.H., "A treatise on the Mathematical Theory of Elasticity", Cambridge University Press, 1927.

28. Timoshenko, S., Woinowsky-Krieger, S., "Theory of Plates and Shells", McGraw Hill, N.Y. 1959.

29. Flugge, W., "Stresses in Shells", Springer-Verlag, Berlin, 1962, second printing.

30. Donnell, L.H., "Stability of Thin-Walled Tubes Under Torsion", NACA Report-479 (1933).

31. Budiansky, B., Sanders, J.L., "On the Best First Order Linear Shell Theory", Progress in Applied Mechanics. The Prager Anniversary Volume, The MacMillan Company, 1963.

32. Vlasov, V.Z., "Basic Differential Equations in the General Theory of Elastic Shells", NACA TN-1241, Translation, 1951.

33. Naghdi, P.M., "Foundation of Elastic Shell Theory", Progress in Solid Mechanics, Vol. IV, Ed. Sneddon-Hill, North-Holland Publishing Co. - Amsterdam, 1963.

34. Hurty, W.C., Rubenstein, M.F., "Dynamics of Structures", Prentice-Hall, Inc., Englewood Cliffs, N.J., 1965 second printing.

35. Mindlin, R.D., "High Frequency Vibrations of Crystal Plates", Quarterly of Applied Mathematics, Vol. 19, 1961.

36. Herrmann, G., Mirsky, I., "Three Dimensional and Shell-Theory Analysis of Axially Symmetric Motions of Cylinders", Journal of Applied Mechanics, December 1956.

37. Yu, Y.Y., "Viscoelastic Damping of Vibrations of Sandwich Plates and Shells", Non-Classical Shell Problems, Proceedings of the I.A.S.S. Symposium, Warsaw, Sept. 2-5, 1963.

38. Klosner, J.M., Levine, H.S., "Further Comparison of Elasticity and Shell Theory Solutions", AIAA Journal, Vol. 4, No. 3, March 1966.

39. Reissner, E., "Stress Strain Relations in the Theory of Elastic Shells", Journal of Math. Physics, Vol. 31, July 1952.

40. Greenspon, J.E., "Vibrations of a Thick-Walled Cylindrical Shell. Comparison of Exact Theory with Approximate Theories", Journal of the Acoustical Society of America, Vol. 32, No. 5, May 1960.

41. Mirsky, I., "Three-Dimensional and Shell-Theory Analysis for Axisymmetric Vibrations of Orthotropic Shells", Journal of the Acoustical Society of America, Vol. 39, No. 3, 1966.

42. Spillers, W., "Wave Propagation in a Thin Cylindrical Shell", Journal of Applied Mechanics, June 1965.

43. Naghdi, P.M., "On the Theory of Thin Elastic Shells", Journal of Applied Math XIV, 369-380, 1957.

44. Iyengar, K.T., Yogananda, C.V., "Comparison of Elasticity and Shell Theory Solutions for Long Circular Cylindrical Shells", AIAA Journal Vol. 4, No. 12, December 1966.

45. Mindlin, R.D., "Influence of Rotary Inertia and Shear On Flexural Motions of Isotropic, Elastic Plates", Journal of Applied Mechanics, March 1951.

46. Mindlin, R.D., Deresiewicz, H., "Axially Symmetric Flexural Vibrations of a Circular Disk", Journal of Applied Mechanics, March 1955.

47. Goldstein, H., "Classical Mechanics", Addison-Wesley Co., Reading, Mass. 1950.

48. Wang, C., "Applied Elasticity", McGraw Hill, N.Y., 1953.

49. Courant, R., Hilbert, D., Methods of Mathematical Physics, Vol. 1, Interscience, N.Y., 1953.

50. Reissner, E., "On the Form of Variationally Derived Shell Equations", Journal of Applied Mechanics, June 1964.

51. Yu, Y.Y., "Generalized Hamilton's Principle and Variational Equation of Motion in Non-Linear Elasticity Theory, with Application to Plate Theory", Journal of the Acoustical Society of America, Vol. 36, No. 1, January 1964.

52. Yu, Y.Y., "On Linear Equations of Isotropic Elastic Plates and Shells", Air Force Office of Scientific Research Contract AF 49 (638)-1290, Scientific Report No. 2 - Polytechnic Institute of Brooklyn, Feb. 1964.

53. Washizu, K., "On the Variational Principles of Elasticity and Plasticity", M.I.T. Aeroelastic and Structures Research Laboratory, Technical Report 24-18, March 1955.

54. Ince, E.L., "Ordinary Differential Equations", Longmans, Green and Co. Ltd., London, 1927.

55. Kraus, H., Kalnins, A., "Transient Vibration of Thin Elastic Shells", Journal of the Acoustical Society of America, Vol. 38, No. 6, Dec. 1965.

56. Tso, W.K., "Orthogonality Condition for the Vibrational Modes of Elastic Shells", Journal ofApplied Mechanics, Sept. 1967.

57. Yu, Y.Y., "On the Donnell Equations and Donnell Type Equations of Thin Cylindrical Shells, AFOSR TN-57-464, Ad-136455, Syracuse Univ. Res. Inst. Aug. 1951.

58. Deltoro, V., Parker, S., "Principal of Control Systems Engineering", McGraw Hill Book Co., N.Y. 1960.

59. Salvadori, M., Schwarz, R., "Differential Equations in Engineering, Prentice-Hall, Inc., N.Y. 1954.

60. Freudenthal, A.M., "The Inelastic Behavior of Engineering Materials and Structures", John Wiley and Sons, Inc., N.Y., 1950.

61. Wylie, C.R., "Advanced Engineering Mathematics", Second edition, McGraw-Hill Book Co., Inc., N.Y. 1960.

62. Reismann, H. and Pawlik, P., "Plane-Strain Dynamic Response of a Cylindrical Shell - A Comparison of Three Different Shell Theories", Tran. of the ASME, Journal of Applied Mechanics, June 1968.

63. Reismann, H. and Padlog, J., "Forced, Axisymmetric Motions of Cylindrical Shells", J. Franklin Institute, V. 285, No. 5, November 1967.

64. Medige, J., Lin, M.Z., Reismann, H., "Dynamic Response of Cylindrical Shells to Lateral Load", Proc. of the Army Symposium on Solid Mechanics, Sept. 1968.

65. Reismann, H., "Response of a Cylindrical Shell to an Inclined Moving Pressure Discontinuity (Shock Wave)", J. of Sound and Vibration, Vol. 8, No. 2, 1968.

Autobiographical Statement

Selig Fisher is a graduate of C.C.N.Y. (B.M.E, 1957, M.E., 1964). He has eight years of experience as an Engineer in the defense electronics and aircraft industries. Four years were spent as a full-time lecturer in the Mechanical Engineering Department at City College. He is married and has two children.